A MULTI-SCALE COMPUTATIONAL APPROACH TO UNDERSTAND THE CALCIUM DYNAMICS AND ARRHYTHMOGENIC DISORDERS CAUSED BY MUTATIONS IN RYR2/CASQ2 EXPRESSING GENES

by

Roshan Paudel

A Dissertation
Submitted to the
Graduate Faculty
of
George Mason University
in Partial Fulfillment of
The Requirements for the Degree
of
Doctor of Philosophy
Bioinformatics and Computational Biology

Committee:

_____	Dr. M. Saleet Jafri, Committee Chair
_____	Dr. Iosif Vaisman, Committee Member
_____	Dr. Dmitri Klimov, Committee Member
_____	Dr. Iosif Vaisman, Director, School of Systems Biology
_____	Dr. Donna M. Fox, Associate Dean, Office of Student Affairs & Special Programs, College of Science
_____	Dr. Fernando R. Miralles-Wilhelm, Dean, College of Science
Date: _____	Summer Semester 2020 George Mason University Fairfax, VA

A Multi-scale Computational Approach to Understand the Calcium Dynamics and Arrhythmogenic Disorders Caused by Mutations in RyR2/CASQ2 Expressing Genes

A Dissertation submitted in partial fulfillment of the requirements for the degree of Doctor of Philosophy at George Mason University

by

Roshan Paudel
Master of Science
Morgan State University, 2012
Master of Science
Tribhuvan University, 2003

Director: M. Saleet Jafri, Professor
School of Systems Biology, College of Science

Summer Semester 2020
George Mason University
Fairfax, VA

DEDICATION

This dissertation is dedicated to my parents (Chudamani and Mati Kumari), loving wife Kalpana, my two wonderful daughters Imisha and Romisha. I am extremely grateful for their unconditional love, unceasing support, and inspiration.

ACKNOWLEDGEMENTS

First, I am sincerely grateful to my dissertation advisor, Dr. M. Saleet Jafri, for his continuous support and constructive suggestions throughout the year; otherwise, this research work would not be possible. It is my great pleasure to thank all the members of the dissertation advisory committee, Dr. Iosif Vaisman and Prof. Dmitri Klimov, for their constant help and guidance throughout the research process.

I am also thankful to Dr. Aman Ullah for his continuous help, guidance, and encouragement. I am also grateful to Dr. Sarita Limbu for her help and support. It was great fun to share the lab space with fellow lab members, Dr. Lamya AlOmair, Dr. Nasrin Afzal, Bader Alharbi, Fahad Almsned, and Leena Nezamuldeen.

I owe the deepest gratitude to my wife, Kalpana, for her unwavering love, support, and encouragement all the time. I am not sure I could have done it without her. I owe a sincere apology to my two beautiful daughters, Imisha and Romisha Paudel, who had to sacrifice their share of playtime with their father for his research work. I am also thankful to my brother Damodar Paudel and friend of mine, Dr. Fitzroy Nembhard, for their help and support.

TABLE OF CONTENTS

LIST OF TABLES

LIST OF FIGURES

LIST OF ABBREVIATIONS AND SYMBOLS

Action Potential Duration ..... APD
Calsequestrin Type 2 ..... CASQ2
Calcium Induced Calcium Release ..... CICR
Catecholaminergic Polymorphic Ventricular Tachycardia ..... CPVT
Excitation Contraction Coupling ..... ECC
Force-Frequency Relationship ..... FFR
Gain-of-Function ..... GOF
Long/Lasting Calcium Channel LCC
Loss-of-Function ..... LOF
Luminal Regulation Function ..... ϕ
Plasma Membrane Calcium Adenosine Triphosphate ..... PMCA
Ryanodine Receptor Type 2 ..... RyR2
Sarcoplasmic/Endoplasmic Reticulum Calcium Adenosine Triphosphate ..... SERCA
Sarcoplasmic Overload Induced Calcium Release ..... SOICR
Sarcoplasmic Reticulum/Endoplasmic Reticulum ..... SR/ER

ABSTRACT

A MULTI-SCALE COMPUTATIONAL APPROACH TO UNDERSTAND THE CALCIUM DYNAMICS AND ARRHYTHMOGENIC DISORDERS CAUSED BY MUTATIONS IN RYR2/CASQ2 EXPRESSING GENES

Roshan Paudel, Ph.D.

George Mason University, 2020

Dissertation Director: Dr. M. Saleet Jafri

Whole-cell computational models are very beneficial to understand and predict the underlying cellular and ionic mechanism in the heart. We developed a stochastic ventricular myocyte model of Guinea pig with 20000 stochastically gating CRUs incorporating a six-state L-type Ca^{2+} channel (LCC) and a three-state ryanodine receptor (RyR2). The model was used to understand the Calcium (Ca^{2+}) dynamics in the subcellular level with the computational analysis of Ca^{2+} sparks, their amplitudes and durations in the exploration of force-frequency relationship (FFR) and arrhythmogenesis of mutations in the genes expressing the luminal Ca^{2+} buffer, Calsequestrin (CASQ2) and sarcoplasmic reticulum (SR) Ca^{2+} channels, RyR2. In FFR, the model predicted that diastolic SR [Ca^{2+}] and RyR2 adaptation increased with the increased stimulation frequency giving rise rising than falling amplitude of the cytoplasmic [Ca^{2+}] transients. A simulation on the deletion mutation $CASQ2^{G112+5X}$ responsible for causing

catecholaminergic polymorphic ventricular tachycardia type 2 (CPVT2) found cardiac alternans (action potential duration (APD) and AP amplitude) and early afterdepolarizations (EADs) were the underlying mechanisms to cause arrhythmia in the myocytes during β-arrhythmogenic receptor (β-AR) stimulation. The arrhythmogenic mechanisms instigated by RyR2 mutations are explained by four different hypotheses: gain-of-function (GOF), loss-of-function (LOF), store-overload induced Ca^{2+} release (SOICR), and binding protein destabilization. Our model evaluated all these hypotheses with β-AR stimulation and it predicted that the EADs were the mechanism of CPVT1 in LOF mutation and APD and AP amplitude alternans were the mechanisms in GOF mutation. The abundance Ca^{2+} spark leaks in the binding protein mutation came short to develop any DADs and the SOICR phenomenon was unable to activate RyR2 in the absence of Ca^{2+} induced Ca^{2+} release (CICR).

CHAPTER ONE: INTRODUCTION

Abstract

The heart is a thick muscular pump that serves to circulate blood all over the body. In each beat, the heart supplies oxygen and nutrients via blood to each cell in the body and collects waste generated during metabolism. The heartbeat is initiated by the spontaneous depolarization of pacemaker cells, propagated by the conduction system inside the heart and maintained by influx and efflux ions. A normal heart maintains a well-regulated heart rhythm under different physiological conditions. An understanding of the gating behavior of ionic channels in the myocyte is necessary to understand the proper functioning of the heart. A significant disruption of normal ionic movement can cause irregular rhythm to the heart (arrhythmia) and if severe it may end up sudden cardiac death (SCD). In the young patients (< 35 years), the most common causes of SCD are arrhythmia and the majority of SCDs appear without any known cardiac abnormalities in those patients. Mutation in the Ca^{2+} handling proteins causes arrhythmia during exercise, stress, or catecholamine infusion and the condition is derived as catecholaminergic polymorphic ventricular tachycardia (CPVT). When CPVT occurs due to mutation (dominant) in ryanodine receptor (RyR2) protein, it is known as type 1 CPVT (CPVT1) and if it occurs due to mutation (recessive) in Calsequestrin (CASQ2) protein, it is known as type 2 CPVT (CPVT2). Early afterdepolarization (EAD), delayed

afterdepolarization (DAD) and alternans could be the underlying arrhythmic mechanism in those CPVTs. In this research, we answered the mechanism to cause CPVT1 and CPVT2 due to the mutation in the genes expressing CASQ2 and RyR2.

Background

The beating of the heart pumps blood throughout the body via the circulatory system. The heart muscle provides a strong and periodic force to pump the oxygenated blood to all tissues in the body and transport deoxygenated blood away from the tissues. To generate a regular heartbeat, it requires the translation of electrical impulse (excitation) into mechanical force (contraction) (Stoppel, Kaplan, & Black, 2016). When the membrane potential of cardiac myocytes depolarizes by inward moving Na^+ ions, they activate voltage-gated L-type Ca^{2+} (Cav 1.2) channels. This brings extracellular Ca^{2+} to the myoplasm which will then activate intracellular Ca^{2+} channels, the type 2 ryanodine receptors (RyR2s), to release Ca^{2+} from internal storage called the sarcoplasmic reticulum (SR). The rise in intracellular Ca^{2+} causes a contraction in the myofilaments which results in contraction of the cardiac muscle (Walweel, & Laver, 2015). It is called excitation and contraction coupling (E-C coupling) (Fozzard, 1977). Every heartbeat is the result of the rhythmic EC-coupling mechanism. Any disturbance in this coupling can originate abnormal electrical impulses and which can cause cardiac arrhythmia. Cardiac arrhythmia can lead to heart failure (HF) and sudden cardiac death (SCD) (Wellens, Schwartz, Lindemans, Buxton, Goldberger, Hohnloser, et al., 2014).

Heart

The heart of a mammal is a thick muscular organ that contracts to supply the blood rich with oxygen and nutrients to the body. The heart wall is made up of three layers of tissues – epicardium, myocardium, and endocardium. The internal cavity of a mammal heart contains four cavities used to collect and dispense blood. There are two upper chambers, left and right atria and two bottom chambers left and right ventricles as shown in figure 1A.

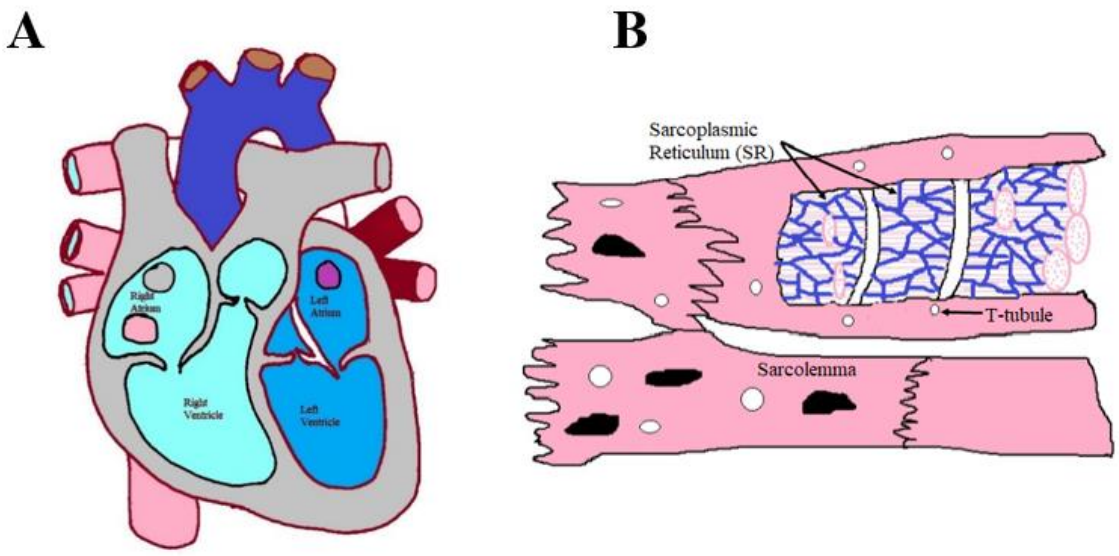

Figure 1: Schematic diagram of a heart and SR and T-tubules in a ventricular myocyte. A four-chambered heart (A), two upper chambers, left and right atria and two lower chambers, left and right ventricles. (B) The internal structure of a myocyte with t-tubules are positioned near SR. Sarcomeres form myofibrils which are responsible for cardiomyocyte contraction upon calcium release.

The right atrium receives deoxygenated blood from the upper and lower body parts via superior vena cava and inferior vena cava, respectively. The left atrium receives oxygenated blood from the lungs via pulmonary veins. The right ventricle pumps the deoxygenated blood from the heart to the lungs while the left ventricle is responsible for sending oxygenated blood all over the body. The heart acts as two pumps left and right sides but both regions contract simultaneously. Out of all four chambers, the left ventricle has the thickest muscular wall to generate enough force to ensure the blood flow to the entire body. The work we have done here was fully concentrated on the left ventricular myocyte and the role of Ca^{2+} ions to play a significant role in the contraction of the heart.

Cellular Structure of Myocytes

Each cardiac myocyte is surrounded by a cell membrane called sarcolemma (Fig. 1A). The sarcolemma is composed of the lipid bilayer and interacts with extracellular and intracellular environments. Besides being a barrier of diffusion like other lipid bilayers, the membrane proteins of sarcolemma contain receptors, pumps, exchangers, and channels basically for sodium (Na^{+}), calcium (Ca^{2+}), and potassium (K^{+}) ions. They are made up of a bundle of myofibrils containing myofilaments. The myofilaments within a myocyte are surrounded by sleeves of sarcoplasm reticulum (SR). These myofibrils have contractile repeated units called sarcomeres. The sarcomere is a region in myofilaments in between two Z – lines. A separate tubular transverse invagination in a myocyte named T tubules cross at the Z – line, as shown in figure 1B. The sarcomere has thin and thick protein filaments – actin and myosin, respectively. The thick filaments also contain regulatory proteins – troponin and tropomyosin. The chemical and physical interaction

between the actin and myosin cause the sarcomere length to shorten, resulting in contraction of myocyte during excitation-contraction coupling. Gap junctions are present in between cardiac myocytes providing a low resistance pathway for the spread of excitation from one myocyte to another (Pinnel, Turner, & Howell, 2007). The myocytes are also packed with mitochondria to supply enough adenosine triphosphate (ATP) required for heart contraction. Because of immense energy demand by EC-coupling, the mitochondria occupy 30-40% of myocyte cell volume (Walker, & Spinale, 1999) (Gong, Liu, & Wang, 2014).

Conduction System in the Heart

The heart conduction system is regulated by cardiac muscle cells and conducting fibers. The electrical impulse starts from the sinoatrial (SA) node situated at the top of the right atrium. The SA node is composed of self-firing cardiac tissues, also known as pacemaker cells. The electrical impulse generated by pacemaker cells is transmitted by nodal fibers to the atrioventricular (AV) node located on the bottom of the right atrium. From the AV node, the conduction travels to the left and right ventricles through the AV bundle or bundle of His. The bundle of His penetrates all the tissue in the form of Purkinje fibers to transmit the electrical impulse to each ventricular tissue in the left and right ventricles to initiate heart contraction.

Action Potential

A brief change in membrane potential in the cell membrane of cardiac myocytes is called cardiac action potential (AP). AP (QRS-T in Fig. 2A) is generated by sequential

opening and closing of ionic channels to transport ions into a cell through transmembrane, as shown in figure 2B.

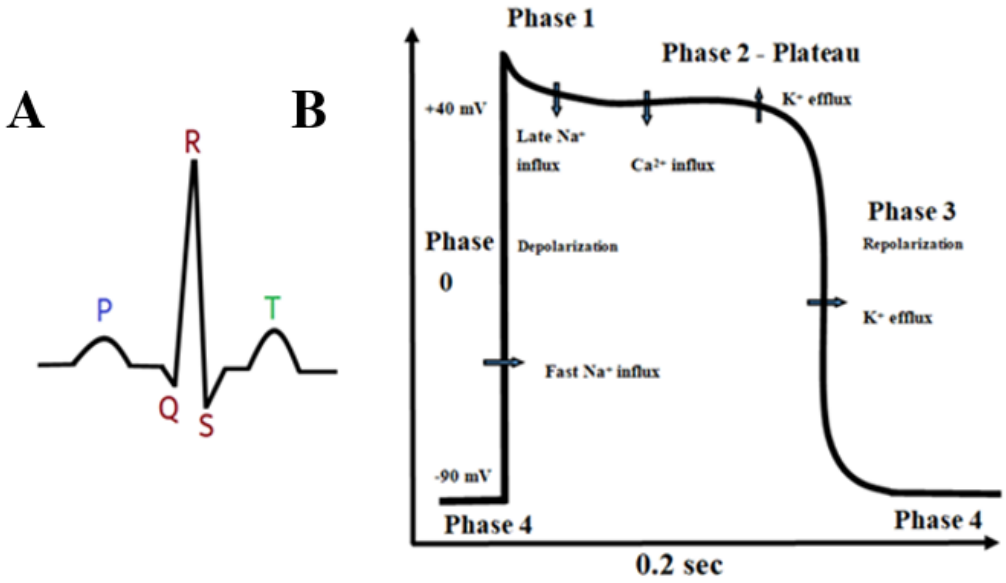

Figure 2: Different phases in electrocardiogram (ECG) and of action potential (AP) in non-pacemaker cardiomyocytes. (A) ECG contains depolarization of atria (P-wave), ventricular depolarization (QRS complex), and repolarization of the ventricles (T-wave). (B) AP is depolarization and repolarization of ventricles, has four phases: phase 0 has steep depolarization because of fast Na^+ current, extracellular and intracellular Ca^{2+} are responsible for long plateau phase and closing of pumping back Ca^{2+} to the intracellular store and exchanging it with Na^+ ions and efflux of K^+ ions repolarize AP back to resting phase.

Atrial and ventricular depolarization-repolarization in the heart is recorded by an electrocardiogram (Fig. 2A). The depolarization of atria is represented by p-wave and the repolarization phase isn't visible because of very low amplitude and overlapping with repolarization of ventricles (Briggs, 1994) (Jayaram, Gandhi, Sangareddi, Mangalanathan, & Shanmugam, 2016). The second wave in the heart is repolarization of ventricles and is represented by the QRS complex in electrocardiogram (Fig. 2A). The T-wave reflects the repolarization of ventricles. A normal cardiac action potential falls into two categories: self-oscillatory or pacemaker and excited by an external stimulus. The action potential in ventricles myocytes is initiated by propagating depolarization coming from pacemaker cells. The action potential explained here is the ventricular action potential of a guinea pig heart.

The action potential of a cardiac cell is composed of 5 different phases which are described below (Nerbonne, & Kass, 2005).

Phase 4: Resting Potential

The resting potential of a heart is -86 mV. It is controlled by a constant outward leak of potassium ions (K^+) through inward rectifier channels. Both sodium (Na^+) and calcium (Ca^{2+}) channels are closed.

Phase 0: Depolarization

Phase 0 is a rapid upstroke of membrane potential caused by the opening fast Na^+ channels. At the beginning of this phase, a triggered from pacemaker cells or neighboring cardiac myocytes slightly increases the membrane potential starts to rise and reaches to -70 mV. This is called a threshold potential. After this, the voltage-gated Na^+ channels

open very quickly and a sharp rise in membrane potential takes place. The L-type Ca^{2+} channels start to open after reaching -40 mV and causes a steady influx of Ca^{2+} down its concentration gradient. In reaching just above 0 mV, the fast Na^{+} channels get closed.

Phase 1: Early Repolarization

Beginning inactivation of fast Na^{+} channels and activation of early K^{+} channels create outward flow of K^{+} resulting reduction in the positivity of myocyte and slight repolarization occurs.

Phase 2: The Plateau Phase

L-type Ca^{2+} channels stay open and generate constant inward Ca^{2+} current following excitation-contraction coupling. An outward movement of K^{+} continues through delayed rectifier K^{+} channels. These countercurrents stabilize the electrical potential and a plateau is formed.

Phase 3: The Repolarization

The L-type Ca^{2+} channels start to inactivate and the inward potential of Ca^{2+} is surpassed by the outward flow of K^{+} and it brings down the AP back to the resting phase. A normal ionic concertation gradient is restored by sending Na^{+} and Ca^{2+} ions to the extracellular space and K^{+} ions inside the cell.

Calcium-Induced Calcium Release

There are two sources of Ca^{2+} required for a heartbeat in the cardiac myocytes – extracellular Ca^{2+} and intracellular Ca^{2+}. Specific Ca^{2+} release channels are available for both sources, for outer Ca^{2+}, it is carried out by L-type channels and for inner Ca^{2+}, it is done by ryanodine receptor. The l-type channel is found in the t-tubule of sarcolemma

and RyR is in the junctional region of the SR (JSR). The restricted region in the myoplasm laying between t-tubule and JSR (see in figure 3) is called subspace where both L-type channels and RyR form a cluster. Each cluster is known as Ca^{2+} releasing unit (CRU). The members of the cluster require a stimulus to get activation and release Ca^{2+} in the subspace. The L-type channel is activated by a change in the membrane potential (voltage) and the ryanodine receptor is activated by sensing Ca^{2+} in the fringe. The electrical impulse generated by the SA node raises the voltage of the sarcolemma. The Na^{+} channels in the sarcolemma open and the depolarization of the membrane occurs. This increased membrane potential activates L-type channels and extracellular Ca^{2+} pours into the subspace. After sensing this Ca^{2+}, the RyR2 channel activates and releases intracellular Ca^{2+} also in the same subspace. A phenomenon where extracellular Ca^{2+} signals a much larger release of Ca^{2+} from the intracellular source is known as calcium-induced calcium release (CICR). L-type channels and RyR2 channels both open in a dyadic subspace and form a cluster. The SR close to t-tubule is categorized as junctional SR and away region of SR is network SR. Four intracellular compartments based upon time evolution of Ca^{2+} - subspace, bulk myoplasm, JSR, and NSR.

Excitation and Contraction Coupling (EC-coupling)

In 1883, Sydney Ringer found cardiac myocytes contract if you put the cells into extracellular fluid (ECF) with calcium (Fye, 1984). If the fluid is without calcium, the myocytes don’t contract. It is quite the opposite of skeletal muscles; they show contraction in non-calcium extracellular fluid too. So, the fundamental element inducing

excitation and contraction is Ca^{2+}. Excitation-contraction coupling is a phenomenon of the myocytes to contract the heart by the electrical stimulation due to a change in the ionic concentration in the cytosol. Calcium ion (Ca^{2+}) is the only activator to the

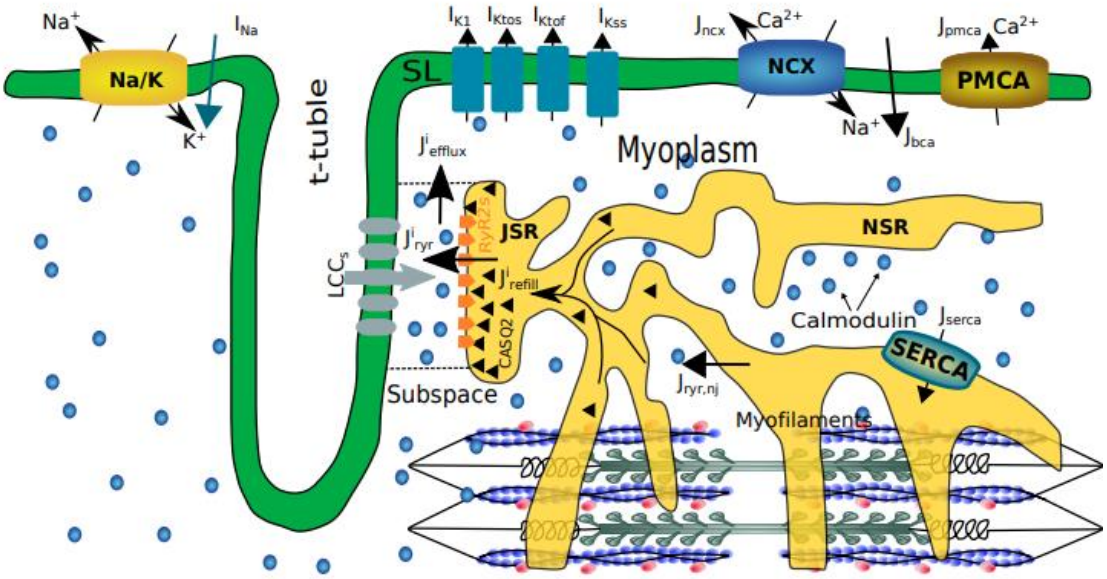

Figure 3: Schematic diagram of CICR, adapted from Williams *et al.* (2011)

myofilaments which can cause the contraction in the heart. When Ca^{2+} enters the cell via voltage-gated calcium (L-type) channels located in sarcolemma and t-tubules, triggers ryanodine receptors (RyR2) present in the sarcoplasmic reticulum (SR) to be excited and release more Ca^{2+} into the myoplasm. The concentration of Ca^{2+} in the cytosol significantly increases during this process. The free cytosolic Ca^{2+} binds to troponin C which causes conformational changes in the tropomyosin. Now more and more Ca^{2+}

attach to the myofilaments. When more and more Ca^{2+} are attached to the myofilaments, they cause them to contract which ultimately contracts all cardiac myocytes for action potential (Bers, 2002). The intracellular Ca^{2+} in myoplasm is pumped back to the SR by the SERCA pump and exchanged with outside Na^{+} by the help of sodium-calcium exchanger (NCX). This results in the depletion of Ca^{2+} level from myoplasm resulting in the relaxation of myocytes during the diastolic phase. The EC-coupling is achieved through the change in cytosolic Ca^{2+} from 100 nanomolar/liter (100 nmol/L) to 10 micromolar/liter (10 μmol/L) concentration (Berne, & Levy, 1997).

Sarcoplasm Reticulum

The sarcoplasm reticulum (SR) is an intracellular specialized Ca^{2+} handling cellular organelle and it is the major component to regulate cytosolic Ca^{2+} (Kadambi, & Kranais, 1997) (Walker, & Spinale, 1999). The SR is divided into two compartments: region close to the sarcolemma and T-tubule, junctional SR (JSR), and the away region, network SR (NSR). The SR maintains a continuous excitation-contraction coupling with the release of Ca^{2+} from its storage and reuptake it back to the storage. A class of three protein is utilized to maintain Ca^{2+} homeostasis- the SR Ca^{2+} ATPase (SERCA 2a), Ca^{2+} release channels (ryanodine receptors, RyR2), and luminal Ca^{2+} binding protein, calsequestrin (CASQ2) (Rossi, & Dirksen, 2006) (Walker, & Spinale, 1999). CASQ2 is a major Ca^{2+} binding protein and it forms a quaternary complex along with triadin and junctin to RyR2. This complex confers Ca^{2+} sensitivity to RyR2 (Györke, Hester, Jones, & Györke, 2004). Phospholamban is believed regulatory protein for SERCA2a function (Tada, & Toyofuku, 1996). The key function of SERCA2a is to minimize the

myoplasmic Ca^{2+} concentration low by pumping it out to the SR; hence the activity of SERCA2a depends upon the availability of cytosolic Ca^{2+} ($[Ca^{2+}]_{myo}$) (Eisner, 2014) (Tran, Smith, Loiselle, & Crampin, 2011).

Calcium Sparks

Calcium sparks are brief, elementary, and local Ca^{2+} release events in the subspace of myoplasm by the opening of one or cluster of RyR2s (Izu, Wier, & Blake, 1998) (Guatimosim, Guatimosim, & Song, 2011) (Lukyanenko, & Gyorke, 2004) (Hoang-Trong, Ullah, & Jafri, 2015). When RyR2s release Ca^{2+} from internal storage, they form sparks and increase the Ca^{2+} concentration in myoplasm required for E-C coupling. Ca^{2+} sparks can occur spontaneously or RyR2 activation by L-type Ca^{2+}. Cheng *et al*. in 1993 (Cheng, Lederer, & Cannell, 1993) used laser scanning confocal microscopy and Fluo-3 Ca^{2+} indicator to record Ca^{2+} sparks in a single cardiac myocyte (Lopez-Lopez, 1995). Ca^{2+} release during EC-coupling is the result of the summation of Ca^{2+} sparks (Lukyanenko, & Gyorke, 2004). When numerous Ca^{2+} sparks occur simultaneously in a myocyte, it creates a uniform Ca^{2+} transient (Guatimosim, et al., 2011) (Tuan, Williams, Chikando, Sobie, Lederer, & Jafri, 2011). In the experiments, the sparks are measured with Ca^{2+}-sensitive fluorescent dye under the confocal laser-scanning microscope (Picht, Zima, Blatter, & Bers, 2007).

Force-Frequency Relationship

The beat to beat cardiac function is affected by mechanical restitution and postextrasystolic potentiation which is decided by the amount of Ca^{2+} available to the contractile filaments (Hardman, 1994). Hence, the concentration of intracellular Ca^{2+} has

a major role in the increase and decrease in the pumping force of a heart. The contractility of myocardium depends on the frequency or rhythm of the heart (Woodworth, 1902) too. The frequency-dependent increase in myocardial contractility is associated with an increase in the amount of Ca^{2+} ions entering the myocytes in each beat (Koch-Weser, & Blinks, 1963). The changes in force development are directly related to the changes in the intracellular Ca^{2+} transients (Yue, 1992). In an experiment, it was reported that when the frequency of electrical stimulation increases, it also raises the amplitude of Ca^{2+} transient (Allen, & Blinks, 1978) (Blinks, Blinks, Wier, Hess, & Prendergast, 1982). The interval-force relation deals with the changes in Ca^{2+} transient and force generated by cardiac myocytes with varying pacing frequencies. The change in the force in each pacing is termed as an interval-force relationship (Williams, Smith, Sobie, & Jafri, 2010) or force-frequency relationship (FFR). In general, when there is a change in pacing frequency, it also changes myoplasmic Ca^{2+} transient and the force generated by the myocytes. Mature myocyte of higher mammals exhibits a positive FFR and it is called Bowditch phenomenon (Godier-Furnémont, Tibucry., Wagner, Dewenter, Lammle., El-Armouche, Lehnart, et al., 2015) (Schotten, Schotten, Greiser, Braun, Karlein, & Schoendube, 2001). A negative FFR and alterations in EC-coupling are key features in arrhythmic heart failure (Bers, 2001) (Katz, 2000). FFR is an important intrinsic regulatory mechanism in cardiac myocytes' contraction (Endoh, 2004). The positive FFR is crucial for the adaptation at the time of increased physical activities or exercise (Hasenfus, Holubarsch, Hermann, Astheimer, Pieske, & Just, 1994). The negative FFR in humans is suggested to exhibit a maladaptation of the heart in rapid

pacing. The FFR is an intrinsic regulatory factor that adjusts the contractile function of the myocytes to change them rapidly if required for more blood supply (Joulin, Marechaux, Hassoun., Montaigne, Lancel, & Neviere, 2009), and depression in cardiac function serves better in negative FFR (Bohm, La Rosee, Schmidt, Schulz, Schwinger, & Erdmann, 1992). Cardiomyocytes of failing human heart display reversal in the FFR, there is a decrease in the contractile performance at higher rates of stimulation (Davies, Davia, Bennett, Pepper, Poole-Wilson, et al., 1995). The mechanisms of the force-frequency relationship primarily depend upon changes in the intracellular Ca^{2+} transients (Joulin, Joulin, Marechaux, Hassoun., Montaigne, Lancel, & Neviere, 2009) as well as some other factors such as SERCA pump activities, $Na^{+,}$ and Ca^{2+} exchangers (NCX) and adrenergic control (Lompre, Lompre, Anger, & Levitsky, 1994) (Kurihara, & Allen, 1982) (Ross, Miura, Kambayashi, Eising, & Ryu, 1995).

FFR is described as a phenomenon in which interplay between the increase in the concentration of SR Ca^{2+} with an increase in pacing frequency and the accumulation of RyR in the adaptation state (Jafri, 2012). The mechanism of impairment in myocardial Ca^{2+} during heart failure is important in interval-frequency response. Other abnormalities include reduced Ca^{2+} release from the SR as well as delayed reuptake, in a reduction in the number of SR Ca^{2+} channels and abnormal mRNA levels of Ca^{2+} transport proteins (Ross, et al., 1995). We are conducting this research with a highly stable ventricular myocyte model with the update with new experimental features and integrating stochasticity in the deterministic model developed by Jafri, Rice, and Winslow (1998).

The variability in the biological system and heterogeneity in nature can be best represented by stochastic processes.

The Ca^{2+} transients are the result of the stochastic summation of Ca^{2+} spark elementary events in the diadic subspace and hence they form the basis of EC coupling (Cheng, & Lederer, 2008) (Hoang-Trong, Ullah, & Jafri, 2015). The force generated by myocyte depends greatly on local Ca^{2+} dynamics and can be explained by the characteristics of these Ca^{2+} sparks. The amplitude of these sparks also varies based upon numbers of RyR2 open in the given time. The Ca^{2+} spark analysis should predict a more realistic relationship between force generated by the cardiomyocytes with the variation in the frequency over the classical methods.

Calsequestrin (CASQ2)

Calsequestrin (CASQ) is a highly abundant and major calcium-binding protein or Ca^{2+} buffer protein in the SR of cardiac myocyte (known as CASQ2) and endoplasmic reticulum (ER) of skeletal muscle (known as CASQ1). It is highly acidic and contains high affinity Ca^{2+} binding sites. Because of the Ca^{2+} buffering capacity of CASQ2 in luminal space, it stores free Ca^{2+} below the inhibitory level (1 mM) of SERCA2a (Park, Park II, Kim, Youn, Fields, & Dunker, 2004). A molecule of CASQ2 can bind 40 – 60 Ca^{2+} and releases them with a high off rate (Beard, Leaver, & Dulhunty, 2004) (Hajeung, Park, Kim, Youn, Dunker, & Kang, 2004) (Kim, Kim, Young, Kemper, Campbell, Milting, & Varsanyi, et al., 2007). The monomers in CASQ have a molecular mass of ~40 kDa and contain close to 415 amino acids (Song, Alcalai, Arad, Wolf, Toka, Conner, et al., 2007). The monomer contains three domains each with a compact α – helical/ β-

sheet thioredoxin which is stable in the presence of Ca^{2+} and the domain is connecting by short loops (Fig. 5) (Faggioni, Krystal, & Knollmann, 2012). CASQ2 is a luminal Ca^{2+} buffer protein and a single molecule of CASQ2 is high affinity Ca^{2+} binding protein, can bind up to 50 Ca^{2+} by a molecule.

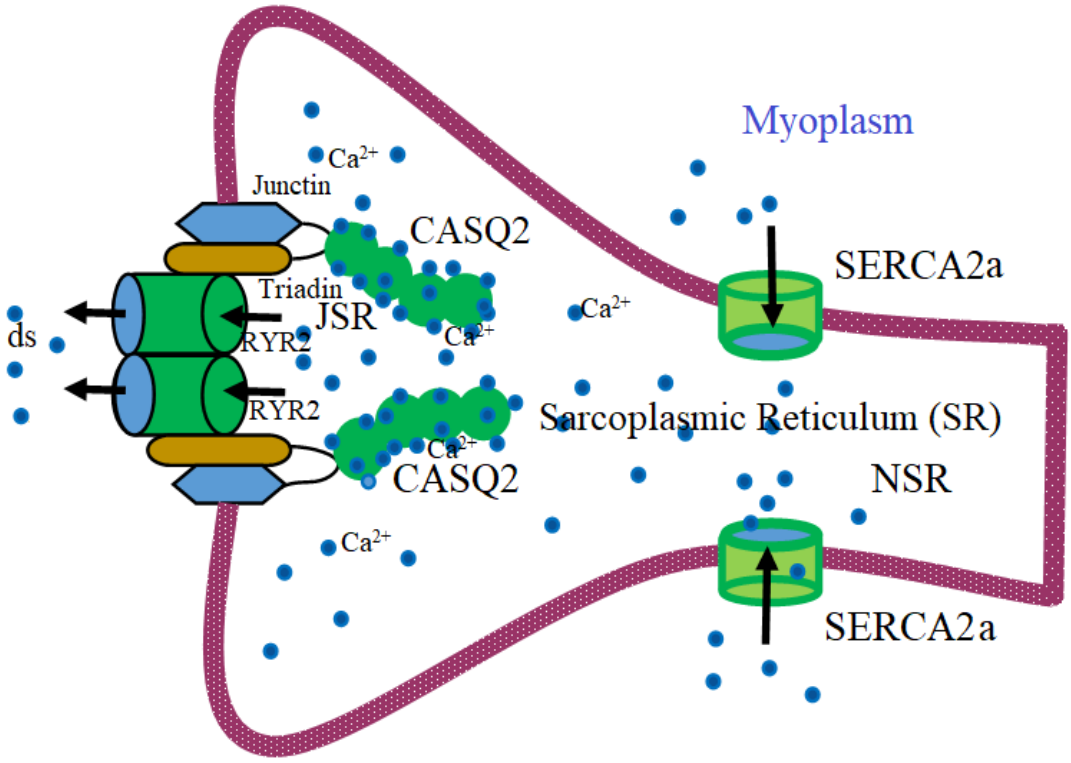

Figure 4: Schematic representation of the RyR2-CASQ2-triadin-junctin complex in the SR.

CASQ2 forms a quaternary complex with RyRs and anchoring proteins, triadin, and junctin (Zhang, Kelley, Schmeisser, Kobayashi, & Jones, 1997) (Novak, & Soukup, 2011) (Beard, Casarotto, Wei, Varsanyi, Laver, & Dulhunty, 2005). The "RyR complex"

(Fig. 4) plays a major role during EC-Coupling by releasing Ca^{2+} from SR via RyRs (Murray, Froemming, Maguire, & Ohlendieck, 1998) (Dulhunty, 2006) (Mackrill, 2010). The triadin and junctin proteins interact with RyR in the junctional area with a readily available larger pool of Ca^{2+} close to the release site (Beard, Wei, & Dilhunty, 2009). CASQ2 allows the Ca^{2+} required for the contraction to be stored at a total concentration of ~ 20 mM (Beard, et al., 2004) and CASQ2 dissociates from the quaternary complex when the luminal [Ca^{2+}] is ~1mM or below (Shin, Ma, & Kim, 2000).

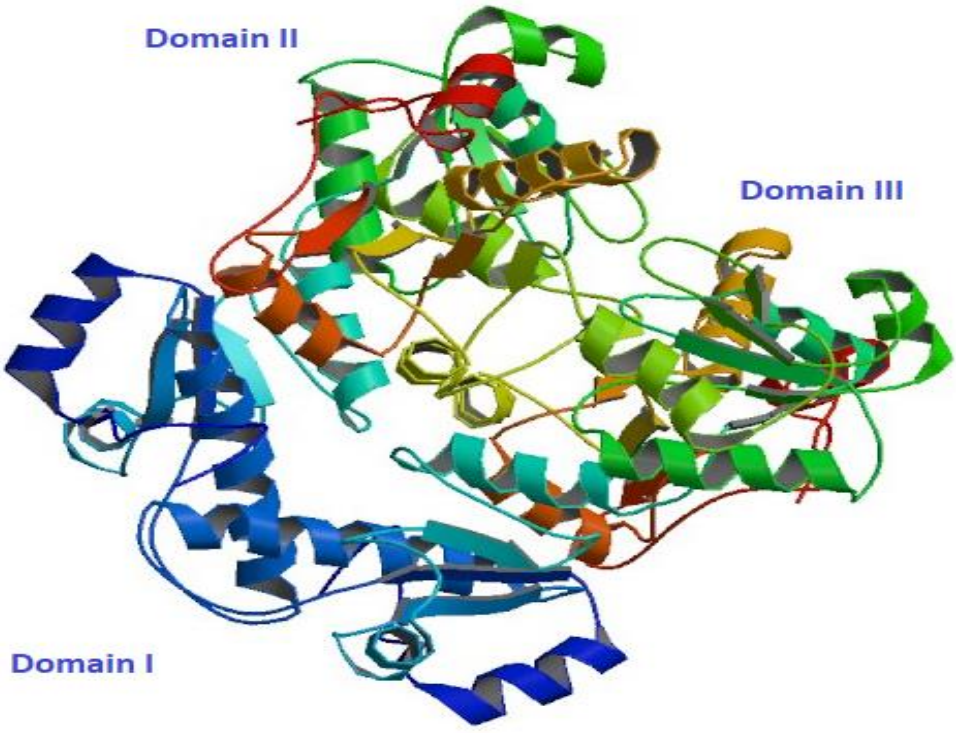

Figure 5: A cartoon diagram of human CASQ2 displaying the arrangement of α-helices and β-sheets in different domains adapted from Kim *et al*. (Kim, et al. 2007).

Ryanodine Receptor

Sarcoplasm reticulum (SR) is the storage of intracellular Ca^{2+} in a myocyte. The availability of this Ca^{2+} in SR plays all the roles in the cellular process of excitation-contraction coupling (E-C Coupling). Two protein components are responsible for releasing and refill the Ca^{2+} in SR- ryanodine receptor (RyR) and the SR Ca^{2+} ATPase (SERCA) pump, respectively. The SR intracellular Ca^{2+} gets a release to myoplasm through a cluster of ionic channels for EC–coupling events which are ryanodine receptors (RyR2s). When RyR2 is activated by Ca^{2+} influx via L-type channels, a calcium-induced calcium-release (CICR) phenomenon takes place (Fabiato, 1975) (Peng, Shen, Wu, Guo, Pan, & Wang, 2016). These RyRs are among the largest Ca^{2+} channels and the majority of them located in the junction between the t-tubule part of the sarcolemma (SL) and junctional sarcoplasmic reticulum (JSR) in striated muscle (Otsu, Willard, Khanna, Zorzato, Green, & MacLennan, 1990) (Blayney, & Lai, 2009). In humans, the t-tubule measures 125 nm in diameter and separated with a gap called dyad cleft (15 nm) to the SR (McGrath, Yuki, Manaka, Tamaki, Saito & Takekura, 2009) (Radermacher, Rao, Grassucci, Frank, Timerman, & Fleischer, 1994). In mammal cells, there are three mammalian isoforms of ryanodine receptors namely RyR1, RyR2 and RyR3 (Lanner, Georgiou, Joshi, & Hamilton, 2010) (Yan, Bai, Yan, Wu, Li, Xie, et al., 2015) (Kushnir, & Marks, 2010) and RyR2 shares almost 70% out of three mammalian RyR isoforms (Ma, Hayek, & Bhat, 2004). Major forms for RyR1 and RyR3 are reported from skeletal muscle and brain cells, respectively (Takeshima, Matsumoto, Ishida, Kangawa, Minamino, Matsuo, et al., 1989) (Santulli, Lewis, Georges, Marks, & Frank, 2018) and

cardiac myocytes are rich in RyR2s (Zorzato, Fujii, Otsu, Philips, Green, Lai, et al., 1990) (Otsu, et al., 1990). In non-cardiac cells, these RyRs are co-located with inositol 1, 4, 5-triphosphate receptors (IP3Rs) to release Ca^{2+} (Patterson, Boehning, & Snyder, 2004). RyR2s are generally modulated by the dihydropyridine receptor (DHPR) or L-type Calcium channels (Fig. 3) and small molecules, ions or myoplasmic proteins such as calmodulin (CaM), calcium-dependent protein kinase II (CaMKII), calsequestrin (CSQ), triadin, junctin (Nakai, Sekiguchi, Rando, Allen, & Bean, 1998) (Györke, Hester, Jones, & Györke, 2004) (Mohler, & Wehrens, 2007). RyR2s are fully regulated by the presence of Ca^{2+}, in the absence of it virtually closed with the open probability below 10^{-4} (Laver, & Honen, 2008).

Molecular Structure of Ryanodine Receptor

The RyR2s are homo-tetramer transmembrane subunits formed by 4967 amino acids. (Walweel, & Laver, 2015) (Wei, Zhang, Clift, & Yamaguchi, 2016) (Medeiros-Domingo, Bhuiyan, Tester, Hofman, Bikker, Tintelen, et al., 2009). They form large protein complexes comprising of four 560-KD RyR subunits, four 12-KD FK506-binding proteins, and various accessory proteins (Meissner, 2017). Under electron microscopy,

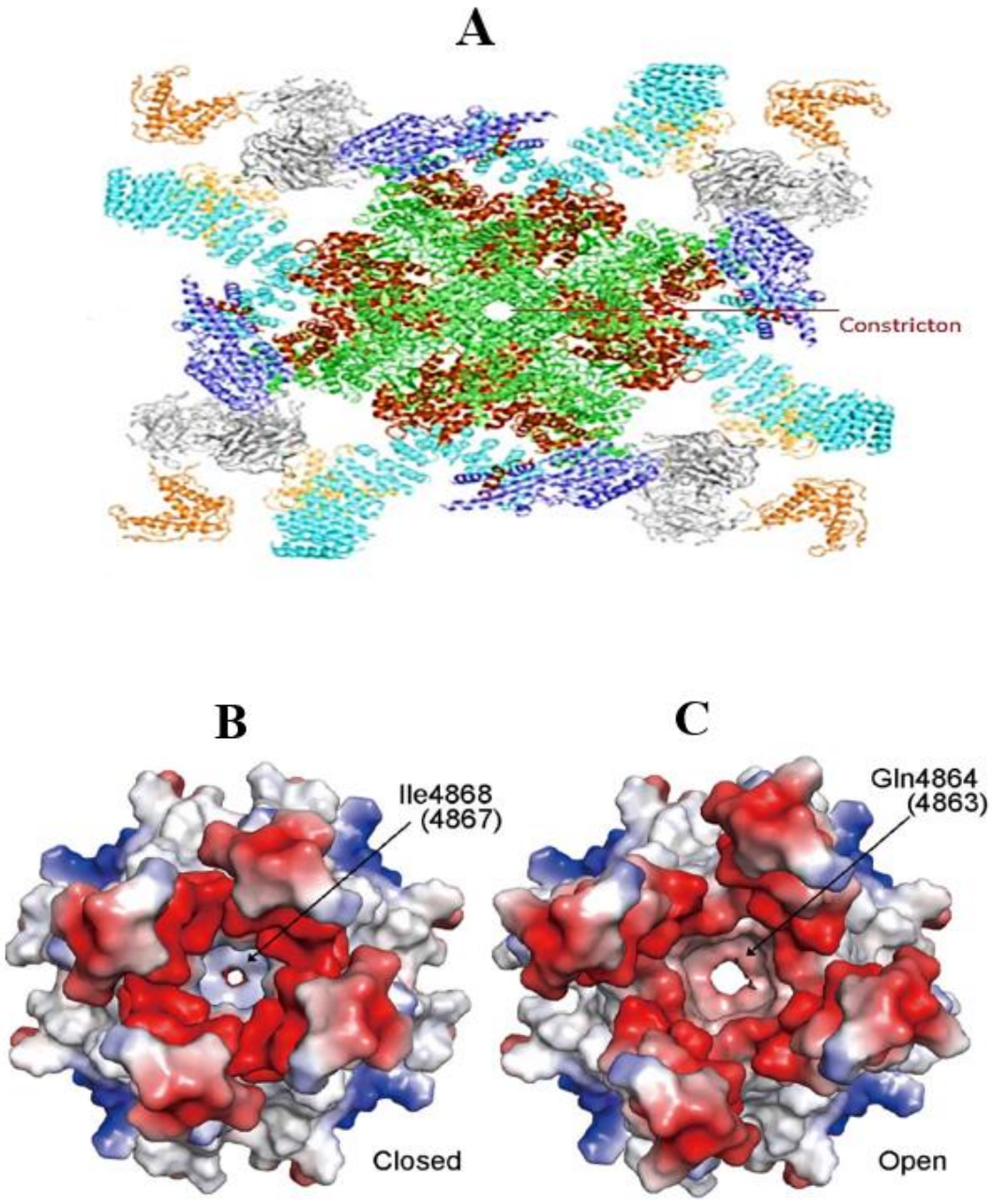

Figure 6: The cartoon structure of RyR2 with constriction in closed and open state. (A) The cryo-EM structure of RyR2 from the porcine heart in a closed state (Yan, et al., 2015) (Peng, 2016). Cryo-EM structure of RyR2 in an open state (B) and closed state (C). Extracted from porcupine RyR2, where ille4868 and Gln4864 are constriction residues in

respective states (Peng, et al., 2016) (Kawata, Ohno, Aiba, Sakaguchi, Miyazaki, Sumitomo, et al., 2016).

the RyR2 has a pyramid appearance. There are nine conspicuous domains in the cytoplasmic region of each protomer. The domains are N-terminal domain, three SPRY (SplA kinase and RyRs) domains, the $P_1$and P_2 domains, the handle, helical and central domains (Yan, et al., 2015). The N-terminal is a hot spot for disease-causing mutations and the first SPRY domain (SPRY1) is a binding site for FKBP12.6, calstabin2 (Gonano, & Jones, 2017) (Meissner, 2017). The central domain comprises an armadillo repeat-like a twenty alpha-helices assembly, an EF-hand domain on the ridge of the assembly, and a U-motif at the C terminus as shown as cartoon structure in the figures 6(A) and RyR2 closed state (6B) and open state (6C). The RyR2 receptors are activated open to release SR Ca^{2+} with the influx of Ca^{2+} from voltage-gated Ca^{2+} channels, DHPRs.

β-Adrenergic Receptors

β-adrenergic receptors (β-ARs) are the transmembrane receptors and are the members of the family of G-protein-coupled receptors. There are three isoforms of these receptors: β_1-, β_2 - and β_3 – adrenoceptors, and β1-adrenoreceptors are found in the cardiac muscles (Myagmar, Flynn, Cowley, Swigart, Montgomery, & Thai, 2017). The structure of the receptor reveals that it has three intercellular loops, three extracellular loops, one and one intracellular C-terminal and extracellular N-terminal domain, and seven-transmembrane-spanning domain (Wallukat, 2002) (Rockman, Koch, & Lefkowitz, 2002). These adrenoceptors are activated upon binding the sympathetic

neurotransmitter norepinephrine or the hormone epinephrine during the fight-or-flight response. Epinephrine is released by the adrenal medulla while norepinephrine is released by sympathetic nerve endings (de Lucia, Femminella, G. D., Gambino, G., Pagano, G., Alloca, E., & Rengo, 2014). The signaling of the receptors plays a critical role in the regulation of function and processes of the cardiovascular system such as an increase in heart rate, increase the contractile property of cardiomyocytes, increase in the relaxation rate of cardiomyocytes and modulation in the metabolism to satisfy the increase in energy requirements during the process (Saucerman, & McCulloch, 2006). The signaling of β-ARs increases the activity of L-type channels bringing more Ca^{2+} into the cardiac myocytes which results in larger contraction of the heart. (Tsien, Giles, & Greengard, 1972). Phosphorylation of phospholamban reduces inhibition of the SERCA pump and sequesters more Ca^{2+} into the SR for the larger subsequent contractions (Solaro, Moir, & Perry, 1976).

Mutation

A mutation brings alteration in the DNA sequence of a gene. As the altered gene expresses a protein, the amino acid sequences are modified and it may affect the function of the final product. The mutation could be hereditary or somatic. If the mutation is inherited from parents to off-springs, it is called a hereditary mutation. There is a chance a person can develop a mutation during own's life, it is termed as somatic or acquired mutation. Not all the gene mutations are harmful; only a few percentages of those mutations affect the function of a protein expressed by the mutated gene.

Point mutation – A single nucleotide changes from a base pair. It could be transition mutation - one purine to another purine (A → G or G → A) or transversion mutation - one pyrimidine to another pyrimidine (C → T or T → C) (Torgerson, & Ochs, 2015). Point mutation could be nonsense, missense, frameshift, and silent mutations.

Nonsense mutation – A nucleotide change in the DNA sequence creates an immature stop codon (TGA, TAG or TAA) and ceases the amino acid polymerization. The result is truncated or unstable protein.

Missense (amino acid substitution) mutation – It is a single nucleotide change in DNA that leads to change one kind amino acid form another one. The expressed protein form missense mutation becomes unstable or dysfunctional.

Silent mutation – In this mutation, the DNA sequence will change with the change in nucleotide (third nucleotide) and translate into the same amino acid and protein.

Frameshift mutation – An addition or deletion of a base, and it creates every subsequent genetic code different from the previous one due to shifting in the reading frame.

Loss of Function or Gain of Function Mutations

There are two types of mutations based upon their impact on the function of protein - loss of function and gain of function. When both alleles of a gene are mutant, it results in a recessive mutation. A recessive mutation inactivates the affected gene and leads to loss of function of the protein. In contrast, when a single allele of the gene is mutant and another one is normal, the consequence becomes a dominant mutation. A dominant mutant may enhance the activity of the protein and leads to a gain of function mutation (Lodish, Berk, Zipursky, Matsudaira, Baltimore, & Darnell, 2000).

Cardiac Arrhythmia, Heart Failure, and Sudden Cardiac Death

Arrhythmia is an irregular beating of heart due to an abnormality in the electrical impulse in the origination or during propagation. Heart failure is a clinical syndrome of a heart when it cannot pump enough blood to the body required for the metabolic process of the cells (Xiao, Guo, Sun, Hunt, Wei, Liu, et al., 2016). Any disruption in the coordinated electrical propagation in the heart tissues results in arrhythmia (Tse, 2016) and it could happen in atrial or ventricular regions the heart. Three basic mechanisms are responsible for cardiac arrhythmia- automacity, triggered activity, and reentry (Gaztanaga, Marchlinski, & Betensky, 2012). Automacity is the specialized function of cardiac myocytes to initiate spontaneous AP (Antzelevitch, & Burashnikov, 2011). Automacity happens due to suppressions in the origination of impulse (SA node) or conduction of impulse (AV node and His-Purkinje system) (Matteo, & Nargeot, 2008). Disturbed Intracellular Ca^{2+} signaling and changes in Ca^{2+} dynamics are determined to cause ventricular arrhythmias such as tachycardia or ventricular fibrillation (Venetucci, Denegri, Vapolitano, & Priori, 2008) (Wagner, Maier, & Bers, 2015) and atrial arrhythmia such as atrial fibrillation and flutter (Heijman, Voigt, Nattel, & Dobrev, 2014) (Nattel, & Dobrev, 2012) (Deo, Weinberg, & Boyle, 2017). Ventricular tachycardia or fibrillation can cause hyperexcitability of the sarcolemma, disturbed repolarization, or defective conduction of electrical impulse across the myocardium (Pandit, & Jalife, 2013). The tachycardia can occur due to a block of electrical impulse with non-electric scar tissues and they force the impulse to propagate around the blockage. If the block is unidirectional, then the impulse can re-enter and re-excite the tissue in front of the block.

This is called the reentry mechanism of arrhythmia. It will cause alteration in the excitation, repolarization, or conduction of the electrical wave front and can happen to tissue with injury or inflammation (Pandit, & Jalife, 2013). However, the disturbed functions of ionic channels also can bring changes in excitation, repolarization, or even conduction in normal myocytes. Abnormal impulse propagation with consequent reentrant excitation can result in Ca^{2+}- alternans (Wagner, et al., 2015). Another mechanism of electrical irregularity is triggered activity which occurs because of abnormal ionic currents within the single cardiomyocytes and results in afterdepolarizations (Bers, 2002) (Antzelevitch, & Burashnikov, 2011).

Sudden Cardiac Death (SCD) is traditionally associated with the structural abnormalities of the heart and appears causing some damages to the heart but 10 -20% of those cases are happening without any damage to the cardiac muscles and any prior known causes. Action potential causes of SCD in the absence of known heart diseases are electrical disorders such as Catecholaminergic polymorphic ventricular tachycardia (CPVT), Brugada syndrome, long QT syndrome and short QT syndrome (Schimpf, Veltmann, Wolpert, & Borggrefe, 2010) (Viskin, & Belhassen, 1998). Almost 50% of the heart failure deaths are related to arrhythmia and rest are caused by insufficient muscle force (Mozaffarian, Anker, & Anand, 2007). Heart disorder causing HF is associated with aberrant Ca^{2+} transport across SL and SR (Bers, 2003), and the abnormal regulation of RyR2 (Wehrens, Lenhart, & Huang, 2003), (Marks, 2003). The ion channel composition of each cardiomyocyte contributes to the formation of action potential (AP). Calcium ions aid the generation and propagation of AP in cardiomyocytes and are

responsible for calcium-induced calcium release and mechanical contraction (EC-coupling) phenomena in the heart. The Ca^{2+} in the myocytes are the dynamic entities and their oscillations, as well as their intracellular and extracellular concentrations, are managed by influx and efflux of ions by ionic pumps, exchangers, receptors and channels. For a heart to function normally, intracellular Ca^{2+} homeostasis requires throughout the cardiomyocytes. Any disorder in this Ca^{2+} dynamics brings irregular electrical impulses in the heart and disturbance in the AP. The intracellular Ca^{2+} dysregulations can cause AP alternans and provide a perfunctory connection with ventricular tachycardia and ventricular fibrillation (Narayan, Bayer, & Trayanova, 2008).

Afterdepolarization

There are two types of afterdepolarization depending on their occurrence in the phases of AP - Early afterdepolarization and delayed afterdepolarization. Afterdepolarizations occur in some pathological conditions such as heart failure, ischemic heart disorders (Vereko, Veldkamp, Baartscheer, Schumacher, Klopping, Ginneken, & Ravesloot, 2001), or otherwise healthy individuals during exercises, or rapid heart rate (Stambler, Fenelon, Shephard, Clemo, & Guiraudon, 2003).

Early Afterdepolarization

Early Afterdepolarization (EAD) is a triggered activity in cardiac myocyte before action potential repolarizes completely (January, & Riddle, 1989). When depolarization occurs during phase 2 or phase 3 of an AP, it is termed as EAD as shown in figure 9 below (Weiss, Nivala, Garfinkel, & Qu, 2010) (Tse, 2016). EADs occur, in principle, when it is reduced outward current or increase inward current or both such that the net

inward current is higher which stops myocytes from repolarizing (Weiss, et al., 2010). The L-type current and (I_{LCC}) and Na^{+}-Ca^{2+} exchange current (I_{NCX}) are the major contributors of EADs. An increase in l-type activity or decrease in NCX activities can compromise the Ca^{2+} dynamics in the cardiomyocytes. EADs are favored by prolonged AP (Fozard, 1992).

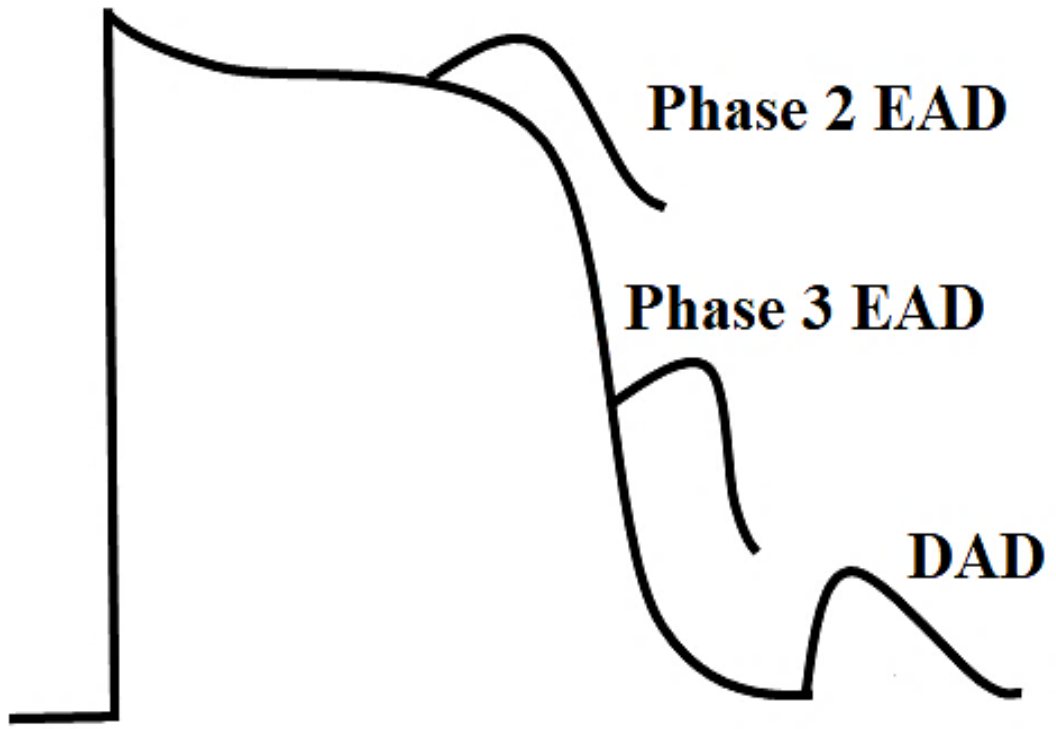

Figure 7: Early afterdepolarization (EAD) and delayed afterdepolarization are considered as precursors of Arrhythmia. The EAD occurs in phase 2 or phase 3 and the DAD occurs during phase 4 of the AP, adapted from (Tse, 2016).

Delayed Afterdepolarization

Delayed afterdepolarization (DAD) typically occurs during phase 4 of AP (Fig. 7) when the systolic phase is complete and is believed to be the precursor of arrhythmia (Fink, Noble, & Noble, 2011). DADs appear because of Ca^{2+}-overloading in intracellular organelles which can result from exposure to digitalis, catecholamines, hypokalemia, and hypercalcemia (Ferrier, Sounders, & Mendez, 1973)

Cardiac Alternans

Cardiac alternan is a condition when there is a periodic beat-to-beat oscillation in electrical activity and the strength of myocytes contraction at a constant heart rate. At the cellular level, alternans are defined as beat-to-beat alternations in contraction amplitude (mechanical alternans), AP duration (APD or electrical alternans), and Ca^{2+} transient amplitude (Ca^{2+} alternans). Many studies believe the cause of alternans is the instabilities of bi-directional coupling of membrane voltage, $V_{m,}$ and Ca^{2+} during AP (Blatter, & Edwards, 2014). Bi-directional coupling refers to the Vm depolarization during AP causes the elevation of Ca^{2+} which ensures the contraction of myocytes and at the same time, the change in Ca^{2+} also controls membrane voltage because of many membrane currents depend on Ca^{2+} (Shiferaw, Garfinkel, Weiss Qu, & Karma, 2005). In short, any disturbances in Ca^{2+} signaling result in alternans. There are two types of alternans:

Pulsus or mechanical alternans – A beat-to-beat oscillations in systolic dysfunction of left ventricular myocyte causes pulsus or mechanical alternans (Michaels, Browne, Varghese, & Chou, 2000) as shown in figure 8. It may cause due to cardiomyopathy, systematic hypertension, or in the patients after supraventricular tachycardia (Nguyen,

Cao, & Movahed, 2013). The alteration in cellular handling of calcium during heart contraction or abnormality of intracellular calcium cycling in the SR is behind the pulsus alternans and (Kotsanas, Holroyd, Young, & Gibbs, 1996) (Schmidt, Kadambi, Ball, Sato, Walsh, Kranias, et al., 2000). Schmidt et al. (2000) discovered the overexpression of CASQ2 could cause alternans when the heart beats rapidly. Kotsanas et al. (Kotsanas, Holroyd, Young, & Gibbs, 1996) reported that the alternation of the amplitude of Ca^{2+} transient produced pulsus alternans.

Electrical or T-wave alternans – A beat-to-beat alternations of the electrical activity of heart causes electrical or T-wave alternans. In this alternan, the beat-to-beat variation will

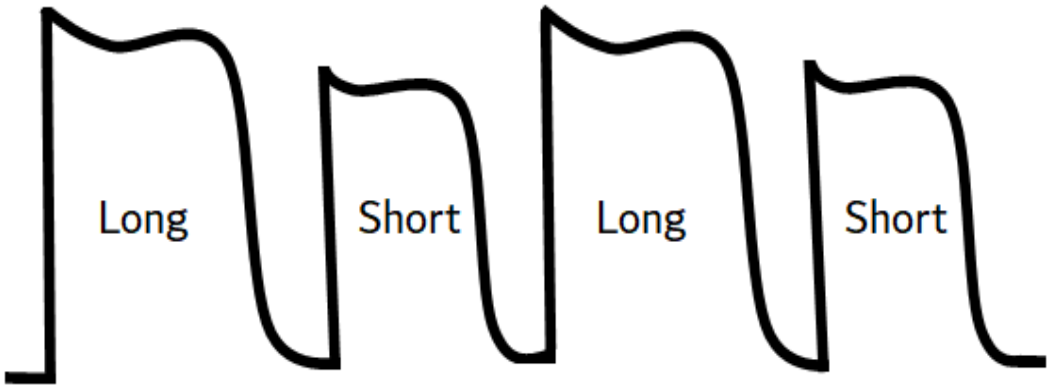

Figure 8: Schematic diagram of alternans in the duration (electrical or APD) and contraction amplitude (mechanical) of the action potential. The APs have alternation both in amplitude and duration.

be in direction, amplitude, and duration of any components in echocardiogram waveform. Both T-wave and pulsus alternans have been known as precursors of lethal arrhythmias for long (Qu, Liu, & Nirvala, 2016). The mechanisms responsible for alternans are incompletely understood (Eisner, 2006) (Qu, & Weiss, 2007) (Walker, & Rosenbaum, 2003). There is a constant debate that what is responsible for alternans, the change in membrane potential or SR Ca^{2+} (Weiss, Nivala, Garfinkel, & Qu, 2006) (Jordan, & Christini, 2007) (Shiferaw, et al., 2006).

The Ca^{2+} store and release organelles in SR play a major role in the relaxation and contraction of cardiac muscles. Most of the Ca^{2+} required for the EC-Coupling mechanism comes from SR. That calcium is made available to RyR by CASQ2.

Catecholaminergic Polymorphic Ventricular Tachycardia (CPVT)

In 1975, Reid *et al*. (Reid, 1975) discovered the first case of CPVT in a 6-year-old girl having no structural abnormality in her heart. In 2001, Priori et al. (Priori, Napolitano, Tiso, Memmi, Viganti, Bloise, et al., 2001) identified missense mutations in RyR2 gene are responsible for CPVT. They also claimed that the arrhythmia is due to Ca^{2+} overload and delayed afterdepolarizations (DADs). Later in the same year, Lahat, Pras, Olender, Avidan, Ben-Asher, E., Man, et al. (2001) reported that mutation in the CASQ2 gene also cause CPVT.

Catecholaminergic polymorphic ventricular tachycardia (CPVT) is an adrenergically-induced highly malignant, the familial arrhythmic disorder appears during stress or exercise (Liu, Rizzi, Boveri, & Priori, 2009) (Garcia-Elias, & Benito, 2018) (Laitinen, Brown, Piippo, Swan, Devaney, Brahmbhatt, & Donarum, 2001) (Gray,

Bagnall, Lam, Ingles, Couns, Turner, et al., 2016). Mutations in RyR2 or CASQ2 expressing genes can cause CPVT (Song, Alcalai, Arad, Wolf, Toka, Conner, et al., 2007) (Postma, Denjoy, & Kamblock, 2005) (Sumitomo, Harada, Nagashima, Yasuda, Nakamura, Aragaki, et al., 2003), (Venetucci, Denegri, Vapolitano, & Priori, 2012). The mutations bring alteration in the intracellular Ca^{2+} handling which results in this arrhythmogenic disorder (Fischer, Gottschalk, & Schuler, 2017). In CPVT, the patients experience severe cardiac dysfunction when an individual is going high emotional stress or performing exercises and they don't have any sign of structural abnormalities in their heart (Napolitano, Bloise, Memmi, & Priori, 2014) (Allouis, Probst, Jaafar, Scott, & Marec, 2005) (Lieve, Werf, & Wilde, 2016). One-third of the patient with CPVT mutation experience some symptoms by the age of 10 and the mortality rate reaches up to 30-50% by the age of 35 if condition went untreated (Kujala, Pavola, Lathi, Larsson, Pekkanen-Mattila, & Viitasalo, 2012) (Shashank, & Weindling, 2016) (Christopher, et al., 2007). The episodic syncope of CPVT results in (Priori, Napalitano, Memmi, Colombi, Drago, & Gasparini, et al., 2002). Spontaneous recovery of a patient with self-termination of arrhythmia or CPVT may further deteriorate into ventricular fibrillation (VF) and may cause sudden cardiac death (SCD).

CASQ2 is highly susceptible to CPVT genes (Garcia-Elias, & Benito, 2018) (Priori, Mazzanti, Blom, Borggrefe, Camm, & Elliott, et al., 2015). Scientists are reporting there are seven different gene mutations in Ca^{2+} receptors or Ca^{2+} buffer proteins cause CPVT, but mutations in CASQ2 are the second most event (Table 1) (Garcia-Elias, & Benito, 2018) (Landstrom, Dobrev, & Wehrens, 2017). In addition to

the CASQ2 gene, there are mutations in the ryanodine receptor (RyR2), triadin, calmodulin (CaM1, CaM2, CaM3) (Hajeung, et al., 2004), (Gomez-Hurtado, Boczek, Kryshtal, Johnson, Sun, Nitu, et al., 2016) and newly found TECLR genes (Devalla, Gélinas., Aburawi, Beqqali., Goyette, P., Freund, et al., 2016) may cause CPVT. TECRL gene encodes the trans-2, 3-enoyl-CoA reductase-like protein which participates in the synthesis of fatty acids. It is expressed in cardiac myocytes and localized in the SR. Except for CPVT causes by RyR2, the other CPVTs are extremely rare. When a CPVT caused by a mutation in the RYR2 gene, it is known CPVT1 and it is inherited in an

Table 1: Fraction of CPVT caused by different mutation types

Gene	Protein	Type	Prevalence (%)
RyR2	Ryanodine receptor	CPVT1	50 – 60
CASQ2	Calsequestrin 2	CPVT2	5
TRDN	Triadin	CPVT5	< 1
CALM1	Calmodulin	CPVT4	< 1
CALM2	Calmodulin	CPVT4	< 1
CALM3	Calmodulin	CPVT4	< 1
TECLR	Trans-2,3-enoyl-CoA-reductase-like	CPVT3	< 1

autosomal dominant manner while CPVT caused by a mutation in the CASQ2 gene called CPVT2 which is inherited in an autosomal recessive manner (Napolitano, et al., 2014) (Faggioni, et al., 2012). The gain-of-function RyR2 mutation is an account for more than 50% of CPVT1 (Kawata, et al., 2016). RyR2 has a major role in the pathogenesis of heart failure and lethal arrhythmia with a reduced affinity of FKBP12.6 to the RyR2 in the closed state by creating a defective inter-domain interaction between N-terminal and central domain. Besides its mutations in RyR2, the mutations in accessory proteins such as FKBP12.6, CASQ2, and calmodulin destabilize the modulation of RyR2 gating which results in heart failure and lethal arrhythmia (Yano, Yamamoto, Kobayashi, & Matsuzaki, 2009).

Review of Computational Models of Cardiac Myocytes

A computational model is a mathematical system that carries out an understanding of a complex system by running simulations on a computer. The purpose of developing a model is to translate a set of hypotheses into predictable observation events of any natural system (Potse, 2012). After the success of the Hodgkin-Huxley (Hodgkin, Huxley, & Kartz, 1952) model for the ionic mechanism, many cardiac related models were developed. Reutar and Beeler (1977) constructed the first ventricular myocyte model to simulate action potential by using ionic currents measured in voltage-clamp experiments. This model included the simulation of inward Na^+, Ca^{2+} currents, and outward K^+ currents. In early year, Nobel and Francesco (1985) developed a Purkinje fiber model introducing activities of Na^+- K^+ pump and Na^+-Ca^{2+} exchanger in the model. Hilgemann and Noble (1987) developed a rabbit atrial cell model and they incorporated

the interaction of Ca^{2+} dynamics, intracellular and extracellular calcium transients, Na^{+}-Ca^{2+} exchanger, and SR in the mammalian heart. In the year 1991, Luo and Rudy (1991) published Luo-Rudy I model for ventricular myocyte of guinea pig. The ionic formulations in the Luo-Rudy model were based upon the Hodgkin-Huxley model. This model formulates different ionic currents related to Na^{+}, $K^{+,}$ and Ca^{2+} ions based on experimental data though it lacks an account on Ca^{2+} cycling, Na^{+}-K^{+} pump, and Na^{+}-Ca^{2+} exchanger. In 1994, Luo and Rudy (Luo & Rudy, 1994a) (Luo, & Rudy, 1994b) made major improvements in the first model and published the Luo-Rudy II model. After few years, Jafri, Rice, and Winslow (1998) and Winslow, Rice, Jafri, & O'Rourke (1999) included whole-cell Ca^{2+} dynamics (Ca^{2+} homeostasis) in the ventricular myocyte models of guinea pig (J-F-W model) and canine (W-R-J model) respectively. The J-R-W is the first model to incorporate Markovian formulation for LCC and they also updated the Luo-Rudy model with experimentally verified features such as mode switching behavior in L-type Ca^{2+} channel (Imredy, & Yue, 1994), SR release mechanism was replaced by RyR adaptation experiment (Gyorke, & Fill, 1993) with the modification in Keizer-Levine RyR model (Keizer, & Levine, 1996), a restricted subspace was added in between junctional SR and t-tubule and they also scaled ionic magnitude of some ionic currents. The W-R-J model was also a heart failure model which predicted an increase inward (L-type Ca^{2+}) current is the mechanism of longer AP duration (APD) during heart failure.

The publication of the Luo-Rudy II model began the new era of computation modeling (Winslow, Cortassa, O'Rourke, Hashambhoy, Rice, & Greenstein, 2011) and this model did an outstanding job in the modeling of ionic currents. The Jafri-Rice-

Winslow model blended whole-cell Ca^{2+} homeostasis more realistically in the model (Shannon, Wang, Puglisi, Weber, & Bers, 2004). These models provide an important insight into Ca^{2+} dynamics, understanding of cardiac arrhythmia but still, they possess some limitations such as they used the same compartment (common pool) for the discharge of triggered Ca^{2+} and released Ca^{2+}. The common pool models also lacked a physiologically realistic description of RyRs and were unable to predict positive feedback mechanism caused by the regenerative nature of CICR (Williams, Smith, Sobie, & Jafri, 2010). The common pool method was also unable to reproduce graded (an elevation of Ca^{2+} with depolarization) SR Ca^{2+} release and those models also supported strong VDI and weak CDI opposite to experimental findings and this also destabilized AP plateau (Greenstein, & Winslow, 2011). This could be the reason common pool models easily produced alternans and had difficulties to identify to the mechanism causing alternans (Diaz, O'Neil, & Eisner, 2004) (Chudin, Goldhaber, Garfinkel, Weiss, & Kogan, 1999).

To address SR graded Ca^{2+} release, a group of researchers (Stern, Song, Cheng, Sham, Yang, Boheler, et al., 1999) developed a local control (recruitment of CRUs from where Ca^{2+} release occurs) stochastic model based on SR Ca^{2+} release is achieved by graded recruitment of individual, autonomous and stochastic release events. Rice, Jafri and Winslow (1999) also developed a stochastic (with 500 CRUs) model of SR Ca^{2+} release along with RyR2 adaptation which played no major role in the RyR2 termination. A model developed by Shirfew, Watanabe, Garfinkel, Weiss, Karma (2003) also develop a model that produced SR graded release, Ca^{2+} sparks as a sum of local release, and model was also able to produce alternans in rapid pacing. Adaptive behavior wasn’t the

part of the gating mechanism, time decay of Ca^{2+}, and SR depletion causes the spark termination. Shannon *et al.* (Shannon., Wang, Puglisi, Weber, & Bers, 2004) developed a model using a bulk JSR with graded SR Ca^{2+} release. In their model, they combined luminal and junctional Ca^{2+} combinedly initiate and terminate Ca^{2+} release. The role of RyR adaptation and inactivation in RyR gating is debatable. Fill et al. (Fill, Villalba-Galea, Zahradnik, Escobar, & Gyorke, 2000) believed high Ca^{2+} inactivation and low Ca^{2+} adaptation are the two different gating mechanisms in RyR. Sobie and him team (Sobie, Dilly, Cruz, Lederer, & Jafri, 2002) formed a "sticky" model without RyR adaptation and suggested Ca^{2+} sparks arise during the release from the sticky RyR2 cluster. For Ca^{2+} spark termination, local SR Ca^{2+} depletion (>90%) is required but experimental results found as much as 40% free JSR Ca^{2+} when sparks terminate (Hoang-Trong, et al., 2015). This model didn't deny RyR2 adaptation in the gating mechanism but found no contribution to the spark termination. Greenstein and Winslow (2011) developed a local control stochastic model with 12,500 CRUs and tried to improve in EC-coupling, SR graded release and variable gain. Though it's an advancement in the existing models, it was unable to imitate proper Ca^{2+} spark feature and there was no explanation of SR Ca^{2+} leak. Williams et al. (2011) applied 20,000 CRUs in their local control stochastic model of Ca^{2+} dynamics. This model accounted for SR Ca^{2+} leak, Ca^{2+} sparks, stochastic activation, and termination of RyR channels. In this model, RyR2 opening depends both cytosolic and luminal [Ca^{2+}] but RyR adaptation had no role in gating mechanisms.

Priebe and Beuckelmann (1998) developed the first ionic model of heart failure and described EADs, DADs, and alternans are the underlying causes in ventricular arrhythmia. EADs and alternans happened because of a reduction in K^+ (fast delayed rectifier, $I_{Kr,}$ and slow delayed rectifier current, I_{Ks}) while an increased I_{ncx} found responsible for DADs from spontaneous SR Ca^{2+} release. A model formed by Puglisi and Bers (2001) combines reduced inward rectifying current (I_{k1}) and raised I_{ncx} to produce alternans. The views that the downward regulation of repolarizing currents (K^+) play a major role in triggered arrhythmia rather than an increase in depolarizing Ca^{2+} currents (I_{LCC}, I_{ncx}) didn't perceive well. Experimentally, disturbances in intracellular Ca^{2+} dynamics are found responsible for heart failure (Winslow, et al., 1999), (Chudin, et al., 1999) (Mahajan, Shiferaw, Sato, Baher, Oles, Xie, et al., 2008) (Gomez, Cardona, & Trenor, 2015) (Edwards, & Blatter, 2014). Shannon et al. (Shannon, Wang, & Bers, 2005) developed a model of Ca^{2+} homeostasis that triggers DADs and arrhythmia by increasing Ca^{2+} affinity of RyR2.

There are limited numbers of the model developed to study mutations in SR Ca^{2+} handling proteins but the trend is growing. Many models representing RyR2 mutations the gene expressing RyR2 increases its open probability and spontaneous Ca^{2+} release occurs during the diastolic phase which causes DADs and arrhythmia (Iyer, Hajjar, & Armoundas, 2007) (Chen, Aistrup, Wasserstrom, & Shiferaw, 2011). Similarly, a mutation in the genes to express CASQ2 impairs regulation of RyR2 by CASQ2 that causes reduced Ca^{2+} transients and development of DADs (Iyer, et al., 2007). Faber and Rudy (Faber, & Rudy, 2007) reported a mutation $CASQ2^{D307H}$ protein caused store-

overload-induced Ca^{2+} release (SOICR) and DADs were produced due to excess free SR Ca^{2+}. The role of CASQ2 as RyR2 regulator is in discussion and only certain is CASQ2 acts as buffer protein (Kubalova, Gyorke, Terentyeva, Viatchenko-Karpinski, Terentyv, Williams, Gyroke, 2004) and at higher concentration, there is CASQ2-independent luminal Ca^{2+} mechanism (Qin, et al., 2009). Zhao *et al*. (Zhao, Valdivia, Gurrola, Powers, Willis, Moss, et al., 2015) generated an animal model with RyR2-A4860G mutation to have hypo-active RyR2s which trigger EADs and cause arrhythmia. Xiao *et al.* (2016) tested eight different RyR2 mutations in HEK293 cells and found RyR2 mutations enhanced the Ca^{2+}-dependent activation of RyR2 binding, increased cytosolic Ca^{2+}-induced fractional Ca^{2+} release, and reduced the activation and termination thresholds for spontaneous Ca^{2+} release Danielsen et al. (Danielson, Manotheepan, Sadredini, Laren, Edwards, Vincent, et al., 2018) reported from clinical, experimental and computational studies that increased heart rate and β-AR stimulation combine to increase the risk of arrhythmias but increase heart rate alone was not enough to induce arrhythmias in CPVT1 mutant RyR2-R2474S.

Research Objectives

The main aim of this research is to study Ca^{2+} dynamics to understand the mechanisms of how catecholaminergic polymorphic ventricular tachycardia (CPVT) arises in higher mammals with longer action potential during exercises or emotional distress having mutations in Ca^{2+} handling proteins. Based on literature reviews, the underlying mechanisms of CPVT in both mutations are EADs or/and DADs, or/and alternans. Mutations in CASQ2 is an autosomal recessive type and this is also known as

loss of function mutation. Mutation in RyR2 is an autosomal dominant type and it is also known as a gain of function mutation (Lodish, et al., 2000). The main function of CASQ2 is Ca^{2+} buffering (Kubalova, et al., 2004)) and mutation causes a loss in buffering capacity which means a rise in free luminal Ca^{2+}. It increases RyR2 P_O and much larger SR Ca^{2+} releases to the subspace in each beat. The SR Ca^{2+} overload during adrenergic stimulation will be assessed and whether diastolic SR enough to trigger DADs will be investigated. Similarly, a mutation in RyR2 increases RyR2 PO, and SR Ca^{2+} overload might not exist in this condition too. Using our model, we explore how such mutations lead to arrhythmia under conditions of beta-adrenergic stimulation and what is the underlying mechanism behind them. Scientists have proposed four different mechanisms to explain the causes of CPVT1 with mutant myocyte. They are GOF, LOF, SOICR, and FKBP12.6 destabilization. There are more disagreements than agreements in all three mechanisms except GOF. We are shedding light on those mechanisms to find out the best hypothesis to support and explain arrhythmogenesis caused by the mutations in the RyR2 expressing proteins.

Intracellular Ca^{2+} transients are measuring to calculate the contractile force of a myocyte. Since Ca^{2+} sparks are the building blocks of those Ca^{2+} transients. Another objective of this research is to understand the mechanisms by which interval-force relations are established in the heart. The Guinea pig has longer action potential and a stable plateau, it gives us a better understanding of Ca^{2+} dynamics in the cardiac myocytes of larger mammals such as humans.

The triggered cluster opening of RyR2 from the Ca^{2+} sparks causes to release of Ca^{2+} to the cytoplasm. The frequency and amplitudes of each of those sparks depend upon the transient opening of RyR2 clusters and they vary the pace to pace. The recording of the frequency of Ca^{2+} sparks, average spark duration, and computing their average amplitude in each beat provide the information on Ca^{2+} transients in the subspace, the availability of Ca^{2+} in the SR, and the physiological state of the RyR2. The contractility of cardiac myocyte is determined by the size of the Ca^{2+} transients and those Ca^{2+} transients depend upon the frequency and amplitudes of Ca^{2+} sparks. However, the opening probability of RyR2 dictates all these outcomes and it depends upon the sensitivity and luminal dependency of RyR2. The mutation in RyR2 and CASQ2 has a role in the opening probability of RyR2 and which leads to CPVT1 and CPVT2, respectively. The understanding of these Ca^{2+} sparks is required to find out the detailed in force generated by Ca^{2+} transients and the effect of mutations in the Ca^{2+} handling proteins in the opening probability of the RyR2.

There is the incremental release of Ca^{2+} from SR in response to an incremental step change in cytosolic Ca^{2+} but that graded release will be impacted by lower concentrations of NSR Ca^{2+} and adaptive nature of RyR2. Many models don't include adaptation in the gating mechanism and we believe for a complete understanding of RyR2 gating, RyR2 adaptation must be part of it. Our model includes a novel three-state model adding an adaptive state to the closed and open states.

References

Allen, D. G. & Blinks, J. R. (1978). Calcium transients in aequorin-injected frog cardiac muscle. *Nature, 273*, 509-513.

Allouis, M. V., Probst, V., Jaafar, P., Scott, J.J., & Marec, L. (2005). Unusual clinical presentation in a family with catecholaminergic polymorphic ventricular tachycardia due to a G14876A ryanodine receptor gene mutation. *American Journal of Cardiology, 95*(5), 700-702.

Antzelevitch, C. & Burashnikov. A. (2011). Overview of basic mechanisms of cardiac arrhythmia. *Cardiac Electrophysiology Clinics, 3*(1), 23-45.

Beard, N. A., Leaver, D., & Dulhunty, A. F (2004). Calsequestrin and the calcium release channel of skeletal and cardiac muscle. *Progress in Biophysics & Molecular Biology, 85*(1), 33-69.

Beard, N. A., Casarotto, M. G., Wei, L., Varsanyi, M., Laver, D. R., & Dulhunty, A. F. (2005). Regulation of ryanodine receptors by calsequestrin: effect of high luminal Ca2+ and phosphorylation. *Biophysical Journal, 88*(5), 3444-3454.

Beard, N. A., Beard, N. A., Wei, L., & Dilhunty, A. F. (2009). Ca^{2+} signaling in striated muscle: the elusive roles for triadin, junctin, and calsequestrin. *European Biophysical Journal, 39*, 27-36.

Berne, R. M. & Levy, M. N. (1997). *Cardiovascular physiology.* St. Louis: Mosby.

Bers, D. M., Eisner, D. A., & Valdivia, H.H. (2003). Sarcoplasmic reticulum Ca2+ and heart failure: roles of diastolic leak and Ca2+ transport. *Circulation Research, 93*, 487-490.

Bers, D. M. (2001). *Excitation-contraction coupling and cardiac contractile force.* Dordrecht, Netherlands: Kluwer Academic.

Bers, D. M. (2002). Cardiac excitation-contraction coupling. *Nature*, 198-205.

Blatter, E. J. & Blatter, L. A. (2014). Calcium alternans and intracellular calcium cycling. *Clinical and Experimental Pharmacology and Physiology, 41*(7), 524 - 532.

Blayney, L. M. & Lai, F. A. (2009). Ryanodine receptor-mediated arrhythmias and sudden cardiac death. *Pharmacology & Therapeutics, 123*, 151 - 177.

Blinks, J. R. Wier, W. G., Hess, P., & Prendergast, F.G. (1982). Measurement of Ca^{2+} concentrations in living cells. *Progress in Biophysics and Molecular Biology, 40*, 1-114.

Bohm, M. K., La Rosee, K., Schmidt, U., Schulz, R., Schwinger, R. H., & Erdmann, E. (1992). Force-frequency relation and inotropic stimulation in the non-failing and failing human myocardium: Implications for the medical treatment of heart failure. *Journal of Clinical Investigation, 70*, 471-475.

Briggs, K. L. (1994). A digital approach to cardiac cycle. *IEEE Engineering and Medical Biology, 13*, 454-456.

Chen, W., Aistrup, G., Wasserstrom, J. A., & Shiferaw, Y. (2011). A mathematical model of spontaneous calcium release in cardiac myocytes. *American Journal of Physiology. Heart and Circulatory Physiology, 300*(5), H1794-1805.

Cheng, H. & Lederer, W. J. (2008). Calcium sparks. *Physiological Reviews, 88*(4), 1491-1545.

Cheng, H., W. Lederer, W. J., & Cannell, M. B. (1993). Calcium sparks: Elementary events underlying excitation-contraction coupling in heart muscle. *Science, 262*(5153), 740-744.

Christopher, H. G., Jundi, H., Thomas, N. L., Fry, D. L., & Lai, F. A. (2007). Ryanodine receptors and ventricular arrhythmias: Emerging trends in mutations, mechanisms and therapies. *Journal of Molecular and Cellular Cardiology, 42*, 34-50.

Chudin, E., Goldhaber, J., Garfinkel, A., Weiss, J., & Kogan, B. (1999). Intracellular Ca dynamics and the stability of ventricular tachycardia. *Biophysical Journal, 77*, 2930-2941.

Danielson, T. K., Manotheepan, R., Sadredini, M., Laren, I. S., Edwards, A.G., Vincent, K.P., et al. (2018). Arrhythmia initiation in catecholaminergic polymorphic ventricular tachycardia type 1 depends on both heart rate and sympathetic stimulation. *PLOS ONE, 13*(11), 1-21.

Davies, C., Davia, K., Bennett, J.G., Pepper J. R., P. A. Poole-Wilson, P. A., et al. (1995). Reduced contraction and altered frequency response of isolated ventricular myocyte from patients with heart failure. *Circulation, 92*(9), 2540-2549.

de Lucia, C., Femminella, G. D., Gambino, G., Pagano, G., Alloca, E., & Rengo, C. (2014). Adrenal adrenoceptors in heart failure. *Frontier Physiology, 5,* 246.

Deo, M., Weinberg, S. H., & Boyle, P. M. (2017). Calcium dynamics and cardiac arrhythmia. *Clinical Medicine Insights: Cardiology, 11*, 1177-1179.

Devalla, H. D., Gélinas, R., Aburawi, E. H., Beqqali, A., Goyette, P., Freund, C., et al. (2016). TECRL, a new life-threatening inherited arrhythmia gene associated with overlapping clinical features . *EMBO Mol Med, 8*(12), 1390-1408.

Diaz, M. E., O'Neil, S. C., & Eisner, D. A. (2004). Sarcoplasmic reticulum calcium content fluctuation is the key to cardiac alternans. *Circulation Research, 94*(5), 650-656.

Dulhunty, A. F. (2006). Excitation-contraction coupling from 1950s into the new millenium. *Clinical Experimental Pharmacology, 33,* 763-772.

Edwards, J. N. & Blatter, L. A. (2014). Cardiac alternans and intracellular calcium cycling. *Clinical and Experimental Pharmacological and Physiology, 41*(7), 524-532.

Eisner, D. (2014). Calcium in the heart: from physiology to disease. *Experimental Physiology, 10,* 1273-1282.

Eisner, D. A. (2006). Alternans of intracellular calcium: mechanism and significance. *Heart Rythm, 3*(5), 743-748.

Endoh, M. (2004). Force frequency relationship in intact mammalian ventricular myocardium: physiological and paraphysiological relevance. *European Journal of Pharmacology, 500,* 73-86.

Faber, G. M. & Y. Rudy. (2007). Calsequestrin mutation and catecholaminergic polymorphic ventricular tachycardia: A simulation study of cellular mechanism. *Cardiovascular Research, 75*(1), 79-88.

Fabiato A. (1975). Contractions induced by a calcium-triggered release of calcium from the sarcoplasmic reticulum of single skinned cardiac cells. *Journal of Physiology, 249*(3), 469-495.

Faggioni, M. D., Krystal, D. O., & Knollmann, B. C. (2012). Calsequestrin mutations and catecholaminergic polymorphic ventricular tachycardia. *Pediatric Cardiology*, 959-967.

Ferrier, G. R., Sounders, J. H., & C. Mendez, C. (1973). A cellular mechanism for the generation of ventricular arrhythmias by acetylstrophanthidin. *Circulation Research, 32,* 600-609.

Fill, M., Villalba-Galea, C. A., Zahradnik, I., Escobar, A. L., & Gyorke, S. (2000). Ryanodine receptor adaptation. *Journal of General Physiology, 116*(6), 873-882.

Fink, M. P., Noble, P. J., & Noble, D. (2011). Ca2+- induced delayed afterdepolarizations are triggered by dyadic subspace Ca2+ affirming that increasing SERCA reduces aftercontractions. *American Journal of Heart Circulatory Physiology, 301*(3), H921-H935.

Fischer, E. A., Gottschalk, A., & Schuler, C. (2017). An optogenetic arrhythmia model to study catecholaminergic polymorphic ventricular tachycardia mutations. *Scientific Reports, 7*(1), 17514.

Fozard, H. A. (1992). Afterdepolarization and triggered activity. *Basic Research Cardiology, 87*(2), 105-113.

Fozzard, H. A. (1977). Heart: Excitation-contraction coupling. *Annual Review of Physiology, 39,* 201-220.

Fye, W. B. (1984). Sydney Ringer, calcium and cardiac function. *Circulation,* 849- 853.

Garcia-Elias, A. & Benito, B. (2018). Ion channel disorders and sudden cardiac death. *International Journal of Molecular Science, 19*(3), 692.

Gaztanaga, L., Marchlinski, F. E., & Betensky, B. P. (2012). Mechanisms of cardiac arrhythmia. *Revista Espanola De Cardiologia, 65*(2), 174-185.

Godier-Furnémont, A. F., Tibucry, M., Wagner, E., Dewenter, M., Lammle, S., El-Armouche, A., Lehnart, S. E., et al. (2015). Physiologic force-frequency in engineered heart muscle by electromechanical stimulation. *Biomaterials, 60,* 82-91.

Gomez, J. F., Cardona, K., & Trenor, B. (2015). Lesson learned from multi-scale modeling of the failing heart. *Journal of Molecular and Cellular Cardiology, 89,* 146-159.

Gomez-Hurtado, Boczek, N. J., Kryshtal, D. O., Johnson, C. N., Sun, J., Nitu, F. R., et al. (2016). Novel CPVT-Associated Calmodulin Mutation in CALM3 (CALM3-

A103V) Activates Arrhythmogenic. *Circulation: Arrhythmia and Electrophysiology, 9*(8), 1-22.

Gonano, L. A. & Jones, P. P. (2017). FK506-binding proteins and 12.6 (FKBPs) as regulators of cardiac ryanodine receptors: Insights from new functional and structural knowledge. *Channels (Austin), 11*(5), 415-425.

Gong, G., Liu, X. & Wang, W. (2014). Regulation of metabolism in individual mitochondria during excitation-contraction coupling. *Journal of Molecular Cell and cardiology, 0*, 235-246.

Gray, B., Bagnall, R. D., Lam, L., Ingles, J., Couns, G. D. G., Turner, C. et al. (2016). A novel heterozygous mutation in cardiac calsequestrin causes autosomal dominant catecholaminergic polymorphic ventricular tachycardia. *Heart Rhythm, 13*(8), 1652-1660.

Greenstein, J. L. & Winslow, R. L. (2011). Integrative systems models of cardiac excitation-contraction coupling. *Circulation Research, 108*(1), 70-84.

Guatimosim, S. C., Guatimosim, C. & Song, L. -S. (2011). Imaging calcium sparks in cardiac myocytes. *Methods in Molecular Biology, 689*, 205-214.

Györke, I., Hester, N., Jones, L. R., Györke, L. & Gyorke, S. (2004). The Role of calsequestrin, triadin, and junctin in conferring cardiac ryanodine receptor responsiveness to luminal calcium. *Biophysical Journal, 86*(4), 2121-2128.

Gyorke, S. & Fill, M. (1993). Ryanodine receptor adaptational mechanism of Ca^{2+} -induced Ca2+ release in the heart. *Science, 260*, 807-809.

Hajeung, P. Y., Park, Y., Kim, E., Youn, B., Dunker, A. K. & Kang, C. (2004). Comparing skeletal and cardiac calsequestrin structures and their calcium-binding. *Journal of Biological Chemistry, 279*(17), 18026-18033.

Hardman, S. M. (1994). Clinical implications of the interval-force relationship of the heart. *Postgraduate Medical Journal, 70*, 553-557.

Hasenfus, G., Holubarsch, C., Hermann, H. P., Astheimer, K., Pieske, B. & Just, H. (1994). Influence of force-frequency relationship on hemodynamics and left ventricular function in patients with non-failing hearts and in patients with dilated cardiomyopathy. *European Heart Journal, 15*, 164-170.

Heijman, J., Voigt, N., Nattel, S. & Dobrev, D. (2014). Cellular and molecular electrophysiology of atrial fibrillation initiation, maintenance and progression. *Circulation Research, 114*(9), 1483-1499.

Hilgemann, D. & Noble, D. (1987). Excitation-contraction coupling and extracellular calcium transients in rabbit atrium: reconstruction of basic cellular mechanism. *Proceedings of Royal Society of London B Biological Science, 230*(1259), 163-205.

Hoang-Trong, T. M., Ullah, A. & Jafri, M.S. (2015). Calcium sparks in the heart: Dynamics and regulation. *Research and Reports in Biology, 6*, 203-214.

Hodgkin, A. L., Huxley, F. A. & Kartz, B. (1952). Measurement of current-voltage relations in the membrane of the giant axon of Loligo. *Journal of physiology, 117*, 424-48.

Imredy, J. P. & Yue, D. T. (1994). Mechanism of Ca2+ -sensitive inactivation of l-type Ca^{2+} channels. *Neuron, 12*, 1301-13018.

Iyer, V. R., Hajjar, R. J. & Armoundas, A. A. (2007). Mechanisms of abnormal calcium homeostasis in mutations responsible for catecholaminergic polymorphic ventricular tachycardia. *Circulation Research, 100*, e22-e31.

Izu, L. T., Wier, W. G. & Blake, W. (1998). Theoretical analysis of the Ca2+ spark amplitude distribution. *Biophysical Journal, 75*(3), 1144-1162.

Jafri, M. S., Rice, J. J. & Winslow, R. L. (1998). Cardiac Ca2+ Dynamics: The roles of ryanodine receptor adaptation and sarcoplasmic reticulum load. *Biophysical Journal*, 1149 - 1168.

January, C. T., & Riddle, J. M. (1989). Early afterdepolarization: Mechanism of induction and block, a role for L-type Ca^{2+} current. *Circulation Research, 64*(5), 977- 990.

Jayaram, S., Gandhi, U., Sangareddi, V., Mangalanathan, U. & Shanmugam, R. M. (2016). Unmasking of atrial repolarization waves using simple limb lead system. *The Anatolian Journal of Cardiology, 15*(8), 605-610.

Jordan, P. N., & Christini, D. J. (2007). Characterizing the contribution of voltage- and calcium dependant coupling to action potential stability: implications for repolarization alternans. *American Journal of Heart Circulatory Physiology, 293*, H2109-2118.

Joulin, O., Marechaux, S., Hassoun, S., Montaigne, D., Lancel, S. & Neviere, R. (2009). Cardiac force-frequency relationship and frequency-dependent acceleration of relaxation are impaired in LPS-treated rats. *Critical care, 13*(1), R14.

Kadambi, V. J. & Kranais, E. G. (1997). Phospholamban: a protein coming of age. *Biochemical Biophysics Research Communication, 239*, 1-5.

Katz, A. M. (2000). *Heart Failure pathophysiology, molecular biology and clinical management.* Philadelphia, USA: Lippcott Williams and Wilkins.

Kawata H., Ohno, S., Aiba, T., Sakaguchi, H., Miyazaki, A. & Sumitomo, N., et al. (2016). Catecholaminergic polymorphic ventricular tachycardia (CPVT) associated with ryanodine receptor (RyR2) gene mutations - long-term prognosis after initiation of medical treatment. *Circulation Journal, 80*, 1907-1915.

Keizer, J. & Levine, L. (1996). Ryanodine receptor adaptation and Ca2+-induced Ca2+ release-dependant Ca2+ oscillations. *Biophysical Journal, 71*(6), 3477-3487.

Kim, E., Youn, B., Kemper, L., Campbell, C., Milting, H. & Varsanyi, M., et al. (2007). Characterization of human cardiac calsequestrin and its deleterious mutants. *273*(2), 1047-1057.

Koch-Weser & Blinks, J. R. (1963). The influence of the interval between beats on myocardial contractility. *Pharmacological Review, 15*, 601-652.

Kotsanas, G., Holroyd, S. M., Young, R. & Gibbs, C. L. (1996). Mechanism contributing to pulsus alternans in pressure-overload cardiac hypertrophy. *American Journal of Physiology, 271*(6), 2490-2500.

Kubalova, Z., Gyroke, I., Terentyeva, R., Viatchenko-Karpinski, S., Terentyv, D., Williams, S. C., Gyroke, S. (2004). Modulation of cytosolic and intra-sarcoplasmic reticulum calcium waves by calsequestrin in rat cardiac myocytes. *The Journal of Physiology, 561*(2), 515-524.

Kujala, K., Pavola, J., Lathi, A., Larsson, K., Pekkanen-Mattila, M. & Viitasalo, M. (2012). Cell Model of Catecholaminergic polymorphic ventricular tachycardia reveals early and delayed afterdepolarizations. *PLOS ONE*, 1-10.

Kurihara, S. & Allen, D. G. (1982). Intracellular Ca2+ transients and relaxation in mammalian cardiac muscle. *Japan Circulation Journal, 46*, 39-43.

Kushnir, A. & Marks, A.R. (2010). The ryanodine receptor in cardiac physiology and disease. *Advanced in Pharmacology, 59*, 1-30.

Lahat, H., Pras, E., Olender, T., Avidan, E., Ben-Asher, E., Man, O. et al. (2001). A Missense Mutation in a Highly Conserved Region of CASQ2 Is Associated with Autosomal. *American Journal of Human Genetics, 69*(6), 1378-1384.

Laitinen, J., Brown, K. M., Piippo, K., Swan, Devaney, J. M., Brahmbhatt, B., & Donarum, E. A. (2001). Mutations of the cardiac ryanodine receptor (RyR2) gene in familial polymorphic ventricular tachycardia. *Circulation, 103*(4), 485-490.

Landstrom, A. P., Dobrev, D. & Wehrens, X. H. T. (2017). Calcium signaling and cardiac arrhythmias. *Circulation Research, 120*(12), 1969-1993.

Lanner, J. T., Georgiou, D. K., Joshi, A. D., & Hamilton. S. L. (2010). Ryanodine receptors: structure, expression, molecular details, and function in calcium release. *Cold Spring Harbor Perspectives in Biology, 2*(11), 1 - 27.

Laver, D. R. & Honen, B. N. (2008). Luminal Mg^{2+}, a key factor controlling RyR2 mediated Ca^{2+} release: cytoplasmic and luminal regulation modeled in a tetrameric channel. *Journal of General Physiology, 132*, 429-446.

Lieve, K. V., Werf, C. V. D. & Wilde, A. A. (2016). Catecholaminergic polymorphic ventricular tachycardia. *Circulation Journal, 80*, 1285-1291.

Liu, N., Rizzi, N., Boveri, L. & Priori. S. G. (2009). Catecholamine polymorphic ventricular tachycardia. *Journal of molecular and cellular cardiology, 46*(2), 149-159.

Lodish, H., Berk, A., Zipursky, S. L., Matsudaira, P., Baltimore, D. & Darnell, J. (2000). *Molecular cell biology* (4th ed.). New York: W. H. Freeman.

Lompre, A. M., Anger, M. & Levitsky, D. (1994). Sarco(endo)plasmic reticulum calcium pumps in the cardiovascular system: function and gene expression. *Journal of Molecular and Cellular Cardiology, 26*, 1109-1121.

Lopez-Lopez, J. R., Shacklock, P. S., Balke, C. W. & Wier, W. G. (1995). Local calcium transients triggered by single L-type calcium channel currents in cardiac cells. *Science, 268*, 1042-1045.

Lukyanenko, V. & Gyorke, S. (2004). Ca2+ sparks and Ca2+ waves in saponin-permeable rat ventricular myocytes. *The journal of Physiology, 521*(3), 575-585.

Luo, C. H. & Rudy, Y. (1994a). A dynamic model of the ventricular cardiac action potential. I. Simulations of ionic current and concentration changes. *Circulation Research, 74*(6), 1070-1096.

Luo, C. H. & Rudy, Y. (1994b). A dynamic model of the cardiac ventricular action potential. II. Afterdepolarizations, triggered activity, and potentiation. *Circulation Research, 74*(6), 1097-1113.

Ma, J. S., Hayek, S. M. & Bhat, M. B. (2004). Membrane topology and membrane retention of the ryanodine receptor calcium release channel. *Cell Biochemistry and Biophysics, 40*(2), 207-204.

Mackrill, J. J. (2010). Ryanodine receptor calcium channels and their partners as drug targets,. *Biochemical Pharmacology, 79*, 1535-1543.

Mahajan, A., Shiferaw, Y., Sato, D., Baher, A., Oles, R., Xie, L.-H., et al. (2008). A rabbit ventricular action potential model replicating cardiac dynamics at rapid heart rates. *Biophysical Journal, 94*, 392-410.

Marks, A. R. (2003). A guide for perplexed: towards an understanding of the molecular basis of heart failure. *Circulation, 107*, 1456-1459.

Matteo, E. & Nargeot, J. (2008). Genesis and regulation of the heart automacity. *Physiological Reviews, 88*, 919-982.

McGrath, K. F., Yuki, A., Manaka, Y., Tamaki, H., Saito, K. & Takekura, H. (2009). Morphological characteristics of calcium release units in animals with metabolic and circulatory disorders. *Journal of Muscle Restriction and Cell Motility, 30*, 225-231.

Medeiros-Domingo, Bhuiyan, Z. A., Tester, D. J., Hofman, N., Bikker, H., Tintelen, J. et al. (2009). Comprehensive open reading frame mutational analysis of the RyR2-encoded ryanodine receptor/calcium channel in patients diagnosed previously with either catecholaminergic polymorphic ventricular tachycardia or genotype negative, exercise-induced long QT s. *Journal of American College of Cardiology, 54*(22), 2065-2074.

Meissner, G. (2017). The structural basis of ryanodine receptor ion channel function. *Journal of general physiology, 149*(12), 1065-1089.

Michaels, A. D., Browne, A. E., Varghese, P. & Chou, T. M. (2000). Intracoronary measurement of pulsus alternans. *Catheterization Cardiovascular Interventions, 51*(3), 335-338.

Mohler, P. J. & Wehrens, X. H. T. (2007). Mechanisms of human arrhythmia syndromes: Abnormal cardiac macromolecular interactions. *Physiology, 22*(5), 342-350.

Mozaffarian, D. S., Anker, S. D. & Anand, I. (2007). Prediction of mode of death in heart failure: the Seattle heart failure model. *Circulation Arrhythmia and Electrophysiology, 116*, 392-398.

Murray, B. E., Froemming, G. R., Maguire, P. B. & Ohlendieck, K. (1998). Excitation-contraction-relaxation cycle: role of Ca2+ regulatory membrane proteins in normal, stimulated and pathological skeletal and muscle. *International Journal of Molecular Medicine, 1*, 677-687.

Myagmar, B. E., Flynn, J. M., Cowley, P. M., Swigart P. M., Montgomery, M. D. & Thai, K. (2017). Adrenergic receptors in individual ventricular myocytes: the beta-1 and alpha-1b are in the cells, the alpha-1a is in a subpopulation, and the beta-2 and the beta-3 are mostly absent. *Circulation Research, 120*, 1103-1115.

Nakai, J., Sekiguchi, N., Rando, T. A., Allen, P. D. & Bean, K. G. (1998). Two regions of ryanodine receptor involved in coupling with L-Type Ca2+ channels. *Journal of Biological Chemistry*, 13403 - 13406.

Napolitano, C., Bloise, R., Memmi, M. & Priori. S. G. (2014). Clinical utility gene card for: Catecholaminergic Polymorphic Ventricular Tachycardia (CPVT). *European Journal of Human Genetics, 22*(1), 55.

Narayan, S. M., Bayer, J. D. &Trayanova, N. A. (2008). Actional potential dynamics explain arrhythmic vulnerability in human heart failure. A clinical and modeling study implicating abnormal calcium handling. *Journal of the American College of Cardiology, 52*(22), 1782-1792.

Nattel, S. & Dobrev, D. (2012). The multidimensional role of calcium in atrial fibrillation pathophysiology: mechanistic insights and therapeutic opportunities. *European Heart Journal, 33*(15), 1870-1877.

Nerbonne, J. M. & Kass, R. S. (2005). Molecular Physiology of Cardiac Repolarization. *Physiological Reviews*, 1205 - 1253.

Nguyen, T., Cao, L.-B. & Movahed, A. (2013). Biventricular pulsus alternans: An echocardiographic finding in patients with pulmonary embolism. *World Journal of Clinical Cases, 1*(5), 162-165.

Noble, D. & Francesco, D. (1985). A model of cardiac electrical activity incorporating ionic pumps and concentration changes. *Philosophical Transactions of the Royal Society of London. B, Biological Sciences, 307*, 353-398.

Novak, P. & Soukup, T. (2011). Calsequestrin distribution, structure and function, it's role in normal and pathological situations and the effect of thyroid hormones. *Physiological Research, 60*, 439-452.

Otsu, K., Willard, H. F., Khanna, V. K., Zorzato, F., Green, N. M. & MacLennan, D. H. (1990). Molecular cloning of cDNA encoding the Ca2+ release channel (ryanodine receptor) of rabbit cardiac muscle sarcoplasmic reticulum. *Journal of Biological Chemistry, 265*, 13472 - 13483.

Pandit, S. V. & Jalife, J. (2013). Rotors and the dynamics of cardiac fibrillation. *Circulation Research, 112*(5), 849-862.

Park, H., Park II, Y., Kim, E., Youn, B., Fields, K., & Dunker, A. K. (2004). Comparing skeletal and cardiac calsequestrin structures and their calcium-binding a proposed mechanism for coupled calcium binding and protein polymerization. *Journal of Biological Chemistry, 279*, 18026-18033.

Patterson, R. L., Boehning, D., & Snyder, S. H. (2004). Inositol 1, 4, 5-trisphosphate receptors as signal integrators. *Annual Review of Biochemistry, 73*, 437-465.

Peng, W., Shen, H., Wu, J. P., Guo, W., Pan, X. and Wang, R. (2016). Structural basis for the gating mechanism of the type 2 ryanodine receptor RyR2. *Science, 354*(6310), 1-10.

Picht, E., Zima, A. V., Blatter, L. A. & Bers, D. M. (2007). SparkMaster: automated calcium spark analysis with ImageJ. *American Journal of Physiology - Cell Physiology, 293*(3), C1073-C1081.

Pinnel, J., Turner, S., & Howell, S. (2007). Cardiac muscle physiology. *Continuing Education Anaesthesia Critical Care and Pain*, 85 - 88.

Postma, A. V., Denjoy, I. & Kamblock. J. (2005). Catecholaminergic polymorphic ventricular tachycardia: RyR2 mutations, bradycardia and follow up the patients. *Journal of Medical Genetics, 42*, 863-870.

Potse, M. (2012). Mathematical modeling and simulation of ventricular activation sequence: Implications for cardiac resynchronization therapy. *Journal of Cardiovascular Translational Research, 5*(2), 146-158.

Priebe, L. & Beuckelmann, D. J. (1998). Simulation study of cellular electric properties in heart failure. *Circulation Research, 82*, 1206-1223.

Priori, S. G., Mazzanti, A., Blom, N., Borggrefe, M., Camm, J. & Elliott, P. M., et al. (2015). ESC Guidelines for the management of patients with ventricular arrhythmias and the prevention of sudden cardiac death. *European Heart Journal, 36*(41), 2793-2867.

Priori, S. G., Napolitano, C., Tiso, N., Memmi, M., Viganti, G., Bloise, R. et al. (2001). Mutations in the cardiac ryanodine receptor gene(hRyR2) underlie catecholaminergic polymorphic ventricular tachycardia. *Circulation, 103*(2), 196-200.

Priori, S. G., Napalitano, C., Memmi, M., Colombi, B., Drago, F. & Gasparini, M. L. et al. (2002). Clinical and Molecular characterization of patients with catecholaminergic polymorphic ventricular tachycardia. *Circulation, 106*, 69-74.

Puglisi, J. L. & Bers, D. M. (2001). LabHEART: an interactive computer model of rabbit ventricular myocyte ion channels and Ca transport. *American Journal of Physiology, 281*(6), C2049-C2060.

Qin, J., Valle, G., Nani, A., Chen, H., Ramos-Franco, J., & Nori, A. (2009). Ryanodine receptor luminal Ca2+ regulation: swapping calsequestrin and channel isoforms. *Biophysical Journal, 97*(7), 1961-1970.

Qu, Z., Liu, M. B. & Nirvala, M. (2016). A unified theory of calcium alternans in ventricular myocytes. *Scientific Reports, 6*(35625), 1 - 14.

Radermacher, M., Rao, V., Grassucci, R., Frank, J., Timerman, A. P. & Fleischer, S. (1994). Cryo-electron microscopy and three-dimensional reconstruction of the calcium release channel/ryanodine receptor from skeletal muscle. *Journal of Cell Biology, 127*, 411-423.

Reid, D. S., Tynan, M., Braidwood, L. & Fitzgerald, G. R. (1975). Bidirectional tachycardia in a child. A study using His bundle electrography. *British Heart Journal, 37*(3), 339-344.

Reuter, G. W. & Beeler, H. (1977). Reconstruction of the action potential of ventricular myocardial fibers. *The Journal of Physiology, 268*(1), 177-210.

Rice, J. J., Jafri, M. S. & Winslow, R. L. (1999). Modeling gain and gradedness of Ca^{2+} release in the functional unit of the cardiac diadic space. *Journal of Biophysics, 77*, 1871-1884.

Rockman, H. A., W. J. Koch, & R. J. Lefkowitz. (2002). Seven-transmembrane-spanning receptors and heart function. *Nature, 415*, 206-213.

Ross, J., Miura, T., Kambayashi, M., Eising, G. P., & Ryu, K. (1995). Adrenergic control of the force-frequency relation. *Circulation, 92*, 2327 - 2332.

Rossi, A. E. & Dirksen, R. T. (2006). Sarcoplasm reticulum: The dynamic calcium governing of muscle. *Muscle Nerve, 33*, 715-731.

Rudy, Y. A. & Luo, C. H. (1991). A model of ventricular cardiac action potential. Depolarization, repolarization and their interaction. *Circulatory Research, 68*, 1501-1526.

Santulli, G., Lewis, D., Georges, A. D., marks, A. R. & Frank, J. (2018). Ryanodine receptor structure and function in health and disease. *Subcellular Biochemistry, 87*, 329-352.

Sato, D. S. (2006). Spatially discordant alternans in cardiac tissue: role of calcium cycling. *Circulatory Research, 99*, 520-527.

Saucerman, J. J. & McCulloch, A. D. (2006). Cardiac β-Adrenergic signaling from subcellular macrodomains to heart failures. *Annals of New York Academy of Sciences, 1080*, 348-361.

Schimpf, R. C., Veltmann, C., Wolpert, C., & Borggrefe, M. (2010). Arrhythmogenic hereditary syndrome: Brugada syndrome, long QT syndrome, short QT syndrome and CPVT. *Minerva Cardioangiology, 58*(6), 623 - 636.

Schmidt, A. G., Kadambi, V. J., Ball, N., Sato, Y., Walsh, R. A., Kranias, E. G. et al. (2000). Cardiac-specific overexpression of calsequestrin results in left ventricular hypertrophy, depressed force-frequency relation and pulsus in vivo. *Journal of Molecular and Cellular Cardiology, 32*(9), 1735-1744.

Schotten, U., Greiser, M., Braun, V., Karlein, C. & Schoendube, F. (2001). Effect of volatile anesthetics on the force-frequency relation in human ventricular

myocardium. The role of the sarcoplasmic reticulum calcium-release channel. *Anesthesiology, 95*, 1160-1168.

Shannon, T. R., Wang, F. & Bers, D. M. (2004). A mathematical treatment of integrated Ca dynamics within the ventricular myocyte. *Biophysical Journal, 87*, 3351-3371.

Shannon, T. R., Wang, F., Puglisi, J., Weber, C., & Bers, D. M. (2005). Regulation of cardiac sarcoplasmic reticulum Ca release by luminal [Ca] and altered gating assessed with mathematical model. *Biophysical Journal, 89*(6), 4096-4110.

Shashank, P. B. & Weindling, S. N. (2016). Catecholaminergic polymorphic ventricular tachycardia: An exciting new era. *Annual Pediatric Cardiology, 9*(2), 137-146.

Shiferaw Y, Sato, D., & Karma, A. (2005). Coupled dynamics of voltage and calcium in paced cardiac cells. *Physical Review of Statistical, Nonlinear and Soft Matter Physics*, 1 - 13.

Shin, D. W., Ma, J. & Kim, D. H. (2000). The asp-rich region at the carboxyl-terminus of calsequestrin binds to Ca2+ and interacts with triadin. *FEBS Letter, 486*, 178-182.

Shirfew, Y., Watanabe, M. A., Garfinkel, A., Weiss, J. N., & Karma, A. (2003). Model of intracellular calcium in ventricular myocytes. *Biophysical Journal, 85*(6), 3666-3686.

Sobie, E. A., Dilly, K. W., Cruz, J. S., Lederer, W. J. & Jafri, M. S. (2002). Termination of cardiac Ca^{2+} sparks: An investigative mathematical model of calcium-induced calcium release. *Biophysical Journal, 86*(5), 3329-3331.

Solaro, R. J., Moir, A. J. & Perry, S. V. (1976). Phosphorylation of troponin I and the inotropic effect of adrenaline in the perfused rabbit heart. *Nature, 262*, 615-617.

Song, L. R., Alcalai, R., Arad, M., Wolf, C. M., Toka, O., Conner, D. A. et al. (2007). Calsequestrin 2 (CASQ2) mutations increase the expression of calreticulin and ryanodine receptors, causing catecholaminergic polymorphic ventricular tachycardia. *Journal of Clinical Investigation, 17*, 1814-1823.

Stambler, B. S., Fenelon, G., Shephard, R. K., Clemo, H. F. & Guiraudon, C. (2003). Characterization of sustained atrial tachycardia in dogs with rapid ventricular pacing-induced heart failure. *Journal of Cardiac Electrophysiology, 14*, 499-577.

Stern, M. D., Song, L. S., Cheng, H., Sham, J. S., Yang, H. T., Boheler, K. R. et al. (1999). Local control models of cardiac excitation-contraction coupling. A

possible role for allosteric interactions between ryanodine receptors. *Journal of General Physiology, 113*, 469-489.

Stoppel, W. L., Kaplan, D. L., & Black, L. D. (2016). Electrical and mechanical stimulation of cardiac cells and tissue constructs. *Advanced Drug Delivery Reviews, 96*, 133-155.

Sumitomo, N. K., Harada, K., Nagashima, M., Yasuda, T., Nakamura, Y., Aragaki, Y. et al. (2003). Catecholaminergic polymorphic ventricular tachycardia: electrocardiographic characteristics and. *Heart, 89*(1), 66-70.

Tada, M. & Toyofuku, T. (1996). SR Ca-ATPase/phospholamban in cardio-myocyte function. *The Journal of Cardiac Failure, 2*, 77-85.

Takeshima, H., Takeshima, H., Matsumoto, N. S., Ishida, H., Kangawa, K., Minamino, N., Matsuo, H. et al. (1989). Primary structure and expression from complementary DNA of skeletal muscle ryanodine receptor. *Nature, 339*(6224), 439-445.

Torgerson, T. & Ochs, H. (2015). Genetic of primary immune deficiencies. In K. E. Sullivan, *Stiehm's immune deficiencies* (p. 1156). Cambridge: ScienceDirect.

Tran, K., Smith, N. P., Loiselle, D. S. & Crampin, E. J. (2011). A thermodynamic model of the cardiac sarcoplasmic/endoplasmic Ca2+ (SERCA) pump. *Biophysical Journal, 100*(11), 2029-2042.

Tse, G. (2016). Mechanism of cardiac arrhythmias. *Journal of Arrhythmia, 32*(2), 75-81.

Tsien, R. W., Giles, W. & Greengard, P. (1972). Cyclic AMP mediates the effects of adrenaline on cardiac Purkinje fibers. *Nature, 240*, 181-183.

Tuan, H.-T. M., Williams, G. S. B., Chikando, A. C., Sobie, E. A., Lederer, W. J. & Jafri, M. S. (2011). Stochastic simulation of cardiac ventricular myocyte calcium dynamics and waves. *Conference Proceedings of IEEE Engineering in Medicine and Biological Society, 2011*, 4677-4680.

Venetucci, L. A., Trafford, A. W., O'Neill, S. C. & Eisner, D. A. (2008). The sarcoplasmic reticulum and arrhythmogenic calcium release. *Cardiovascular Research, 77*(2), 285-292.

Venetucci, L. M., Venetucci, L., Denegri, M., Vapolitano, C. & Priori, S. G. (2012). Inherited calcium channelopathies in the pathophysiology of arrhythmias. *Nature Review Cardiology, 9*, 561-575.

Vereko, A. O., Veldkamp, M. W., Baartscheer, A., Schumacher, C. A., Klopping, C., Ginneken, A. G., & Ravesloot, J. H. (2001). Ionic mechanism of delayed afterdepolarizations in ventricular cells isolated from human end-stage failing hearts. *Circulation, 104*, 2728-2733.

Viskin, S. & Belhassen, B. (1998). Polymorphic ventricular tachyarrhythmias in the absence of organic heart diseases: classification, differential diagnosis, and implications for therapy. *Progress in Cardiovascular Diseases, 41*(1), 17-34.

Wagner, S., Maier, L. S., & Bers, D. M. (2015). Role of sodium and calcium dysregulation in tachyarrhythmias in sudden cardiac death. *Circulation Research, 116*(12), 1956-1970.

Walker, C. A. & Spinale, F. G. (1999). The structure and function of cardiac myocyte: A review of fundamental concepts. *Journal of Thoracic Cardiovascular Surgery, 118*, 375-382.

Walker, M. L. & Rosenbaum, D. S. (2003). Repolarization alternans: implications for the mechanism and prevention of sudden cardiac arrest. *Cardiovascular Research*, 599 - 614.

Wallukat, G. (2002). The β-adrenergic receptors. *Herz, 27*(7), 683-690.

Walweel, K. & Laver, D. R. (2015). Mechanism of SR calcium release in healthy and failing human hearts. *Biophysical Reviews, 7*(1), 33 - 41.

Wehrens, X. H. Lenhart, S. E. & Huang, F. (2003). FKBP12.6 deficiency and defective calcium release channels (ryanodine receptor) function linked to exercise. *Cell, 113*, 829-840.

Wei, H. X., Zhang, X.-H., Clift, C. & Yamaguchi, N. (2016). CRISPR/Cas9 gene editing of RyR2 in human stem cell-derived cardiomyocytes provides a novel approach in investigating dysfunctional Ca^{2+} signaling. *Cell Calcium, 73*, 104 - 111.

Weiss, J. N., Garfinkel, A., Karagueuzian, H. S. & Chen, P.-S. (2010). Early afterdepolarization and cardiac arrhythmias. *Heart Rythm, 7*(12), 1891-1899.

Weiss, J. N., Nivala, M., Garfinkel, A., & Qu, Z. (2006). Alternans and arrhythmias: from cell to heart. *Circulation Research, 98*(10), 1244 - 1253.

Weiss, J. N. & Qu. Z. (2007). The chicken or the egg? Voltage and calcium dynamics in the heart. *American Journal of Heart Circulatory Physiology, 293*(4), 2054-2059.

Wellens, H. J., Schwartz, P. J., Lindemans, F.W., Buxton, A. E., Goldberger, J. J., Hohnloser, S. H. et al. (2014). Risk stratification for sudden cardiac death: current status and challenges for the future. *European Heart Journal, 35*(25), 1642-1651.

Williams, G. S., Smith, G. D., Sobie, E. A. & Jafri, M. S. (2010). Models of cardiac excitation-contraction coupling in ventricular myocytes. *Mathematical Bioscience, 226*(1), 1-15.

Williams, G. S., Chikando, A. C., Tuan, H. T., Sobie, E. A., Lederer, W. J., & Jafri, M. S (2011). Dynamics of Calcium sparks and calcium leak in the heart. *Biophysical Journal*, 1287 - 1296.

Winslow, R. L., Rice, J. J., Jafri, M. S., & O'Rourke, B. (1999). Mechanisms of altered excitation-contraction coupling in canine tachycardia-induced heart failure, II: model studies. *Circulation Research, 84*(5), 571-586.

Winslow, R. L., Cortassa, S., O'Rourke, B., Hashambhoy, Y. L., Rice, J. J. & Greenstein, J. L. (2011). Integrative modeling of the cardiac ventricular myocyte. *Wiley Interdisciplinary Review of Systems Biology of Medicine, 3*(4), 392 -413.

Woodworth, R. S. (1902). Maximal contraction "staircase" contraction, refractory period, and compensatory pause, of the heart. *American Journal of Physiology, 8*, 213-249.

Xiao, Z., Guo, W., Sun, B., Hunt, D. J., Wei, J., Liu, Y. et al. (2016). Enhanced cytosolic Ca2+ Activation Underlies a common defect of central domain cardiac ryanodine receptor mutations linked to arrhythmias. *The Journal of Biological Chemistry, 291*, 24528-24537.

Yan, Z., Bai, X., Yan, C., Wu, J., Li, Z., Xie, T. et al. (2015). Structure of the rabbit ryanodine receptor RyR1 at near-atomic resolution. *Nature, 517*, 50-55.

Yano, M., Yamamoto, T., Kobayashi, S. & Matsuzaki, M. (2009). Role of ryanodine receptor as a Ca2+ regulatory center in normal and failing hearts. *Journal of Cardiology, 53*(1), 1-7.

Yue, D. T. (1992). Relationships between intracellular free calcium and force with changes of interval. In W. A. Noble M. I. M., *The interval-force-relationship of the heart: Bowditch revised* (pp. 95-110). Cambridge, MA: Cambridge University.

Zhang, L., Kelley., Schmeisser, G., Kobayashi, Y. M. & Jones, L. R. (1997). Complex formation between junctin, triadin, calsequestrin and the ryanodine receptor. Proteins of the cardiac junctional sarcoplasm reticulum membrane. *Journal of Biological Chemistry, 272*, 23389-23397.

Zhao, Y. G., Valdivia, C. R., Gurrola, G. B., Powers, P. P., Willis, B. C., Moss, R. L. et al. (2015). Arrhythmogenesis in a catecholaminergic polymorphic ventricular tachycardia mutation that depresses ryanodine receptor function. *Proceedings of the National Academy of Sciences, 112*(113), 1669-1677.

Zorzato, F., Fujii, J., Otsu, K., Philips, M., Green, N. M., Lai, F. A. et al. (1990). Molecular cloning of cDNA encoding human and rabbit forms of the Ca2+ release channel (ryanodine receptor) of skeletal muscle sarcoplasm reticulum. *Journal of Biological Chemistry, 265*, 2244 - 2256.

CHAPTER TWO: CA^{2+} SPARK EVENTS ARE THE SUB-CELLULAR MECHANISM TO EXPLAIN FORCE FREQUENCY RELATIONSHIPS OF A CARDIAC MYOCYTE

Abstract

Calcium sparks are the elementary Ca^{2+} release events in excitation-contraction (E-C) coupling. The frequency-dependent contractile force generated by cardiac myocytes depends upon the characteristics of the Ca^{2+} transients derived by the number of Ca^{2+} sparks events. A stochastic computational local control model of Guinea pig ventricular cardiomyocyte had developed to get insight into mechanisms of force-frequency relationship (FFR). We developed a new three-state RyR2 model that reproduced the adaptive behavior of RyR2 in which the RyR2 channels equilibrate into a different phase when exposed to prolonged elevated subspace $[Ca^{2+}]$. The model was tested for agreement with previous experimental and modeling studies on force-interval relations. Our local control model displayed a stable action potential trains at 7 Hz, unlike previous common pool models. The duration and the amplitude of the $[Ca^{2+}]_{myo}$ transients increase in pacing rates consistent with the experiments. The $[Ca^{2+}]_{myo}$ transient reaches to its peak value at 4Hz and decreases afterward, consistent with experimental force-frequency curves. The model predicts, in agreement with our previous modeling studies that diastolic sarcoplasmic reticulum (SR), $[Ca^{2+}]_{sr,}$ and RyR2 adaptation increase with the increased stimulation frequency giving rise rising than falling amplitude of the myoplasmic $[Ca^{2+}]$ transients. In analyzing the FFR at the subcellular level, it was also

found the peak Ca^{2+} transient means the highest numbers of SR Ca^{2+} sparks, larger average amplitudes of those sparks, and the longer duration of the Ca^{2+} sparks.

Introduction

The contraction of the heart muscle pumps the blood to the body. The EC-coupling phenomenon is the basis of this contractility. When extracellular Ca^{2+} entry triggers the release of intracellular Ca^{2+}, the amount of Ca^{2+} released from SR governs the strength of the heart contraction and contract to pump the blood. The contractile force depends upon the beating frequency of the heart. The change in the force in each pacing is termed as an interval-force relationship or force-frequency relationship (FFR). In general, when there is a change in pacing frequency, it also changes the myoplasmic Ca^{2+} transient and the force generated by the myocytes. In the guinea pig, the Ca^{2+} transients critically determine the force generation at the level of stimulus frequency (Morii, Kihara, Konishi, Inubushi, Sasayama, 1996). Mature myocyte of higher mammals exhibits a positive FFR and it is called Bowditch phenomenon (Godier-Furnémont, Triburcy, Wagner, Dewenter, Lammle, El-Armouche, et al., 2015) (Schotten, Greiser, Braun, Karlein, & Schoendube, 2001). A negative FFR and alterations in EC-coupling are key features in arrhythmic heart failure (Bers, 2001) (Katz, 2000). FFR is an important intrinsic regulatory mechanism in cardiac myocytes' contraction to match the demand for increased blood supply (Endoh, 2004) (Joulin, Marechaux, Hassoun, Montaigne, Lancel, & Neviere, 2009). The positive FFR is crucial for the adaptation at the time of increased physical activities or exercise (Hasefus, Holubarsch, Hermann, Astheimer, Pieske, & Just, 1994) because force increases with increasing pacing frequency. The

negative FFR in humans is suggested to exhibit a maladaptation of the heart in rapid pacing (Bohm, Rosee, La, Schmidt, Schulz, Schwinger, & Erdmann, 1992). Cardiomyocytes of failing human heart display reversal in the FFR, there is a decrease in the contractile performance at higher rates of stimulation (Davies, Davia, Bennett, Pepper, Poole-Wilson, & Harding, 1995). The mechanisms of the force-frequency relationship primarily depend upon changes in the intracellular Ca^{2+} transients (Joulin, 2009) as well as some other factors such as SERCA pump activities, $Na^{+,}$ and Ca^{2+} exchangers (NCX) and adrenergic control (Lompre, Anger, & Levitsky, 1994) (Kurihara, & Allen, 1982) (Ross, Miura, Kambayashi, Eising, & Ryu, 1995).

The frequency-dependent contractile strength of the heart varies with the species of the animals. For example, in rest, the human heart beats once in one second (1 Hz) which means 60 times in one minute. During exercise, the sustainable beat reaches 180 times in 1 minute (~ 3Hz) without causing any damage to the heart. The resting heartbeat frequency in the rabbit is 2.5 beats in 1 sec and the sustainable heartbeat reaches 5 beats per second during exercise. In mice, resting heartbeat is 10 beats in 1 second and during exercise, it reaches 14 beats per second. From these heart frequencies what we can find human heart can contract up to 200% while rabbit and mice hearts contact 100% and 40% respectively (Janssen, & Periasamy, 2007). In a rat, a normal heartbeat is 400 beats per second (~7Hz – 7 beats/sec) and it can withstand to 11 beats per second during the exercise. The heart of a Guinea pig beats 240 times per minute (Shiba, 2012) (~4Hz – 4 beats/sec) in normal condition and with the 100% contraction capacity can sustain 8 beats per sec during exercise or stress.

In higher mammals such as human, rabbit and guinea pig, the relationship between cardiac contractile force and stimulation frequency recorded to be positive under physiological rates (Buckley, Penefsky, & Litwalk, 1972) (Endoh, 2004) (Gwathmey, Slawsky, Hajjar, Briggs, & Morgan, 1990) and it is found to be negative in small animals like rats, mouse (Namekata, Takeda, Moriwaki, Kazama, Sato, Tanaka, et al., 2004) (Narayan, McCune, Robitaille, Hohl, & Altschuld, 1995), turtle, lizards, snakes (Rumberger, & Riechel, 1972) (Driedzic, & Gesser, 1985) and fish (El-Sayed, Abu-mara, & Badr, 2012) (Shiels, & Farrell, 1997) (Keen, Vazon, Farrell, & Tibbits, 1994). The activities of the SERCA pump and extracellular extrusion of Ca^{2+} determine the availability of intracellular Ca^{2+} during systole. Higher mammals such as human, rabbit, and Guinea pig receive 65–80% of the Ca^{2+} from SR, and the rest of the Ca^{2+} comes from outside via L-type channel. In smaller mammals such as rats and mice depend on ~92% of Ca^{2+} to bind myofilaments during contraction (Bers, 2002) (Monasky, & Jansen, 2009) (Bassani, Bassani, & Bers, 1994). In small mammals like a rat, the majority of the Ca^{2+} for contraction coming from SR needed to be pumped back by SERCA quicker to be ready for the next beat. It has been suggested that the negative force-frequency relationship is due to diminished SR Ca^{2+} release in case of rapid pacing (Orchard, & Lakatta, 1985).

The mechanism of impairment in myocardial Ca^{2+} during heart failure is important in interval-frequency response. Other abnormalities include reduced Ca^{2+} release from the SR as well as delayed reuptake, in a reduction in the number of SR Ca^{2+} channels and abnormal mRNA levels of Ca^{2+} transport proteins (Ross, Miura,

Kambayashi, Eising, & Ryu, 1995). Our goal in this research is to formulate a more stable model with the update in new experimental features and integrate stochasticity in the model developed by Jafri et al. (Jafri, Rice, & Winslow, 1998).

Generally accepted mechanism of FFR is the change in the Ca^{2+} handling of SR. With the increase in beating frequency, the amplitude of Ca^{2+} transient also increases and so as the Ca^{2+} load in the SR. With the increase in the numbers of beats in each period, more Ca^{2+} is brought to inside via L-type channels. With the increased concentration of Ca^{2+} in the cytosol, SERCA pump activities increase; hence more Ca^{2+} is pumped to the SR and in the more Ca^{2+} becomes available for release via RyRs in the subsequent beats (Endoh, 2004). (Janssen, & Periasamy, 2007). When a switch from a given frequency to a higher one occurs, more Ca^{2+} enters in the beginning to the myocytes than leaving out till a steady-state does not form.

As we mentioned previously, excitation-contraction coupling in the heart is controlled by cell-wide Ca^{2+} transients and those transients are formed by elementary Ca^{2+} releasing events (Ca^{2+} sparks). Additionally, those events could be Ca^{2+} triggered or spontaneous (Cheng, Lederer, & Cannell, 1993) and Ca^{2+} transients depend upon triggered events. With the advent of laser confocal microscopy, it became easier to study individual Ca^{2+} sparks in the subspace. It is evident that during the diastolic phase there are ~100 sparks s^{-1} myocyte $^{-1}$ and spark rate raises 1000 to 1000000 times in each molar increase in subspace $[Ca^{2+}]_{myo}$ during systole (Lehnart, Maier, & Hasenfuss, 2009). It is also believed that the modulation in Ca^{2+} spark rate controls the Ca^{2+} transient amplitudes and contractile force generated by cardiac myocytes.

In this research, besides computing Ca^{2+} transient and its role in force-frequency generation, we also explored and analyzed Ca^{2+} spark amplitude and frequency in each beat. The model predicts, in agreement with our previous modeling studies (Jafri et al., Biophys J. 1998 Mar;74(3):1149-68), that diastolic sarcoplasmic reticulum (SR) $[Ca^{2+}]_{SR}$ and RyR2 adaptation increases with increased stimulation frequency giving rise rising than falling amplitude of the myoplasmic $[Ca^{2+}]$ transients. A similar conclusion was also made from spark analysis, with the increase of SR Ca^{2+}, $[Ca^{2+}]_{sr}$ the mean as well as peak amplitudes of the Ca^{2+} sparks raises force generated by the heart and with the increase adaptation of RyR2s, both peak and mean amplitudes start falling giving decline in the force generation.

Methods

Computational Model Development

We built a new whole-cell stochastic model of Guinea pig cardiac ventricular myocyte EC coupling. It integrates a modified model of stochastic Ca^{2+}dynamics from our published rat model formulated by Williams, Chikando, Tuan, Sobie, Lederer, & Jafri (2011), with our published common pool model (Jafri, et al., 1998) for the Guinea pig ventricular myocyte. The resulting model is local control, Monte Carlo simulation model which uses 20,000 stochastically gating Ca^{2+} releasing units that open in dyadic subspaces of cytoplasm. The CRUs are the cluster of 12 L-type and 50 RyR2 channels coupled with a dyadic subspace. We have integrated RyR adaptation to the gating mechanism of the intracellular Ca^{2+}. The ionic current formulations of the new model are borrowed from L-R models (Luo, & Rudy, 1991) (Luo, & Rudy, 1994a) (Luo, & Rudy,

1994b). The Ca^{2+} dynamics of the model are based upon J-R-W (Jafri, et al., 1998) model.

A Novel RyR2 Model

In 1998, Jafri *et al.* (Jafri, 1998) developed a new model by integrating the L-R II (Luo, & Rudy, 1994b) model with a more realistic formulation of the myocyte Ca^{2+} dynamics by replacing the Ca^{2+} SR release mechanism in Luo-Rudy II with a dynamics RyR model with adaptation interacting the L-type Ca^{2+} channels in the dyadic subspace. The RyR model had four states – two closed states and two open states. Combining features upon that model with the stochastic spark model (Williams, et al., 2011), we developed a new three-state model – two closed states and one open state as shown in figure 9. The second closed state (C3) shown in Figure 11 is an adaptive state. The gating mechanism of this RyR2 adaptation model borrowed from the leak model and the stochasticity formulation of the opening probability of the RyR2 in the model are based upon the Monte Carlo method.

In this model, luminal regulation function (Φ) modifies the channel opening rate, SR load, $[Ca^{2+}]_{SR}$ available to be released played a major role in the developing force-frequency relationship (Bers, 2002). RyR release flux reaches to the near its peak with the increase in pacing frequency $[Ca^{2+}]_{SR}$ availability to be released is calculated by the following equation (Jafri, et al., 1998)

$$SR_{rel} = v_1(N_O^i)([Ca^{2+}]_{jsr} - [Ca^{2+}]_{ds}) \quad \text{---------- (1)}$$

Where v_1 is the Ca^{2+} release rate via RyR2 channel, $[Ca^{2+}]_{ds,}$ Ca^{2+} concentration in diadic subspace, and $[Ca^{2+}]_{jsr}$ luminal Ca^{2+} concentration at the junction. N_O^i is the number of open RyR2 channels at the i^{th} release sites.

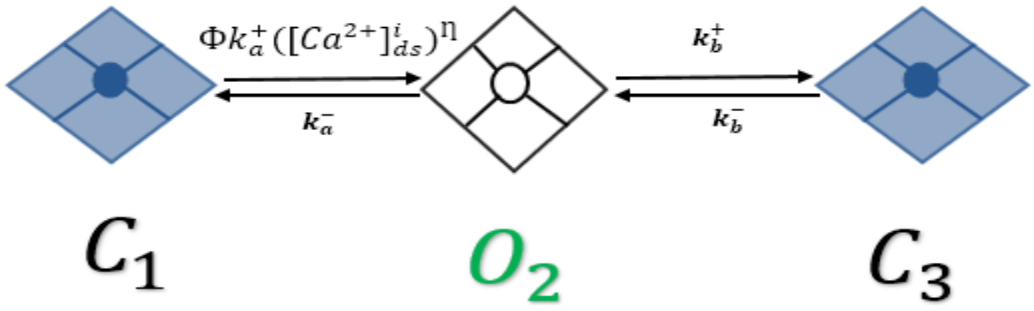

Figure 9: A novel three state RyR2 model with new adaptation state. In the resting phase, almost all RyR2s stay in the close state (C_1), with the arrival of Ca^{2+} in the dyadic subspace, the channels activate into an open state (O_2) and after some time the channels might inactivate into an adaptive state (C_3).

L – type Ca^{2+} Channel Model

In our research, we are using a six-state L-type Ca^{2+} channel model as shown in figure 10. In this model state 2 (O2) and state 3 (O3) are open states, state 1 (C1) and state 6 (C6) are the closed states. The remaining two states (C4 & C5) are inactivated states. The inactivation of opening states of the LCC model happens in two different

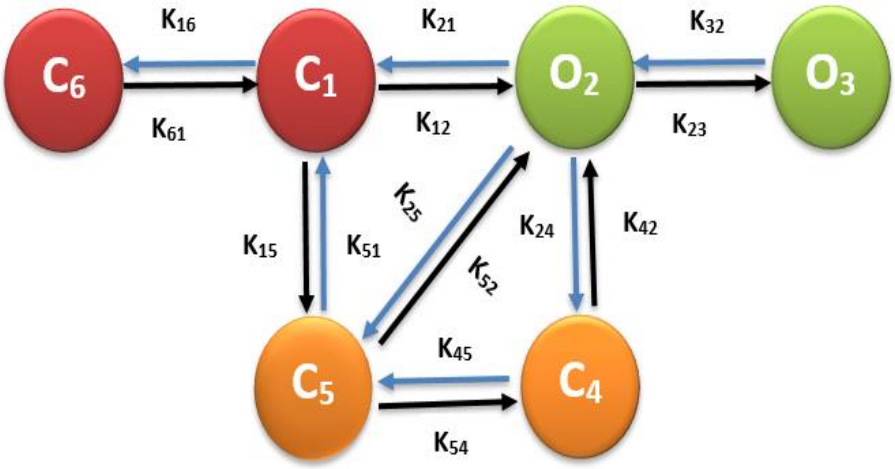

Figure 10: Schematic diagram of the 6-state Markov model of the L-type Ca^{2+} channel. During resting potential, all L-type channels are in a closed state (C_1), and change in the membrane potential active them into an open state (O_2). Channel in O_2 state may continue to open state (O_3) or change in the voltage bring them into inactivate state (C_5) or excess Ca^{2+} in dyadic subspace may bring them into another inactivated state (C_4).

ways – Voltage-dependent inactivation (VDI, O2 → C5), and Ca^{2+} -dependent inactivation (CDI, O2 → C4). The Ca^{2+} in subspace is the one to controls inactivation in each release site. More the level of Ca^{2+} elevates in the subspace, it increases the rate of inactivation of LCC and prevents Ca^{2+} overload in the myoplasm (Wagner, Lauterbach, Kohl, Westphal, Williams, Steinbrecher, et al., 2012). The 6th state, C6, was added in the 5-state original model of Sun *et al.* (Sun, Fan, Clark, & Palade, 2000) to have the stronger depolarization (≥ -30 to ≤ -40 mV) and all the channels during the resting period stay in

this state. The CDI and VDI behaviors were updated from Morotti *et al.* (Morotti, Grandi, Summa, Ginsburg, & Bers, 2012).

Frequency-Dependent Simulation of Myocyte

This newly built Guinea pig model was used to measure Ca^{2+} transients in the cytosol with the varying pacing frequencies. Force is monotonically related to the size of the cytosolic calcium transient (Fabiato, 1985). The foundation of the model was developed in 1 Hz pacing (basic cycle length (BCL) - 1). All the parameters were adjusted for 1 Hz and compared all the plots with the experimental results and the previous model works. After this, we simulated FFR with BCL as low as 0.2 Hz (1 beat in 5 seconds) to as high as 8 Hz (8 beats in 1 second). The other simulation frequencies were 0.20 Hz (1 beat in 5 sec), 0.25 Hz (1 beat in 4 sec), 0.33 Hz (1 beat in 3 sec), 0.5 Hz (2 beats in 2 sec), 1 Hz (1 beat in 1 sec), 2 Hz (2 beats in 1 sec), 3 Hz (3 beats in 1 sec), 4 Hz (4 beats in 1 sec), 5 Hz (5 beats in 1 sec), 6 Hz (6 beats in 1 sec) and 7 Hz (7 beats in 1 sec). For every pacing frequency, each simulation was run for 10 seconds. We recorded all the data from the simulation and plotted them against the time. Then, we extracted amplitude and duration of AP, amplitudes of L-type current (I_{LCC}), Na^{+}-Ca^{2+} current (I_{ncx}), Na^{+} current (I_{Na}), delayed rectifier K^{+} current (I_{ktos}), transient outward K^{+} current (I_{ktof}), inward rectifier (I_{K1}) K^{+} current , cytoplasmic Ca^{2+} concentration ($[Ca^{2+}]_{myo}$), NSR Ca^{2+} concentration ($[Ca^{2+}]_{nsr}$), and RyR opening probability ($P_{o,\,RyR}$) from each beat. Then the peak values of each ionic current were collected and plotted against the pacing frequencies.

The subcellular and molecular analysis of the FFR at Ca^{2+} level was done by calculating average Ca^{2+} sparks, Ca^{2+} spark amplitudes, and the Ca^{2+} spark duration. To compute these data, we picked up the ten beats when simulation arrived in a stable state. After that, an algorithm was designed to pick up the segments of the systolic phase only and exclude any data from the diastolic phase. From the systolic segment, the Ca^{2+} rise which was at least 25 μM tall counted as a spark and sum them up in that beat. Similarly, the sparks were counted from the rest of the beats and the average numbers of the sparks were calculated. Likewise, the average amplitudes of the sparks from different beats of the same frequency were measured by adding the amplitude of each beat and dividing the total amplitude by the number of beats. After collecting average spark amplitudes of each beat, the amplitudes of 10 beats were combined and again the mean amplitude was computed. The average spark duration was calculated akin to Ca^{2+} amplitudes. The total sparks durations were combined in each beat and the sum was divided by the number of sparks, and mean spark duration was concluded from the ten beats.

Numerical Methods

PGI CUDA Fortran was used to compile, execute, and simulate the program in the Linux platform, Ubuntu operating system. CUDA (compute unified device architecture) is a parallel computing platform and programming language developed for graphic processing units (GPUs) by NVIDIA. The CUDA clusters we are using in our lab contain Fermi-based C2050 graphics processing cards with CUDA Toolkit 6.0 and higher. To capture calcium dynamics at a single-channel level a novel computational algorithm Ultra-Fast Markov chain Monte Carlo (UMCMC) method was used for the

stochastics gating from CRUs (US Patent No. US9009095, 2015). All ordinary differential equations were calculated using Euler methods. The time step is for the differential calculation is ten nanoseconds.

The programming software interactive data language (IDL) and Python were used to plot the graphs and compute data from the simulation. IDL is a programming language used for data analysis in astronomy and medical imaging. Python is an open-source interpreted, object-oriented high-level programming language. Python supports many packages and modules. For our plot and graphs, we used some packages such as matplotlib, panda, NumPy, & SciPy, which make python lot easier to work on. IDL also provides a meticulous graphical representation of the data.

Results

Ca^{2+} transient Peaked at 4 Hz Frequency

In simulations, the amplitude of the Ca^{2+} peak transient, $[Ca^{2+}]_{myo}$ increased with the increase in the pacing frequency from 0.20 (0.33 µM) to 4 Hz (0.64 µM), peaking at 4Hz (Fig 11A). A decline in the peak amplitude was observed from 5 Hz (0.61 µM) to 7 Hz (0.56 µM). In experiments and previous models, the overall shape of Ca^{2+} transient from lower to higher beating frequency used to be called a dome-shaped curve (Buckley, 1972) (Hasefus, Holubarsch, Hermann, Astheimer, Pieske, & Just, 1994) (Jafri, et al., 1998) now it is simply known as the positive or negative slope (Godier-Fornemont, 2015). The model showed a positive slope till 4 Hz frequency and negative slope after that and overall, it is a positive force-frequency relation (FFR) curve. A positive FFR is

an intrinsic contractile property of a ventricles myocyte in higher mammals and it is the result of a frequency-dependent acceleration of relaxation (Endoh, 2004) (Godier-Furnémont, et al., 2015) and our model reproduced this behavior. Varian and Janssen (2007) performed an FFR experiment in rabbit (in-vivo) and calculated FFR (Fig. 11B). They have shown the both FFR and Ca^{2+} transient was positive till they reached to 4Hz and figure 11B shows our model followed the similar pattern. They were unable to get the data in higher pacing because it was thought with the high metabolic demand and greater rundown, data might be compromised. Endoh (2004) also reported similar results from rabbit papillary muscle, the Ca^{2+} transient was still positive till 4 Hz but the contractile force associated with the amplitude of Ca^{2+} transients showed positive FFR from 0.13Hz to 3.30 Hz, then started to dissociate just before 4 Hz. He also observed negative FFR in Rabbit in higher frequency and believed it happened because of altered Ca^{2+} handling and Ca^{2+} overload.

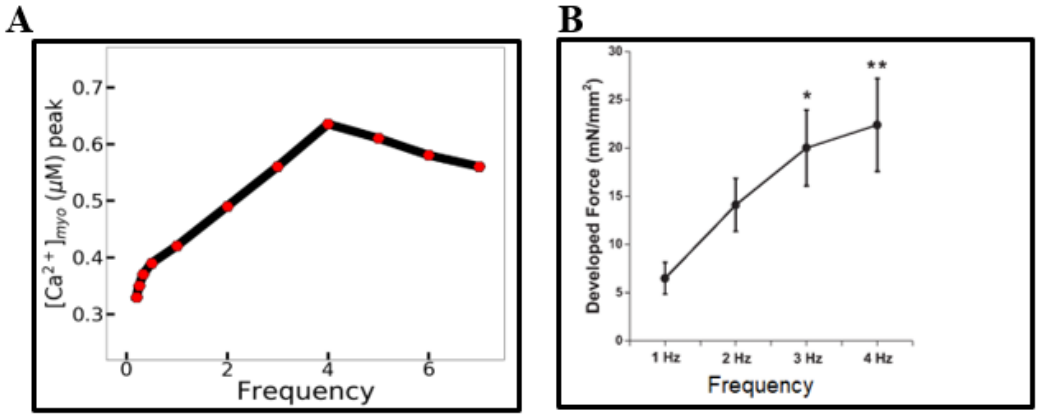

Figure 11: The Ca^{2+} transient peak (FFR curve) (A) derived from our model with simulation from 0.2 to 7Hz, with primary positive FFR (0.2 – 4Hz) and secondary phase negative FFR (5–7Hz) (B) An experimental FFR of rabbit ventricular trabeculae showing positive FFR (1 – 4Hz) (adapted from (Varian, 2007)).

With the increase in pacing frequency, we also recorded the RyR2 P_O (Fig 12A), $[Ca^{2+}]_{nsr}$ (Fig. 12B), the coupling of RyR2 P_O with $[Ca^{2+}]_{nsr}$ (Fig. 12C), and AP amplitude (Fig. 12D), all of them behaved similar to FFR, peaked at 4Hz pacing and slowed down thereafter. In the meantime, we also looked at the adaptation feature of RyR2 with the increase in cytosolic Ca^{2+} in the rapid pacing and discovered the diastolic adaptation fraction of RyR2 (Fig. 12E) was still peaking up after 4 Hz but slowed down only after 6 Hz pacing. The rapid pacing rate means bringing more extracellular Ca^{2+} per unit time and it increased the level of Ca^{2+} ($[Ca^{2+}]_{myo}$, $[Ca^{2+}]_{jsr}$ & $[Ca^{2+}]_{nsr}$) in the intracellular compartments. As stated in equation 1 above, the collective response of SR Ca^{2+} along with RyR P_O provides the Ca^{2+} availability for the release via RyR2 was enough for the

further increase of FFR but it also went down because of decrease in RyR P_O. Endoh (2004) stated that SR Ca^{2+} plays the central role in determining the FFR but the only way to get it out is RyR2. But some RyR2 channels stay inactive in the diastolic

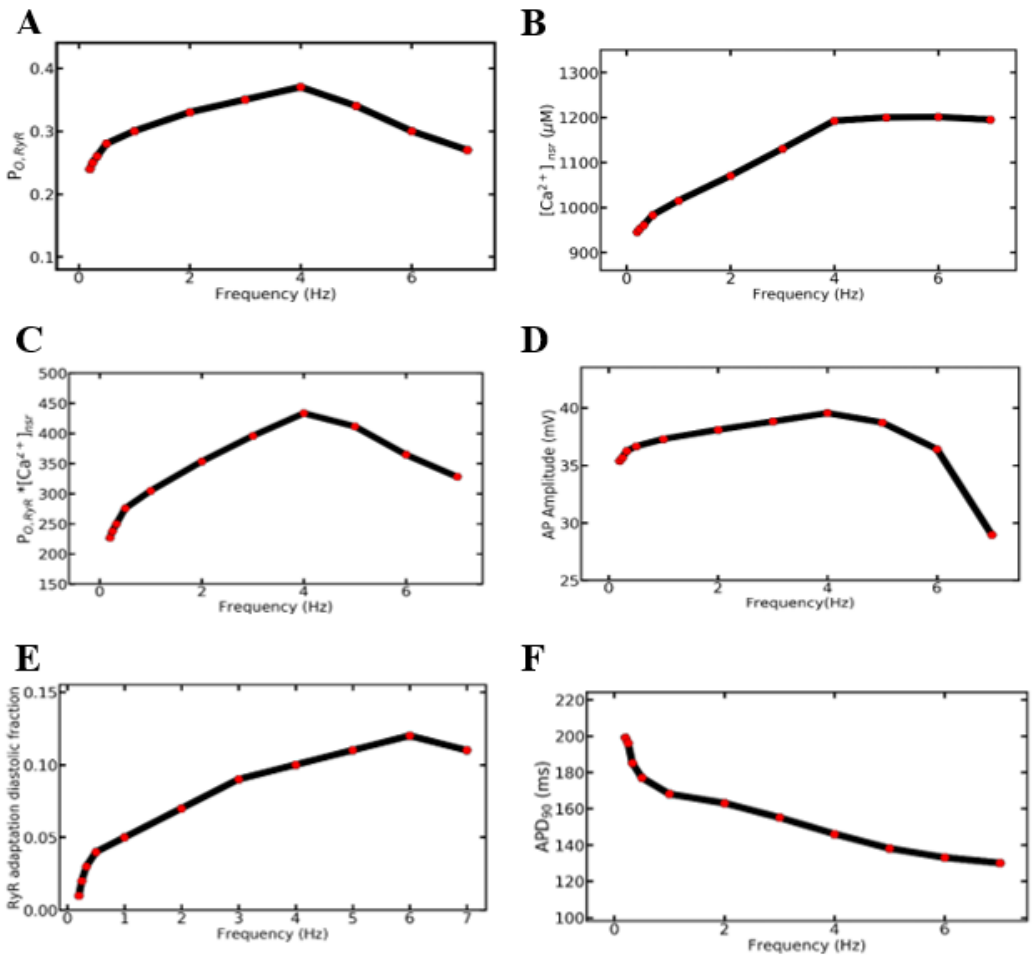

Figure 12: The FFR is determined by Ca^{2+} transient in the intracellular chambers of a myocyte. (A) The RyR2 PO is the main component to release SR Ca^{2+} and increase SR release to produce large Ca^{2+} transients with the rapid pacing. (B) Increase activity of SERCA2A pumps take the benefit of per unit time increase extracellular Ca^{2+} via L-type channels

and refill quickly to increase SR Ca^{2+} load. (C) A coupling of RyR2 P_O with SR Ca^{2+} displays their capacity to increase the contractile force with an increase in pacing frequency. (D) An increase in AP amplitude noticed with the pacing frequency increase. (E) The adaptation of RyR2 is still very high during the diastolic phase. (F) APD gradually declines in our model with an increase in pacing frequency.

phase and continue to do so during the systolic phase too due to their nature of slow adaptation after activated by a strong Ca^{2+} stimulus. The RyR2 adaptation is a regulatory mechanism that triggers when there is high $[Ca^{2+}]_{myo}$ and successive $[Ca^{2+}]_{myo}$ might open them but become inactive (adapt) right after activation (Gyroke 1993). In our model, we found the 5% RyR2 in adaptation state in 1 Hz and it reached 13% in the 6Hz during diastole and the number increased during the systolic phase. This RyR2 in the adaptive state played the role of the fewer opening of RyR2 and release less SR Ca^{2+} to the cytosol. The increase in RyR2 adaptation with the rapid accession of cytosolic Ca^{2+}, many of the RyR2 channels went to the adapted state and stayed inactive which lowered the available number to initiate sparks in the higher pacing. The force of contraction of the heart depends upon the amount of SR Ca^{2+} released but the adaptation limited the Ca^{2+} release and so the force of contraction gets smaller the and the positive FFR dissociates in higher pacing.

With the increase in pacing frequency, we spotted the APD constantly decreasing from 0.2 Hz to 7 Hz (Fig. 12F). It has been said that the faster pacing rate leads to a physiological shortening of APD. Szigligeti *et al.* (Szigligeti, Pankucsi, Banyasz, Varro,

& Nanasi, 1996) changed positive FFR to negative FFR by shortening APD. The frequency dependence of APD is caused by a decrease of the inward current, L-type current, and increase of outward current, Na^+-Ca^{2+} exchange current (Wang, Chen, Liu, Xiao, & Wang, 2014). In our model, we also observed the frequency dependence decrease of I_{LCC} and the increase of I_{ncx}.

L-type current decreases and I_{ncx} current increases with the Rapid Pacing

With the increase of pacing frequency, the per-second flux of Ca^{2+} increases but the entry of Ca^{2+} in each beat via L-type channel decreases (Fig. 13A). On the contrary, the electrogenic I_{ncx} current elevated with the increase in the pacing frequency (Fig 13B). We found a constant decrease in amplitude from -8.19 μA/Cm^2 in 0.20 to -6.22 μA/Cm^2 in 7 Hz (Fig. 15A) pacing. The Ca^{2+} dependent inactivation of L-type channels is shorter in lower frequency (Fig. 15C) but it was rising in the higher frequency (15D) (1Hz vs 6Hz). With the frequency-dependent increase in RyR2 P_O (12A), the LCC channels were inactivated by increase release of SR Ca^{2+} into the cytosol. The loss of L-type current leads to a decrease in plateau phase in AP which also decreases the APD with increasing pacing rate. The SR Ca^{2+} serves as the feedback mechanism to the L-type channels and their amplitude decrease with the increase in pacing frequency (Kubalova, 2003). In our simulation, the extrusion of Ca^{2+} from Na^+-Ca^{2+} exchanger constantly increases from 0.2 Hz to 7 Hz (Fig. 13B). An increase in I_{ncx} current means the extrusion of Ca^{2+} from the myocyte in exchange for Na^+ with Ca^{2+} (three Na^+ in & one Ca^{2+} out) which brings net

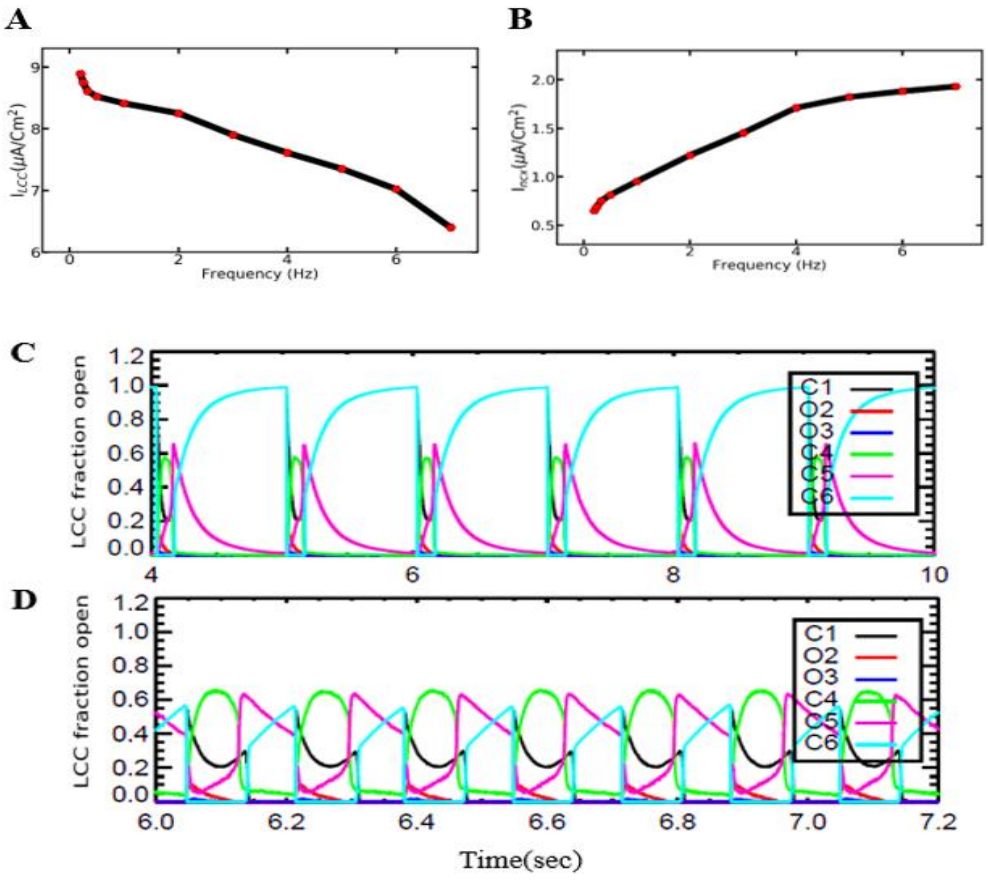

Figure 13: Influx of Ca^{2+} decreases with the surge in Ca^{2+} dependent inactivation of L-type channels and extrusion of Ca^{2+} goes up with the surge in cytosolic Ca^{2+} in rapid pacing frequency. (A) I_{LCC} amplitude decreases with the increase in the beating rate. (B) An increase in I_{ncx} occurs when pacing frequency increases. (C) & (D) showing different opening, closing, or inactivation states of L-type channel in 1 Hz and 6 Hz pacing frequencies respectively. C4 (green) represents CDI state and it is higher in 6Hz than 1 HZ. C_1 (black) & C_6 (cyan) closed states, O_2 (red) & O_3 (blue) open states, and C_5 (magenta) VDI state.

the positive charge in as the depolarizing current. In the model, we noticed the amplitude of I_{ncx} gained ~3 folds in between 0.2 Hz to 7 Hz (0.65 to 1.93 μA/Cm^2). The content of SR Ca^{2+} accounts for the force-frequency relationship and it is reliant on the extracellular Ca^{2+} entered via LCC and competition with cytoplasmic extrusion, especially I_{ncx} (Bassani, et al., 1994) (Terracciano, & MacLeod, 1997). The increased amplitude of I_{ncx} in rapid pacing should help to the dissociation of the FFR. The role of L-type current in FFR., other than bringing more extracellular Ca^{2+} and initiating the CICR, is controversial. Rossman *et al*. (2004) found that increased I_{LCC} couldn't reverse negative FFR in failing heart but pumping more Ca^{2+} to the SR changed it to the positive FFR. In the model, we did not see it increasing with primary positive or secondary negative FFR.

Calcium sparks are the Subcellular Mechanisms of FFR

The above results enumerate very well the role of Ca^{2+} transient in reproducing force-frequency relationship (FFR). The model allows an analysis of how Ca^{2+} spark frequency and Ca^{2+} spark amplitude regulate the Ca^{2+} transient and the resulting contractile force of a myocyte. Ca^{2+} spark properties show similar behavior to Ca^{2+} transients (Fig. 13A). The average number of Ca^{2+} sparks in each beat at different frequencies increases from 0.2 Hz continuing to 4 Hz pacing and the number of sparks gradually decreased thereafter (Fig. 14A). The maximum number of sparks appeared at 4 Hz pacing (83,553 ± 5105). Lukyanenko and Gyorke (1999) found the frequency of the sparks increases with the increase in SR Ca^{2+} load and due to the loss in SR Ca^{2+} load would decrease it. A coupling of Ca^{2+} sparks with SR Ca^{2+} ($[Ca^{2+}]_{nsr}$) load (Fig. 14B), the product also became the largest in 4 Hz pacing. As we mentioned above, every surge in

frequency also brought a similar upsurge in Ca^{2+} spark numbers, when it was coupled with the fractional RyR2 P_O (Fig. 14C), it showed a negative slope after 4 Hz.

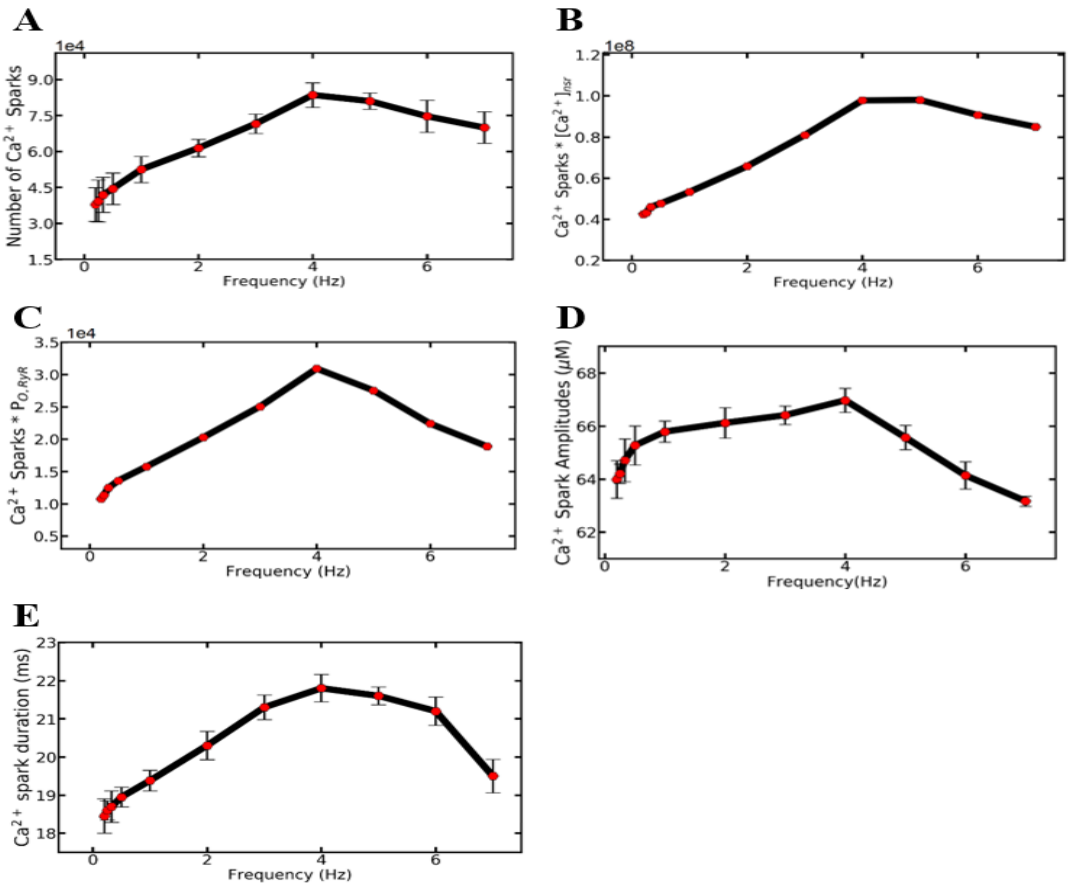

Figure 14: Ca^{2+} sparks frequency and amplitudes are better in predicting FFR. (A) An increase in Ca^{2+} sparks frequency with the increase in the beating rate. (B) Higher the pounding of cardiac myocyte so as the average Ca^{2+} spark amplitude. (C) Highest Ca^{2+} spark amplitude found in the 4 Hz pacing. (D) Counting of the larger sparks (> 100 µM) (E) A product of Ca^{2+} spark and RyR open fraction has peaked at 4 Hz. (F) A combined product of Spark count and NSR $[Ca^{2+}]$ has a peak at 4 Hz.

due to decreasing in RyR2 opening fraction. Both couplings showed the Ca^{2+} spark activities were very high at 4 Hz frequency and they generated maximum contractile force in 4 Hz. The fast increase and decrease RyR2 P_O coupled with the sparks (Fig. 14C) looked more like frequency-dependent phenomenon, so besides SR load, the Ca^{2+} sparks also depend upon the number available channels of RyR2 or simply RyR2 P_O. After this, the spark numbers in compared to 4 Hz value went down by ~5%, ~11%, ~17% with 5, 6, and 7 Hz, respectively. Besides sparks frequency, the average spark amplitudes also pursued the same trend and the peak amplitude (62.95±0.55 μM) also occurred in 4 Hz pacing and constant fall after that (Fig. 14D). Comparable to Ca^{2+} sparks, the SR load also affects the possibility of occurrence of larger or smaller spark amplitudes (Song, Stern, Lakatta, & Cheng, 1997) (Izu, Wier, & Blake, 1998). The model found the largest average amplitudes when SR load was higher in 4 Hz. A larger amplitude means a greater force is generated; hence the contractile force became higher in 4 Hz pacing. The Ca^{2+} spark duration is another activity performed by intracellular Ca^{2+} and it was also gradually increased from low pacing frequency to higher frequency being the longest for 4 Hz. This means the spark duration was also maximum at 4 Hz and underway to be shorter thereafter. All the above results, Ca^{2+} sparks, Ca^{2+} spark amplitudes, and Ca^{2+} spark duration suggested that the peak intracellular Ca^{2+} activities occurred during 4 Hz pacing and it was translated into the FFR curve. When the SR load, the number of available RyR2 started to dwindle, the FFR became negative too. The mechanism behind the increase in Ca^{2+} transient hence surge in the force generated by myocyte, is related to subcellular activities of Ca^{2+}.

Luminal Dependence and SR Ca^{2+} Play Major Role in FFR

The release of SR Ca^{2+} during CICR is regulated by luminal Ca^{2+}. When RyR2 is activated by cytosolic Ca^{2+}, the SR Ca^{2+} towards the luminal region plays an important part to modulate RyR2 P_O (Györke, 2008), higher luminal Ca^{2+} availability amplifies P_O

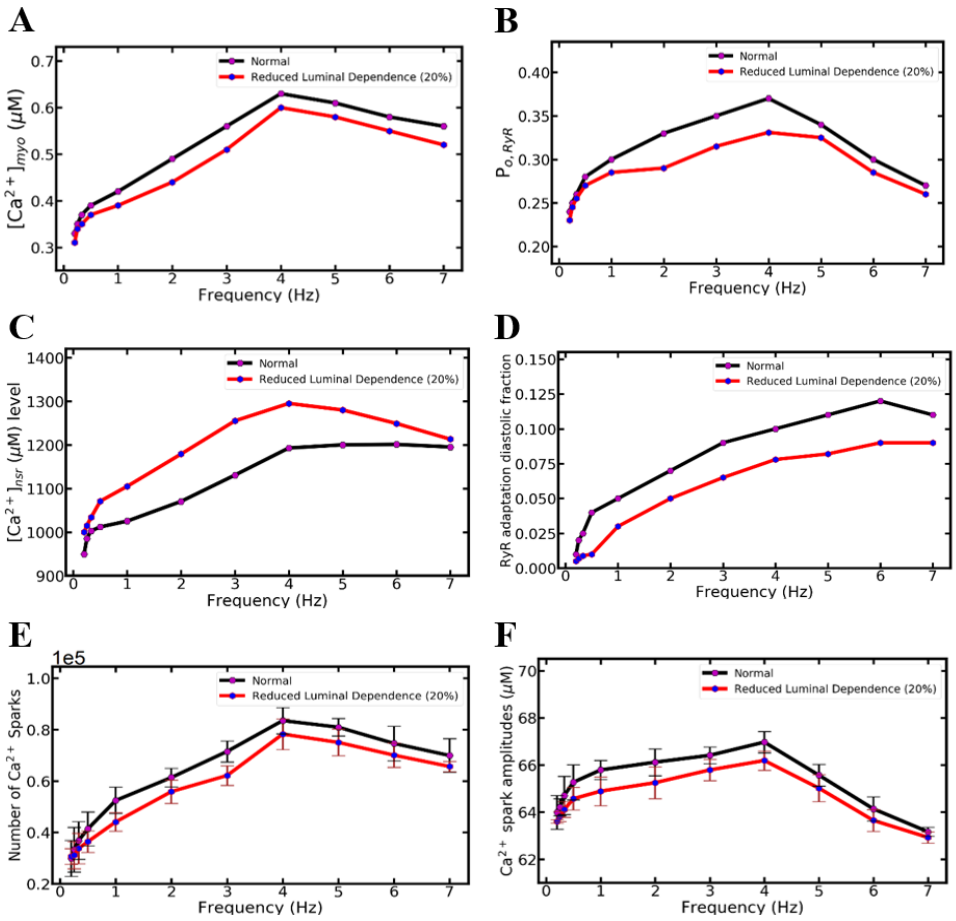

Figure 15: Luminal Ca^{2+} does not activate RyR2 in CICR but plays a major role to increase or decrease the RyR2 P_O to regulate the dynamics of intracellular Ca^{2+}. Here are the comparison plots of the original value of Luminal Ca^{2+} and a 20% reduction.

(A) Ca^{2+} myoplasm peak transients get smaller with a reduction in luminal dependence. (B) SR luminal Ca^{2+} is the modulator of RyR2 PO, any decrease in its value directly affects the opening probability of RyR2 channels (C) Smaller the RyR2 Po, less SR Ca^{2+} release while lower value reduces it. (D) Adaptation is another feature that is linked to cytosolic Ca^{2+}, smaller the myoplasmic transients, so as the RyR2 adaptation. (E) Smaller SR luminal value decreases RyR2 PO and it also lowers the formation of Ca^{2+} sparks. (F) The average Ca^{2+} spark amplitudes also reduced with the reduction in luminal dependence.

A simulation ran after lowering luminal dependency by 20%; we observed the Ca^{2+} transient peaks were smaller (~6%) in comparison to the normal luminal value (Fig. 15A). This happened because of the lowering of RyR2 P_O (15B) released depressed the SR Ca^{2+} required for the CICR. As a result of this, we also found an increase in the SR Ca^{2+} load (Fig. 15C). The decreasing luminal activity also played a role in lowering the diastolic fraction of RyR2 because a decrease in the cytosolic Ca^{2+} lowered the RyR2 adaptation rate (15D) and it solely depends upon cytosolic Ca^{2+}. Similarly, the numbers of Ca^{2+} sparks (Fig. 15E) and the average amplitude of the sparks were lower with the reduced luminal Ca^{2+}. Since SR Ca^{2+} load decides the Ca^{2+} sparks but lower P_O caused them to decrease. Sobie, Dilly, Cruz, Lederer, and Jafri (2002) reported RyR2 activity linearly depend on luminal Ca^{2+}, lowering the luminal value shifted the luminal regulation away from the RyR2 and the CICR related activities were affected and a smaller number of Ca^{2+} sparks and sparks with smaller average amplitudes were detected.

In comparing simulations, we found ~8% 57837±18935 vs 53322±17377) fewer sparks per beat were released with a 20% reduction in luminal dependence than in the normal simulation. During CICR, the results showed more SR Ca^{2+} residue.

Adaptation Brings Negative Feedback Mechanism to the RyR2 P_O

Adaptation in our model acts as a time-dependent phenomenon that shifts the modal gating behavior of RyR2. A 20% lowering of the adaptation rate of the RyR2 channel, we found a 4% increase in the size of Ca^{2+} transients (Fig. 16A). It happened because of the RyR2 P_O (Fig. 16B) went up with the lower shifting of adaptation property of the channels. The increased RyR2 P_O made helped to drain more SR Ca^{2+} (16C) to produce larger Ca^{2+} transients. The adaptation rate itself went down which can be seen in figure 18D. The increased SR release also produced a greater number of Ca^{2+} sparks (Fig. 16E) and larger average spark amplitudes (Fig. 16 F). In analyzing Ca^{2+} spark behavior, it was found a 5% increase (57837±18937 vs 60768±19752) Ca^{2+} sparks per beat with this simulation. Jafri *et al.* (Jafri, 1998) reported that the adaptation of RyR2 decreased its P_O with the beginning of rapid pacing. In this model, the RyR2 P_O and its adaptation got bigger as the pacing frequency increased but RyR2 P_O declined with the negative FFR. After simulating with the reduced adaptation value, we also found the RyR2 P_O went up by 7% so it was up before because both luminal dependency and stimulus by subspace Ca^{2+} provide positive feedback to the P_O. Sobie *et al.* (2002) showed that even in the absence of L-type current stimulation, the subspace Ca^{2+}, $[Ca^{2+}]_{ss}$ increased four times more Ca^{2+} sparks from 100 nM to 1 µM.

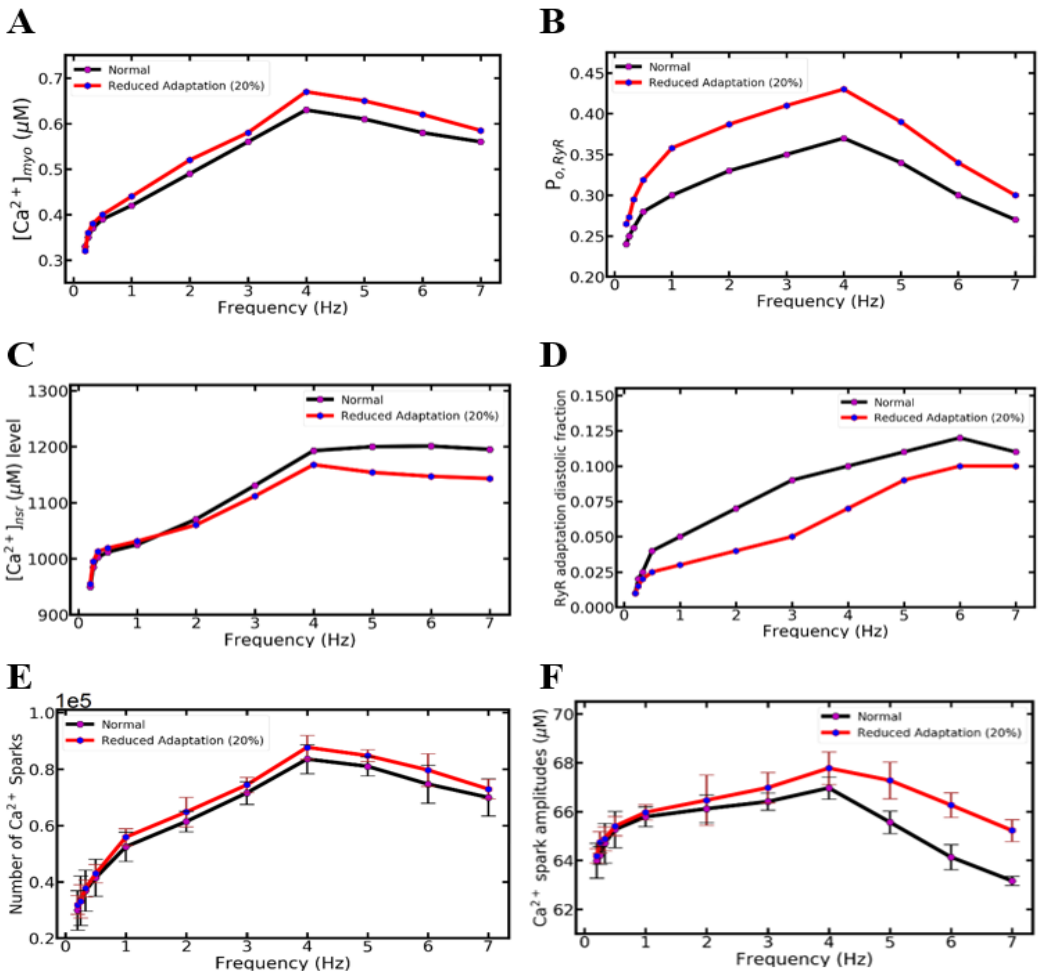

Figure 16: The RyR2 activity increases to the fast Ca^{2+} stimulus and decays spontaneously thereafter because some channels enter the adapted phase. (A) When the adaptive behavior of RyR2 channels is reduced, the channels continuously open and release more SR Ca^{2+} with higher RyR PO (B). (C) The higher RyR2 Po depletes the level of SR Ca^{2+}. (D)The diastolic adaptive fraction of RyR2 also stays low with smaller adaptation values. Higher RyR2 PO due to lower adaptation value increases both Ca^{2+} sparks (E) and their average amplitudes (F).

A Role of RyR2 Opening Rate Constant in FFR

A lowering of 20% RyR2 opening rate constant decreased the peak amplitude of Ca^{2+} transient by 4% (Fig. 17A) than the normal one. The opening probability plays a major role in the starting of CICR but after this luminal Ca^{2+} becomes the main modulator of the opening rate than the probability of RyR2 open. The decreased opening rate of RyR2 (Fig. 17B) rendered the release of SR Ca^{2+} slow and SR load increased (Fig. 17C). The diastolic adaptation of RyR2 (Fig. 17D) almost remains the same because the Ca^{2+} transient did not increase enough to adapt in compared to normal conditions and it stayed the same. The Ca^{2+} sparks (Fig. 17E) and Spark amplitude (Fig. 17F) were also decreased due to a decrease in RyR2 P_O. A 3% decrease per beat was found with the lowering of RyR2 open constant (57837±18937 vs 55991±18182). The phosphorylation of in RyR2 increases the diastolic Ca^{2+} leaks (Marx, Reiken, Hisamatsu, Jayaraman, Burkhoff, Rosembit, et al., 2000) and a decrease in RyR2 P_O should decrease Ca^{2+} leak. In comparing the model data of 1 Hz pacing we found a small number of leak increase (1441±914) with reducing rate constant. The total diastolic leak rate for 1 Hz pacing was 28687±1632 for the normal simulation while it was 27246±1589 for the 20% reduced constant rate simulation.

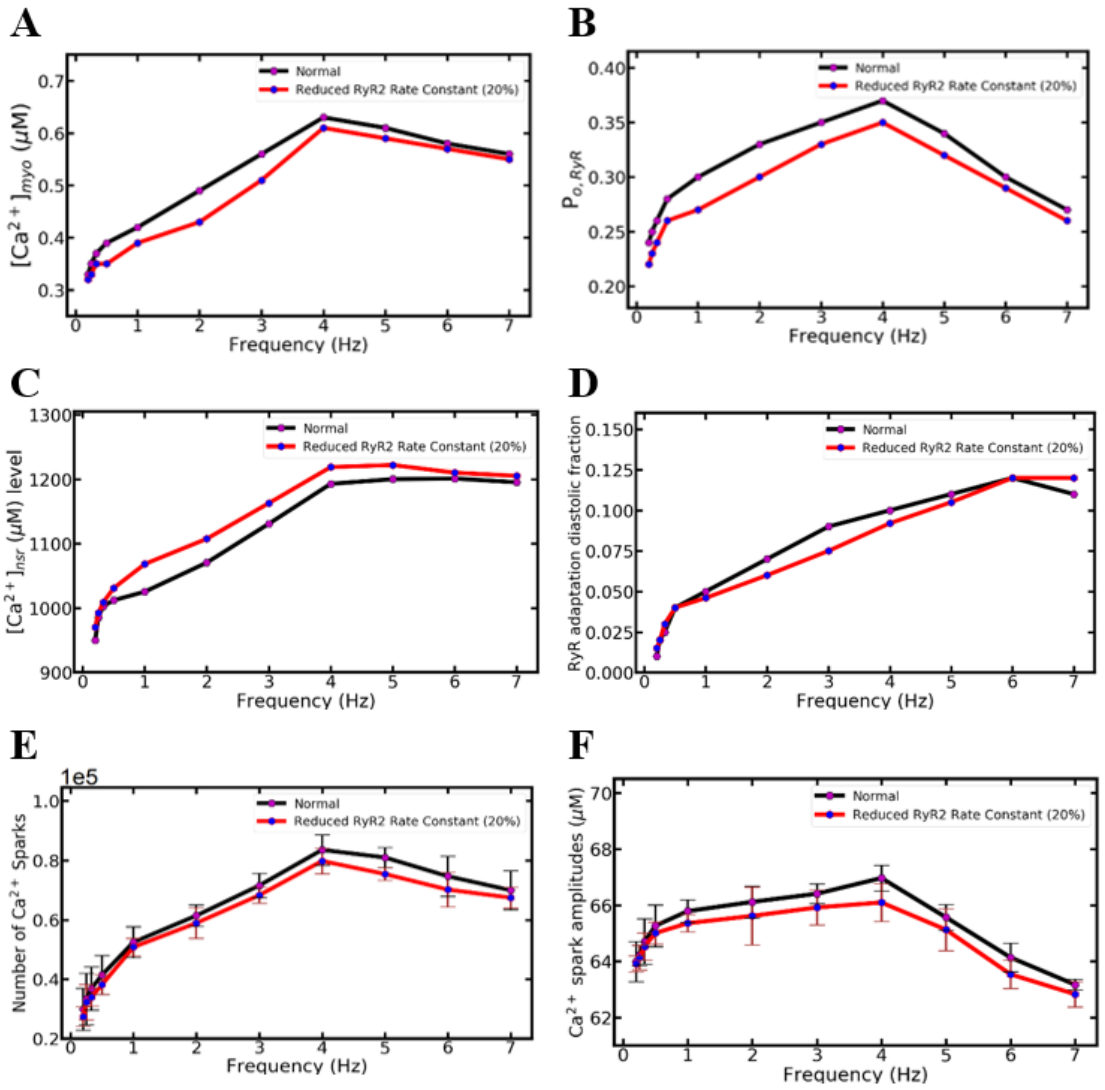

Figure 17: Reducing opening rate constant means there are lower numbers of RyR2 will open in a cluster per second, the result will be smaller Ca^{2+} transients (A) lower probability of opening of RyR2 channels (B), the increase SR Ca^{2+} load (C). It was also seen the lower RyR2 PO made smaller changes in adaptive behavior, probably low cytosolic Ca^{2+} (D). The number of Ca^{2+} sparks (E) and average Ca^{2+} spark amplitudes were also down with the decrease in the opening rate constant (F).

The altering value of the rate constant to move closed RyR2 channels to open states in each state showed that it has a negative effect on RyR2 P_O but in all other simulations, it always remains a fixed value so it has no role in affecting the outcome. On the other hand, the luminal Ca^{2+} and RyR2 adaptation play a positive and negative role in controlling RyR2 PO, respectively.

Pacing Protocols in FFR

We simulated with the widely used pacing protocol in the FFR experimentation of cardiac myocyte. Based upon this protocol - first, we simulated 0.5 Hz pacing, then it was raised to 1.5 Hz pacing and again brought back to 0.5 Hz pacing as shown in figure 16. For all these 3 steps, the simulation ran for 60 seconds for stable output. It was noticed a minimal decrease in the amplitude of AP (39.49 to 39.23 mV) (Fig. 18A) from lower to higher and a 9 ms difference in the AP duration (172 ms to 163 ms) in a similar way. Like classic staircase response, Ca^{2+} transient in myoplasm exhibited lower amplitude during the transitional steps between lower to higher pacing (Fig. 18B). Due to shorter diastolic interval for SR refilling (Fig. 18C), unable of RyR2 channels to recover fully from previous inactivation (Fig. 18D), and a fraction of RyR2 is also in adaptive state C_3, the first few transients are smaller than the normal one but they are forming a positive staircase and after 6-7 beats, they converted into a steady state. On the other hand, in the transition between higher to lower pacing, the first transient of 0.5 Hz is relatively higher because of longer diastolic phase for SR refilling and greater time available for RyR2 to reactivation, a larger load of $[Ca^{2+}]_{SR}$ released into subspaces which make the first transient to jump up. The larger SR release and longer diastolic interval also increase the

extrusion of Ca^{2+} with the increase of I_{ncx} current. Gradually, the transients form a negative staircase and enter the stable state, which means the contractile force was higher in the beginning and changed into a steady-state in a short while.

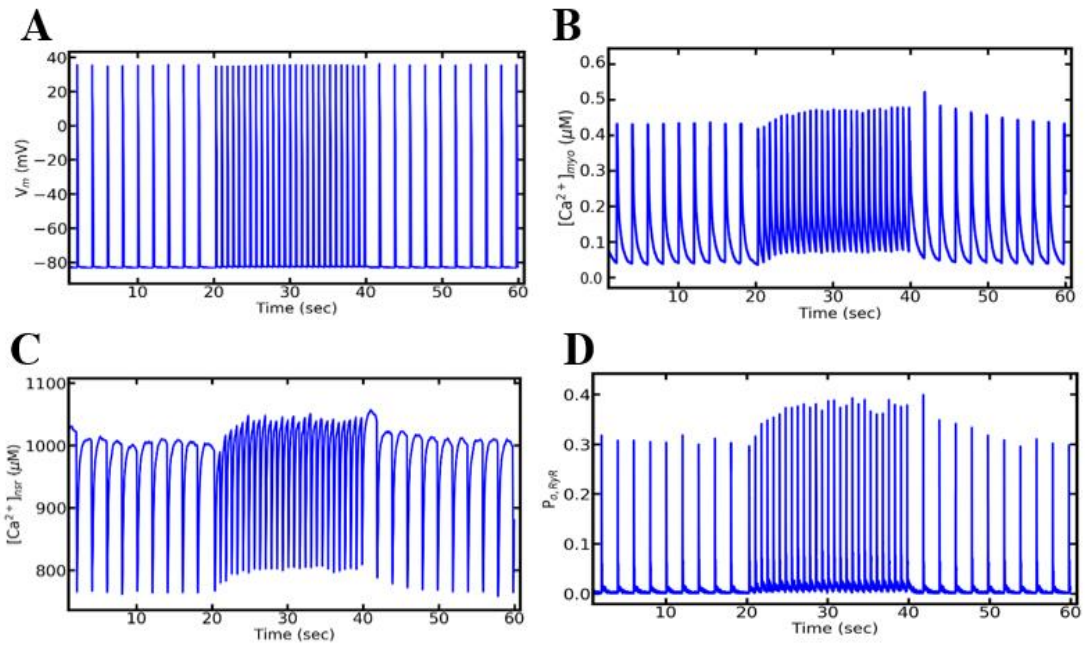

Figure 18: The force-frequency relationship in slow-rapid-slow pacing.

(A) A minimal decrease in AP amplitude and duration in rapid pacing (B) A few smaller Ca^{2+} transients, $[Ca^{2+}]_{myo}$ at the beginning of faster pacing form positive staircase then turn into a steady state. (C) The NSR Ca^{2+} load gradually increases in the rapid pacing (1.5 Hz) and it decreases gradually at the beginning of slow pacing (0.5 Hz). The first transient at the beginning of low pacing is very high and transients gradually lowered in amplitude thereafter to attain a steady-state (D) The peak RyR2 open fraction showed a fewer opening at the start of rapid pacing before reaching into a stable state.

Due to the stochastic opening and closing of Ca^{2+} channels, it was always noticed variations in the amplitude of RyR open fraction in the consecutive beats even steady state. An increase in the open fraction rate seen at the beginning of a lower frequency of pacing. From above it was noticed that when there is higher availability of SR Ca^{2+} to be released, the open fraction of RyR2 is also high and oppositely, if SR refill is less, the open fraction of RyR2 is also reduced. The interplay of these two plays a major role in the force-frequency relationship and this is a widely studied phenomenon in both experimental and model settings. This protocol pacing is well studied in both experimental (Bers, 2001) and model settings (Jafri, et al., 1998) and our model was also able to mimic similar results.

Discussion

The frequency-dependent performance of the myocardium changes the contractile strength of the heart. For human, rabbit or Guinea pig, the beating strength of the cardiomyocytes increases in the subsequent increase in the beating frequency. With a model of ventricular myocytes of Guinea pig, we studied the role Ca^{2+} dynamics in predicting the FFR during the rapidly-paced cardiomyocytes with the classical approach of the Ca^{2+} transient method and quantified it with the behavior of Ca^{2+} sparks in the subcellular level. The contractile force depends upon the Ca^{2+} transients formed by Ca^{2+} sparks but the answer we were looking for was what is the control mechanism to guide the release of SR Ca^{2+}. The developed model captured and counted every Ca^{2+} spark formation when they occur. The model displayed a positive FFR starting from 0.2 Hz to

ending at 4 Hz pacing the calcium transients constantly increase to the RyR2 P_O, RyR2 adaptation, and SR Ca^{2+} load. The RyR2 P_O started to decline when it transitioned to 5 Hz from 4 Hz pacing. At the same time, the upward trajectory of SR Ca^{2+} ceased and started to dwindle slowly but the adaptation behavior of the RyR2 channels did not decline yet. The positive FFR is the characteristic of the higher mammalian myocardium including Guinea pig and rabbit (Endoh, 2004) (Szigligeti, 1996). Endoh (2004) and Varian and Janssen. (2007) reported in the rabbit the Ca^{2+} transient is positive till 4 Hz pacing and starts to be negative after that and our model exactly reproduced this behavior. The question to be answered is what is the beginning of negative FFR in frequency-dependent stimulation. The mechanism of FFR as the function of frequency-dependent activation is still moderately understood (Janssen, 2007), we are looking positive and negative feedback mechanism to the RyR2 PO by luminal dependence or SR Ca^{2+} load and RyR2 adaptation respectively and their interplay to generate positive FFR.

It was thought in the beginning RyR2 adaptation is relatively slow as a negative control mechanism but Valvadia, Kaplan, Ellis-Davies, and Lederer (1995) found that the adaptation was ~10-fold faster with Mg^{2+}. The adaptation rate for this model was seven per second. The result of this stochastic model agrees with the deterministic model developed by Jafri *et al.* (1998). In that model, they found adaptation was necessary to produce FFR related behavior. After running simulation reducing adaptation value by 20%, there was an increase in Ca^{2+} transients, Ca^{2+} sparks and their amplitudes, and RyR2 P_O. In negative FFR, after very high frequency, when both SR Ca^{2+} release and Ca^{2+} transient became smaller, then diastolic adaptation went lower too. In lower pacing,

the contractile force cannot be high because of low $[Ca^{2+}]_{sr}$ though there was very adaptive control of RyR2. In higher pacing, there was a higher SR load, $[Ca^{2+}]_{sr}$ to yield bigger contractile force but RyR2 undergoes accumulation and reduces P_O. Puglisi Negroni, Chen-Izu, and Bers (2013) stated it was not RyR2 adaptability only, was the adaptation of the heart to keep it intact in the extreme Ca^{2+} load in the intracellular compartments when it continuously pumps in high-frequency rate. For instance, in β-adrenergic stimulation, it prepares the ventricles to accommodate the higher beating rate.

The frequency-dependent increase of SR Ca^{2+} load is the major contributor to FFR (Endoh, 2004). Our model displayed a loaded SR with each pacing rate increase. The higher SR load produced larger Ca^{2+} transients via upward trending RyR2 P_O modulated luminal dependency. The role of SR Ca^{2+} is further illustrated by a positive staircase phenomenon (Bers, 2001). An increase in heart rate increases the force of contraction generated by the myocyte and the phenomenon is associated with intracellular Ca^{2+} handling in the myoplasm. In steady-state, with every depolarization, the influx of Ca^{2+} from L-type channels leads to Ca^{2+} release from SR. Myocyte relaxes when Ca^{2+} returns to its original concentration by removing Ca^{2+} from cytosol refill back to the SR by SERCA and efflux via Incx. But when pacing frequency increases, there is an increase per second flux of L-type channels and SERCA concentration increases with the increase in $[Ca^{2+}]_{myo}$ which increases refill of Ca^{2+} to the SR. With the increase in pacing frequency, there is a shorter time interval between consecutive beats which decreases Ca^{2+} efflux via I_{ncx}. The increase in SR Ca^{2+} load also increases contraction force generated by myocyte in rapid pacing. The first Ca^{2+} transient from lower pacing to

higher becomes shorter due to smaller recovery time to RyR from the previous inactivation with a shortened diastolic phase either. Continuous pacing in higher frequency leads to a gradual increase in a positive staircase before reaching into a steady state. If the pacing rate decrease from higher to lower frequency, opposite to previous condition the first Ca^{2+} transient becomes greater and a falling continuous before entering a steady state. This is because of increased SR load due to an increased influx of Ca^{2+} per unit time in rapid pacing as well as enough time to reactivation of RyR channels due to the elongated diastolic phase. We have also found 3 factors contributing positive staircase similar to Bers (2001) in higher pacing – (a) Increase in L-type Ca^{2+} per unit time (not per unit beat), (b) Higher diastolic $[Ca^{2+}]_{myo}$, and (c) Increased SR Ca^{2+} load $[Ca^{2+}]_{sr}$ available to be released in subsequent beats.

The FFR is an important indicator in finding failing or non-failing hearts. The twitch tension (FFR) rises in a normal heart but does not rise in the failing one (Mulieri, Hasenfuss, Leavitt, Allen, & Albert, 1992). Heart failure is characterized by the decay of contraction and small systolic Ca^{2+} transients (Eisner, & Tafford, 2002). They also explained the small Ca^{2+} transients in two theories – decreased activities of SERCA2a to reload SR and decreased RyR2 $P_{O.}$ Though SERCA2a activity was not the direct focus of current research, with the negative FFR (after 5 Hz) we found decreased in SR Ca^{2+} load and reduced RyR2 PO, both played the role to release the SR Ca^{2+} in the smaller transients. The model also showed there was a reduction in I_{LCC} and improved I_{ncx}, the former is responsible for decreasing RyR2 activation and the later one competes with SERCA2a to extrude Ca^{2+} out of the myocyte. In the model, with the 20%

dephosphorylation of the RyR2, we found a small decrease (5%) in the SR Ca^{2+} spark leak which increased SR Ca^{2+}. In the failing heart, the opposite occurs, there is an increase in RyR2 Po due to hyperphosphorylation but it also increases diastolic Ca^{2+} leak and limits the amount of Ca^{2+} in the SR (Wagner, et al., 2015) (Marx, et al., 2000). In agreement with Endoh, (2004), the SERCA2a pumps in the failing heart exhaust their capacity to reload SR Ca^{2+} and the positive FFR turns into negative FFR and the function of the heart is ceased (Endoh, 2004), the model also gave more reasons to believe that decrease SR load caused negative FFR rather than SR leak. For a normal myocyte, the force-frequency curve tells us an increase in pacing rate results in higher Ca^{2+} levels in the myocytes and increases in the contractile force but a dissociation in that force is necessary to prevent the myocyte from any mechanical damages. A healthy myocardium needs the positive FFR to continue a contractile behavior and in heart failure, the heart loses its ability to refill SR to continue to the frequency-dependent positive FFR (Pieske Maier, Bers, & Hasenfus, 1999).

Conclusions

The force-frequency relationship is a survival feature in many organisms. It allows the heart to adjust itself with contractile property and control the cardiac output during rapid or frequent pacing. The continuous refill and replenish of SR by SERCA pump and enhancement SR Ca^{2+} release is highly critical for increased force-frequency response. Our model predicts both the cellular and subcellular mechanism of FFR. In cellular mechanism, the model predicts, in agreement with our previous modeling studies

(Jafri *et al.*, Biophys J. 1998 Mar;74(3):1149-68), that diastolic sarcoplasmic reticulum (SR) $[Ca^{2+}]_{SR}$ and RyR2 adaptation increases with increased stimulation frequency giving rise rising than falling amplitude of the myoplasmic $[Ca^{2+}]_{myo}$ transients. The model also allowed us to dissect these frequency-dependent changes down to the spark level getting new insight into mechanism governing cardiac calcium dynamics. The computational model of Ca^{2+} dynamics in the Guinea pig ventricular myocyte suggests the following:

- In guinea pig myocyte like other higher mammals, the FFR is positive, the peak of force generation occurred in 4 Hz pacing.
- Adaptation of RyR2 channels after the large stimuli of Ca^{2+} is equally important as SR Ca^{2+} load to bring negative FFR in the very high pacing myocyte.
- $[Ca^{2+}]_{myo}$ transient is highest at 4 Hz. Similarly, the frequency of Ca^{2+} sparks, average Ca^{2+} spark amplitude, Ca^{2+} spark duration, and RyR Po, all had a peak at 4 Hz.
- Like Ca^{2+} transients, Ca^{2+} sparks also have the same FFR in all pacing frequencies as they are Ca^{2+} sparks are the fundamental units to Ca^{2+} transients.
- The average spark amplitudes and the spark durations increased with increasing pacing frequency play.
- The product of the number of sparks and the average spark amplitude yields similar shapes as the force-frequency relation in the experiment.
- The complex dynamics of the force-frequency relation depends greatly on local Ca^{2+} dynamics and can also be explained by the characteristics of Ca^{2+} sparks.

References

Bassani, J. W., Bassani, R. A. & Bers, D. M. (1994). Relaxation in rabbit and rat cardiac cells: species-dependent differences in cellular mechanisms. *Journal of Physiology, 476*, 279-293.

Bers, D. M. (2001). *Excitation-contraction coupling and cardiac contractile force.* Dordrecht, Netherlands: Kluwer Academic.

Bers, D. M. (2002). Cardiac excitation-contraction coupling. *Nature, 415*, 198-205.

Bohm, M., Rosee, K. La., Schmidt, U., Schulz, R., Schwinger, R. H. & Erdmann, E. (1992). Force-frequency relation and inotropic stimulation in the non-failing and failing human myocardium: Implications for the medical treatment of heart failure. *Journal of Clinical Investigation, 70*, 471-475.

Buckley, N. M., Penefsky, Z. J. & Litwalk, R. S. (1972). Comparative force-frequency relationships in human and other mammalian ventricular myocardium. *Pflugers Archives: European Journal of Physiology, 332*(4), 259-270.

Cheng, H., Lederer, W. J. & Cannell, M. B. (1993). Calcium sparks: Elementary events underlying excitation-contraction coupling in heart muscle. *Science, 262*(5153), 740-744.

Davies, C., Davia, K., Bennett, J. G., Pepper, J. R., Poole-Wilson, P. A. & Harding, S.E. (1995). Reduced contraction and altered frequency response of isolated ventricular myocyte from patients with heart failure. *Circulation, 92*(9), 2540-2549.

Driedzic, W. R. & Gesser, H. (1985). Ca2+ protection from negative inotropic effect of contraction frequency on teleost hearts. *Journal of Experimental Biology, B 156*, 135-142.

Eisner, D. A. & Trafford, A. W. (2002). Heart failure and the ryanodine receptor. *Circulation Research, 91*, 979-981.

El-Sayed, M. F., Abu-mara, E. & Badr, A. (2012). Effects of changes in temperature on the force-frequency relationship in the heart of catfish (Clarias gairepinus). *The Journal of Basic & Applied Zoology, 65*, 274-281.

Endoh, M. (2004). Force frequency relationship in intact mammalian ventricular myocardium: physiological and paraphysiological relevance. *European Journal of Pharmacology, 500*, 73-86.

Fabiato, A. (1985). Simulated calcium currents can both cause calcium loading in and trigger calcium release from the sarcoplasmic reticulum of a skinned canine cardiac Purkinje cell. *Journal of General Physiology, 85*(2), 291-320.

Franz, M. R. (1983). Electrical and mechanical restitution of the human heart at different rates of stimulation. *Circulation Research, 53*, 815-822.

Godier-Fornemont, A. F., Triburcy, M., Wagner, E., Dewenter, M., Lammle, S., El-Armouche, S. et al. (2015). Physiologic force-frequency in engineered heart muscle by electromechanical stimulation. *Journal of Biomaterials, 60*, 82-91.

Gwathmey, J. K., Slawsky, M. T., Hajjar, R. J., Briggs, G. M., & Morgan, J. P. (1990). Role of intracellular calcium handling in force-interval relationships of the human ventricular myocardium. *Journal of Clinical Investigation, 85*(5), 1599-1613.

Györke, S. & Terentyev, D. (2008). Modulation of ryanodine receptor by luminal calcium and accessory proteins in health and cardiac disease. *Cardiovascular Research, 77*(2), 245-255.

Gyroke, S. & Fill, M. (1993). Ryanodine receptor adaptational mechanism of Ca2+ - induced Ca2+ release in heart. *Science, 260*, 807-809.

Hasefus, G., Holubarsch, C., Hermann, H. P., Astheimer, K., Pieske, B. & Just, H. (1994). Influence of force-frequency relationship on hemodynamics and left ventricular function in patients with non-failing hearts and in patients with dilated cardiomyopathy. *European Heart Journal, 15*, 164-170.

Izu, L. T., Wier, W. & Blake, W. (1998). Theoretical Analysis of the Ca2+ spark amplitude distribution. *Biophysical Journal, 75*, 1144-1162.

Jafri, M. S., Rice, J. J. & Winslow, R. L. (1998). Cardiac Ca2+ Dynamics: The roles of ryanodine receptor adaptation and sarcoplasmic reticulum load. *Biophysical Journal*, 1149 - 1168.

Jafri, M., Hoang-Trong, M. & Williams, G. S. (2015, April 14). *US Patent No. US9009095*. Retrieved from https://patents.google.com/patent/US9009095

Janssen, P. M. & Periasamy. M. (2007). Determinants of frequency dependant contraction and relaxation of mammalian myocardium. *Journal of Molecular and Cellular Cardiology, 43*(5), 523-531.

Joulin, O. S., Marechaux, S., Hassoun, S., Montaigne, D., Lancel, S. & Neviere, R. (2009). Cardiac force-frequency relationship and frequency-dependent acceleration of relaxation are impaired in LPS-treated rats. *Critical care, 13*(1), R14.

Katz, A. M. (2000). *Heart Failure pathophysiology, molecular biology and clinical management.* Philadelphia, USA: Lippcott Williams and Wilkins.

Keen, J. E., Vazon, D. M., Farrell, A. P., & Tibbits, G. F. (1994). Effect of temperature and temperature acclimation on the ryanodine sensitivity of the trout myocardium. *Journal of Comparative Physiology B, 164*, 438-443.

Kubalova, Z. (2003). Inactivation of l-type calcium channels in cardiomyocytes. Experimental and theoretical approaches. *General Physiology and Biophysics, 22*, 441-454.

Kurihara, S. & Allen, D.G. (1982). Intracellular Ca2+ transients and relaxation in mammalian cardiac muscle. *Japan Circulation Journal, 46*, 39-43.

Lehnart, S., Maier, L. S. & Hasenfuss, G. (2009). Abnormalities of Calcium metabolism and myocardial contractility depression in the failing heart. *Heart Failure Reviews, 14*, 213-224.

Lompre, A. M., Anger, M. & Levitsky, D. (1994). Sarco(endo)plasmic reticulum calcium pumps in the cardiovascular system: function and gene expression. *Journal of Molecular and Cellular Cardiology, 26*, 1109-1121.

Lukyanenko, V. & Gyorke, S. (1999). Ca2+ sparks and Ca2+ waves in saponin-permeable rat ventricular myocytes. *The Journal of Physiology, 521*(3), 575-585.

Luo, C. H. & Rudy, Y. (1991). A model of the ventricular cardiac action potential. Depolarization, repolarization, and their interaction. *Circulation Research, 68*(6), 1501-1526.

Luo, C. H. & Rudy, Y. (1994a). A dynamic model of the ventricular cardiac action potential. I. Simulations of ionic current and concentration changes. *Circulation Research, 74*(6), 1070-1096.

Luo, C. H. & Rudy, Y. (1994b). A dynamic model of the cardiac ventricular action potential. II. Afterdepolarizations, triggered activity, and potentiation. *Circulation Research, 74*(6), 1097-1113.

Marx, S. O., Reiken, S., Hisamatsu, Y., Jayaraman, T., Burkhoff, D., Rosembit, N. et al. (2000). PKA phosphorylation dissociates FKBP12.6 from the calcium release channel (ryanodine receptor): Defective regulation in failing hearts. *Cell, 101*(4), 365-376.

Monasky, M. M. & Jansen, P. M. (2009). The positive force-frequency relationship is maintained in the absence of sarcoplasmic reticulum function in rabbit, but not in rat myocardium. *Journal of Comparative Physiology B, 179*, 469-479.

Morii, I. Y., Kihara, Y., Konishi, T., Inubushi, T., Sasayama, S. (1996). Mechanism of the negative force-frequency relationship in physiological intact rat ventricular myocardium studies by intracellular Ca2+ monitor with indo-1 and by 31P-nuclear magnetic resonance spectroscopy. *Japanese Circulation Journal, 60*, 593-602.

Morotti, S. E., Grandi, E., Summa, A., Ginsburg, K. S. & Bers, D. M. (2012). Theoretical study of L-type Ca2+ current inactivation kinetics during action potential repolarization and early afterdepolarizations. *The Journal of Physiology, 590*(18), 4465-4481.

Mulieri, L. A., Hasenfuss, G., Leavitt, B., Allen, P. D. & Albert, N. R. (1992). Altered myocardial force-frequency relation in human heart failure. *Circulation, 85*(5), 1743-1750.

Namekata, I. K., Takeda, K., Moriwaki, R., Kazama, A., Sato, A., Tanaka, H., et al. (2004). Role of sodium-calcium exchanger in excitation-contraction coupling of mouse myocardium. *Journal of Pharmacological Science, 92*, 272p.

Narayan, P. S., McCune, S. A., Robitaille, P. M., Hohl, C. M. & Altschuld, R. A. (1995). Mechanical alternans and the force-frequency relationship in failing rat hearts. *Journal of Molecular and Cellular Cardiology, 27*, 523-530.

Orchard, C. H. & Lakatta, E. G. (1985). Intracellular calcium transients and developed tensions in rat heart muscle: a mechanism for the negative interval-strength relationship. *Journal of General Physiology, 86*, 637-651.

Pieske, B. L., Maier, L. S., Bers, D. M. & Hasenfus, G. (1999). Ca^{2+} handling and sarcoplasmic reticulum Ca2+ content in isolated failing and nonfailing human myocardium. *Circulation Research, 85*(1), 38-46.

Puglisi, J. L., Negroni, J. A., Chen-Izu, Y. & Bers, D. M. (2013). The force-frequency relationship: insights from mathematical modeling. *Advanced Physiological Education, 37*(1), 28-34.

Ross, J. T., Miura, T., Kambayashi M., Eising, G. P. & Ryu, K. (1995). Adrenergic control of the force-frequency relation. *Circulation, 92*, 2327 - 2332.

Rossman, E. R., Petre, R., Chaudhary, K. W., Piacentino, V., Janssen, P. M., Gaughan, J. P., et al. (2004). Abnormal frequency-dependent responses represent the pathophysiologic signature of contractile failure in human myocardium. *Journal of Molecular and Cellular Cardiology, 36*(1), 33-42.

Rumberger, E. & Riechel, H. (1972). The force-frequency relationship: a comparative study between warm and cold-blooded animals. *Pflugers Archives, 332*, 206-217.

Schotten, U., Greiser, M., Braun, V., Karlein, C. & Schoendube, F. (2001). Effect of volatile anesthetics on the force-frequency relation in human ventricular myocardium. The role of the sarcoplasmic reticulum calcium-release channel. *Anesthesiology, 95*, 1160-1168.

Shiba, Y., Fernandes, S., Zhu, W.-Z., Filice, D., Mushkeli, V., Kim, J., et al. (2012). Human ES-cell-derived cardiomyocytes electrically couple and suppress arrhythmias in injured hearts. *Nature, 489*, 322-325.

Shiels, H. A. & Farrell, A. P. (1997). The effect of temperature and adrenaline on the relative importance of the sarcoplasmic reticulum in contributing calcium to force development in isolated ventricular trabeculae from rainbow trout. *Journal of Experimental Biology, 200*, 1607-1621.

Sobie, E. A., Dilly, K. W., Cruz, J. S., Lederer, W. J. & Jafri, M. S. (2002). Termination of cardiac Ca2+ sparks: An investgative mathematical model of calcium-induced calcium release. *Biophysical Journal, 86*(5), 3329-3331.

Song, L. -S., Stern, D., Lakatta, E. G. & Cheng, H. (1997). Partial depletion of sarcoplasmic reticulum does not prevent calcium spark formation and detection in cardiac myocytes. *Journal of Physiology, 505*, 665-675.

Sun, L., Fan, J.-S., Clark, J. W. & Palade, P. T. (2000). A model of the L-type Ca2+ channel in rat ventricular myocytes: ion selectivity and inactivation mechanisms. *The Journal of Physiology, 15529,* 139-158.

Szigligeti, P. C., Pankucsi, C., Banyasz, T., Varro, A. & Nanasi, P. P. (1996). Action potential duration and force frequency relationship in isolated rabbit, guinea pig and rat cardiac muscle. *Journal of Comparaive Physiology*, 150-155.

Terracciano, C. M. & MacLeod, K. T. (1997). Reticulum Ca2+ content during the cardiac cycle in Guinea pig and rat ventricular myocytes. *Biophysical Journal, 72*(3), 1319-1326.

Valdivia, H. H., Kaplan, J. H., Ellis-Davies, G. C. & Lederer, J. W. (1995). Rapid adaptation of cardiac ryanodine receptors: modulation of Mg2+ and phosphorylation. *Science, 267*(5206), 1997-2000.

Varian, K. D. & Janssen, P. (2007). Frequency dependent acceleration of relaxation involves decreased myofilament calcium sensitivity. *American Journal of Physiological Heart and Circulation Physiology, 292,* H2212-H2219.

Wagner, E., Lauterbach, M. A., Kohl, T., Westphal, V., Williams, G. S. B., Steinbrecher, J. H. et al. (2012). Stimulation emission depletion live-cell super-resolution imaging shows proliferative remodeling of T-tubule membrane structures after myocardial infarction. *Circulation Research, 111*(4), 402-414.

Wang, Y., Chen, M. S., Liu, H. C., Xiao, J. H. & Wang, J. L. (2014). The relationship between frequency dependence of action potential duration and the expression of TRPC3 in rabbit ventricular myocyte. *Cellular physiology and Biochemistry, 33*, 646-656.

Williams, G. S., Chikando, A. C., Tuan, H. T., Sobie, E. A., Lederer, W. J. & Jafri, M. S. (2011). Dynamics of Calcium sparks and calcium leak in the heart. *Biophysical Journal*, 1287 - 1296.

CHAPTER THREE: ALTERNANS AND EADS ARE THE UNDERLYING CAUSES OF CPVT2 IN THE MYOCYTE HARBORING CASQ2 DELETION MUTATION, CASQ2$^{G112+5X}$ DEPENDING ON THE PACING DYNAMICS

Abstract

Calsequestrin type 2 (CASQ2) is a high capacity and low-affinity Ca^{2+}-binding protein expressed in the sarcoplasmic reticulum (SR) of the cardiac myocyte. The mutation that occurs in CASQ2 expressing gene has been linked to catecholaminergic polymorphic ventricular tachycardia (CPVT2) and possibly sudden cardiac death (SCD) with acute emotional stress or exercise. CASQ2$^{G112+5X}$ is a 16 bp (339-354) deletion CASQ2 mutation that prevents the protein expression due to premature stop codon. Understanding the subcellular mechanisms of CPVT2 is experimentally challenging because arrhythmias are rare and. To get an insight into the characteristics of this rare disease, we have developed a local control stochastic model of the cardiac myocyte to investigate how the mutant CASQ2s may be responsible for the development of an arrhythmogenic episode under the condition of beta-adrenergic stimulation or in the pauses afterward. An adjustment of the parameters was made based upon the changes brought by the CASQ2 mutation and a simulation ran with the β-adrenergic receptor (βAR) stimulation by changing pacing frequencies from a normal to rapidly pacing myocyte. The simulations results suggested that under rapid pacing (6 Hz), the electromechanically concordant alternans appeared under β-AR stimulation in the CPVT mutant, but not in the wild-type and unstimulated mutant. Similarly, the simulations of accelerating pacing from slow to rapid and back to the slow pacing didn't display

alternans but did generate early afterdepolarizations (EADs) during the period of second slow pacing subsequent acceleration of rapid pacing.

Introduction

Catecholaminergic polymorphic ventricular tachycardia (CPVT) is an irregular rhythm of the heart induced by physical activities, emotional stress, or catecholamine infusion, which may further deteriorate the heart into ventricular fibrillation (VF) (Bhuiyan, Berg, Tintelen, Bink-Boelkens, Wisefield, Alders, et al., 2007). The heart of CPVT patients does not display any morphological indifferences and their pathogenicity is often not identified before the symptoms appear (Coumel, Fidelle, Lucet, Attuel, & Bouvrain, 1978). It is one of the malignant young patients' cardiac channelopathy with the mortality rate of 30-50 percent (Medeiros-Domingo, Bhuiyan, Tester, Hoffman, Bikker, Tintelen, et al., 2009). CPVT type 2 (CPVT2) transpires by common single nucleotide polymorphism (SNP) or point mutation in the gene to express the Calsequestrin type 2 (CASQ2) protein (Refaat, Aouizerat, Pullinger, Malloy, Kane, & Tseng, 2014). It is an inherited autosomal recessive (both copies of allele mutated) trait of mutation. The CASQ2 expressing gene has 11 exons and encodes a protein containing 399 amino acids (Lahat, Pras, & Eldar, 2004).

CASQ2 is a high capacity and low-affinity Ca^{2+} buffering protein located near the RyR2 channel which binds to Ca^{2+} to keep low free [Ca^{2+}] in the luminal region of SR. The binding site is the aspartic acid (Asp) rich region in the C-terminus where CASQ2 monomers aggregate to form dimers then tetramers which turn into negatively charged Ca^{2+} binding pockets (Wang, Trumble, Liao, Wesson, Dunker, & Kang, 1998) (Handhle,

Ormonde, Thomas, Bralesford, Williams, Lai, et al., 2016). An extended C-terminal end is comprised of more than 70% acidic residue (Wei, Hanna, Beard, & Dulhunty, 2009). The three domains in CASQ2 molecule form disc shape like structure and they are connected by loops (Novak, & Soukup, 2011).

A total of fifteen CASQ2 mutations have been identified in humans, two out of them belong to deletion mutations – $CASQ2^{L23fs+14X}$ & $CASQ2^{G112+5X}$ (Faggioni, Krystal, & Knollmann, 2012). Experimental studies revealed this mutation brings morphological changes in the SR by reducing the buffering capacity of CASQ2 in the SR luminal region and an increase in the volume of SR. These are the morphological changes incorporated in our model to mimic the SR changes by the onset of $CASQ2^{G112+5X}$ mutant CASQ2 and we were able to study the mechanism of arrhythmia during β-adrenergic stimulation.

$CASQ2^{G112+5X}$ is a homozygous deletion mutation and causes disruption of CASQ2 polymerization in protein expression. The 16 base pairs (c.339-354) deletion causes a frameshift to generate premature stop codon after removal of 5 amino acids. This mutation causes the omission of whole parts of II and III domains and some parts of the first domains. The mutant protein lacks total acidic residue required for the binding of Ca^{2+}. The mutant also lacks the amino acids which are part of front-to-front or back-to-back interaction for the CASQ2 polymerization (Novak, & Soukup, 2011). This mutation causes a reduction in the SR Ca^{2+} buffer, prolonged release of SR Ca^{2+}, an increase in SR volume, and impaired clustering of CASQ2 (di Barletta, Viatchenko-Karpinski, Nori, Memmi, Terentyev, Turcato, et al., 2006).

To run this simulation, we modified the parameters for SR volume, CASQ2 buffer, L-type channel activities, and SERC2A pump activities in our newly developed stochastic Guinea pig myocyte model to imitate CPVT2 in a myocyte carrying the $CASQ2^{G112+5X}$ mutation in the CASQ2 expressing gene. The result of the present study demonstrated the arrhythmia during β-adrenergic stimulation in the mutant myocyte. The underlying mechanism of the arrhythmia is Ca^{2+} alternans. We also found EADs produced when rapidly pacing myocyte paces slowly under catecholamine treatment.

Methods

Model Development

The CASQ2 ventricular model was developed from the ventricular myocyte model explained in chapter 2. On that model, we altered the parameters related to β-AR stimulations and $CASQ2^{G112+5X}$ mutations to represent experimental approved features that explain and compare the behavior and morphological features of mutant myocyte to wild type one. Our research focus was on the effect of the mutation in the Ca^{2+} dynamics in intracellular compartments in normal pacing and rapid pacing compared to the β-adrenergic stimulation in both wild type and mutant myocyte to see whether any arrhythmia occurs in mutant myocytes, if that happens what the mechanisms behind it are. To prepare a model with β-adrenergic stimulation consistent with experiments, we updated the parameters for L-type Ca^{2+} channels (LCC) and SERCA2-ATPase pump cycling rates (V_{cycle}). Similarly, for CASQ2 mutation, the luminal Ca^{2+} dependency, (Φ_m) of RyR2 was increased and two morphological features (SR volume increase and

reduction in CASQ2 buffer) were added. Ginsburg and Bers (Ginsburg, 2004) reported the ISO treatment in cardiac myocyte increased L-type Ca^{2+} and enhanced SR Ca^{2+} uptake. Terentyev, Viatchenko-Karpinski, Valdivia, Escobar, & Gyroke (2002) in their experiment in rat ventricular myocyte, reported that there is a 2-3-fold increase in Ca^{2+} sparks due to an increase in the volume of luminal Ca^{2+}. Similarly, Kornyeyev et al. (Kornyeyev, 2011) reported that the loss of CASQ2-mediated Ca^{2+} buffering causes a faster rise in luminal free Ca^{2+}. Song, Alcalai, Arad, Wolf, Toka, Conner, et al (2007) reported an enhanced SERCA2a pump SERCA-ATPase Cycling rate (V_{cycle}) activities in CASQ2 deficient myocytes. $CASQ2^{G112+5X}$ mutation behaves similarly to knockout CASQ2 ($CASQ2^{-/-}$) (di Barletta, et al. 2006), and Knollmann Chopra, Hlaing, Akin, Yang, Ettensohn, et al. (2006) found that ~50% SR volume was increased in $CASQ2^{-/-}$ deficient ventricular myocyte to compensate the total loss of Ca^{2+} buffer.

Simulation Protocols

We created an environment for two types of myocytes – wild type and mutant myocytes. The mutant myocytes also have two morphological changes – an increase in the volume of SR and a reduction in the buffering capacity of CASQ2 compared to wild type myocyte. First, the simulations were performed side by side wild type myocyte and mutant myocyte in 1 hertz (Hz) pacing until a qualitative agreement with steady-state Ca^{2+} dynamics in each type of myocytes was reached. These conditions were used as the initial state for our model for further simulations. The following categories of simulation were performed for 1 to 6 Hz pacing: a) wild type control pacing, b) Mutant myocyte control pacing, c) Wild type β-adrenergic stimulation pacing, and d) Mutant myocyte β-

adrenergic stimulation pacing. The simulation protocol is given in Table 1 which represents the modified simulation parameters in WT and mutant myocytes for the β-AR stimulation.

Table 2: Simulation parameters for β-adrenergic stimulation in WT and mutant myocyte

Parameters	**Change (%)**
L-type Channel (P_dhpr)	40
Luminal dependence (K_jsr0)	90
SERCA Pump (Ap)	50
Morphology	
jSR Volume (V_JSR_T)	50
NSR Volume (V_NSR_T)	50
CASQ Buffer (B_SR_T)	(-95)

The β-AR receptor stimulation increases SR Ca^{2+} content by increasing L-type current and SERCA2a activity (Ginsburg, & Bers, 2004). For the β-AR stimulation in a WT and CASQ2 mutant myocytes, we altered to alter the following features.

B-AR Stimulation Parameters

a) Increase in L-type channel activity: All the experimental researchers believe there is a sudden amplified L-type current when the level of catecholamine increases by the activation of adrenergic receptors in the sarcolemma. We raised a 40 percent L-type

current (P_dhpr) for the simulation result. Ginsburg and Bers (2004) found a 53% increase in the LCC peak value with the treatment of isoproterenol (ISO).

b) Increase in luminal dependence: CASQ2 is a densely staining major Ca^{2+} storage protein in the SR and its absence from it has a major implication in the availability of free Ca^{2+} in the luminal region. Luminal sensitivity regulation function (ϕ) depends upon free Ca^{2+} in the SR as shown in figure 19, when there is more independent Ca^{2+} available in the lumen, it is going to enhance the opening rate of RyR2. Since there is a total reduction of Ca^{2+} buffer in $CASQ2^{G112+5X}$, a 90% increase in luminal dependence (K_{jsro}) provided a steady-state Ca^{2+} transient by distressing free SR Ca^{2+} availability. Gyorke and Gyorke (Györke, 1998) reported the RyR2 PO increased 0.26±0.04 to 0.49±0.09 with doubling luminal doubling SR free $[Ca^{2+}]$.

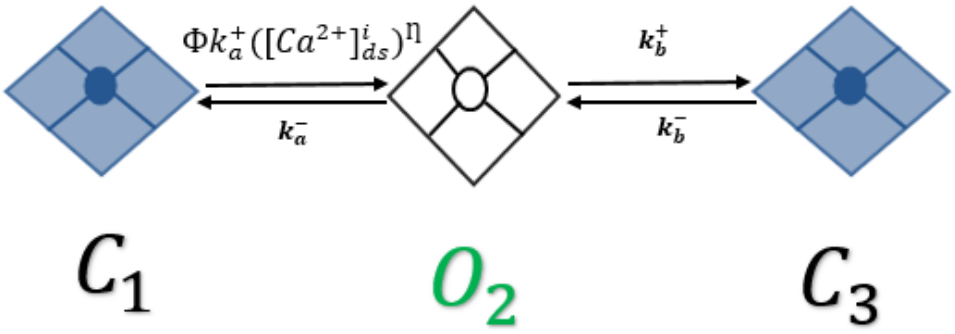

Figure 19: Opening probability (P_o) of RyR2 channels from closed state (C_1) to open state (O_2), is controlled by luminal regulation function (Φ) in the RyR2

In our the RyR2 model, the luminal regulation function (Φ) depends upon luminal dependence (Φ_m),

$$\Phi = \Phi_m [Ca^{2+}]_{sr} + \Phi_b$$

where, $[Ca^{2+}]_{sr}$ represents both $[Ca^{2+}]_{jsr}$ and $[Ca^{2+}]_{nsr}$

c) Enhanced SERCA-ATPase Cycling rate (V_{cycle}): Increased Ca^{2+} in cytosol due to an increase in L-type current as well as increased RyR channel activity, it is going to affect the activity of SERCA2A cycling rates, and they pump Ca^{2+} back to SR rapidly. Phospholamban (PLB) inhibits the SERCA2A activities in the SR but the inhibition is reduced by the stimulation of β-adrenergic receptors which results in increased SERCA2A pump activities (Metzger, & Westfall, 2004). When more Ca^{2+} in cytosol due to an increase in Ca^{2+} influx via L-type current, it is also going to increase SR Ca^{2+} load (Bers, 2000) with the activation of SERCA2A (Kashimura, Briston, Trafford, Napolitano, Priori, Eisner, et al., 2010). In our simulation, the whole-cell SERCA pump flux is given by,

$$J_{serca} = 2v_{cycle} A_p$$

where,

v_{cycle} is cycling rate per molecule, and

Ap is the concentration of SERCA molecules per liter cytosol and the unit of Ca^{2+} flux, J_{serca} is mol s^{-1}.

Alteration of morphological parameters in the mutant myocyte

d) Increased SR volume: The morphometric analysis of volume fraction of SR membrane of CASQ2 knockout myocyte, Knollmann *et al.* (2006) found SR volume

related to cytoplasm increased by ~51% while the volume related to myofibril was up by ~45%. And, they have found a 50% increase in the SR volume enough to maintain the normal SR storage capacity.

e) Abolition of SR buffering Capacity: $CASQ2^{G115+5x}$ deletion mutation removes the entirety of CASQ2 protein, leaving no place to SR Ca^{2+} to buffer (di Barletta, et al., 2006). To accommodate the steady-state to our model, we left a 5% buffer in the SR.

Numerical Methods

A scientifically, computationally powerful, and high-level programming language, Fortran 95 was used to write code and calculate differential equations for the model. Fortran was first appeared in 1957 and continuously used after that in the field of science and engineering to solve highly complex problems. Fortran 90 was major hauled over FORTRAN 77; it became case insensitive (supports both lower- and upper-case characters) in writing code and allowed operator overloading. Fortran 95 is a continuation of an earlier version, Fortran 90.

The PGI CUDA Fortran compiler was used to execute and simulate the program in the Linux platform, Ubuntu operating system. CUDA (compute unified device architecture) is a parallel computing platform and programming language developed for graphic processing units (GPUs) by NVIDIA. The original CUDA was developed in C programming language. CUDA and NVIDIA GPUs have been widely used in higher education research in computational biology, numerical analytics, physics, and scientific visualization. The CUDA clusters we are using in our lab contain Fermi-based C2050 graphics processing cards with CUDA SDK 6.0 and higher. To capture calcium dynamics

at a single-channel level a novel computational algorithm Ultra-Fast Markov chain Monte Carlo (UMCMC) method was used for the stochastics gating from CRUs (Jafri, et al., 2015).

The programming software interactive data language (IDL) and Python were used to plot the graphs and compute data. All ordinary differential equations were calculated using Euler methods. The time step is for the differential calculation is ten nanoseconds.

Model Simulations

The cardiac action potential is measured by the difference in the electrical potential between the interior and exterior surfaces of a myocyte. It is generated by in and out movements of the positively and negatively charged ions through the specific ionic channels forming ionic currents. In our model (explained in chapter 2), we have simulated the following ionic currents - sodium current (I_{Na}), L-type Ca^{2+} current (I_{LCC}), Na^{+}-Ca^{2+} current (I_{ncx}), Inward rectifier K^{+} current (I_{K1}), Delayed rectifier K^{+} current (I_{Ktos}), Transient outward K^{+} current (I_{Ktof}), Na^{+}-K^{+} current (I_{NaK}), Ca^{2+} pump current (I_{PMCA}), background Ca^{2+} current (I_{bCa}), background Na^{+} current (I_{bNa}), and background K^{+} current (I_{bK}). Besides ionic currents, the simulation of myoplasmic Ca^{2+} transients ($[Ca^{2+}]_{myo}$), NSR Ca^{2+} variation ($[Ca^{2+}]$nsr), JSR Ca^{2+} release ($[Ca^{2+}]_{jSR}$), RyR opening ($P_{O,\,RyR}$), L-type Ca^{2+} channel opening ($P_{O,\,LCC}$) and sparks in subspace region ($[Ca^{2+}]_{subspace}$) were also performed. This chapter includes all the applicable plots of ionic currents, Ca^{2+} transients, and channel opening rates in 6 Hz pacing which provides stability and basic comparison to counterparts pacing protocols. Most of the simulations were run for 10 seconds until stable pacing was achieved. On the other hand, the

alternans were generated in 6 Hz β-adrenergic stimulation ran for 30 seconds to achieve stable pacing. Similarly, 6 Hz pacing simulations were used for all pacing protocols to compare plots and find out the changes in the AP and other ionic currents because of myocyte instability and change in Ca^{2+} dynamics in rapid pacing and mutation. An adult Guinea pig's normal heartbeat is around 240 beats per minute or 4 Hz (beats per second). When β-adrenergic receptors activated either by exercise or emotion, the heartbeat is going to above five beats per second (5 Hz) or six beats per second (6 Hz) and so on. In our simulation, we found a mutant myocyte can retain its stability till 5 Hz pacing but when it starts beating at 6 Hz, the myocyte displayed changes in shape and size of AP, changes in I_{Na} currents, there was a rapid increase in basal [Ca^{2+}] in the cytosol and SR. From our numerous simulations, we have noticed even a wild type myocyte started to develop AP noises in 7 Hz pacing and alternans in 8 Hz pacing. We found that it has changed in mutant myocyte and instability in the AP appears early pacing.

Table 3: Simulation Parameter used in wild-type and mutant myocytes

Simulations	**Wild-type myocyte**	**Mutant myocyte**
Control Simulation	Original model parameters with a change in the pacing frequency	Morphological changes (SR Volume Increase, SR Ca^{2+} buffering diminished)
B-adrenergic stimulation	Increase L-type activity, SERCA activity, and luminal Ca^{2+}	Morphological changes plus β-AR stimulation

Besides alternans simulation, we also performed EAD simulations in slow-rapid-slow (1Hz-5Hz-1Hz) pacing following the same protocols used in the adrenergic stimulation. This simulation was also run for a total of 30 seconds: first 10-sec slow pacing then another 10 sec of rapid pacing and last 10-sec slow pacing again.

There were four types of CPVT2 for simulations as shown in table 3 above: (a) Control simulation in wild type: Simulations were performed in the original parameters only changing pacing frequencies, (b) Control simulation in mutant myocyte: only morphological changes (SR volume, Ca^{2+} buffer) was modified in the mutant myocyte in this simulation, (c) β-adrenergic stimulation in wild type myocyte: Adrenergic stimulation ran into wild type myocyte by mimicking catecholamine treatment by modifying parameters to L-type activity, SERCA activity, and luminal dependence. (d) Adrenergic stimulation simulation in mutant myocyte: Both parameters from b & c were used for this simulation.

Results

The mutations in the Ca^{2+} handling proteins like CASQ2 are responsible for causing imbalance to the Ca^{2+} homeostasis which affects the shape, size, and structure of AP between beat to beat or one frequency to the other. The β-AR stimulation of the CASQ2 mutant myocyte in our model profiled three phenomena of CPVT: 1) EADs, found in low frequency right after switching from the rapid pacing, 2) alternans, recorded in the rapid pacing, and 3) an alternate beat skipping, also in the rapid pacing. This is the

important aspect of this model which displayed all these different phenomena of arrhythmia without altering any parameter other than changing the pacing frequencies.

Slow-Rapid-Slow Pacing Developed EADs

EADs have been observed at slow pacing rates following periods of rapid pacing in experiments involving CASQ2 variants associated with CPVT, presumably due to the longer APD with slow pacing and higher SR Ca^{2+} load following a period of rapid pacing. Therefore, we tested the likelihood of EADs at lower pacing lower frequency before and after rapid pacing. While running the simulation, we used the features of CASQ2 mutant $CASQ2^{G1125X}$ and ran the simulations with the protocols explained above and performed the simulations slow-fast-slow mode. In the starting, the myocyte was in 1 Hz pacing to simulated for 10 seconds, then the simulation continued to another 10 seconds with the pacing rate of 5 Hz, and the pacing rate was dropped back into 1 Hz to ran another simulation for ten more seconds. In initial low frequency, the myocyte was found to have normal pacing then also paced well without any irregularity in 5 Hz before it initiated to go back to slow pacing (1 Hz), then the AP ended up having EADs (Fig 20A) in many beats. In figure 20A, we spotted the EADs in the AP of 22, 23, 26, 27, 28 & 29 seconds during the second phase of slow pacing. We also ran a similar simulation in the WT myocyte with β-AR stimulation but the APs before and after rapid pacing were normal as shown in figure 20B. The average APDs were found higher in mutant myocyte than WT myocyte (229.1±15.93 vs 211.7±10.1) during β-AR stimulation. We tallied calcium sparks in each beat before rapid pacing (Fig. 20C) and after rapid pacing (20D)

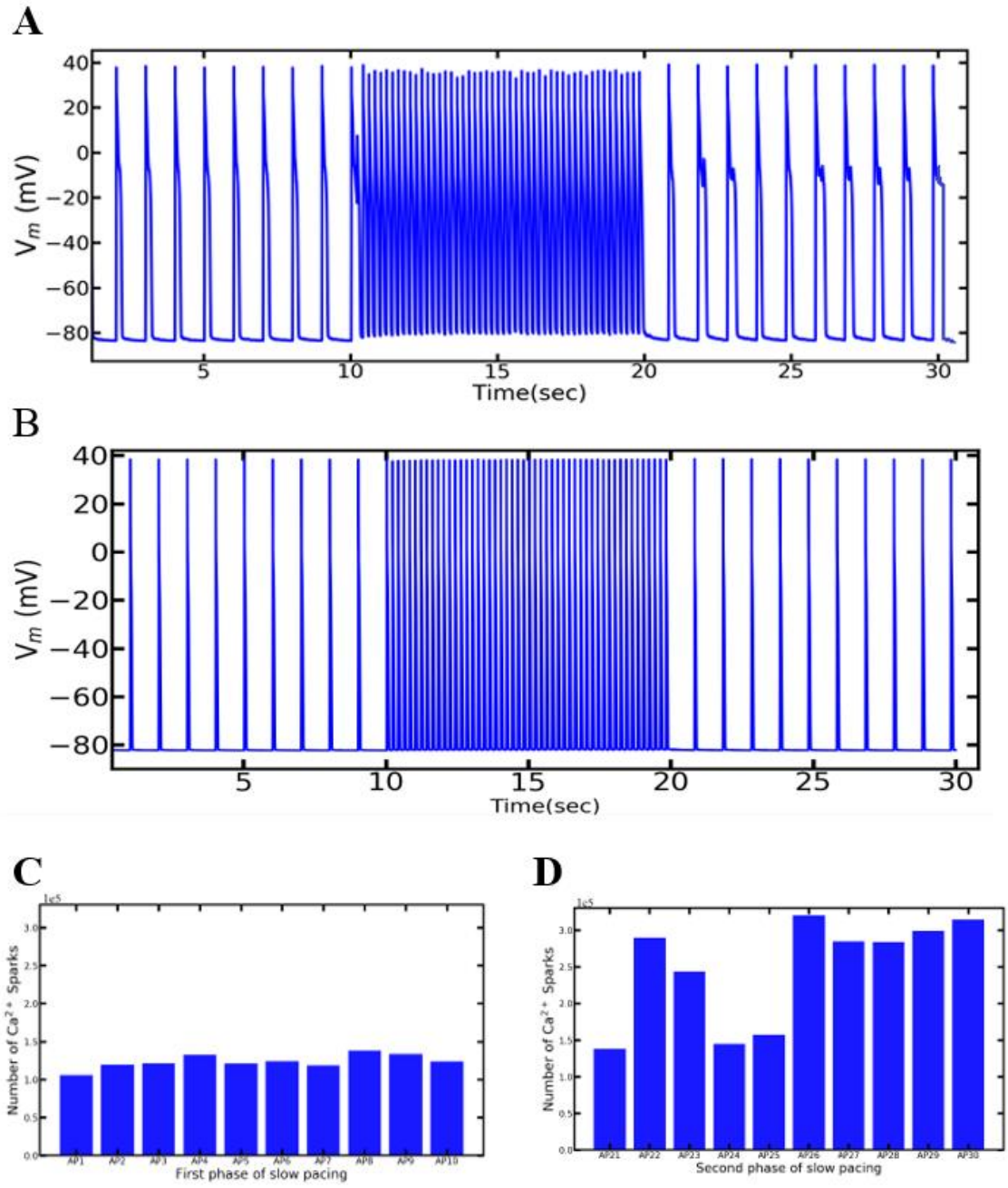

Figure 20: Slow-rapid-slow pacing in a CASQ2$^{G112+5X}$ mutant myocyte generates EADs in the second phase of slow pacing during β-adrenergic stimulation. (A) β-AR AP for 30 seconds in the mutant myocyte (1-10 sec first phase slow pacing, 11-20 sec rapid pacing, and 21-30 sec second phase slow pacing). (B) β-AR stimulation in WT myocyte with first

and second slow phases with rapid pacing in the center. The number of Ca^{2+} sparks were counted and compared in the first phase slow pacing (C) and second phase slow pacing (D) after the rapid pacing. The huge difference in their number of sparks before and after the rapid pacing represents the increased SR load right after the rapid pacing.

per beat after rapid pacing (247,320±68,967) than before rapid pacing (123,847±8638) with the same pacing frequency should have played a major role in destabilizing the myocyte. We further analyzed per second Ca^{2+} sparks in both phases and compared them.

The main difference between pacing at these two rates is the higher availability of the SR Ca^{2+} level (Fig. 21A) in generating more numbers of Ca^{2+} sparks in the second phase than the first phase (Table 4). Guo *et al*. (Guo, 2012) reported the Ca^{2+} spark frequency increases with increased SR load. The higher variability in the average APD in the second slow phase (330±56.95) than in the first slow phase (229.1±15.93) supports the EADs that are favorable in the elongated APDs (Fig. 21B) and all the APs might not have EADs. An increased electrogenic I_{ncx} (21C) due to elevated cytosolic calcium also supported the further elongation of the APD. The generation of the EADs is generally related to elongated AP and late I_{LCC}, late $I_{Na,}$ or inward I_{ncx} currents (21C) (Karagueuzian, 2017) (Sipido, 2007). We have also found slightly higher AP amplitudes (39.3±0.33) in the second slow phase over the first one (38.47±0.22) but their values are not spread out enough to support the amplitudes play any role in EADs. The high average Ca^{2+} sparks count (20D) per beat after rapid pacing (247,320±68,967) than before rapid pacing (123,847±8638) with the same pacing frequency should have played a major role

in destabilizing the myocyte. We further analyzed per second Ca^{2+} sparks in both phases and compared them with control WT and β-adrenergic WT (Table 4). The initial slow phase had 155,082±8633 while it was 368,841±26,995 in a second.

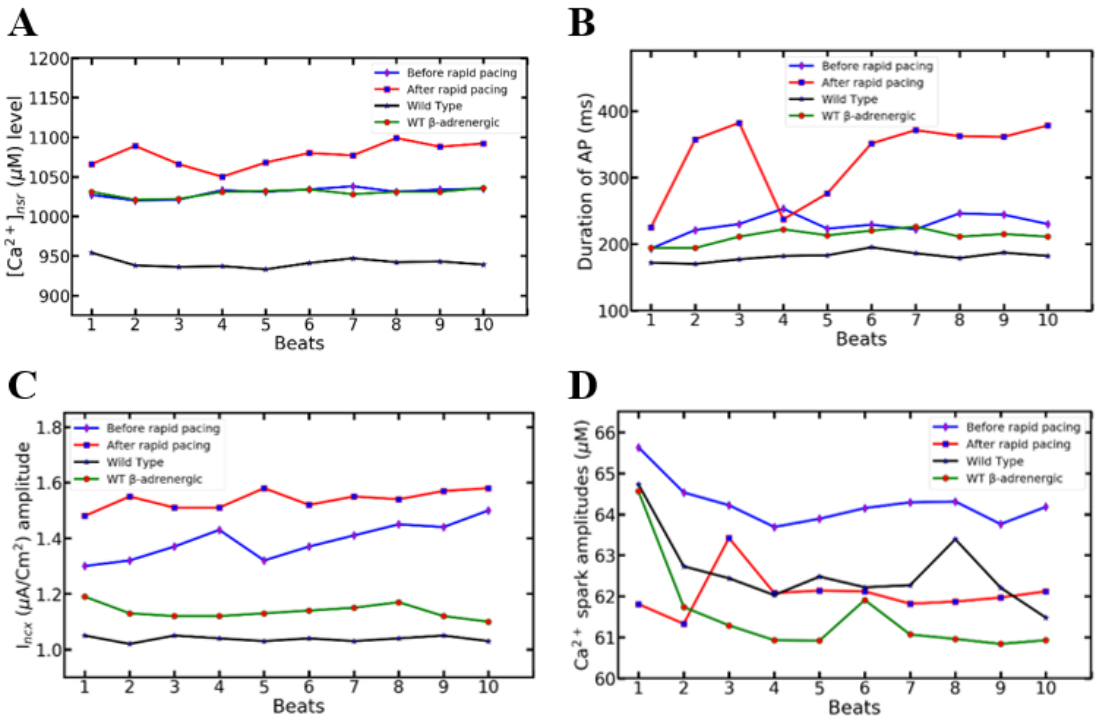

Figure 21: A comparison of intracellular Ca^{2+} activities of first and second slow phases with WT myocyte with or without β-adrenergic receptor-stimulated. A higher SR load, $[Ca^{2+}]_{nsr}$, (A) initiates a spontaneous Ca^{2+} release via RyR2 in the second slow phase. The APDs (B), get further elongated with the increased activities of electrogenic I_{NCX} current (C). The decreased average Ca^{2+} spark amplitudes (D) per beat in the second rapid phase opposite to all other components supported the notion that indeed a spontaneous Ca^{2+} release occurred.

The difference between per sec Ca2+ sparks per beat in the second slow phase is four times higher than the first slow phase (122,521±12,252 vs 31,235±3,452). This data suggested that there was a diastolic Ca2+ leak in the second phase but it might not be

Table 4: APD, average Ca^{2+} sparks count and their amplitudes in myocytes (1 Hz)

Myocyte	APD (beat)	Ca^{2+} sparks/sec	Ca^{2+} sparks/beat	Spark Amp. (beat)
WT Control	181.3±6.96	60951±2439	50695±1986	62.6±0.85
WT β-adrenergic	211.7±10.1	156302±9592	112388±5480	61.52±10.7
First slow phase	229.1±15.93	155082±8638	123847±8638	64.27±0.52
Second slow phase	330±56.95	368841±26994	247392±68966	62.07±0.51

enough to make it visible in the AP plots or engendering delayed afterdepolarizations (DADs). In the WT myocyte, the per second frequency of Ca^{2+} spark was 60,495±2,439, whereas per beat frequency was 50,694±1986. However, the average spark amplitudes (Fig. 21D) displayed different behavior as they were higher in the initial slow phase (64.27±0.52) than the second one (62.07±0.51) (Table 5). Previously (chapter 2), we have found the average Ca^{2+} spark amplitudes get taller concerning SR load increase, but the difference here should be because of the abnormal APs with EADs. The overloaded SR after rapid pacing had removed some of the excess Ca^{2+} during diastolic Ca^{2+} leak with the spontaneous Ca^{2+} release but not enough to generate any DADs.

Mechanism of EADs

To understand how the EADs were formed in our model, we brought different plots side by side as shown in figure 21. There are APs before rapid pacing (Fig. 22A, blue) and after rapid pacing (Fig. 22A, red) and both APs do not have any diastolic Ca^{2+} leak. But in counting sparks (table 4), we found a huge average sparks numbers of the Ca^{2+} sparks after rapid pacing that certainly brought the changes in the intracellular Ca^{2+} dynamics but it was hard to pinpoint how it caused the spontaneous Ca^{2+} release and ended up an EAD. We saw the late reactivation in LCC (Fig. 22B) around 0.421 sec (in the first AP in figure 22B) and in the meantime, the reopening of RyR2 (Fig. 22C) took place at 0.405 sec which showed there was spontaneous RyR2 opening before reactivation of LCC. As a result of spontaneous Ca^{2+} release, the shifting of the curve to the right in $[Ca^{2+}]_{nsr}$ (Fig. 22D) took place at 0.407 sec. In comparing the first phase and the second phase, we have also found a notable difference in the Na^{+}-Ca^{2+} exchange current with the availability of excess Ca^{2+} in the cytoplasm (Fig. 22E). In the first phase of slow pacing as shown in figure 22F, the I_{ncx} is extending from 0.587 to -0.856 with an absolute increase of 1.443 ($\pi A/Cm^2$). The same I_{ncx} current during the second phase of slow pacing is extending from 0.577 to -1.172 with an absolute increase of 1.752 ($\pi A/Cm^2$). It is 0.309 ($\pi A/Cm^2$) higher in the second slow phase than the first slow phase. During the rapid pacing of 5 Hz, we found it is extending from 0.48 to -1.55, with an absolute rise of 2.03 ($\pi A/Cm^2$). The I_{ncx} generates an inward current when Ca^{2+} is extruded from the myocyte. The inward current during the repolarization elongates the APD (Janvier, 1997) (Schouten, 1990). Similarly, there is a difference between SR Ca^{2+}

level before rapid pacing and after it. In figure 22D, it can be seen the diastolic Ca^{2+} level is high (1092 µM vs 1009 µM) after rapid pacing as compared to the initial slow phase. Volders et al. (Volders, 2000) stated that during stimulation of β-adrenergic receptor stimulation, the arrhythmogenic responses are accompanied by spontaneous Ca^{2+} release during systole and inward I_{ncx} contribute to the generation of EADs.

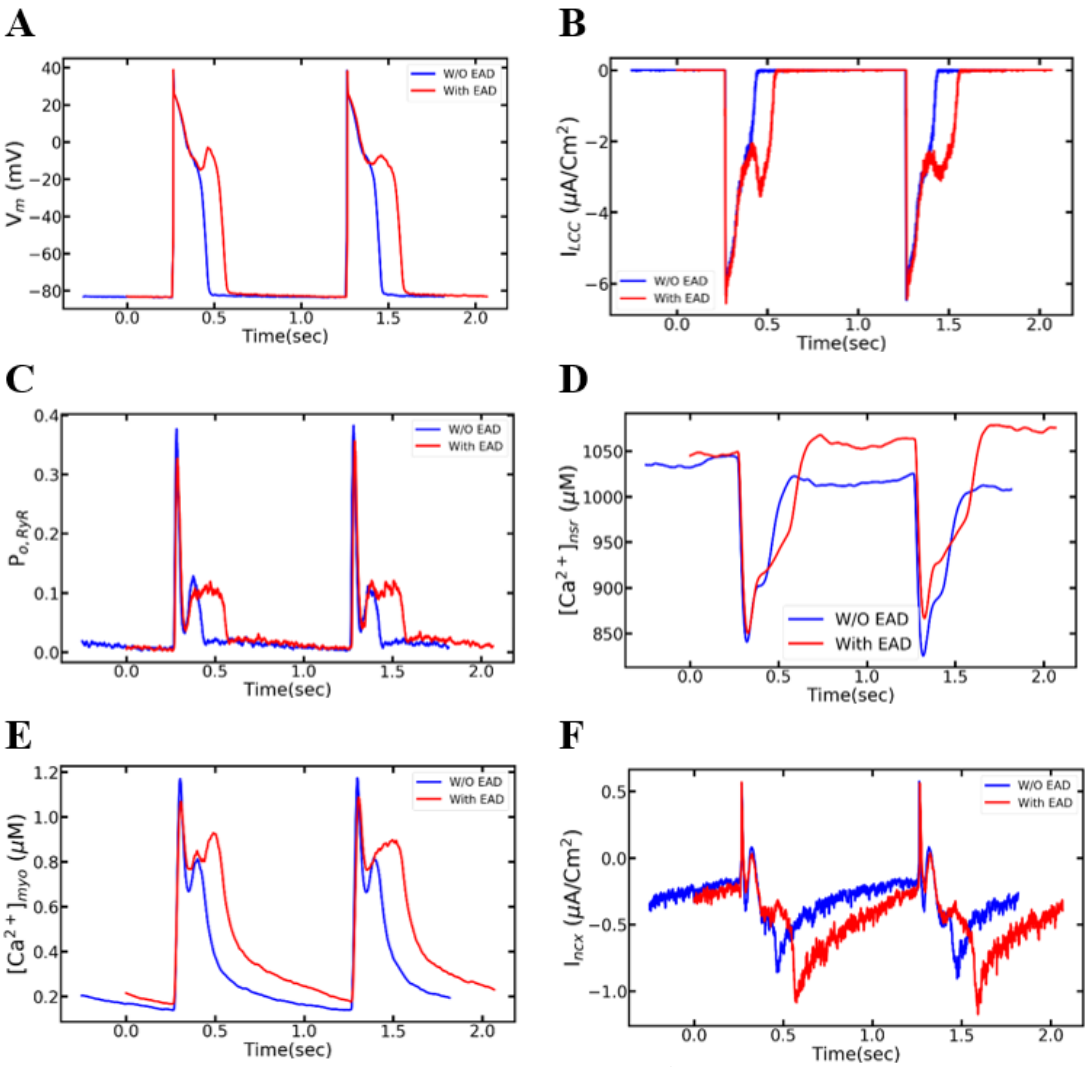

Figure 22: A comparison of AP, channel gating, Ca^{2+} transients, and ionic currents

during β-AR receptors, activated myocytes show spontaneous Ca^{2+} release develops EADs in the second slow pacing after myocyte went through rapid pacing.
The plots represent the combined simulations of 7.5 sec to 9.5 (blue) sec and 21.5 sec to 23.5 sec (red). (A) A normal AP in the slow pacing ahead of the rapid pacing (blue), but it changed in the subsequent slow phase right after the rapid pacing where AP developed EADs. (C) The RyR2 channels spontaneously release Ca^{2+}. (D) An overloaded SR, $[Ca^{2+}]_{SR,}$ is responsible for spontaneous Ca^{2+} release. (E) Cytoplasmic Ca^{2+} level ($[Ca^{2+}]_{myo}$) changes after spontaneous Ca^{2+} release and late reactivation of LCC. (F) Increased activity of Na^{+}-Ca^{2+} exchange current (I_{ncx}) is supportive of elongate APD.

In our simulation, it was seen the spontaneous Ca^{2+} release from the overloaded SR and the elongated APD caused by electrogenic inward I_{ncx} causes EADs to happen. On blocking NCX current by benzamil, Priori et al. (Priori, Napolitano, Tiso, Memmi, Viganti, Bloise, et al., 2001) were able to suppress the EADs. In a rabbit model, by reducing 55% SR Ca^{2+} uptake of ISO exposed myocytes found controlling spontaneous Ca^{2+} release, then EADs (Xie, Grandi, Puglisi, Sato, & Bers, 2013).

AP and Ionic currents During Rapid Pacing

Though the SR Ca^{2+} overload arose due to rapid pacing was responsible for spontaneous Ca^{2+} release in slow pacing produced EADs but the APs and other ionic currents in 5 Hz pacing found to be normal. We checked AP and other Ca^{2+} related plots to know whether there were any abnormalities in those components during the time of rapid pacing, we sliced a segment between 18.5 to 20.5 sec (Fig.23A-F). The AP plot

(Fig. 23A) didn't have any reflection of abnormality, LCC (Fig. 23B) had a usual decrease in amplitude with the increase rate but didn't display any abnormality.

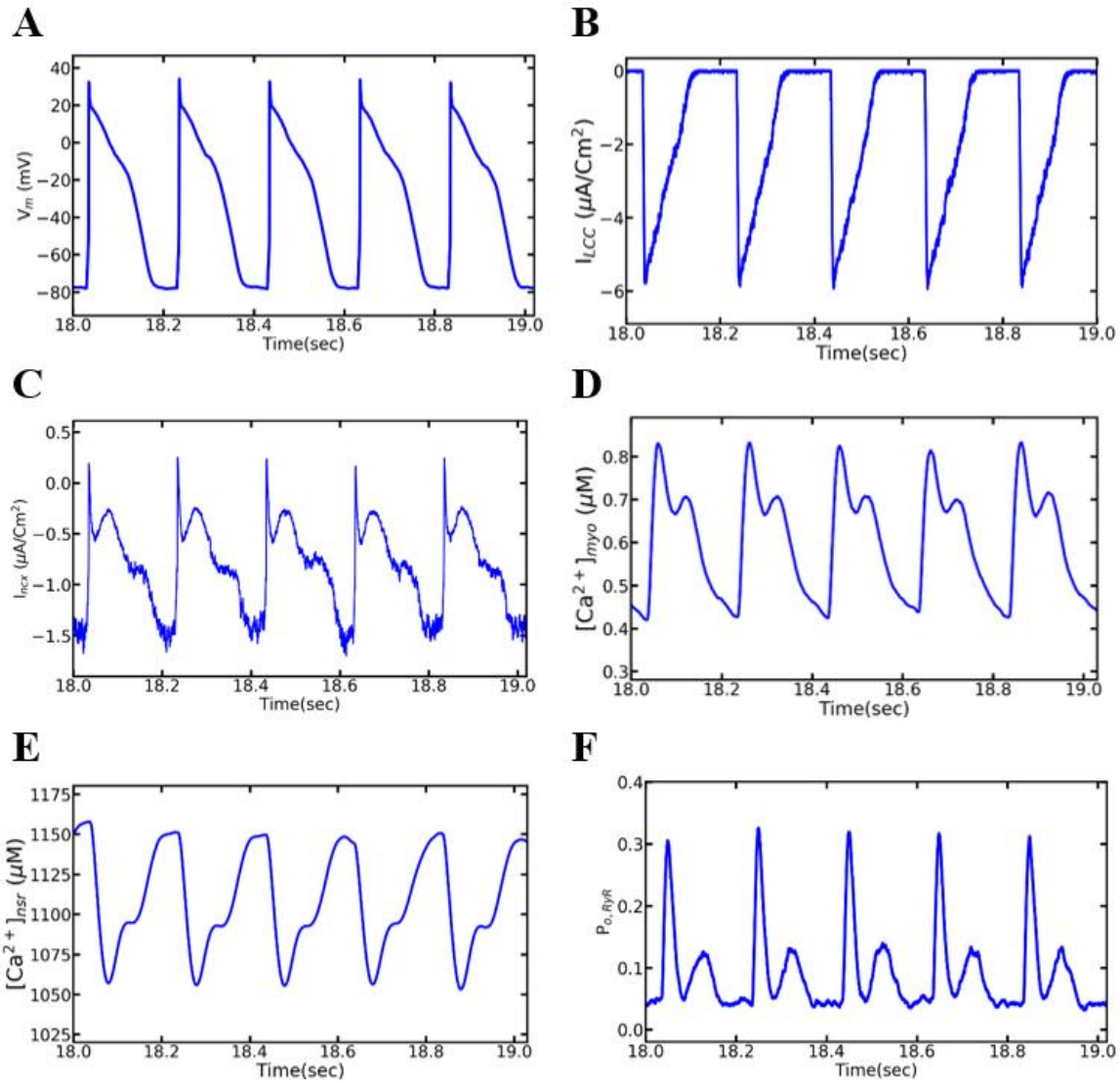

Figure 23: No EADs or alternans were recorded in 5 Hz pacing after the first slow phase pacing. A segment between 18 to 19 sec was enlarged from figure 19A to find out about

the state of AP and other ionic currents during rapid pacing but none of them captured any abnormality. (A) AP (B) L-type channels, (C) Na^{+}-Ca^{2+} exchange current (I_{ncx}), (D) Myoplasmic Ca^{2+} concentration ($[Ca^{2+}]_{myo}$) (E) NSR Ca^{2+}, $[Ca^{2+}]$nsr, and (F) RyR opening.

Similarly, the results obtained for I_{ncx} (Fig. 23C) were normal, and not any unexpected changes in the amplitude were observed. The Ca^{2+} transient $[Ca^{2+}]_{myo}$ (Fig. 23D), SR Ca^{2+} release $[Ca^{2+}]_{nsr}$ (Fig. 23E) and RyR2 P_o (Fig. 23F) displayed late reactivation of the RyR2 channels in the plots but the release was not enough to bring the changes in the AP.

Alternans and alternately Skipping beats

The myocyte simulated for WT control, mutant control, and WT β-adrenergic receptors were mostly normal in the pacing frequency of 1 Hz to 6 Hz. Overall, the APD was longer in the β-adrenergic stimulated myocytes than the WT or control mutant while comparing in the same pacing level. I_{ncx} was also longer in the stimulated myocytes than control ones. As usual, SR Ca^{2+} load found to be higher in the β-adrenergic stimulation than control myocytes and it went higher as pacing frequency increased. In comparing control WT and control mutant, the SR Ca^{2+} level was lower in mutant myocytes. The β-adrenergic stimulated myocytes had more load than the WT or control mutant in comparing the result with the same pacing level. I_{ncx} was also longer in the stimulated myocytes than control ones. The SR Ca^{2+} load found to be higher in the β-adrenergic

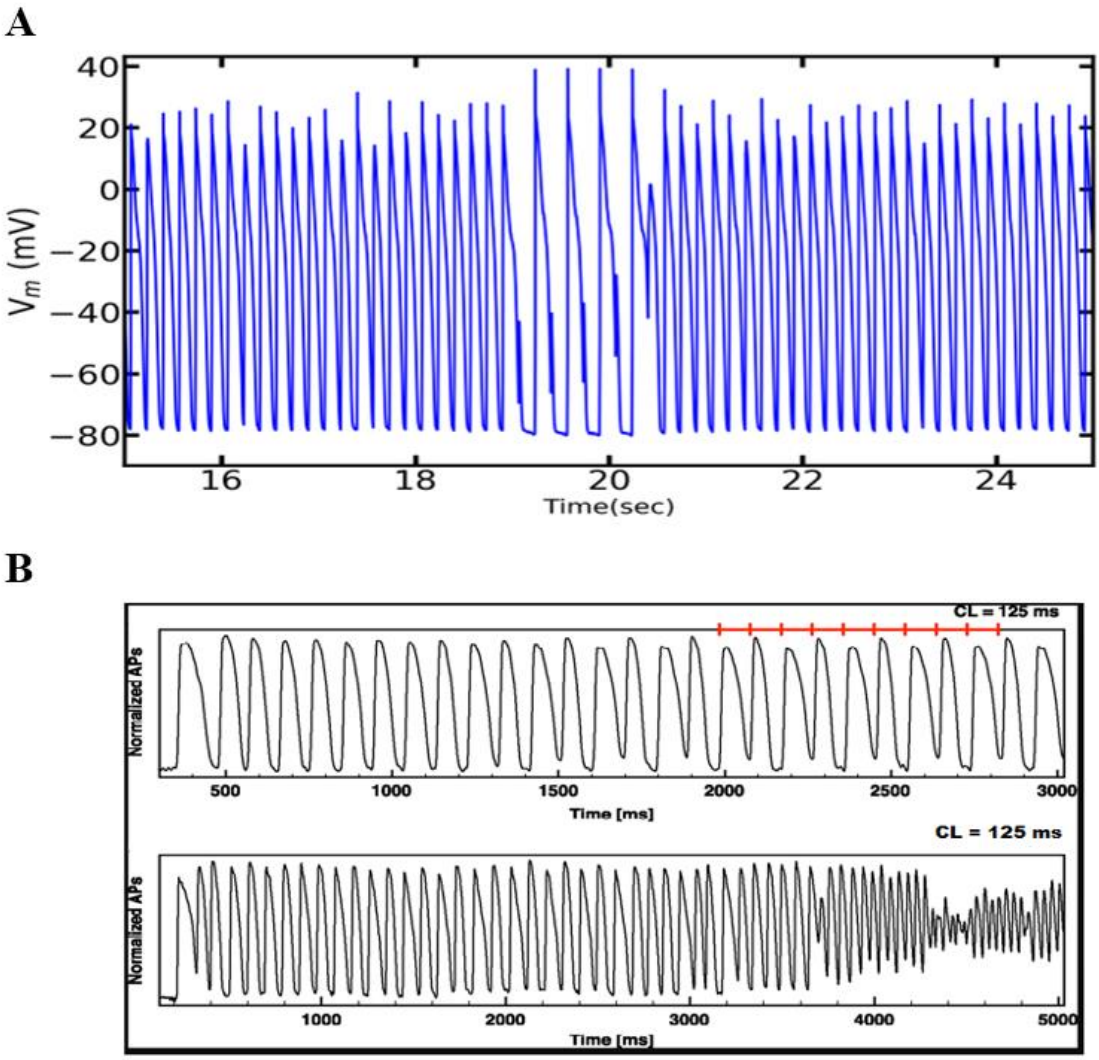

Figure 24: Alternans and alternate beat skipping cause arrhythmia in a myocyte having mutation in the gene expressing CASQ2 protein Alternans along with beats missing in longer simulation. (A) AP shows alternans most of the time and there is also alternate beat skipping in 18.5-20.5. (B) An experimental AP plot of canine myocyte showing alternans (Gizzi, 2013), they plotted it from the optical signal of ventricles with the cycle length (CL) of 0.125 sec, upper plot showed APs up to 3 sec while lower had it till 5 secs.

stimulation than control myocytes because of higher pacing frequency brought more extracellular Ca^{2+} in per unit time.

In comparing control WT and control mutant, the SR Ca^{2+} level was lower in mutant myocytes. A simulation of 30 sec was able to display alternans as well as alternate beat missing (Fig. 24A). The alternans are both in retrenchment amplitude (mechanical) alternans and AP duration (APD or electrical) alternans. The alternate beat missing was for about 2 seconds from 18.5 to 20.5 seconds (Fig.24A) and alternans of different shapes and sizes were noticed in the rest of the time. In comparing our AP plot with the experimental plot (Fig. 24B) (Gizzi, Cherry, Gilmour Jr., Luther, Filippi, & Fenton, 2013), it showed similar patterns of alternate APs in our model plot with an experimental plot. In their plot, the alternans start to appear after 1500 ms (shown by the red line) and further rapid pacing leads to heart failure in 4400 ms. The model plot was from the simulation of CASQ2 mutant myocyte with a constant pacing rate of 6 beats (6000 ms).

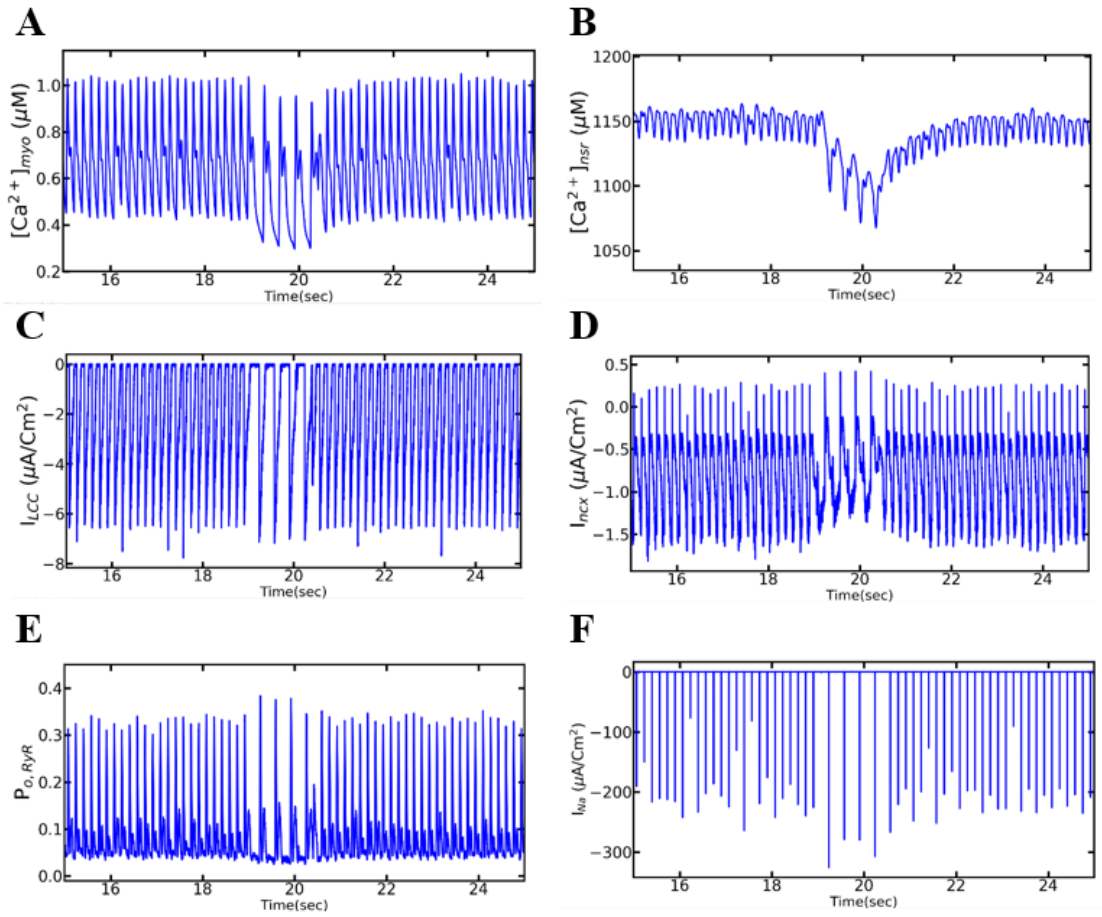

Figure 25: The Ca^{2+} transients, channel openings and ionic currents also reflect the alternans and the beat skipping in them. (A) Myoplasmic Ca^{2+} concentration ($[Ca^{2+}]_{myo}$ (B) NSR Ca^{2+} concentration ($[Ca^{2+}]_{nsr}$), (C) L-type channels, (D) Na^{+}-Ca^{2+} exchange current (I_{ncx}), (E) RyR openings, (F) Na^{+} current (I_{Na}).

The figures in 24 includes alternans plots of cytoplasmic Ca^{2+}, $[Ca^{2+}]_{myo}$ (Fig. 25A), SR Ca^{2+} transient, $[Ca^{2+}]_{nsr}$ (Fig. 25B). L-type ionic currents (I_{LCC}) (Fig. 25C), Na^{+}-Ca^{2+} exchanger current (I_{ncx}) (Fig. 25D), RyR openings, $P_{O,\,RyR}$, (Fig. 25E) Na^{+} current

(I_{Na}), (Fig. 25F). All these plots are showing alternans behavior as shown by AP and their characteristics during alternans are explained later.

Mechanism of Alternans

With the change in the AP, there were changes in other ionic currents and Ca^{2+} transients as shown in figure 25 however further detailed analysis was required to dissect which factors were responsible for the alternation of AP (Fig. 26A) one-second segment in between 8.5 to 9.5 seconds was zoomed in for ionic currents and Ca^{2+} transients and they were plotted as shown in figure 26 (though the alternate patterns were not the same across simulation time a similar pattern was noticed after some interval). We measured both the amplitude and duration of those beats as shown in table 5. The average APD in WT myocyte was measured 141±3 which seems higher than APD of shorter beats but lower than longer beats in alternans (table 4). In comparing peak AP amplitudes, we have recorded the average peak amplitude in WT 38.38 ±0.4 which is higher both shorter and longer beat in alternans. These data on durations, amplitudes, and standard deviation showed mutant myocyte was having both mechanical and electrical alternans. We also investigated the activities of Ca^{2+} sparks in each successive beat (table 5), by counting their numbers (Fig. 26B) and calculating their average amplitudes as well as peak amplitudes per beat. Both shorter and longer beats displayed a massive number of Ca^{2+} sparks in comparison to wild type myocyte. Among the shorter and longer beats, the

Table 5: AP amplitudes, duration, and number of sparks in alternate beats

AP	**Beat 1**	**Beat 2**	**Beat 3**	**Beat 4**	**Beat 5**	**Beat 6**	**St. Dev.**
Duration (ms)	157	131	156	132	156	139	11.45
Amplitude (mV)	31.15	17.23	31.51	16.83	31.51	17.31	7.14
Spark Count	129638	92570	139542	91152	132970	99334	20219

longer beat produced one-third more sparks than shorter beat (table 5). Both average amplitudes (57.03±0.01 vs 60.99±0.02) and peak amplitudes (180.11±0.03 vs 190.79±0.03) of sparks were found shorter than wild type myocyte. It was also observed an alternate diastolic interval (DI) between two consecutive beats. The DI in between shorter and longer (0.025 ms) beat was quantitatively higher than longer and shorter (0.001 ms) (Fig. 26A). A longer DI allowed to increase SR Ca^{2+} load for an incoming beat and it turned out to be a beat with longer APD. The APD depends upon Incx current, when RyR2 brought more Ca2+ to the cytosol, it activated I_{ncx} current and the myocyte stayed depolarized. The L-type current (Fig. 26C) also displayed alternate behavior opposite to respective APs as well opening probability of LCC, $P_{O,\,LCC}$ (Fig. 26D & Fig. 26E). In the L-type Ca^{2+} the channel, during the systolic phase, the highest fraction of the Ca^{2+} channels undergo Ca^{2+} dependent inactivation (CDI – C4), voltage-gated

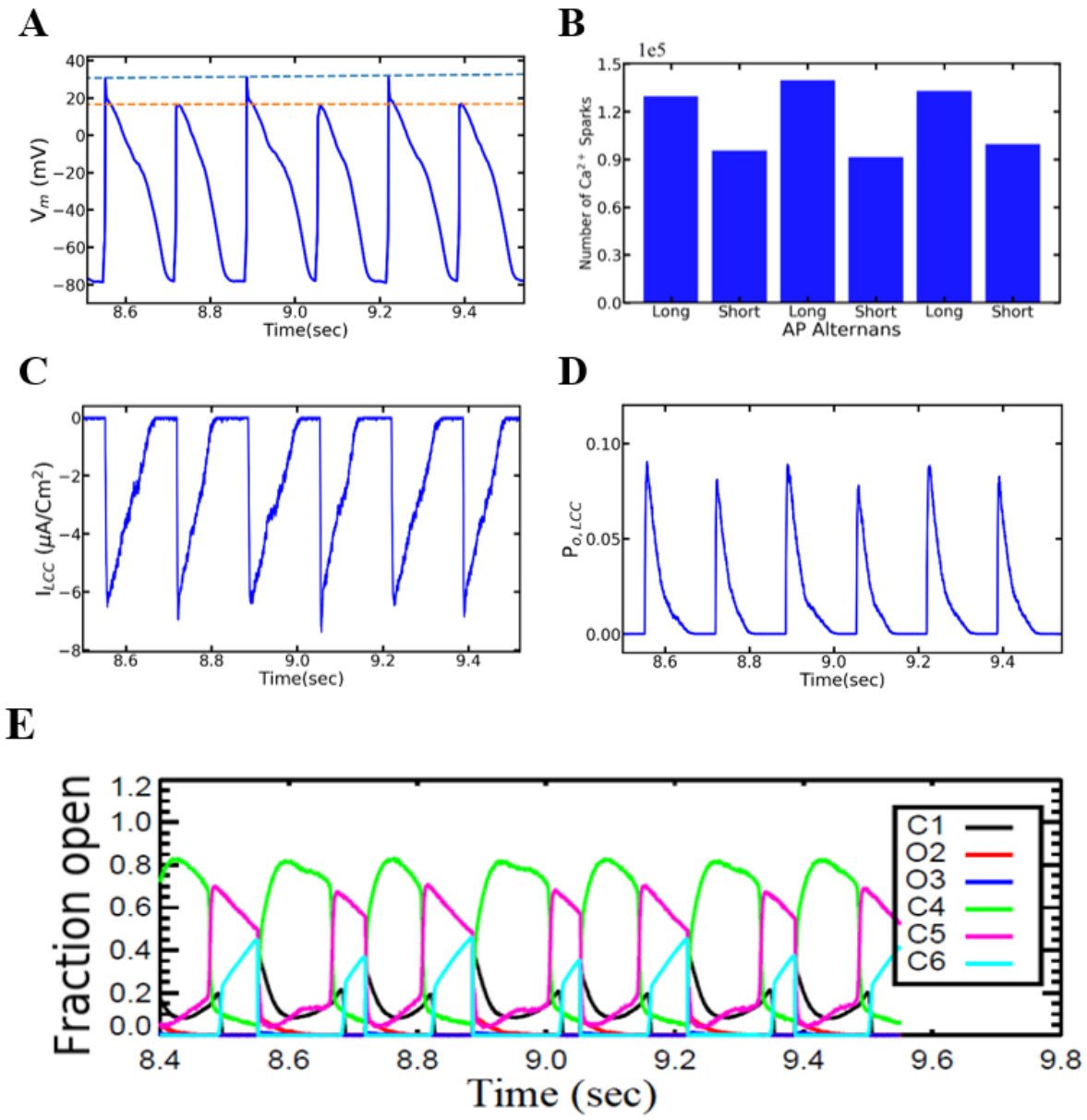

Figure 26: Alternate APs and Ca^{2+} dependent inactivation in alternate L-type current. APs displayed alternations in duration, amplitude, and Ca^{2+} sparks. (A) AP plots in between 8.5 to 9.5 seconds, (B) Bar plot of Ca^{2+} sparks recorded in each beat, (C) Alternate L-type current in the opposite pattern of AP (D) Opening probability of L-type current displayed different pattern than LCC. (E) An open fraction of LCC states

displayed higher calcium-dependent inactivation (CDI) than voltage-dependent inactivation (VDI).

inactivation (VDI – C5) and followed by inactivation state (C6). The open fraction of LCC states showed there was Ca^{2+} dependent inactivation of LCC when the SR load is higher. The SR Ca^{2+} (Fig. 27A) released via RyR2 channels (Fig. 27B) pushed back to the LCC and they displayed different alternate patterns than APs. The beat to beat alternate SR load release of cytoplasm (Fig. 27C) was responsible for the alternate electrogenic I_{ncx} current (Fig. 27D) While plotting Na^{+}-Ca^{2+} exchange currents (Fig. 27D). Those I_{ncx} currents were alternate but unlike L-type currents, they were aligned to the APs, longer the APs then longer the I_{ncx} and vice-versa, and the electrogenic nature helped elongated APs alternately. The plots of I_{Na} (Fig. 27E) and Na^{+} inactivation gate (Fig. 27F)

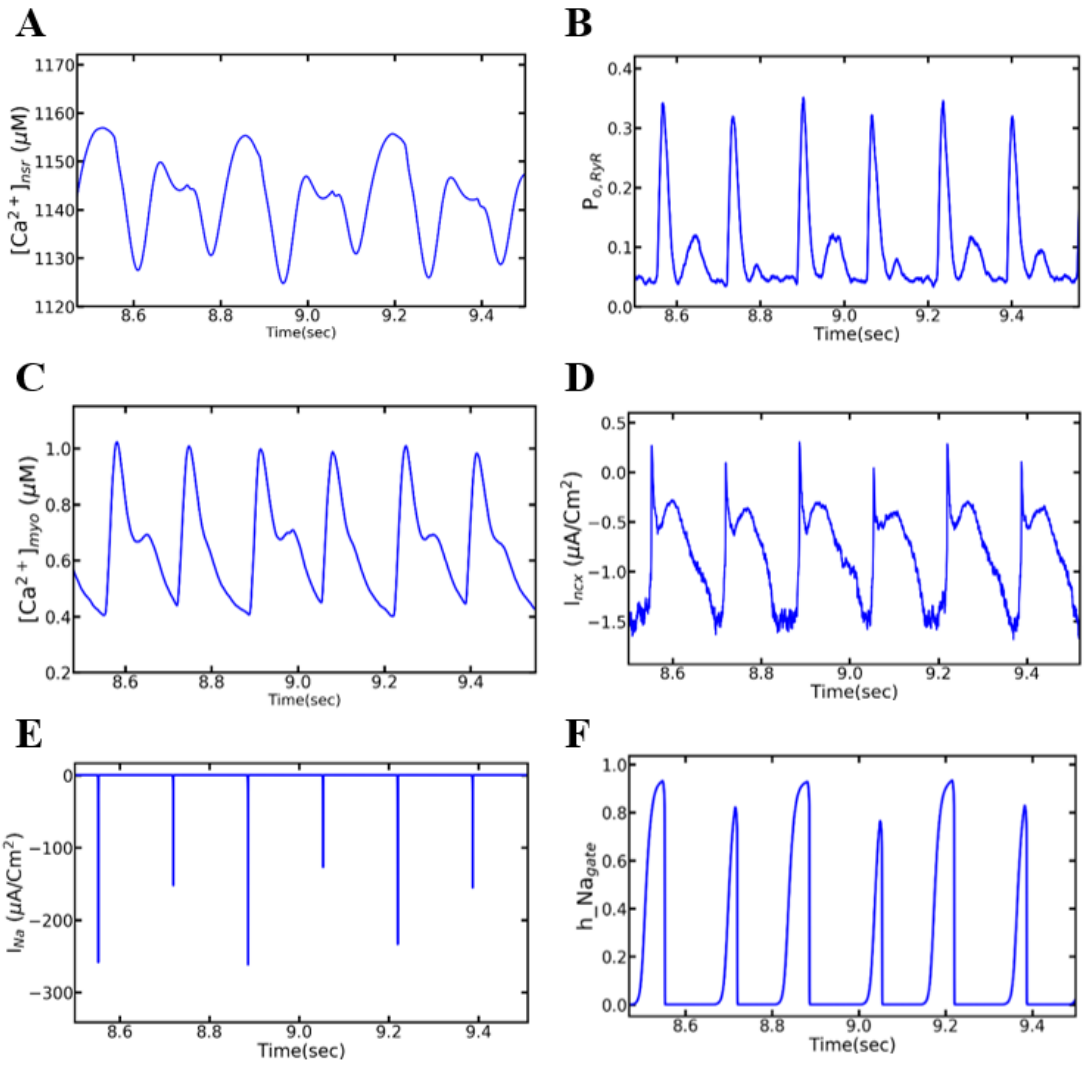

Figure 27: Alternate ionic currents and Ca^{2+} transients can have an alternate pattern. A detailed plots from a segment 8.5-9.5 sec displayed those patterns in different ionic elements (A) NSR Ca^{2+} concentration (B) Opening probability of RyR2 channels, (C) Myoplasmic Ca^{2+} concentration ($[Ca^{2+}]_{myo}$), (D) Na^{+}-Ca^{2+} exchange current (I_{ncx}), (E) Na^{+} current (I_{Na}), (F) Na^{+} inactivation h-gate.

followed the same pattern of APs beats but the alternate arrangements of LCC were opposite to I_{Na}, though they are responsible for the activation of L-type channels in the first place because of the negative feedback mechanism of SR Ca^{2+} towards L-type channels with a larger release in the larger AP. The SR Ca^{2+} serves as the feedback mechanism to the L-type channels and their amplitude decreases (Kubalova, 2003). In table 6, the visual alternate patterns of ionic currents, AP and SR Ca^{2+} transient in consecutive beats were gathered and shown below. In plotting APs from 8.5 to 9.5 sec, we find that the APs were alternate in amplitude and APD. The alternate amplitude is caused by Na^{+} current; when Na^{+} channels were activated fully, they generated taller APs but the shorter APs were because of incomplete recovery of those channels from the previous inactivation. The plot shows that SR Ca^{2+} was mainly responsible for the APD and they also push back LCC with CDI.

Table 6: Alternating ionic currents and transients in consecutive beats

Currents/Transients	**Beat (n- 1)**	**Beat (n)**	**Beat (n + 1)**
I_{Na}	Longer	Shorter	Longer
I_{LCC}	Shorter	Longer	Shorter
AP	Longer	Shorter	Longer
$[Ca^{2+}]_{nsr}$	Longer	Shorter	Longer
I_{ncx}	Longer	Shorter	Longer

But one thing was observable there, during APD alternans the diastolic interval becomes shorter which means shorter time for Na^+ channels to recover from inactivation this makes a smaller number of channels are available for incoming beat hence APD alternans also plays a role in amplitude alternans. In the meantime, the I_{ncx} gets elongated with the Ca^{2+} availability in the cytoplasm and assists the APD to increase further.

Nonrecovery of Sodium Channels Results into Alternate Beat Skipping

In the longer AP plot (Fig. 25A), the graph displayed a few beats were skipping in between 18.5 to 20.5-sec segment and they are zoomed here in figure 28A. The L-type channels were also missing (Fig. 28B) along with APs and they followed a similar pattern but that was opposite in alternans. The I_{Na} currents are also completely disappeared here (Fig. 28C) and were unable to activate the LCC. But during alternans, the Na^+ channels (Fig. 27E) were partially activated and even very low activation was able to activate enough LCCs to sought an AP. The plots of Na^+ inactivation gate (h_Na_{gate}) (Fig. 28D) displayed all the Na^+ channels did not recover from the previous inactivation even late in the systolic phase. Na^+-Ca^{2+} exchange current (Fig. 28E) and NSR Ca^{2+} level (Fig. 28F) were gradually decreased during beat missing period and they were recovering back when the alternate beats started. The voltage-gated Na^+ channels always open for a very short moment to initiate AP and they undergo inactivation. By the time AP repolarizes, the Na^+ channels must be fully recovered for the incoming beats. But this situation may change if there is persistent Na^+ entry in the myocyte. In rapid pacing along with β-adrenergic activation, the level of intracellular in per unit time is very high and due to increased luminal sensitivity of RyR2 towards SR free Ca^{2+}, the activity of I_{ncx}

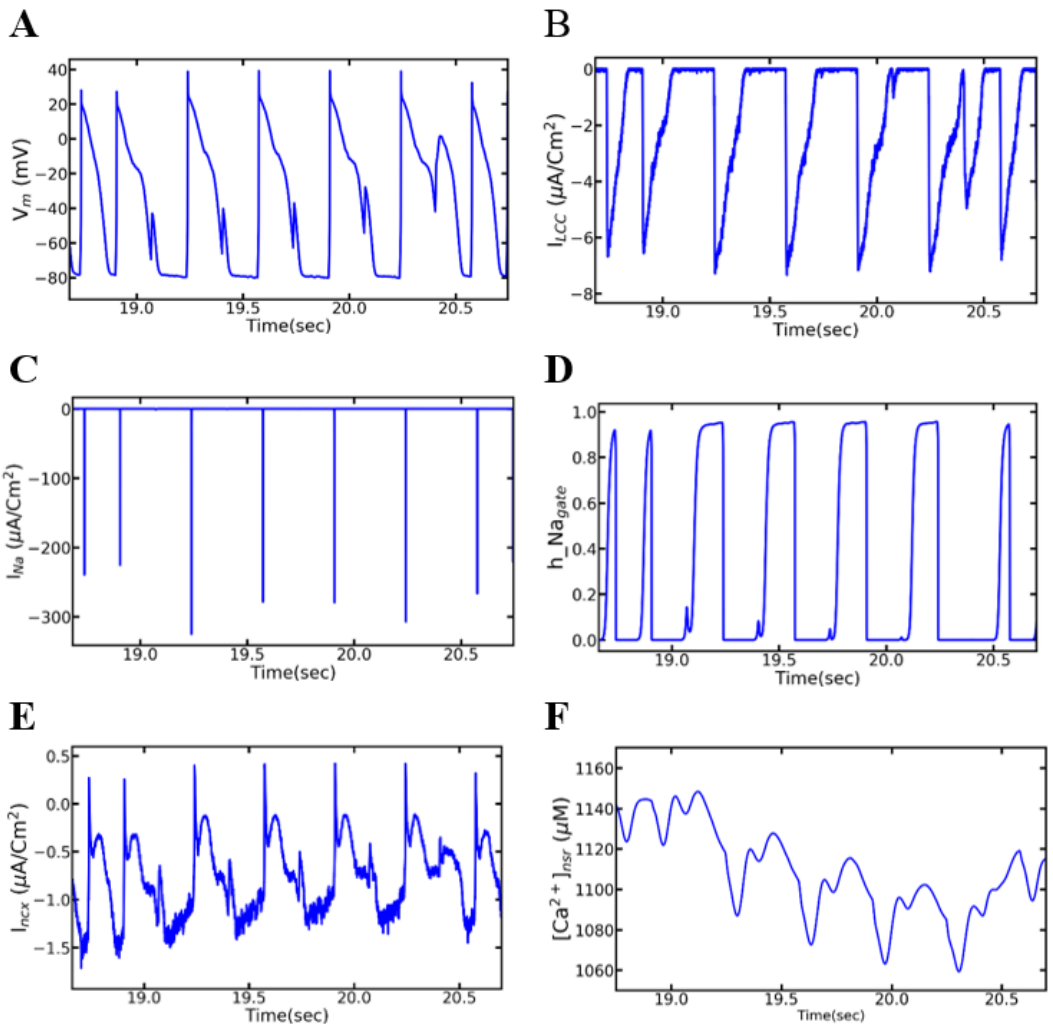

Figure 28: Simulation of AP and other ionic currents in the 6 Hz pacing of a mutant myocyte with β-adrenergic stimulation displayed alternately beat missing**.** The alternation in the beats happens due to the inactivation of Na^+ channels. (A) Inactivation of Na^+ channels is responsible for alternate AP with alternately missing beats. (B) L–type (I_{LCC}) channels are also alternately activated because they need Na^+ current, I_{Na} (C) to increase membrane voltage to activate them. Na^+ channels inactivate themselves in the peak AP by closing their inactivation gates (D). Rapidly paced myocyte has a higher level of

intracellular Ca^{2+} and the late resurgence of Na^{+} occurs by removing excess Ca^{2+} by I_{ncx} (E) and prevents Na^{+} channels from recovering from the previous inactivation. When SR Ca^{2+} level diminishes (F), then myocyte gets back to regular beating.

current also increases. During the rise of intracellular Ca^{2+} concentration, the Na^{+} gradient is used to pump out Ca^{2+} producing an inward (downward) I_{ncx} during the late plateau (Noble, 2006). An increased influx of Na^{+} this late sends the message to the Na^{+} channels they do not need to go through recovery from the previous inactivation

Discussion

Mutations in CASQ2 affects the intracellular Ca^{2+} dynamics and generate CPVT in the heart. Researchers are coming up with different mechanisms behind it both from experimental and simulation settings. To test our hypothesis about the mechanisms, we performed a series of simulations in WT myocytes and mutant myocytes under adrenergic stimulation and presented results above. CPVT is inherited malignant arrhythmia and it can appear in the individuals without prior symptoms or diagnosis which may end up in sudden cardiac death of the patients. Other studies have reported diastolic SR Ca^{2+} overload and leaky RyR2 which results in DADs but we found no evidence leaky RyR2 released enough Ca^{2+} to be able to generate DADs. Gyorke, Hester, Jones, & Gyorke, (2004) reported CASQ2 modulates RyR2 as a luminal Ca^{2+} sensor but Knollmann et al. (2006) demonstrated in a null CASQ2 myocyte RyR2 can sense luminal

Ca^{2+} and handles intracellular Ca^{2+} normally in low SR Ca^{2+} but that may change in higher SR Ca^{2+} load. Our model was able to capture that notion, we have seen the increased SR Ca^{2+} load produced alternans in the continuous rapid pacing but spontaneous Ca^{2+} release occurred if the rapidly pacing myocyte passed in low pacing or pause after and the EADs are produced as the precursor of CPVT.

Alternans

We observed Ca^{2+} alternans in our model with mutant CASQ2 as early as 6 Hz pacing. The simulations suggest under rapid pacing (6 Hz) cellular alternans occurs under β-adrenergic stimulation in the CPVT mutant, but not in the wild-type and unstimulated mutant. There were beat to beat changes in AP (APD & amplitude), ionic currents and Ca^{2+} transients. Due to this multi-faceted impact on AP, it is difficult to pinpoint the responsible ionic behavior for the development of alternans at the cellular level. The benefit of the multi-scale modeling is that it helps us to trace out and detect real-time association of each component to the AP. From the model, the following major points are noted:

- I_{Na} plays a major role in the AP amplitude alternans and SR Ca^{2+} has the main role in the APD alternans.
- Na^{+} channel alternation has a negative feedback on the l-type current alternation
- Intracellular Ca^{2+} has negative feedback to extracellular Ca^{2+} in SR overload
- Very short diastolic interval (DI) for the refilling of Ca^{2+} after a beat with longer APD

- Higher fractions of l-type channels exhibit Ca^{2+}- dependent inactivation (CDI) & voltage-dependent inactivation (VDI)
- NCX current (I_{ncx}) has a positive coupling to the APD

In rapid pacing, the Na^{+} channels are unable to recover from previous beat inactivation and they produce shorter Na^{+} current in the incoming beat. The reduced amplitude of I_{Na} supposed to activate a few LCC reducing the amount of Ca^{2+} influx. This loss is made up of activation of adrenergic receptors during adrenergic stimulation. But we found larger I_{Na} ended up having a smaller LCC. This negative feedback of I_{LCC} towards I_{Na} is controlled by $[Ca^{2+}]_{SR}$. The smaller release of Ca^{2+} in shorter beat leaves higher residue in the SR in the first place and subsequent SR refilling occurs on top of an existing residue. The shorter beat accompanies longer DI which allows a longer time for Ca^{2+} reuptake to SR. All these events create Ca^{2+} overload in the SR for an upcoming beat. When RyR channels are activated by Ca^{2+} via LLC, the massive Ca^{2+} releases from SR inundate diadic subspace benefiting from longer opening RyR2s and LCCs undergo inactivation (CDI) to reduce further intracellular Ca^{2+} toxicity. This is the point where the AP alternans occurs. In the meantime, there are increases I_{ncx} which means more positive charges were brought to the cytosol. The intracellular Ca^{2+} released from SR is responsible for the generation of alternans in cardiac myocyte and the positive coupling of I_{ncx} further adds up into the AP duration.

From spark analysis, it is recorded that more than one-third of Ca^{2+} sparks happened to be in the longer beats that shorter ones. It tells there is fluctuation in Ca^{2+} content in the SR. Diaz, O'Neil, and Eisner (2004) from their experiment reported a

measurable change in the SR Ca^{2+} content produce alternans. They also found reduced openings of LCCs during alternans, we have also got similar patterns in LCCs due to CDI.

L-type channels have two types of inactivation states – voltage-gated inactivation (VDI) and Ca^{2+}- dependent inactivation (CDI) to prevent toxic overload of Ca^{2+} during prolonged depolarization. Primarily Elevated intracellular Ca^{2+} concentration near the junction of SR (dyadic subspace) triggers channel inactivation providing negative feedback to Ca^{2+} influx. The inactivation rate is very high when there is very high $[Ca^{2+}]_{ds}$ in dyad in comparison to bulk myoplasm. Kubalova (2003) distinguished two phases of Ca^{2+} inactivation of L-type channels – a slow phase that depends on Ca^{2+} flow through the channels (Ca^{2+} current-dependent inactivation) and a fast one that depends on Ca^{2+} released from the SR, Ca^{2+} (Ca^{2+} release-dependent inactivation). Hence, SR released Ca^{2+} is the most effective inactivation mechanism in the inhibition of Ca^{2+} entry through the channel. The inactivation of the L-type channel shown to depend linearly on the rate and magnitude of the Ca^{2+} release from the RyRs (Adachi-Akahane, & Cleemann, 1996). Our finding agrees with Saitoh, Bailey, & Surawicz (1989), who demonstrated in dog's ventricular myocyte experiment that the APD alternans are controlled by intracellular Ca^{2+}. The end-systolic SR volume is increased after a shorter beat which leads to a greater end-diastolic volume for the next longer beat and this process is more prominent in the rapidly pacing heart (Euler, 1999). The new APD depends upon the preceding DI, longer the DI, higher the APD, and vice-versa (Tse, Wong, Tse, Lee, Lin, & Yeo, 2016). In our model, it is true longer DI ends up with

longer AP and short DI ends with shorter AP. It is suggested that I_{ncx} is responsible for the prolongation of APD during large Ca^{+} transient (Wan, Cutler, Song, Karma, Matsuda, Baba, et al. 2012). Since three Na^{+} ions enter the cell for every Ca^{2+} ion extruded, this increase in driving force elevates the inward membrane current which prolongs the APD (positive coupling).

In the pattern of the longer and shorter beat in alternans, suddenly the shorter beat goes missing but longer beat continues alternately. This alternate beat missing is also believed to be a form of alternans, but the model suggests different mechanisms other than SR Ca^{2+} overloading in this case. The alternate beat missing is caused by incomplete recovery of Na^{+} channels from inactivation (h-gate) during the relative refractory period (RPP) (Sigg, Laizzo, Xiao, & He, 2010) (Mangold, Brumback, Angsutararux, Volker, Zhu, Kang, et al., 2017). The RPP is the period in between AP depolarization and enough number of Na^{+} channels are available to initiate the incoming beat. Within the milliseconds of their activation, most of the Na^{+} channels undergo inactivation which is faster than total deactivation. The inactivated channels gradually reach the closed state and by the time of RPP, everything is done. When there is late Na^{+} current is available in the myocyte in the late plateau phase or early repolarization, even if the availability of less than 0.5% of the peak Na^{+} travels through the inactivation gates and those channels sense that they do not go recovery from inactivation. In rapid pacing, Na^{+} channels have an extremely short window of RPP; they do not find enough time to recover from the previous inactivation. During alternans, we have found partially inactivated Na^{+} current as well as alternate APs and an increased Incx. It seems the

longer the plateau, the larger the I_{ncx}, which increases the late influx of Na^+ current. These Na^+ ions travel through the inactivated gates and stop them from recovery, it can shut all the Na^+ channels from activation for the incoming beat., in some cases all the channels still inactivated in the time of new beat. When Na^+ channels were unable to activate themselves, the voltage-gated LLCs will not be activated. This complete inactivation of Na^+ channels further inactivates LCCs which shut off the CICR mechanism in the myocyte and a whole beat is lost.

Many researchers believe there are two ways DADs can occur during β-adrenergic stimulation, the aberrant leaking of SR Ca^{2+} during diastole and/or excessive Ca^{2+} influx via L-type channel (Marks, 2001). In our simulations, there was no aberrant leaking of RyR2, and the excessive Ca^{2+} influx because of β-adrenergic stimulation never developed any DADs. We have seen the SR was able to manage Ca^{2+} overload by keeping RyR opening probability longer letting more Ca^{2+} releases from SR, we have also seen more and more L-type channels undergo Ca^{2+} dependent inactivation and RyR2 released Ca^{2+} created a longer beat. After a long beat, there is a very short diastolic phase and might be didn't have enough time required for reloading of SR. The incoming beats become a shorter beat. We have simulated that 40% L-type increases during β-adrenergic stimulation, but we never recorded a diastolic activation of L-type channels and Ca^{2+} influx happening. Based on our simulation findings, we couldn't support the DADs being the mechanism of an arrhythmia in the heart having mutation in the protein of CASQ2 expressing genes.

Early Afterdepolarization (EAD)

When all come down to it, there are three mechanisms of EADs – spontaneous SR Ca^{2+} release caused by intracellular Ca^{2+} loading, β-adrenergic stimulation during stress or exercise, and a resurgence of electrogenic NCX current (Burashnikov, & Antzelevitch, 1998) (Weiss, Garfinkel, Karagueuzian, Chen, & Qu, 2010). However, there is no agreement in the interrelation among those mechanisms. Weiss et al. (2010) reported that EADs occurred due to the reduction in the repolarization reserve but in our simulation, we have noticed an increase in depolarization reserve is responsible for generating EADs. They also claimed EADs occur in a heart during bradycardia but our study finds EADs emerge when a rapidly pacing myocyte enters slow pacing mode. Many researchers agree on is that APD prolongation is necessary to aid EADs, we also found that was true. We noted the irregular intracellular Ca^{2+} dynamics caused by β-adrenergic receptors in the mutant myocyte caused elongated APD. Weiss *et al.* (2010) also believed the major primary current to produce EAD is I_{LCC} and the second major current is I_{ncx} but in our simulations, the primary reason to cause EADs is spontaneous Ca^{2+} release and secondary ones are I_{ncx} and I_{LCC}. Iyer et al. (2007) stated that the stabilization of the SR Ca^{2+} is important in reducing the probability of spontaneous Ca^{2+} release but the stabilization factor, CASQ2 is deleted in $CASQG^{112+5x}$ mutation and it provoked all the instability in the mutant myocyte. January and Riddle (1989) and Sipido *et al.* (2007) suggested that EADs were caused as a result of reactivation of L-type channels following the prolonged plateau phase but we have found spontaneous Ca^{2+} release occurring before reactivation of L-type channels. Because of adrenergic stimulation during exercise

or stress, the L-type channels continuously releasing Ca^{2+} into the dyadic subspace even late in the plateau phase and we have noticed the same phenomenon in our simulation too but we could not support it as a primary source of EADs. At the same time, it was seen the electrogenic I_{ncx} current is also higher than the prior slow phase.

Simulations accelerating pacing from slow (1 Hz) to rapid (5 Hz) and back to slow (1 Hz) did not display cellular alternans but triggered early afterdepolarizations (EADs) during the period of slow pacing after the acceleration to rapid pacing. The model suggests that the rapid pacing loads the cytosol and sarcoplasmic reticulum with Ca^{2+}, which in the CPVT mutant with increased RyR2 open probability can trigger spontaneous Ca^{2+} release which activates Na^{+}-Ca^{2+} exchange resulting in AP prolongation. These studies suggest that spontaneous Ca^{2+} release due to SR overload is the underlying cause of the arrhythmia in these patients.

Conclusion

Ca^{2+} dynamics play a major role for the heart to beat properly. The mutation in the CASQ2 expressing genes affects the Ca^{2+} dynamics by extending the opening probability of RyR2 channels with the increase of luminal dependence. Based on these simulation results, we were able to present that alternans and EADs are the main underlying mechanisms to generate arrhythmia in autosomal dominant CPVT2.

A subcellular disruption in Ca^{2+} dynamics causes a weaker/stronger beat, longer/shorter DI, smaller/larger I_{ncx} and an increase/decrease CDI which all affect the SR Ca^{2+} alternately. When the larger release of SR Ca^{2+} occurs to the cytoplasm, it ends up

creating a stronger beat while smaller SR Ca^{2+} transients produce a weaker beat developing alternans. It was also confirmed by almost double numbers of Ca^{2+} sparks were discharged in a stronger beat than the weaker beat. A beat to beat change in SR Ca^{2+} load give rise to Ca^{2+} alternans which, in turn, result in cardiac alternans and APD alternans. Due to the limitations in our model we are unable to explain this mechanism by Ca^{2+} waves or mini-waves.

Though EADs are also to be the precursor of arrhythmia both in tachycardia and bradycardia because it seems phase 2, EADs prefer low pacing rather than high pacing. Our simulation showed that the heart with mutant myocyte sprints with low pacing to high pacing back and forth, it can generate arrhythmia and the EADs are the mechanism behind it. These EADs generate due to the spontaneous Ca^{2+} release from the loaded SR. The late reactivation of L-type channels and spiking in electrogenic Na^{+}-Ca^{2+} exchange current also aid in generating them.

References

Adachi-Akahane, S. & Cleemann, L. (1996). Cross-signaling between L-type Ca2+ channels and ryanodine receptors in rat ventricular myocytes. *Journal of General Physiology, 108,* 435-454.

Bers, D. M. (2000). Calcium fluxes involved in control of cardiac myocyte concentration. *Circulation Research, 87,* 275-281.

Bhuiyan, Z., Berg, M. P., Tintelen, J. P., Bink-Boelkens, M. T., Wisefield, A. C., Alders, M. et al. (2007). Expanding spectrum of human RYR2-related disease: new electrocardiographic, structural and genetic features. *Circulation, 116,* 1569-1576.

Burashnikov, A. & Antzelevitch, C. (1998). Acceleration-induced action potential prolongation and early afterdepolarizations. *Journal of Cardiovascular Electrophysiology, 9*(9), 934-948.

Coumel, P., Fidelle, J., Lucet, V., Attuel, P. & Bouvrain, Y. (1978). Catecholaminergic-induced severe ventricular arrhythmia with Adams-Stokes syndrome in children: report of four cases. *British Heart Journal, 40*(supplement), 28-37.

di Barletta, M., Viatchenko-Karpinski, S., Nori, A., Memmi, M., Terentyev, D., Turcato, F. et al. (2006). Clinical phenotype and functional characterization of CASQ2 mutations associated with catecholaminergic polymorphic ventricular tachycardia. *Circulation, 114*(10), 1012-1019.

Diaz, M., O'Neil, S. C., Eisner, D. A. (2004). Sarcoplasmic reticulum calcium content fluctuation is the key to cardiac alternans. *Circulation Research, 94*, 650-656.

Euler, D. E. (1999). Cardiac alternans: mechanisms and physiological significance. *Cardiovascular Research, 42*(3), 583-590.

Faggioni, M., Krystal, D. O. & Knollmann, B. C. (2012). Calsequestrin mutations and catecholaminergic polymorphic ventricular tachycardia. *Pediatric Cardiology*, 959-967.

Ginsburg, K. S. & Bers, D. M. (2004). Modulation of excitation-contraction coupling by isoproterenol in cardiomyocytes with controlled SR Ca2+ load and Ca2+ trigger. *Journal of Physiology, 556*, 463-480.

Gizzi, A. E., Cherry, E. M., Gilmour Jr., R. F., Luther, S., Filippi, S. & F. H. Fenton. (2013). Effect of pacing site and stimulation history on alternans dynamics and the development of complex spatiotemporal patterns in cardiac tissue. *Frontiers in Physiology, 4*(7), 1-19.

Guo, T., D. Gillespie, & Fill, M. (2012). Ryanodine receptor current amplitude controls Ca^{2+} sparks in cardiac muscle. *Circulation Research, 111*, 28-36.

Györke, I. & Gyorke, S. (1998). Regulation of the cardiac ryanodine receptor channel by luminal Ca2+ involves luminal Ca2+ sensing sites. *Biophysical Journal, 75*, 2801-2810.

Gyorke, I., Hester, N., Jones, L. R. & Gyorke, S. (2004). The role of calsequestrin, triadin and junctin in conferring cardiac ryanodine receptor responsiveness to luminal Calcium. *J. Biophys., 86*, 2121 - 2128.

Handhle, A., Ormonde, C. E., Thomas, N. L., Bralesford, C., Williams, A. J., Lai, F. A. et al. (2016). Calsequestrin interacts directly with the cardiac ryanodine receptor luminal domain. *Journal of Cell Science, 129*(21), 3983-3988.

Iyer, V., Hajjar, R. J. & Armoundas, A. A. (2007). Mechanisms of abnormal calcium homeostasis in mutations responsible for catecholaminergic polymorphic ventricular tachycardia. *Circulation Research, 100*, e22-e31.

Janvier, N. C., Harrison, S. M. & Boyett, M. R. (1997). The role of Na^+ - Ca^{2+} exchange current in the ferret ventricular action potential. *Journal of Physiology, 498*, 611-625.

Karagueuzian, H. S., Pezhouman, A., Angelini, M. & Olcese, R. (2017). Enhanced late Na and Ca currents as effective antiarrhythmic drug tests. *Frontier Pharmacology, 8*(36), 1-17.

Kashimura, T., Briston, S. J., Trafford, A. W., Napolitano, C., Priori, S. G., Eisner, D. A. et al. (2010). In the RyR2R4496C mouse model of CPVT, beta-adrenergic stimulation induces Ca waves by increasing SR Ca content and not by decreasing the threshold Ca waves. *Circulation Research, 107*, 1483-1489.

Knollmann, B. C., Chopra, N., Hlaing, T., Akin, B., Yang, T., Ettensohn, K. et al. (2006). Casq2 deletion causes sarcoplasmic reticulum volume increase, premature Ca^{2+} release, and catecholaminergic polymorphic ventricular tachycardia. *The Journal of Clinical Investigation, 116*(9), 2510-2520.

Kornyeyev, D., Petrosky, A. D., Zepeda, B., Ferreiro, M., Knollmann, B. & Escobar, A. L. (2011). Calsequestrin deletion shortens the refractoriness of Ca^{2+} release and reduces rate_dependent Ca2+ -alternans in intact mouse hearts. *Journal of Molecular and Cellular Cardiology, 52*, 21-31.

Kubalova, Z. (2003). Inactivation of l-type calcium channels in cardiomyocytes. Experimental and theoretical approaches. *General Physiology and Biophysics, 22*, 441-454.

Lahat H. & Eldar. M. (2004). A missense mutation in CASQ2 is associated with autosomal recessive catecholamine-induced polymorphic ventricular tachycardia in Bedouin families from Israel. *Annals of Medicine, 36*(Suppl), 87-91.

Mangold, K. E., Brumback, B., Angsutararux, P., Volker, T. L., Zhu, W., Kang, P. et al. (2017). Mechanism and models of cardiac sodium channel inactivation. *Channels, 11*(6), 517-533.

Marks, A. R. (2001). Ryanodine receptors/calcium release channels in heart failure and sudden cardiac death. *Journal of Molecular Cell and Cardiology, 33*(6), 615-624.

Medeiros-Domingo, A., Bhuiyan, Z. A., Tester, D. J., Hofman, N., Bikker, H., Tintelen, J. et al. (2009). Comprehensive open reading frame mutational analysis of the RyR2-encoded ryanodine receptor/calcium channel in patients diagnosed previously with either catecholaminergic polymorphic ventricular tachycardia or genotype negative, exercise-induced long QT s. *Journal of American College of Cardiology, 54*(22), 2065-2074.

Metzger, J. M. & Westfall, M. V. (2004). Covalent and noncovalent modification of thin filament action. *Circulation Research, 94,* 146-158.

Noble, D. & Noble, P. J. (2006). Late sodium current in the pathophysiology of cardiovascular disease: consequences of sodium-calcium overload. *Heart, 92*(Suppl. 4), 1-5.

Novak, P. & Soukup, T. (2011). Calsequestrin distribution, structure and function, it's role in normal and pathological situations and the effect of thyroid hormones. *Physiological Research, 60,* 439-452.

Priori, S. G., Napolitano, C., Tiso, N., Memmi, M., Viganti, G., Bloise, R. et al. (2001). Mutations in the cardiac ryanodine receptor gene(hRyR2) underlie catecholaminergic polymorphic ventricular tachycardia. *Circulation, 103*(2), 196-200.

Refaat, M. M., Aouizerat, B. E., Pullinger, C. R., Malloy, M., Kane, J. & Tseng, Z. H. (2014). Association of CASQ2 polymorphism with sudden cardiac arrest and heart failure in patients with coronary artery disease. *Heart Rhythm, 11*(4), 646-652.

Saitoh, H., Bailey, J.C. & Surawicz, B. (1989). Action potential duration alternans in dog Purkinje and ventricular muscle fibers. Further evidence in support of two different mechanisms. *Circulation, 80,* 1421-1431.

Schouten, V. J., ter Keurs, H. E. D. J & Quaegebeur, J. M. (1990). Influence of electrogenic Na/Ca exchange on the action potential in human heart muscle. *Cardiovascular Research, 24,* 758-767.

Sigg, D. C., Laizzo, P. A., Xiao, Y.-F., & He, B. (2010). *Cardiac electrophysiology methods and models.* New York: Springer.

Sipido, K. R., Bito, C., Antoons, G., Volders, P. G. & Vos, M. A. (2007). Na/Ca exchange and cardiac ventricular arrhythmias. *Annals of New York Academics of Sciences, 1099*, 339-348.

Song, L., Alcalai, R., Arad, M., Wolf, C. M., Toka, O., Conner, D. A. et al. (2007). Calsequestrin 2 (CASQ2) mutations increase expression of calreticulin and ryanodine receptors, causing catecholaminergic polymorphic ventricular tachycardia. *J Clin Invest, 17*, 1814-1823.

Terentydev, D., Viatchenko-Karpinski, S., Valdivia, H. H., Escobar, A. L. & Gyroke, S. (2002). Luminal Ca^{2+} controls termination and refractory behavior of Ca^{2+}-induced Ca^{2+} release in cardiac myocytes. *Circulation Research, 91*(5), 414-420.

Tse, G., Wong, S. T., Tse, V., Lee, Y. T., Lin, H. Y. & Yeo, J. M. (2016). Cardiac dynamics: Alternans and arrhythmogenesis. *Journal of Arrhythmia, 32*(5), 411-417.

Volders, P. G., Vos, M. A., Sipido, K. R., de Groot, S. H. M., Gorgels, A. P. M., Willens, H. J. J. et al. (2000). Progress in the understanding of cardiac early afterdepolarizations and torsades de pointes: time to revise current concepts. *Cardiovascular Research, 46*(3), 376-392.

Wan, X., Cutler, M., Song, Z., Karma, A., Matsuda, T., Baba, A., & Rosenbaum, D. S. (2012). New experimental evidence for mechanism of arrhythmogenic membrane potential alternans based on balance of electrogenic I(NCX)/I(Ca) currents. *Heart Rhythm, 9*(10), 1698–1705.

Wang, S., Trumble, W. R., Liao, H., Wesson, C. R., Dunker, A.K. & Kang, C. H. (1998). Crystal structure of calsequestrin from rabbit skeletal muscle sarcoplasmic reticulum. *Nature Structural Biology, 5*(6), 476-483.

Wei, L., Hanna, A. D., Beard, N. A., & Dulhunty, A. F. (2009). Unique isoform-specific properties of calsequestrin in the heart and skeletal muscle. *Cell Calcium, 45*, 474-484.

Weiss, J. M, Garfinkel, A., Karagueuzian, H.S., Chen, P.-S. & Qu, Z. (2010). Early afterdepolarization and cardiac arrhythmia. *Heart Rhythm, 7*(12), 1891-1899.

Xie, Y. E., Grandi, E., Puglisi, J. L., Sato, D. & Bers, D. M. (2013). β-Adrenergic stimulation activates early afterdepolarization transiently via kinetic mismatch of PKA targets. *Journal of Molecular and Cellular Cardiology, 58*, 153-161.

CHAPTER FOUR: GOF AND LOF MUTATIONS IN THE RYR2 EXPRESSING GENE ARE RESPONSIBLE FOR THE ARRHYTHMOGENIC ACTIVITIES IN THE HEART.

Abstract

Mutations that occur in the ryanodine receptor (RyR2) encoding genes in cardiac myocytes have been linked to arrhythmia and possibly sudden cardiac death (SCD) during acute emotional stress, physical activities, or catecholamine perfusion. The most prevalent disorder is catecholaminergic polymorphic ventricular tachycardia (CPVT1). Four primary mechanisms have been proposed to describe CPVT1 in RyR2 mutation: (a) destabilization of binding proteins, (b) store overload-induced Ca^{2+} release (SOICR), (c) gain-of-function (GOF), and (d) loss of function (LOF). To gain some discernment into the nature of this rare disease, we have developed a local control stochastic model of a ventricular cardiac myocyte and used to investigate how the Ca^{2+} dynamics in the mutant RyR2 is responsible for the development of an arrhythmogenic episode under the condition of β-adrenergic (β-AR) stimulation or pauses afterward. We have incorporated a realistic 20,000 stochastic gating of L-type Ca^{2+} channels (LCC) and ryanodine receptors (RyR2) into the model to inquire and analyze many defects caused by the instability of Ca^{2+} handling in molecular level in the mutant RyR2. The recent experimental findings were incorporated into the model parameters to test these proposed mechanisms and the role they play in triggering arrhythmias. The model could not find any connection between SOICR and the destabilization of binding proteins as the arrhythmic mechanisms in the mutant myocyte. Still, it was able to find the LOF, and

GOF mutations developed EADs and alternans as the precursor to generate arrhythmia, respectively.

Introduction

Ryanodine receptor (RyR) is an intracellular Ca^{2+} channel in the cardiac myocyte, which provides Ca^{2+} required for them to contract. Each RyR has a homotetramer functional channel of ~2200 kDa comprising of four monomers. The monomer contains a transmembrane segment located at the N-terminus, which serves as a large platform for regulatory subunits and enzymes to modulate the function of the channel. The small C-terminal transmembrane structure comprises the channel pore

Mutations in the RyR2 genes are thought to cause arrhythmia in the heart through alteration in the Ca^{2+} dynamics. There is no reported disease phenotype associated with RyR3, but RyR1 and RyR2 are associated with over 300 mutations and the number of genetic diseases because of those mutations (Petegem, 2012) (Kimlicka, Lau, Tung, & Petegem, 2013) (Crescenzo, Fogarty, Lefkowitz, Bellve, Zvaritch, MacLennan, et al., 2012). CPVT can be caused by an autosomal dominant mutation in the RYR2 gene, and it is designated as type 1 CPVT (CPVT1) (Behere, & Weindling, 2016) (Napolitano, Napolitano, Bloise, Memmi, & Priori, 2014). The gain-of-function RyR2 mutation accounts for more than 50% of CPVT1 (Kawata, Ohno, Aiba, Sakaguchi, Miyazaki, Sumitomo, et al., 2016). Since the identification of RyR gene mutation causing CPVT by Priori, Napolitano, Tiso, Memmi, Viganti, Bloise, et al. (2001), a total of more 150 different RyR2 mutations have been reported in the CPVT patients (Behere, & Weindling, 2015) (Zhang, & Morad, 2016) (Kontula, Laitinen, Lehtonen, Toivonen,

Viitasalo, & Swan, 2005) (Wei, Zhang, Clift, & Yamaguchi, 2016). Most of these mutations cluster in three different "hot spots" regions, 176-420 amino acids located in N-terminal region (domain I), 2100-2500 amino acids of central region (calstabin2 binding domain II) and after amino acids of 3778-4950 in C-terminal region (domain III) out of 4967 amino acids (Priori, & Chen, 2011) (Robinson, Carpenter, Shaw, Halsall, & Hopkins, 2006) (Leenhardt, Denjoy, & Guicheney, 2012) (Zalk, Lehnart, & Marks, 2007). RyR2 as a gene contains 105 exons, 45 exons of them were reported having CPVT-causing mutations, and substitution mutations are highest in number (Leong, Sucich, Prosser, Skinner, Crawford, Higgins, et al., 2015). Most of the RyR2 mutations cause a gain-of-function (increase RyR2 opening probability) that leads to an increased release of SR Ca^{2+} into the myoplasm (Petegem, 2012) (Kimlicka, et al., 2013). In contrast, there are some mutations responsible for a loss-of-function (Avila, O'Connell, & Dirksen, 2003) (Jiang, Chen, Wang, Zhang, & Chen, 2007), and they cause central core disease and idiopathic ventricular fibrillation. However, this research is focused on gain-of-function mutation and CPVT. Some studies also suggest that the mutations also increase the sensitivity of the channels to the activating agents (Jiang, Xiao, Yang, Wang, Choi, Zhang, et al., 2004). Missense mutations, consisting of single-nucleotide substitutions (point mutations) that lead to the replacement of amino acid, are common in RyR2 (Blayney, & Lai, 2009) (Lanner, Georgiou, Joshi, & Hamilton, 2010) (Bagattin, Veronese, Bauce, Wuyts, Settimo, Nava, et al., 2004). However, in a severe form of CPVT deletion of an entire third exon of 35 amino acids also takes place (Bhuiyan, Berg, Tintelen, Bink-Boelkens, Wisefield, Alders, et al., 2007) (Leong, Sucich, Prosser,

Skinner, Crawford, Higgins, et al., 2015). Surprisingly, this deletion does not cause any misfolding or aggregation and is still a gain of function mutation (Lobo, Kimlicka, Tung, & Petegem, 2011). Any mutation which causes the removal of the entire RyR2 is lethal embryonically (Takeshima, Komazaki, Hirose, Nishi, Noda, & Lino, 1998).

The focus of this study is to understand the mechanism of CPVT1 caused by a mutation in the gene expressing intracellular Ca^{2+} channels, RyR2s. The variations intensify the function of these channels, increasing their open probability (Priori, et al., 2001) (Laitinen, Brown, Piippo, Swan, Devaney, Brahmbhatt, et al., 2001). An elevated release of SR Ca^{2+} affects the intracellular Ca^{2+} dynamics and is thought to trigger arrhythmia during exercises or stress. It is believed that increased SR Ca^{2+} load during rapid pacing combined with the increased RyR2 open probability leads to arrhythmia. However, with increase RyR2 open probability, there are increases SR Ca^{2+} leak, which can limit Ca^{2+} accumulation in the SR complicating this hypothesis. This apparent paradox will be explored using our computational modeling as we address the mechanism of the RyR2 dysfunction approach.

Mechanisms of RyR2 dysfunction in CPVT variants

Researchers have proposed several mechanisms to explain how the dysfunction of mutant RyR2 causes CPVT1, and there is less agreement that exists in those various mechanisms. With the literature reviews, we came up with three main mechanisms – Interdomain unzipping, gain-of-function (GOF), overload threshold change (SOICR), and loss-of-function (LOF).

i) Destabilizations Binding Proteins and interdomain unzipping

The mutation in RyR2 affects the binding proteins between a domain pair and renders them incapable of controlling the opening or closing of the channels. Yamamoto and Ikemoto (2002) reported that the NH2-terminal (N: 0-600) and the central domains (C: 2000- 2500) of RyR2 interact as a domain pair and either of this domain can have CPVT-linked RyR2 mutations which modify the channels to be hyper-active and hyper-sensitive. They were able to synthesize a peptide, DPc10 having RyR2 mutation extending from C:2460 to C:2495 (Gly^{2460} to Pro^{2495}) in a rabbit sequence. The DPc10 is one example of the mutation to cause the unzipping of RyR2 and destabilize the channel. This defect unfastens the zipping in RyR2 channels required for RyR2 closure during the diastolic phase resulting in increased Ca^{2+} leak from the SR, which ultimately causes the development of DADs (Mohler, & Wehrens, 2007) (Suetomi, Yano, Uchinoumi, Fukuda, Hino, Ono, et al., 2011) (Dobrev, Carlsson, & Nattel, 2012). The mutant myocyte in the systolic phase starts with low SR Ca^{2+}, and there is a significant increase in the sensitivity of the RyR2 and longer duration of Ca^{2+} release (George, Higgs, & Lai, 2003).

Similarly, Wehrens Lenhart, Huang, Vest, Reiken, Mohler, et al. (2003) proposed that RyR2 binding protein, calstabin 2 (FKBP12.6 – C:2331-2438), stabilizes RyR2s in wild type myocytes. It is believed that FKBP12.6 to maintain closed state (resting phase) by tightly binding the RyR2 domains, but the binding affinity of FKBP12.6 protein is reduced in mutant RyR2s. All four FKBP12.6 molecules are binding to each tetramer of RyR2 (Marks, 2001). There are two types of proposed mechanism in FKBP12.6 destabilization: a) It is understood that PKA-induced phosphorylation of RyR2 leads the

dissociation of FKBP12.6 protein which increases the open probability of RyR2 channels as well as increase sensitivity towards Ca^{2+} activation (Marx, Reiken, Hisamatsu, Jayaraman, Burkhoff, Rosembit, et al., 2000), b) the reduced RyR2 binding affinity of FKBP12.6 causes abnormal leaks of Ca^{2+} during diastolic phase (Fig. 29) developing DADs with β-adrenergic stimulation (Iyer, Hajjar, & Armoundas, 2007) (Kushnir, & Marks, 2010) (Liu, Papa, Katchman, Zakharov, Roybal, Hennessey, et al., 2009). These binding proteins have their specific sites to bind, the RyR2 binding of DPc10 or FKBP12.6 affects each other (Oda, Yang, Niu, Svensson, Lu, Fruen, et al., 2013) and due to their hyperactivity and premature release of SR Ca^{2+}, these mutations are also termed as gain-of-function mutation (Bhuiyan Berg, Tintelen, Bink-Boelkens, Wisefield, Alders, et al., 2007).

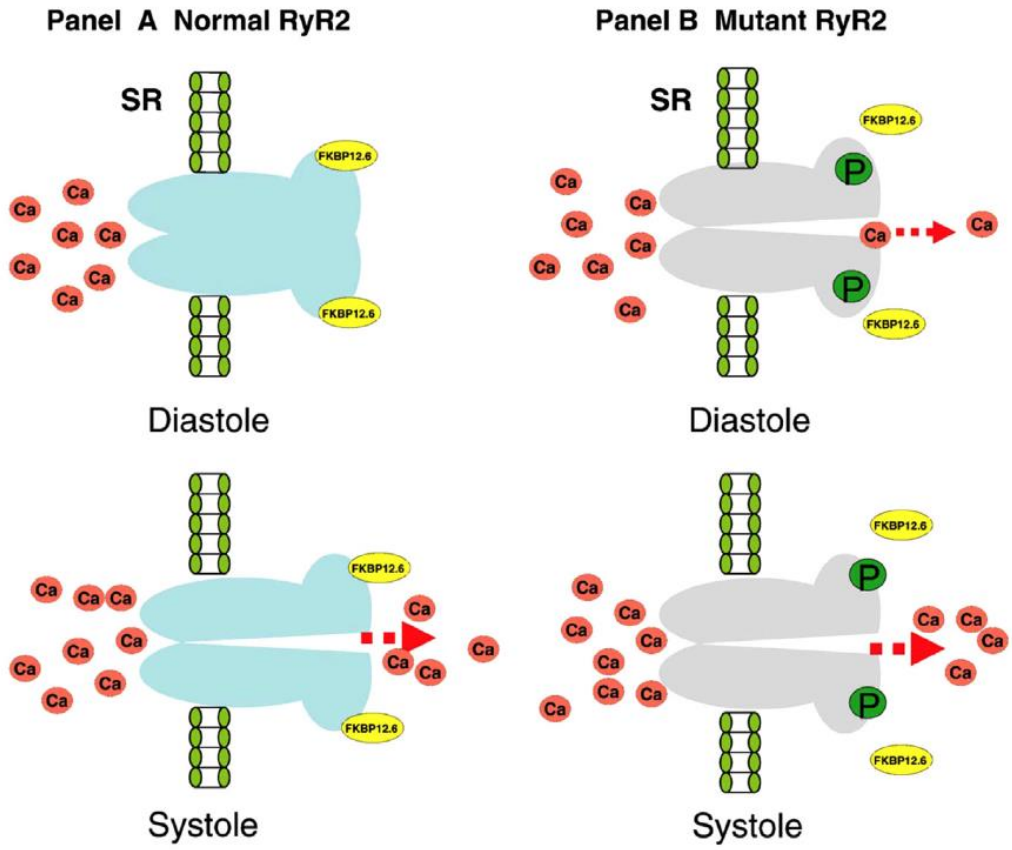

Figure 29: Binding proteins dissociation in RyR2 in the pathogenesis of CPVT (Liu, 2009). DPc10 and FKBP12.6 binding proteins act as stabilizers that preserve the closed RyR2 channel during diastole. Weakened binding affinity with of these proteins may lead to a Ca^{2+} leak during diastole.

ii) Store overload-induced Ca^{2+} Release (SOICR)

Jiang et al. (2004) hypothesized that in the mutant RyR2, the threshold for store-overload-induced Ca^{2+} release (SOICR) in SR is lowered than WT RyR2 due to the

enhanced RyR2 channel sensitivity towards the luminal Ca^{2+}. On the other hand, the sensitivity towards the cytosolic Ca^{2+} remains indifference. The mechanism further states that at the normal CICR, the refilling of SR reaches to a new lower threshold level (shown in Fig. 30 panel B) with the excess Ca^{2+} received from the β-AR stimulation. The threshold is here shifting P_{O_RyR2} from higher luminal dependency to lower one. Due to this sudden change in the SR load, the RyR2 channels open irrespective of the depolarization and spontaneously release SR Ca^{2+} to trigger DADs.

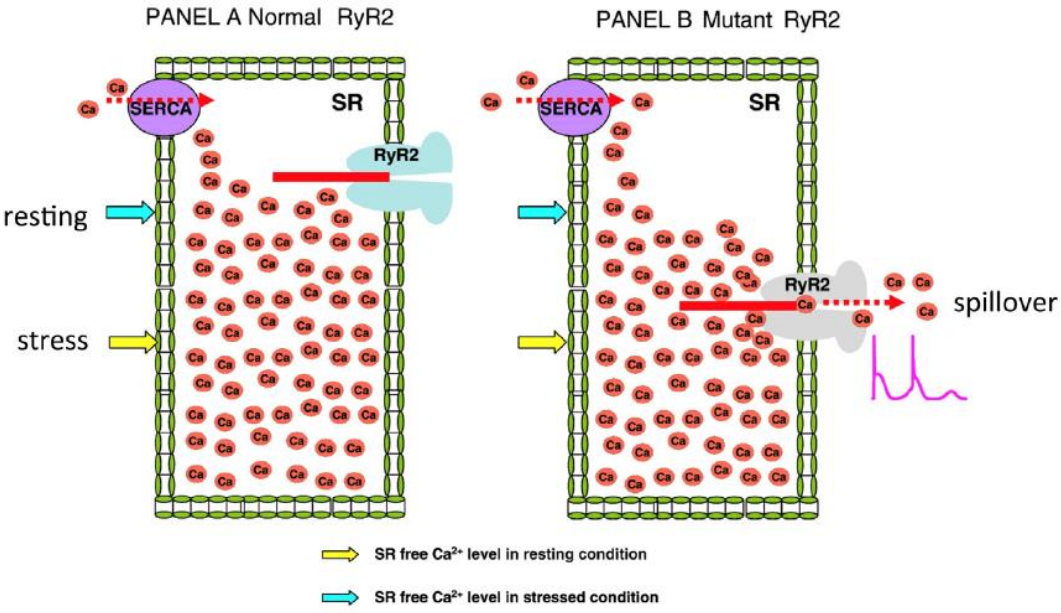

Figure 30: The store overload-induced Ca^{2+} release (SOICR) hypothesis (Liu, 2009). With normal RyR2, the resting and stress levels of free calcium are below the SOICR threshold (panel A). If the SOICR threshold falls below the level of free SR calcium as with mutant RyR2, a leak of Ca^{2+} will occur and generate a DAD.

iii) RyR2 mutation causes loss-of-function

Gomez and Richards (2004) proposed loss-of-function (LOF) hypothesis based upon "non-conventional" findings of Thomas, George, and Lai (2004) and that stated the AP prolongation because of the combination of the normal peak but prolonged Ca^{2+} release to generate EADs in the mutant myocytes. The ventricular arrhythmia in RyR2 mutation can also occur with LOF mutation, the contrary to popular gain-of-function mutation (Jiang, et al., 2007) (Roston, Guo, Krahan, Wang, Petegem, Sanatani, et al., 2017) (Zhao, Valdivia, Gurrola, Powers, Willis, Moss, et al., 2015). According to the LOF mechanism, the mutation causes a decrease in the Ca^{2+} release during systole resulting in a gradual overload of Ca^{2+} in the SR. After a few beats, the overloaded SR randomly releases a burst of Ca^{2+} (Fig. 31) which makes elongated AP and EADs trigger arrhythmia. Zhao et al. (2015) harbored a RyR2 mutation RyR2-A4860.

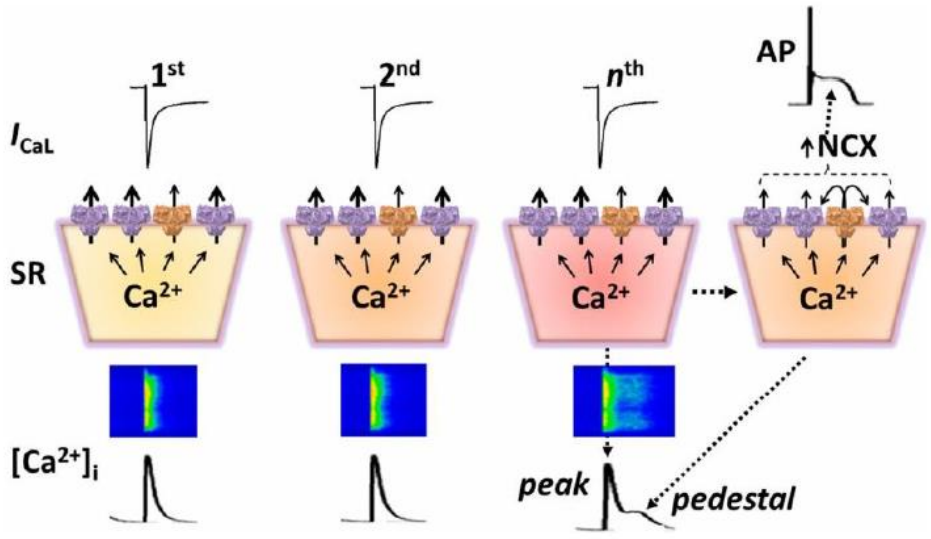

Figure 31: Loss-of-function mutation in RyR2 mutation (RyR2 ^{A4860G}) generates EADs

(Zhao, et al., 2015). In a single RyR2 ^{A4860G} cardiomyocyte containing functionally divergent RyR2 channels (WT has shown in violet, AG shown in bronze).

Materials and Methods

Model Development

During exercise or emotional stress, the response of the sympathetic nervous system activates ("fight" or "flight" response) the catecholamine hormones such as epinephrine or adrenaline, which stimulate the beta-adrenergic receptors (β-adrenoceptor) of the myocardium (Wallukat, 2002). The stimulation of β- adrenoceptor open the L-type calcium channels (LCCs) and release outside Ca^{2+} into the dyadic subspace of myoplasm. This extracellular Ca^{2+} stimulates RyR2 channels to release intracellular Ca^{2+} from the SR. In comparing with wild type myocyte, the opening probability increases in the mutant RyR2 channels. To analyze the effect of beta-adrenergic stimulation quantitatively, we have modified our stochastic computational model of Guinea pig ventricular myocyte and imitated this behavior. The model contains a six-state LCC and three-state RyR2 and gating behavior of these channels derived from the Markovian stochasticity algorithm.

The system of ordinary differential equations (ODEs) used in this model was modified from a stochastic rat model (Williams, Chikando, Tuan, Sobie, Lederer, & Jafri, 2011). The Markov Chain Monte Carlo method incorporated into the model that applied the Euler method to derive Ca^{2+} dynamics from 40002 differential equations. The L-type channel was described by six-state gating mechanisms that incorporate both voltage-

dependent activation/deactivation and Ca^{2+} dependent inactivation like Sun, Fan, Clark, & Palade (2000). The intracellular Ca^{2+} release from junctional SR is based upon Ca^{2+} dependent. We have developed a novel three-state model as shown below. In resting AP, the RyRs are in a closed state (C_1), when the Ca^{2+} in dyad increases, the channels are in the open state (O_2) for a very short period and then go to an adaptive state (C_3). Upon further increase in Ca^{2+}, the RyRs may return to open state (O_2). This model is a modification of the four-state Keizer-Levine model (Keizer, & Levine, 1996). The adaptive state was experimentally proved by Gyorke, Hester, Jones, and Gyorke (2004) and Gonano and Jones (2017). This RyR2 gating in this model is modulated by cytosolic Ca^{2+} sensitivity and luminal Ca^{2+} dependency.

RyR2 Model

In 1998, Jafri et al. (Jafri, 1998) developed a new model by integrating the L-R II (Luo & Rudy, 1994b) model with the improvement of shortcomings of the models at that time. They also replaced the Ca^{2+} SR release mechanism in Luo-Rudy II and added adaptive features in the RyR model to simulate more realistic Ca^{2+} dynamics. The RyR model had four states – two closed states and two open states. Based upon that model, we developed a new three-state model – two closed states and one open state as shown in figure 32. The second closed state (C3) shown in figure 31 is the adaptive state. The gating mechanism of this RyR model borrowed from the leak model and the formulations is based upon Monte simulation.

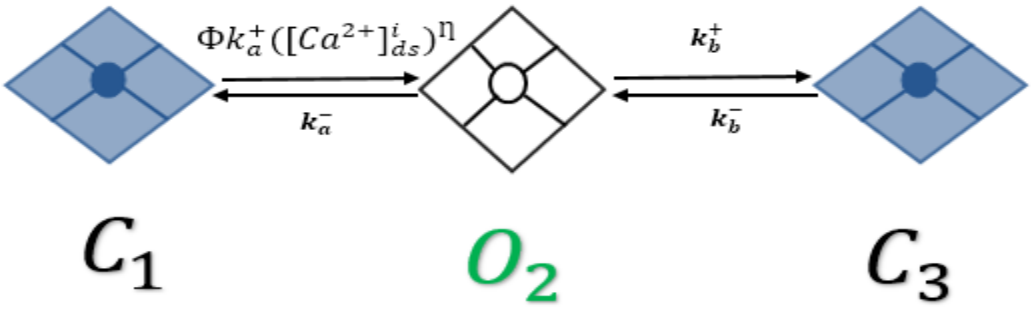

Figure 32: A novel, three-state RyR2 model. In the resting phase, all RyR2s stay in the closed- state (C_1), with the arrival of Ca^{2+} in the dyadic subspace, the channels activate into the open state (O_2), and after some time, the channels might inactivate into an adaptive state (C_3).

In this model, the luminal regulation function (Φ) modifies the channel opening rate, SR load, $[Ca^{2+}]_{SR}$ available to be released (Bers, 2002). RyR release flux reaches to the near its peak with the increase in pacing frequency $[Ca^{2+}]_{SR}$ availability to be released calculated by the following equation (Jafri, et al., 1998)

$$SR_{rel} = v_1(P_{O,RyR})([Ca^{2+}]_{sr} - [Ca^{2+}]_{ds}) \text{ ---------- (1)}$$

Where v_1 is the maximum Ca^{2+} release via RyR channel, $[Ca^{2+}]_{ds,}$ Ca^{2+} concentration in diadic subspace. Opening the probability of RyR ($P_{O,RyR}$) is affected by RyR adaptation in higher frequency.

Simulation Protocols

The simulation protocol for this simulation was designed for increased activity of RyR2 due to mutation and increasing sensitivity towards luminal Ca^{2+} sensitivity and dyadic Ca^{2+}.

A) β-adrenergic stimulation protocols

a) Increased L-type Ca^{2+} influx: The effect of an exercise, emotion, and fight or flight response activates β-adrenergic receptors of protein kinase A (PKA) and increases the Ca^{2+} flow of L-type channels (Liu, et al., 2020). Experiments indicate that the peak L-type amplitude could increase from 53% (Ginsburg, & Bers, 2004) or 95% (Ganesan, Maack, Johns, Sidor, & O'Rourke, 2006) to the three-fold (Miriyala, Nguyen, Yue, & Colecraft, 2008) when the level of isoproterenol (ISO) increases by the activation of β-adrenergic receptors in the sarcolemma (Morales, Hermosilla, & Varela, 2019) (Miriyala, et al., 2008). In adjusting the parameters in our model, a 48% percent increase in L-type current (P_dhpr) was adequate to show the result.

b) Increase in SERC2a pump activity: In higher mammals with positive FFR, there is an increase in SR Ca^{2+} content in elevated pacing frequencies. Phospholamban (PLB) inhibits the SERCA2A activities in the SR but the inhibition is reduced by the stimulation of β-adrenergic receptors which results in increased SERCA2A pump activities (Metzger, 2004). When more Ca^{2+} in cytosol due to an increase in Ca^{2+} influx via L-type current, it is also going to increase SR Ca^{2+} load (Bers, 2000) with the activation of SERCA2A (Kashimura, Briston, Trafford, Napolitano, Priori, Eisner, et al., 2010). In our simulation, we raised the SERCA rate (A_p) by 50 percent. The SERCA formulation is given by,

$$J_{serca} = 2v_{cycle} A_p$$ ---------- (2)

Where, v_{cycle} is cycling rate per molecule, and *Ap* is the concentration of SERCA molecules per liter cytosol

B) Protocols for mechanisms

After setting up the protocols β-adrenergic stimulation, we designed the following protocols for four mechanisms – GOF, SOICR, interdomain unzipping, and LOF mutations.

1. Gain-of-Function simulation

The GOF mutation was modulated with the alteration of the model parameters as given below.

a) Increase in Po of RyR2 channels: Mutations in RyR2 increased the opening probability (sensitivity) of the RyR2, in our RyR2 model, we have K^+ and K^- as opening and closing rate constants for RyR2 channels. Potenza *et al.* (Potenza, Janicek, Fernandez-Tenorio, Camors, Ramos-Mondragon, Valdivia, et al. 2019) recorded a 55% increase in RyR2 phosphorylation during β-AR stimulation. To reproduce the phosphorylation of RyR2, we raised the opening constant (K^+) by fifty percent in this simulation and applied in the equation as shown below.

$$C_1 \underset{k^-_{aryr}}{\overset{k^+_{aryr}}{\rightleftharpoons}} O_2 \underset{k^-_{bryr}}{\overset{k^+_{bryr}}{\rightleftharpoons}}$$ ---------- (3)

$$k^+_{aryr} = *_{18} \left([Ca^{2+}]^{(i)}_{ds}\right)^{2.2} * \left(2.8\, x\, 10^{-4}[Ca^{2+}]^{(i)}_{jsr} + 0.02\right),$$ ---------- (4)

Where, i = number of RyR open channels (0 to 49), k^{-}_{aryr} = 350, k^{+}_{bryr} = 7.0, k^{-}_{bryr} = 1.0 * for non-mutant RyR2, the value of K^{+} is 12.

b) A decrease in half-maximal point (Km): The sensitivity of a single RyR2 channel is prompted by local $[Ca^{2+}]_{myo}$ and local $[Ca^{2+}]_{sr}$. The sensitivity of RyR2 P_O modulated with a half-maximal point (K_m^{myo}), a dynamic buffering fraction of myoplasm as a function of $[Ca^{2+}]_{myo}$ (Qin, Valle, Nani, Chen, Ramos-Franco, Nori, et al., 2009) and it increases the transition rate between closed- to-open state. Still, it declines the open-to-inactivation rate (Danielson, Manotheepan, Sadredini, Laren, Edwards, Vincent, et al., 2018) and they adjusted it by reducing half-maximal value of $[Ca^{2+}]_{myo}$ by 10%. The decrease in half-maximal $[Ca^{2+}]_{myo}$ is the main characteristic of GOF and varies in different RyR2 mutations. For example, it is 1.5 - 4-fold less than WT in N4104K, R4496C, V4653F, and S4153R mutations (Zhabyeyev, Heiss, Wang, Liu, Chen, & Oudit 2013). Hernandez et al. (Hernandez, Herron, Jalife, Maginot, Zhang, Kamp, et al., 2018) in RyR2-H2464D mutation recorded a cytosolic Ca^{2+} sensitivity of RyR2 increased from 19±3% WT to 44±6% in the mutant myocyte. To model Km in our model, we reduced the value of $\boldsymbol{k^{-}_{aryr}}$ from equation 3 by 30% (500 – 150 = 350). Besides these two parameters, the leakiness of RyR2 was adjusted by reducing the value of allosteric coupling (a_*) by 80% which is explained below.

2. Destabilization of binding proteins or Interdomain Unzipping:

As per the RyR2 binding protein theory, there is a reduced binding affinity to RyR2 under basal conditions. To reproduce this behavior in our model, we decreased allosteric coupling (AC) (a_*) by 50% and ~100%, AC deals with the interactions among

the homotetramers in the RyR2. We simulated without current clamps and checked whether the Ca^{2+} leak was able to generate any DADs during the diastolic phase in both cases. The allosteric coupling factors X_{oc} and X_{co} is given by Williams et al. (2011).

$$X_{oc} = \exp\{-a_* 0.5\,[N_c \varepsilon_{cc} - (N_0 - 1)\varepsilon_{00}]\}\,, \text{---------- (4)}$$

$$X_{co} = \exp\{-a_* 0.5\,[N_0 \varepsilon_{00} - (N_c - 1)\varepsilon_{cc}]\}\,, \text{---------- (5)}$$

Where, a_* is average allosteric connectivity, ε_{cc} & ε_{oo} are dimensionless free energy of interaction represents free energy experienced by a channel in closed state C or open state O when allosterically couples with another channel in the respective states. N_c and N_o are the number of closed or open states in the CRUs ($0 \leq No \leq 49$).

There were two modes of the simulation that were done for destabilizing protein mechanism: the first one was with resting mode and the second one was the current-clamp mode. In simulating resting mode, the initial Ca^{2+} concentration in the SR was increased by two folds while RyR2's sensitivity and hyperactivity were added for current-clamp mode.

3. Simulation of Store overload-induced (SOICR)

The CICR is the central phenomenon to the E-C coupling and regulates subcellular Ca^{2+} signaling in the myocyte. It is initiated by the RyR2 sensitivity towards $[Ca^{2+}]_{myo}$ and luminal Ca^{2+} sensitivity has a major influence on it (Prosser, 2010). To test the SOICR hypothesis of SR Ca^{2+} activates RyR2 channels, the cytosolic Ca^{2+} concentration was fixed to the resting level by setting up $[Ca^{2+}]_{ds}$ into the initial value (0.0954 πM) without incrementing it in the equation two above and the simulation was run with β-AR stimulation. The SR was loaded with 100% Ca^{2+} and luminal dependence

was increased by 90%. The goal over here was to slow down the CICR process and to let the SOICR phenomenon get going as claimed by Jiang et al. (2004).

4. Loss-of-function mutation (LOF)

In the lipid bilayer experiment of LOF mutant, RyR2-A4860G, (Jiang, et al., 2007) found RyR2s are very insensitive to the increased luminal Ca^{2+} and average RyR2 opening probability was below 20% with the Ca^{2+} concentration ranging from 100nM to 50 mM during β-AR stimulation. Likewise, Zhao et al. (Zhao, et al., 2015) also found suppressed $P_{O,\,RyR2,}$ and overloaded SR in the knock-in mouse model with the mutant RyR2-A4860G during ISO treatment. To simulate this change in our model, the luminal dependence of RyR2 was reduced till $P_{O,\,RyR2}$ went below 20% percent in the β-AR myocyte.

The changes made in various parameters in different mechanisms are listed in table 7 below. It shows which parameter values were increased, decreased, or stayed the same.

Table 7: Modulation parameters in the for RyR2 mutation simulations

Simulation Types	Half-maximal Point (K^-)	Hyperactivity(K^+)	Luminal Dependency (K_{JSR0})	Allosteric Coupling (a_*)
GOF	Decrease	Increase	No change	Decrease
LOF	No change	No change	Decrease	No change
Binding Protein	No Change	Increase	No change	Decrease
SOICR	No change	No change	Increase	No change

Numerical Methods

The PGI CUDA Fortran compiler was used to execute and simulate the program in the Linux platform, Ubuntu operating system. CUDA (compute unified device architecture) is a parallel computing platform and programming language developed for graphic processing units (GPUs) by NVIDIA. The original CUDA was developed in C programming language. CUDA and NVIDIA GPUs have been widely used in higher education research in computational biology, numerical analytics, physics, and scientific visualization. The CUDA clusters we are using in the lab contain Fermi-based C2050 graphics processing cards with CUDA SDK 6.0 and higher. To capture calcium dynamics at a single-channel level, a novel computational algorithm Ultra-Fast Markov chain

Monte Carlo (UMCMC) method was used for the stochastics gating from CRUs (Jafri, et al., 2015).

Results

While simulating myocytes with adrenergic receptor activated, the wild type myocytes showed normal pacing from 1 Hz to 6 Hz but mutant myocyte was having normal from plots up to 5 Hz and developed alternans as early as 6 Hz frequency. Our result explanation below compares plots of AP and its other components between 6 Hz pacing in WT myocytes and mutant myocytes with and without adrenergic stimulations in both cases.

Binding Proteins Destabilization

The allosteric coupling simulations to produce interdomain unzipping and Ca^{2+} leaks were for thirty seconds and the plots were checked to find any DADs that appeared by the binding protein destabilization in RyR2 mutation. The plots were unable to show any DADs or any other arrhythmic disorders. No change in the membrane potential of the sarcolemma was recorded in the resting potential during the entire simulations. We then picked a ten-second segment (6- 15 sec) and counted the Ca^{2+} release both in spark release and non-spark release. The Ca^{2+} sparks found during the simulation were plotted in a graph shown in figure 33A below. The average numbers of Ca^{2+} sparks were 1575±306 in 50% lower AC while that number went to 6034±506 while the AC was reduced by ~100% (33B), the spark numbers were not good enough to bring abnormality in the resting potential. We also observed the average size of the spark amplitudes in both

periods, and the average size was 47±0.19 μM with the first reduction while it was recorded 55±0.85 in the second reduction. It showed that the spark amplitudes increase with the increase in sparks numbers. In comparing this with WT simulation, the average number of Ca^{2+} sparks were 129±22.27 and the average size of the Ca^{2+} spark amplitude was 51.44±0.56 μM. In comparing non-spark Ca^{2+} release, both WT and mutant myocyte release them enormously. We counted 19.40 million non-spark Ca^{2+} from WT myocyte while it was 19.98 million in mutant myocyte regardless of the value of AC.

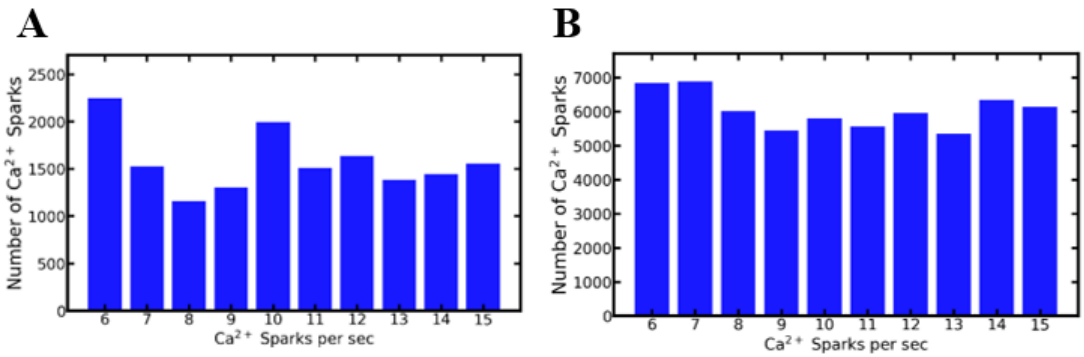

Figure 33: A comparison of Ca^{2+} sparks in the two different levels of allosteric coupling (AC) in the mutant myocytes in resting potential, a leak caused by the destabilization of RyR2 binding proteins. (A) Number of Ca^{2+} sparks in between 5-15 seconds when AC was lowered by 50% (B) Number of Ca^{2+} sparks in between 5-15 seconds when AC was lowered by ~100%. In both cases, no DADs were reported during resting potential.

The occurrence of massive spontaneous Ca^{2+} release during diastole and SR Ca^{2+} leak was observed in the mutant myocyte (Fig. 34A) which is thought to produce DADs.

However, the AP (Fig. 34B) generated by the model was unable to translate them into DADs, which means the increased leak due to RyR2 mutation was not enough to cause the depolarization needed for the DADs. We also found a ~20% decrease in SR Ca^{2+} level as well as smaller peak Ca^{2+} transients in comparison to WT myocyte.

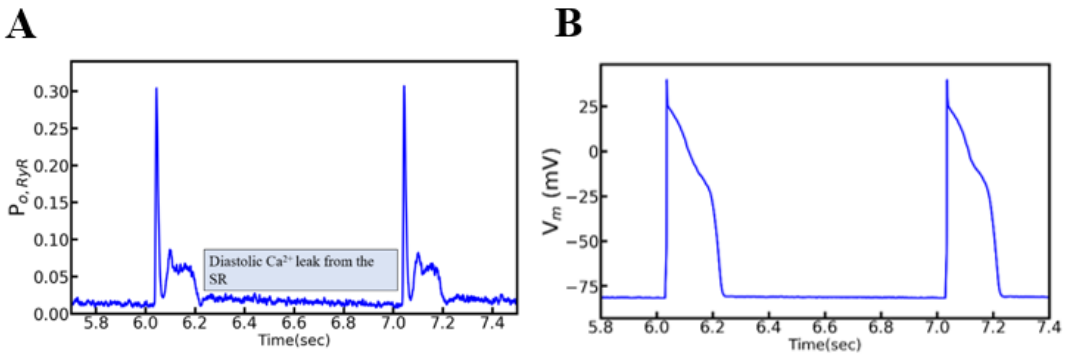

Figure 34: With ~100% lowering of allosteric coupling, there is massive spontaneous Ca^{2+} release during the diastolic phase which can be seen in $P_{o,\,RyR2}$ (A) but there are no signs of DADs in the AP (B).

George et al. (2003) with their study of three CPVT related RyR2 mutations reported that RyR2/FKBP12.6 interaction was undamaged due to the mutations and acted like WT myocytes. They did not find any abnormality in SR Ca^{2+}, $[Ca^{2+}]_{SR}$, or cytosolic Ca^{2+}, $[Ca^{2+}]_{myo}$ in those mutant myocytes during the resting phase. We were also unable to distinguish any changes both in WT and mutant myocytes with the comparison of AP or another ionic current because there were no abnormal activities with the leak. But with

the analysis of Ca^{2+} sparks, we found a higher number of Ca^{2+} sparks during diastole in mutant myocyte than WT one but those sparks weren't enough to trigger DADs.

Loss of function mutation generate EADs

With the reduction in the luminal Ca^{2+} regulation of RyR2 in LOF mutation, we observed longer and slowed SR Ca^{2+} release which resulted into a longer APD (202.18±3.6 vs 189±1.3 WT) and longer average spark durations (32.84 ms vs 19.31 ms WT) in 1 Hz

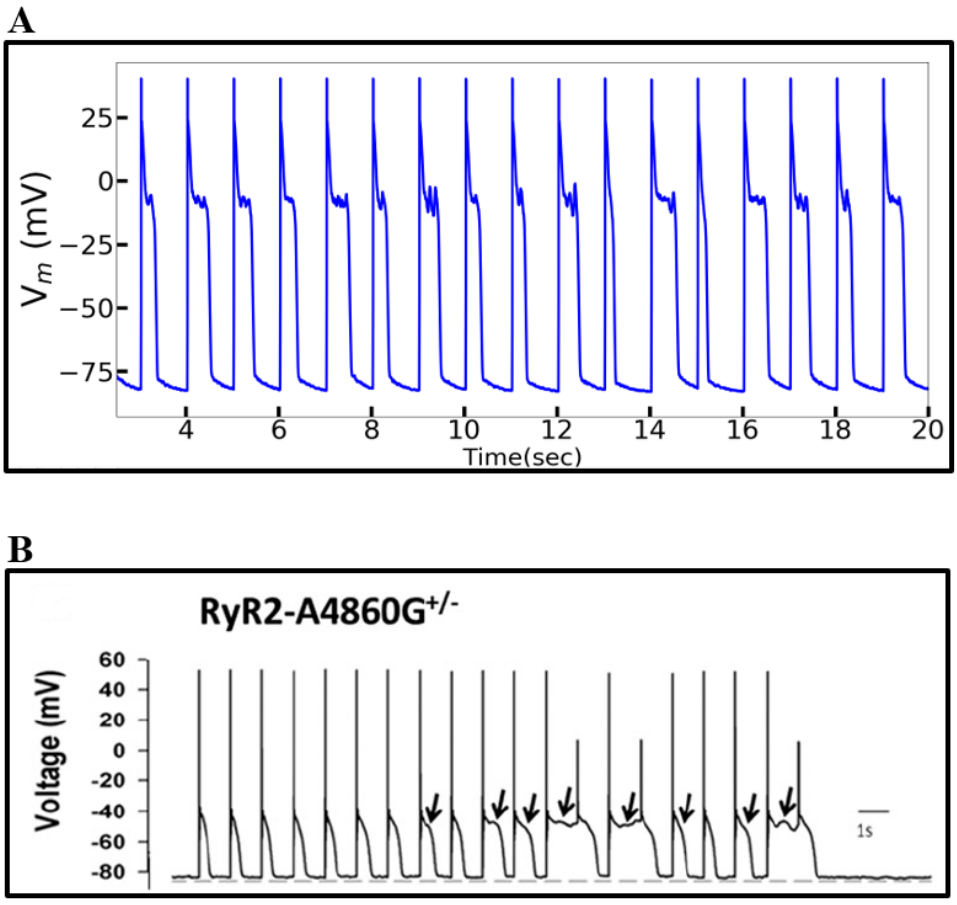

Figure 35: EADs were recorded in a RyR2 LOF mutant myocyte with β-AR stimulation.

(A) APs with the predominant occurrence of EADs from our model, (B) An ISO-stimulated experimental plot of APs with EADs appeared in ventricular myocytes of knock-in mouse model comprising LOF mutation (RyR2-A4860) in ryanodine receptors (Zhao, et al., 2015).

the simulation even before β-AR stimulation. For mutant myocyte, the luminal Ca^{2+} dependency was lowered (~70%) to have the RyR2 the opening rate ~0.20 in the simulation-based upon Jiang *et al.* (Jiang, 2007). Attributable to lower RyR2 open probability and constantly increasing L-type influx in β-AR activation, the APD and spark durations were getting very long (Fig. 35A) (APD; 202.18±3.6 ms & spark duration; 48.25 ms) and it was repolarizing and depolarizing to develop an EAD within a beat. This showed the recorded average APD was huge in comparison to WT as well as mutant myocyte before β-AR stimulation. The result obtained from our model resembles an experimental result of the knock-in mouse model having LOF RyR2 mutation (RyR2-A4860), as shown in figure 35B. The Ca^{2+} transients in myoplasm were higher in mutant myocyte and we found it further up with longer APD (Fig. 36A) and in the meantime, the SR was loaded with higher Ca^{2+}recorded average APD was is huge in comparison to WT as well as mutant myocyte before β-AR stimulation.

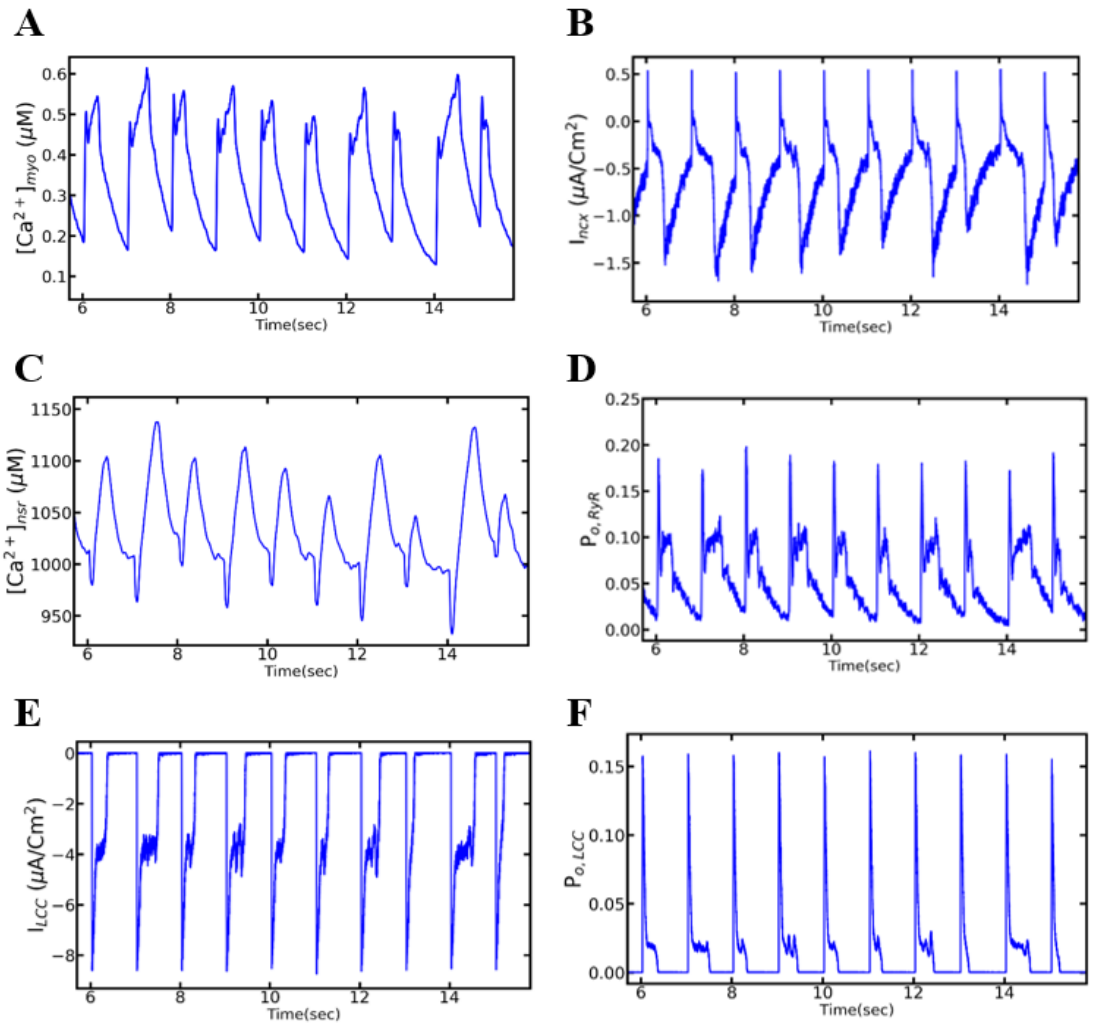

Figure 36: Abnormal Ca^{2+} transients and Ca^{2+} handling channels during EADs (A) An inconsistent looking peak myoplasmic Ca^{2+} transient (B) An elongated electronegative I_{ncx} (C), Abnormal but relatively loaded NSR (D) A longer opening of RyR2 receptors (E) A large and longer L-type current (F) A longer opening of L-type channels show activation and reactivation in the same beat.

The Ca^{2+} transients in myoplasm were higher in mutant myocyte and we found it further up with longer APD (Fig. 36B) and in the meantime, the SR was loaded with

higher Ca^{2+} level (Fig. 36C) and longer opening with prolonged-release Ca^{2+} from RyR2 channels (Fig. 36D). It is believed that the prolonged Ca^{2+} release translated into EADs but it is required to unload SR Ca^{2+} and prevent SR overfilling (Zhao, 2015). Similarly, a longer L-type current (36E) brings an excess influx of extracellular Ca^{2+} which elongates the plateau phase in the AP with the β-AR stimulation of L-type channels. Another highly important components to aid elongated APD is Na^{+}-Ca^{2+} exchange current, I_{ncx} (Fig. 36F). Because of the electrogenic nature of I_{ncx}, it brings extra positive charge in the myoplasm to remove excess Ca^{2+} from the cytosol. It is not always true the lengthening APD causes EADs (Zhilin, 2013) but in our model, we saw the elongated APD increased the chances of reactivation L-type channels (Fig. 36F). It has been found that the EAD oscillations vary with the time and the last oscillation is always larger than preceding oscillations and we have in that in our result to as shown in figure 36A.

Ionic Mechanism of EADs

There are 3 Ca^{2+} related mechanisms to generate EADs are explained in the literature: reactivation and reverse repolarization of L-type current, spontaneous SR Ca^{2+} release, and predominantly inward I_{ncx} current (Weiss, Garfinkel, Karagueuzian, Cheng, & Qu, 2010). In our model, the EADs (Fig. 37A) were produced due to the reactivation of the L-type current (Fig. 37B). The late reactivation brought activation in RyR2 channels (Fig. 37C) and trigger to release more SR Ca^{2+} for the further depolarization of the AP. Then SR release in the cytosol would further activate I_{ncx} current and the plateau continued to stay. Second, the diastolic spontaneous Ca^{2+} release (Fig. 37C) was also recorded in $P_{o,\,RyR2}$ but was inept to bring any abnormality in the AP. A slow-release and

continuous release SR Ca^{2+} due to LOF mutation elongate I_{ncx} current (Fig. 37D). The late opening of RyR2s provided extra Ca^{2+} in the cytosol and Incx elongated the AP duration. It has been said I_{ncx} would synergistically work with I_{LCC} by providing positive feedback to it and facilitates EAD formation. This view of I_{ncx} is supported by almost double amplitude in EADs over WT myocyte (209±0.18 vs 1.10±0.05).

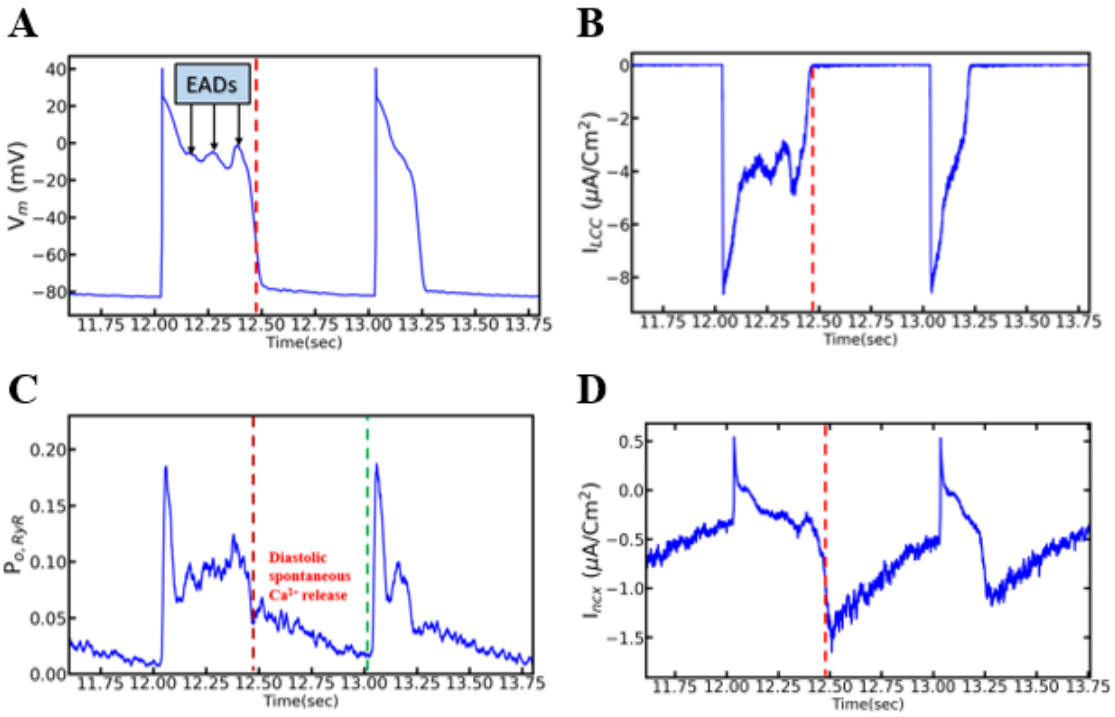

Figure 37: Late reactivation of LCC and SR Ca^{2+} release is essential to generate EADs. (A) AP with EADs, (B) L-type current with late reactivation, (C) RyR2 channels activated by LCC current and spontaneous Ca^{2+} release during diastole, (D) In LOF mutation stretched out I_{ncx} current assisting L-type channels with the elongation of APD. The red dotted lines in the figures are to separate a beat.

To determine which ionic component was responsible for triggering EAD in LOF mutation, we laid together the time of initiation of AP, I_{LCC}, I_{ncx} and RyR2 P_O from figure 36 into a table (Table 8) below. In the first EAD in the left (EAD1), it was observed the L-type current began at 12.118 sec and it was followed by RyR2 more channels were open at 12.1359 sec, then I_{ncx} further activated by the cytosol Ca^{2+} and depolarized at 12.1445 sec and ultimately AP developed EAD at 12.1508 seconds. The remaining two EADs (EAD2 & EAD3) followed a similar process to trigger EADs like the first one. The data clearly displayed the late reactivation of L-type channels triggered the EADs but Incx worked in synergy to provide longer APD to let reactivation of L-type channels again.

Table 8: Depolarization of I_{LCC}, I_{ncx} & AP and opening of RyR2 in EADs

	Time of Initiation of each component			
EADs	ILCC	RyR2	Incx	AP
EAD1	12.1180	12.1359	12.1445	12.1508
EAD2	12.2151	12.2245	12.2255	12.2271
EAD3	12.3295	12.3433	12.3467	12.3502

Role of I_{ncx} in the generation of EADs

To understand the ionic mechanism of the EAD generation concerning I_{ncx}, we ran the simulations blocking I_{ncx} by 25% and 50% and observed the results. In the first, the I_{ncx} was reduced by 25% and ran the simulation. When the results were obtained for

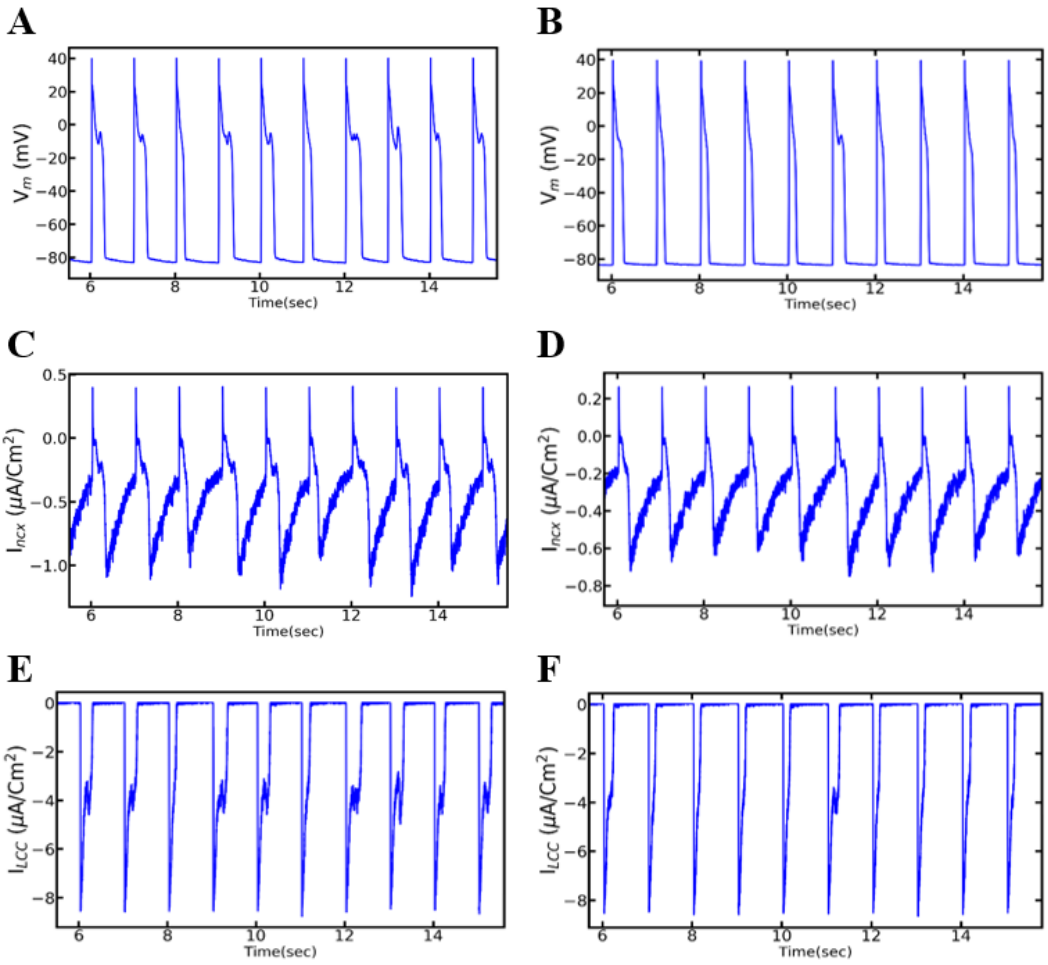

Figure 38: Frequency of EADs and APDs were lowered in a myocyte with the Loss of function RyR2 mutation by reducing I_{ncx} by 50%. The left side (A), (C) & (E) represent AP, I_{ncx}, and ILCC with the 25% blocking with the Incx respectively. On the right panel,

the counter elements of left panel (B) AP (D) Incx and (F) LCC with the 50% blocking of I_{ncx}.

25% reduction, we found the AP (Fig. 38A) still had many EADs but the APD shrunk to 338.97±54.5 ms from 438.97±123.8 ms and the APD (Fig. 38B) was further decreased with the 50% I_{ncx} reduction (238.7±38.55) and the frequency of EADs were significantly removed too. Similarly, the amplitude of the I_{ncx} current was also heavily varied reducing it from 50% to 25% (Figs. 38C & 38D). The I_{ncx} amplitude with EADs was 2.05±0.18, it was lowered to 1.50±0.08 with 25% less I_{ncx} and reached to 0.95±0.04 with the 50% less I_{ncx}. This reduction in the Incx also affected the duration of L-type channels (Figs. 38E & 38F), 314.75±109.20 ms from EADs to 272.55±57.19 ms with 25% I_{ncx} reduction and it further reduced to 169.09±30.22 ms in 50% reduction. In the model, the wild type duration of I_{LCC} was 110.06±0.5.

A comparison of APD90 (Fig. 39A) before and after reducing I_{ncx} provides a clearer clue of how I_{ncx} plays a role in removing heavy occurrence of EADs from the AP. The amplitude of I_{ncx} was greatly reduced (Fig. 39B) but it was able to successfully eliminate most of the EADs.

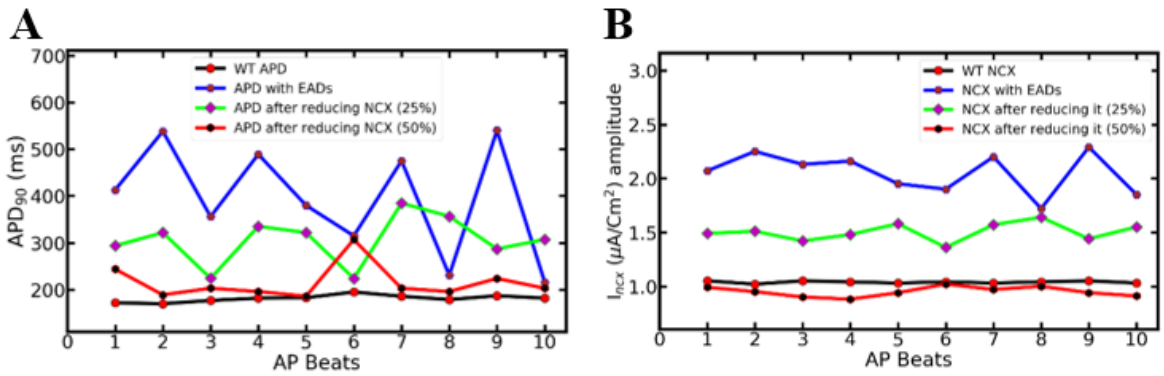

Figure 39: Blocking of I_{ncx} current by 25% and 50% reduced the frequency of EADs occurring in RyR2 LOF mutation. (A) APD_{90} in WT myocyte (black), EADs with β-AR stimulation and original I_{ncx} (blue), APD_{90} after reducing I_{ncx} by 25% (green), and 50% (red), in both reduction β-AR stimulation, was unchanged, (B) I_{ncx} amplitude in WT (black), with original NCX value during EADs (blue), after reducing it by 25% (green) and by 50% (red).

It was nicely observed that the reduction in the I_{ncx} current removed the frequency of EADs occurrence but this change did not affect other than APD, activation time of LCC, and the spark duration, all of these were lowered with a lower value of I_{ncx}. There was no significant difference in $[Ca^{2+}]_{myo}$ peak transient (66.7±2.41 (EAD), 63.6±2.1 (50%), & 63.5±1.8 (25%)) and the same sort of values on opening probabilities of LCC and RyR2, SR Ca^{2+} level, and even in the I_{Na} and inactivation gate. As mentioned by Weiss et al. (2010) I_{ncx} works in synergy with I_{LCC} and we believe the opposite is also true, the I_{LCC} entertains positive feedback mechanisms from the I_{ncx}. Zhao et al. (2015)

also found that treating myocyte with I_{ncx} inhibiting drug the APD was decayed by 75-90 percent and EADs incidents were decreased drastically.

There are many disagreements about LOF hypotheses. Priori and Napolitano (2005) stated the proposed mechanism of loss of function mutation (Gomez, & Richard, 2004) shifts away from the ground reality that majority of the EADs are found in the setting of the low heart rate and getting them the way, they presented in their canine experiment is very unlikely. We also saw that the luminal dependency is the major modulator of RyR2 sensitivity and any downturn in it affects the whole Ca^{2+} dynamics of the heart causing cardiac abnormality like the way an increase in the luminal dependency affects the stability. As they also mentioned the loss-of-function hypothesis as a provocative hypothesis and blame its divergence from the common knowledge of EADs but we believe more study is necessary before concluding anything here.

SOICR mechanism unable to develop any Arrhythmia

The RyR2 mutants in the SOICR mechanism have luminal sensitivity but they not activated by cytosolic Ca^{2+}. The main characteristic of this mechanism is SR Ca^{2+} overload lowers the fill threshold and causes spontaneous Ca^{2+} release and spill over to cytoplasm. In this simulation, we have tested mutant myocyte by keeping dyadic subspace Ca^{2+} as a resting potential to keep CICR mechanism was inactivated. The simulation produced a plateau less (Fig. 40A) (APD = 74.92±1.32 ms) AP, the AP amplitude (38.07±0.02 mV) was a little higher for 6 Hz pacing. The voltage-gated L-type channel which was alone responsible for an AP, was activated fully (Fig. 40B) here. Generally, AP gets shorter in higher pacing because the release of SR Ca^{2+} provides a

negative feedback mechanism but it does not happen if there was no CICR. The Na^{+}- Ca^{2+} exchange current (Fig. 40C) depends upon cytosolic Ca^{2+}, but there was no plateau phase because of the absence of SR Ca^{2+} release which made it shorter and quicker. The cytosolic Ca^{2+} level was highly affected due to the SOICR mechanism, in higher pacing, it is supposed to have a higher concentration of [Ca^{2+}] (Fig. 40D) but the variation in each beat was tiny. In the simulation, we also found non-significant RyR2 channels open (Fig. 40E) and there was a small variation in the SR Ca^{2+} (Fig. 40F). But we counted the Ca^{2+} sparks in each beat, the average number was 1176±48 (WT, 104467±4714) and those sparks the result of spontaneous Ca^{2+} release or leak. When CICR was inactivated, cytosolic Ca^{2+} was not enough for the coordinated openings of mass RyR2 due to many SR Ca^{2+} releases that could not yield the sparks. Even as the very low numbers sparks, their average per beat amplitude was short (55.72±1.02 vs 60.55±1.56, WT).

Based on our findings, we could not support that SOICR as a mechanism of CPVT1 mutation in the genes expressing RyR2 protein. The SR was never loaded by Ca^{2+} to activate spontaneous Ca^{2+} release and to cause DADs. The modulation of the RyR2 opening by the Ca^{2+} in the subspace, not the luminal Ca^{2+}, is the initiation of Ca^{2+} release in the normal or mutant myocyte. It is difficult to understand why someone could add up something like SOICR would replace the CICR.

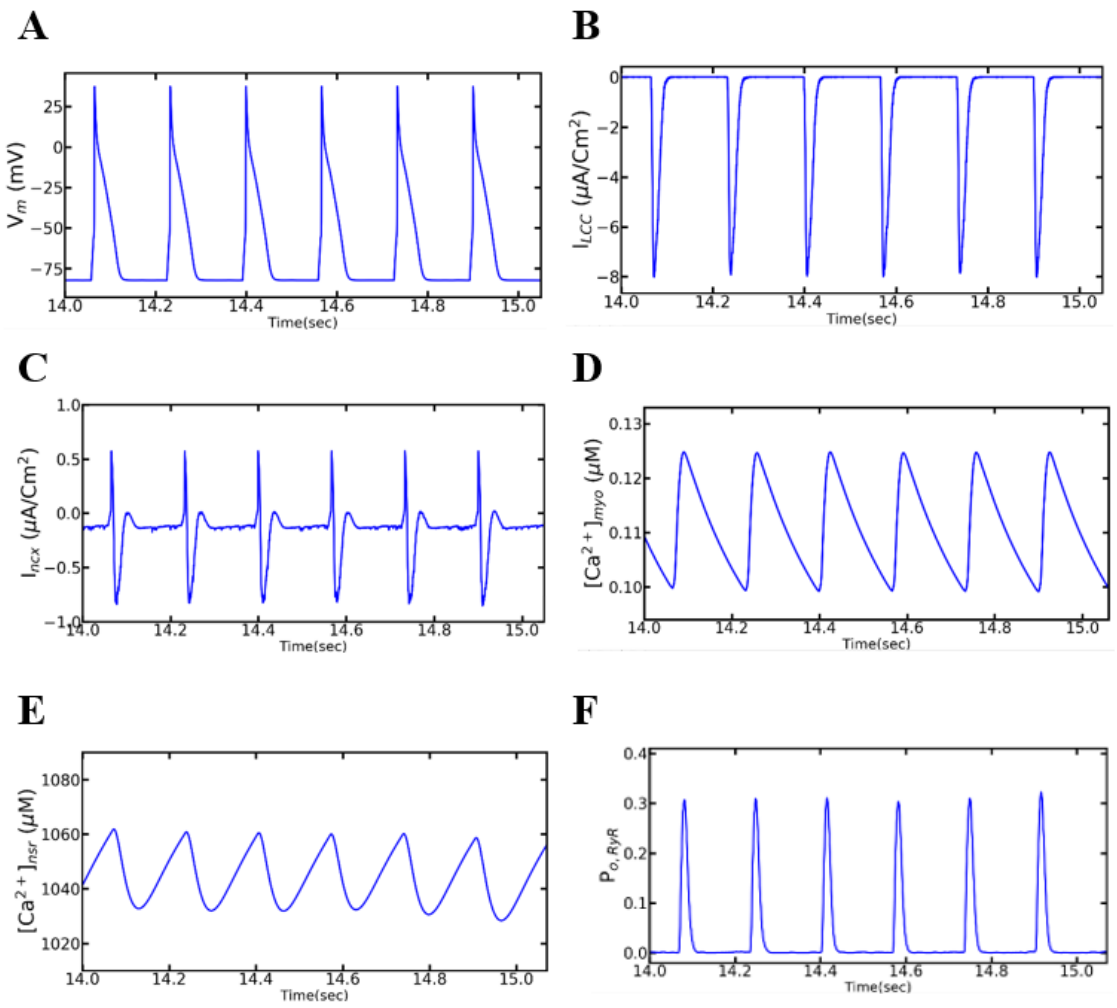

Figure 40: Store overload-induced Ca^{2+} release (SOICR) simulation. The model was unable to predict the SOICR mechanism is responsible for any CPVT1 in RyR2 mutation. (A) A plateau less AP (B) Electrogenic I_{ncx}. (C) I_{LCC}. (D) $[Ca^{2+}]_{myo}$, (E) $P_{O,RyR}$ (F) $[Ca^{2+}]_{nsr}$.

We were unable to observe anything happening in the myocyte without RyR2 sensitivity towards $[Ca^{2+}]_{ds}$ and this is what the beginning of CICR. The cause of spontaneous Ca^{2+} release and producing DADs should be due to overloaded SR, not the

overflow of the SR. Meli *et al.* (Meli, 2011) believed that RyR2 mutation brings hypersensitivity and adds more support to the existing CICR phenomenon rather than SOICR. They showed the CICR mechanism is more than enough to explain CPVT1 in RyR2 mutation and it is not necessary to appeal alternate SOICR mechanisms as an alternative to explain the same thing. Martin, Noble, & Noble (2011) observed thirty-seven previously published computational models and all of them supported the cause of DADs in CPVT by the same CICR mechanism. In short, SOICR is the increase RyR2 open probability concerning luminal dependence and it is always part of the CICR mechanism, you do not need a different name to explain the same mechanism.

Increased RyR2 opening probability due to GOF mutation cause Alternans

Like the previous mechanism, the β-adrenergic stimulation in the mutant myocyte caused by interdomain unzipping was carried out in between 1 Hz pacing and 6 Hz pacing for both WT and mutant myocytes based upon our protocols. The wild type myocytes paced in both control and β-adrenergic receptor stimulation showed normal results except frequency-based changes such as a decrease in APD, an increase in I_{ncx}, intracellular Ca^{2+} level increase, and so on. The control pacing of mutant myocyte obtained similar results to the wild type myocytes. The β-adrenergic stimulation in the mutant myocyte was able to handle well the simulations normally at a lower pacing rate. When the pacing increased to 6 Hz frequency from 5 Hz, the plots displayed alternate

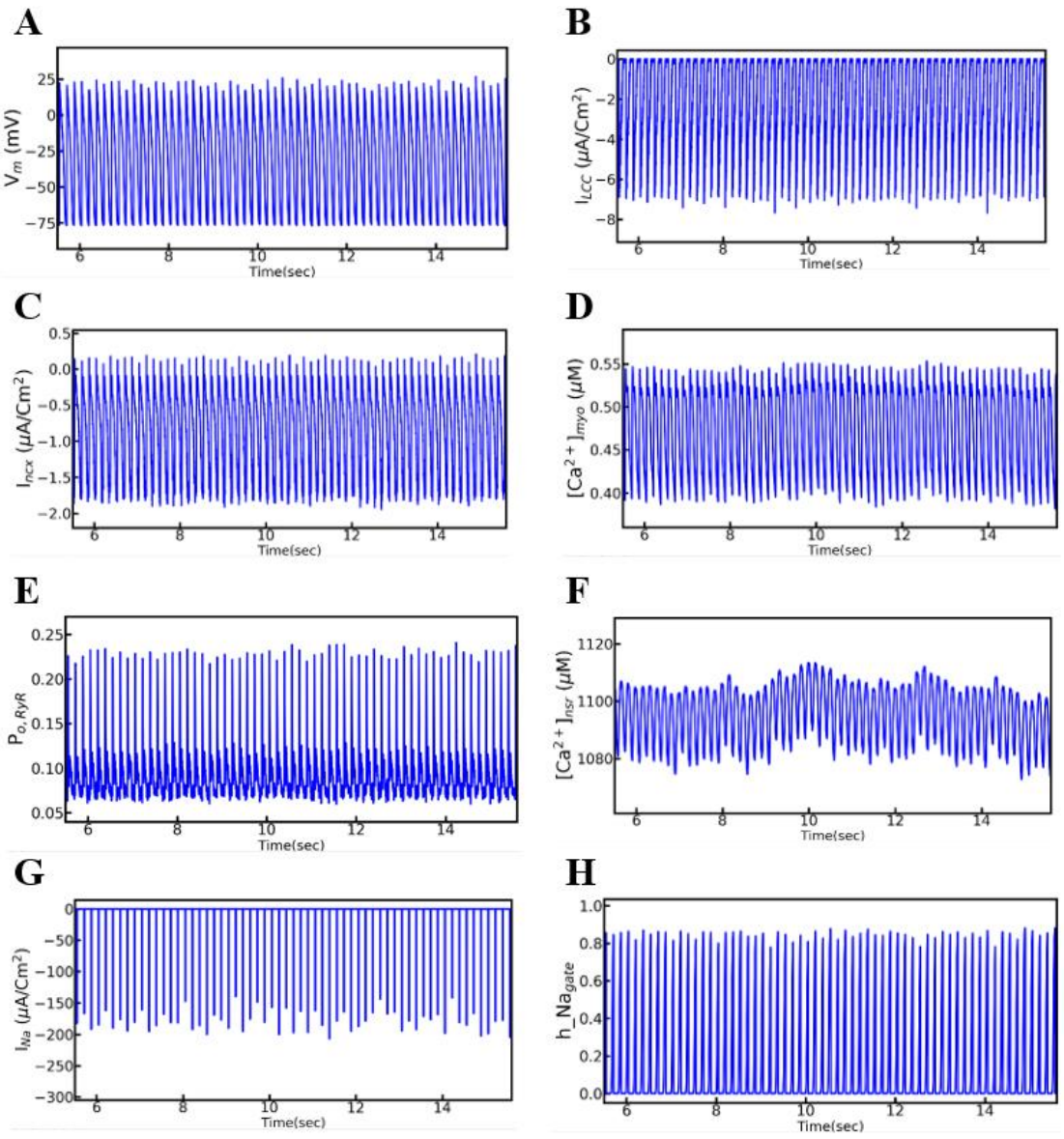

Figure 41: Intracellular Ca^{2+} dynamics greatly disturbed due to β-adrenergic stimulation. Both beat missing and alternans beheld as the arrhythmogenic disorder in the mutant myocytes (A) AP clearly showing alternate beats, (B) L–type current (I_{LCC}), (C) Na^{+}-Ca^{2+} exchange current (I_{ncx}), (D) NSR Ca^{2+} level ($[Ca^{2+}]_{nsr}$), (E)RyR openings (F) Cytoplasmic Ca^{2+} level ($[Ca^{2+}]_{myo}$), (G) Na^{+} current, I_{Na} (H) Na^{+} channel inactivation gate, h_Na_{gate}.

APs and the similar behavior in other ionic currents and Ca^{2+} transients were observed. The AP (Fig. 41A) developed alternate shorter and longer AP. The voltage-gated Ca^{2+} channels, I_{LCC} (Fig. 41B), electrogenic Na^{+} - Ca^{2+} exchange current (I_{ncx}), SR Ca^{2+} level $[Ca^{2+}]_{nsr}$,(Fig. 41C) the opening probability of RyR2 channels (Fig. 41D), $P_{O,RyR}$ (Fig. 41E), the concentration cytosolic Ca^{2+}, $[Ca^{2+}]_{myo}$, (Fig. 41F). voltage-gated fast Na^{+} channels (Fig. 41G) and their inactivation gates (Fig. 41H) all were affected by the alternans one way or other. There was also one AP beat is missing in between 10-11 seconds. The simulations were run for at least 30 seconds but figure 9 represents only 5 - 15 seconds.

Alternation in the diastolic interval (DI) and diastolic SR load develop alternans

The dynamic instability in the intracellular Ca^{2+} translated into the alternans. But it became a difficult task to trace and determine the mechanism of this variability. The alternans were represented in the form of taller & shorter AP amplitude with longer & quicker APD (Fig. 41A) alternately. It was also shown by the spark count of Ca^{2+} with the variations in the number of sparks in those alternate beats (Fig. 41B). A significantly higher number the Ca^{2+} spark in the larger beats than the smaller beats (134629±17344 vs 106970±12215, n = 10) supported that in molecular level Ca^{2+} play a role in creating alternans. The AP amplitude alternations were the result of alternate I_{Na} current (Fig. 40G) due to the non-recovery of Na^{+} channels inactivated from the previous beat (Fig. 40H) and the APD alternations are Ca^{2+} related. There is no question that the activation of β-AR increased the Ca^{2+} influx to the myocyte but the availability of SR Ca^{2+} (Fig. 36C) played an important role here. Leaky RyR2 (Fig. 41D) due to mutation certainly

held a lower total Ca^{2+} volume in the SR than the WT (~15% less) but each beat depends upon the present amount of Ca^{2+} available for it. In the simulation, we found the average spark duration is very long 328 ms vs 19 ms in WT, it showed the leak in each diastolic phase generated a lot of sparks. Our model suggested that diastolic interval (DI) (shown in Fig. 36A) in shorter and longer AP affected the refilling of SR and the level SR Ca^{2+} load available for the incoming beat was different from the current beat. When this trend continued, the longer and shorter Ca^{2+} transients were produced alternately and the myocyte got into the alternans. The amount of Ca^{2+} released from the SR is controlled by the level of Ca^{2+} entry, the activity of RyR2, and the amount of Ca^{2+} content in the SR. On account of the excess Ca^{2+} in the cytosol, many open RyR2 channels switched to the adaptation state (Fig. 41E). The β-adrenergic stimulation increased the frequency of the heartbeat and helped replenish the SR Ca^{2+} content. The elevated Ca^{2+} content in the SR activated negative feedback mechanism by increasing Ca^{2+} dependent inactivation, CDI (Fig. 41F) of L-type channels (Fig. 42A) when there was a higher opening probability of L-type channels, $P_{O,\,LCC}$, (Fig. 42B) it produced smaller LCC while smaller opening produced larger LCC. This autoregulation of the heart is for only one beat and it influences Ca^{2+}- fluxes for the immediate beat only (Eisner, Choi, Diaz, O'Neil, & Trafford, 2000). Because of the negative feedback mechanism, the myocyte released more Ca^{2+} to outside than it is gaining it in that beat which is going to be translated into a larger beat. The larger beat brought more Ca^{2+} to the cytoplasm (Fig. 42C) which increased the activity of I_{ncx} current (42D) and helped to further elongate the APD. The incoming beat started from a depleted SR Ca^{2+} load (compare AP in Fig. 41A with SR

Ca^{2+} in Fig. 41C) which also had a shorter DI (Fig. 41A). A smaller SR content cannot produce a large Ca^{2+} transient and the outcome is a shorter beat. The amount of Ca^{2+} released can be further verified by the level diastolic Ca^{2+} load (DCL) as shown in figure 41C. The DCL also alternated from beat to beat in alternans (Qu, 2016). DCL is part of the fractional Ca^{2+} release curve (FCR). FCR curve is a functional relationship between the amount of Ca^{2+} released from the SR and diastolic Ca^{2+} level (DCL) right before the new release. In figure 41C, we compared the DCL in between levels k, k-1, and $K^{+}1$ and the diastolic difference between two consecutive beats is going to predict the availability of the SR Ca^{2+} for the incoming beat. Hence, the beat to beat diastolic SR Ca^{2+} load is responsible for the APD alternans. Kanaporis et al. (Kanaporis, 2014) showed the disappearance of APD alternans with the suppression of SR Ca^{2+} release in a rabbit myocyte. Picht, DeSantiago, Blatter, & Bers (2006) came up with the idea that not the diastolic Ca^{2+} level fluctuation but the recovery of RyR2 from the previous inactivation are responsible but their conclusion is drawn from frequency induced Ca^{2+} alternans in a normal myocyte since our models dealt with β-AR stimulation-induced alternans that occur in lower frequency than frequency induced ones.

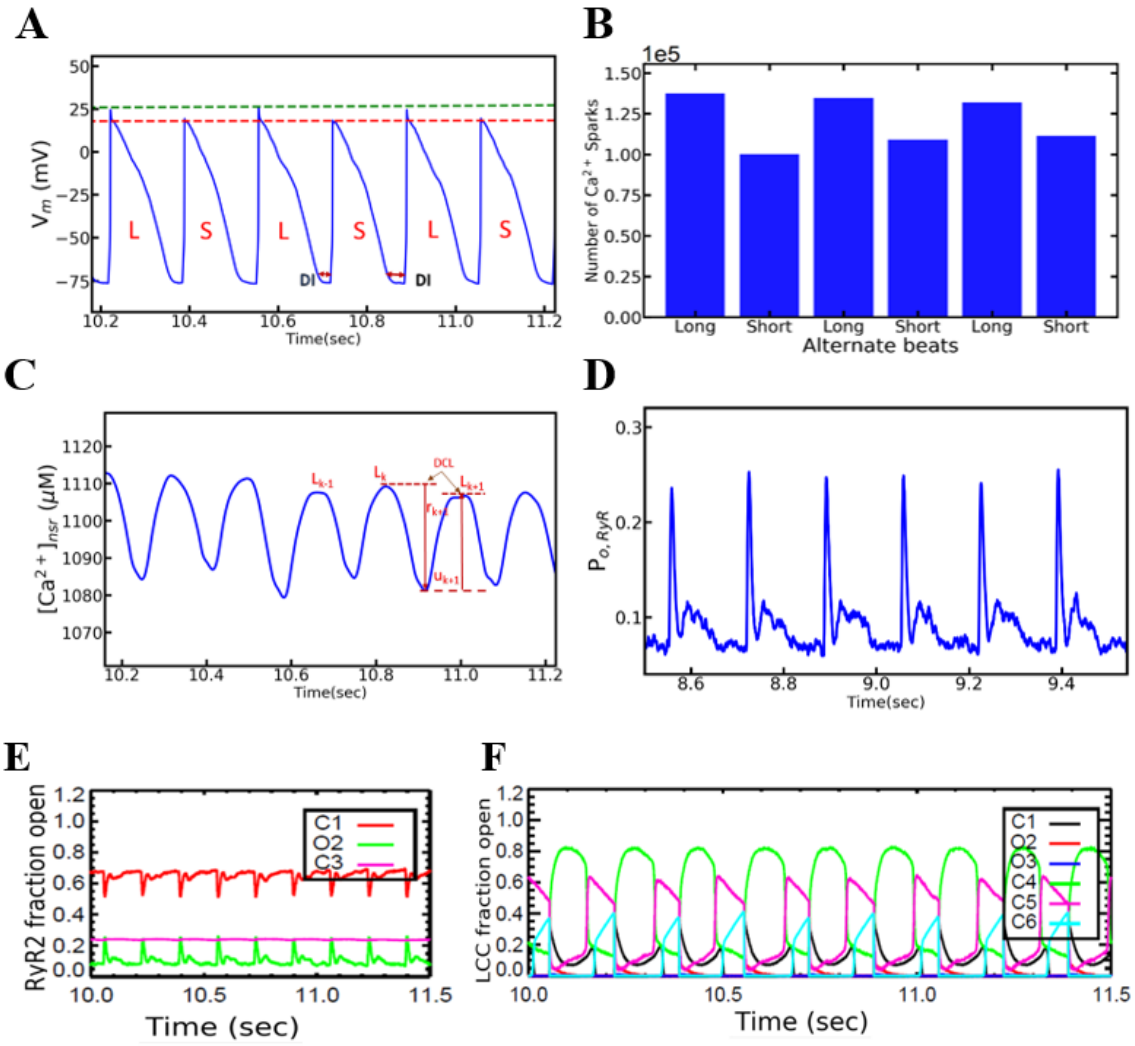

Figure 42: Alternate in the ionic currents and transients can be seen across the plots. This figure showed a detailed plot all of them from the segment (10.0 - 11.0 sec) (A) AP green and red dotted lines measure the amplitude in between shorter and longer beats, L = long beat, S = short beat, DI = diastolic interval, (B) Ca^{2+} spark count in both short and longer beats, (C) NSR Ca^{2+} level, DCL = diastolic Ca^{2+} level. (D) Opening probability of RyR2 channels, (E) The fraction of RyR2 in different opening and closing states, C_1 (red) closed state, O_2 (green) open state and C_3 (magenta) inactivation state (F)

The fraction of L-type channels different states, especially Ca^{2+} dependent inactivation (CDI) and Voltage-dependent inactivation (VDI) alternation during depolarization and repolarization of AP, C_1 (black) & C_6 (cyan) closed states, O_2 (red) & O_3 (blue) open states, C_4 (green) CDI state & C_5 (magenta) VDI state.

We recorded a 20% RyR2 into adaptation state (Fig. 42E) but there was no fluctuation in between the consecutive beats. It cannot be denied there could be a different mechanism in frequency induced alternans but our model did not find it was happening.

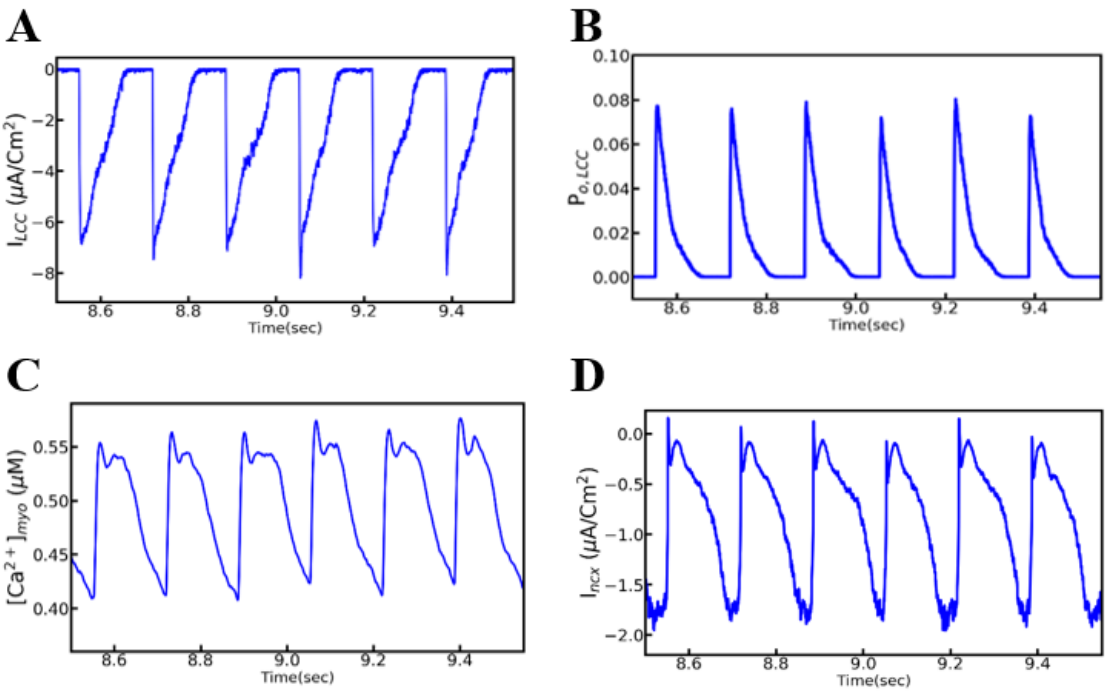

Figure 43: The opening probability of LCC did not control the amplitude of L-type current and increase cytosolic Ca^{2+} raised the activity of the Na^{+}-Ca^{2+} exchange current.

(A) L-type channels, (B) Openings of L-type channels ($P_{O, LCC}$), (C) Cytoplasmic Ca^{2+} level ($[Ca^{2+}]_{myo}$), (D) Na^{+}-Ca^{2+} exchange current (I_{ncx}).

The I_{ncx} current (Fig. 43D) started after a downward deflection of repolarization always with abundance Ca^{2+} in the cytosol to work in the beginning and it is the major Ca^{2+} extruding current. As we discussed above a larger beat means more intracellular Ca^{2+} available for I_{ncx} to pump it out. When I_{ncx} is more active, APD gets prolonged with the increase in inward current (1 Ca^{2+} ion out, 3 Na^{+} ions in) (Tse, 2016) gain of net positive charge to the myocyte. A longer I_{ncx} tends to have a longer AP while the shorter APD means the I_{ncx} is shorter too (compare Figs. 39A and 37D). Diaz et al. (Diaz, 2004) from their experiment reported that more Ca^{2+} escaped from myocyte during large Ca^{2+} transients than smaller ones via I_{ncx}.

Inactivation of non-recovery from earlier activation of Na^{+} channels produce the AP amplitude alternans

In comparing the APs from figure 40A & 41A and I_{Na} current from 40G & 44A, we found that I_{Na} current alternates similarly with the AP and the Na^{+} inactivation gate (Figs. 40 H & 44B) also followed them. It was noticed that the recovery of Na^{+} channels from inactivation played a role in the instability of intracellular Ca^{2+} dynamics. In higher pacing, some of the Na^{+} channels are unavailable for the incoming beat because they are unable to recover from the previous inactivation. This brought alternately opening of Na^{+} channels and the alternation in the amplitude of I_{Na}. We noticed that the activation of L-type channels is affected by the availability of Na^{+} current and larger Na^{+} influx results

larger opening of L-type channels and shorter I_{Na} activates a smaller number of L-type channels. The CICR mechanism requires the opening of L-type channels to activate RyR2 channels; after this, they recruit the neighboring CRUs and activate higher numbers of RyR2. In figure 43A, the I_{LCC} current amplitude did not alternate in the same manner as I_{Na}. This is because of the L-type channels augmented by adrenergic receptors and on the other side in the larger beat, then they were pushed back by CDI. Our results exhibited the alternation of I_{Na} developed AP amplitude alternans in the cardiac myocytes.

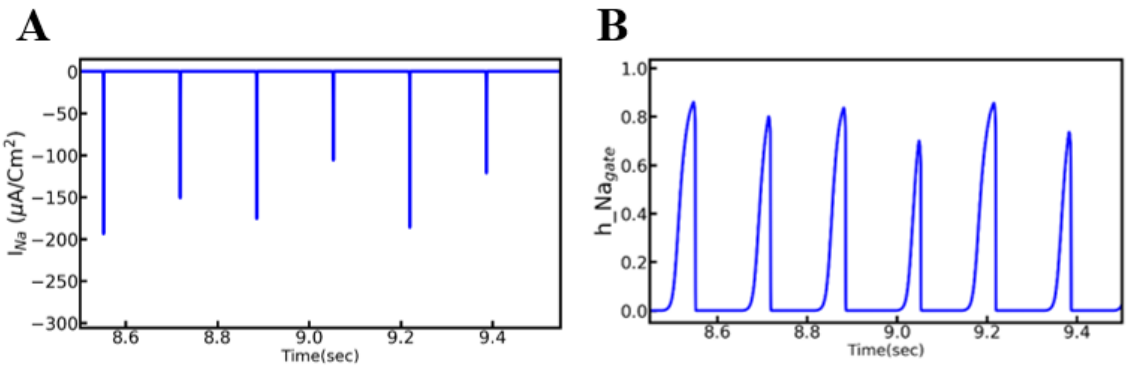

Figure 44: A non-recovery of Na^+ channels from the previous inactivation develop AP amplitude alternans in the myocyte. (A) Na^+ current (I_{Na}) with alternate amplitudes (B) Na^+ channels inactivation gates show alternate recovery from inactivation

Discussion

Most of the Mutations in RyR2 increase the opening probability of RyR2 as it is activated by cytosolic Ca^{2+}. The activation of β-AR brings an increase in the pacing rate of the heart and increases Ca^{2+} flux per unit time. More Ca^{2+} in the cytosol increases the rate of SERCA pump and it replenishes extra Ca^{2+} back to the SR. The pairing of high SR Ca^{2+} load with hyperactive RyR2 produces large Ca^{2+} transients which affect Ca^{2+} dynamics in the myocyte. This condition contributes to the development of alternans and it triggers CPVT1 in the heart. Scientists have proposed four different hypotheses to explain the mechanisms to cause CPVT1. We applied our new stochastic myocyte model of Guinea pig to test all those hypotheses. From our simulation results, we found the GOF mutation to cause alternans, the LOF mutation to cause EADs, the SOICR mechanism failed to activate RyR2 receptors by increased sensitivity in low or null CICR, and binding protein mutations were unable to produce any arrhythmogenic activities in the simulations. The Ca^{2+} spark analysis helped us to understand every basis of this mechanism at the subcellular level and figuring out a variation on the spark's numbers and amplitudes in beat to beat or second to second. The GOF mutation of the RyR2 proteins that increases the opening probability of RyR2 channels and increase propensity towards the cytosolic Ca^{2+} ends up an arrhythmia during rapid pacing with β-AR stimulation. From our model, we found the GOF mutation to cause cardiac alternans as an indication of those arrhythmias. Similarly, the LOF mutation which lowers the luminal dependency of RyR2 channels could cause EADs as the signals of arrhythmia.

Reducing the value of Incx in the AP with EADs lower the frequency of their occurrence working in synergy with I_{LCC}.

Increased RyR2 phosphorylation imitated in our model resulted in alternate weak/strong beats (mechanical alternans) as well as shorter/longer beats (APD or electrical alternans). Our result matches the outcome of Saitoh et al. (Saitoh, 1989) which reported the Ca^{2+} dynamics are the main reason behind the mechanoelectrical alternans in ventricular myocytes (Saitoh, Bailey, & Surawics, 1989). Bers (2001) explained SR Ca^{2+} load is the Ca^{2+} release regulation factor in EC-coupling and CICR. It fully contributes to the underlying mechanism of cardiac alternans. Diaz *et al.* (2004) also reported a variation in the SR Ca^{2+} content is enough to produce cardiac alternans.

The combined effect of the mutation in RyR2 and catecholaminergic stimulation to trigger arrhythmia. The mutations cause a premature or prolonged release of SR Ca^{2+} in the cytosol. At the molecular level study of the number of CPVT1 mutations, the majority of them are the gain-of-function mutations (Lobo, et al., 2011) (Kimlicka, et al., 2013). It is necessary to notice CPVT1 occurs during rapid pacing of the heart under the influence of adrenergic stimulation and it has to do with SR Ca^{2+} load. During CPVT, the myocytes are pacing at a rapid rate and fraction of DI shortens which allows less time for replenishing of SR, removal of $Ca^{2+,}$ and complete relaxation of ventricles. The rapid pacing elevates the diastolic SR Ca^{2+} level (Bassani, Yuan, & Bers, 1995) (McCall, Ginsburg, Bassani, Shannon, Qi, Samarel, et al., 1998). During rapid pacing, in chapter 2, we have found there is an increase in SR Ca^{2+} load in higher pacing alone but with adrenergic stimulation plus rapid pacing, there must be extra Ca^{2+} in the SR. But the

simulation showed there was no unexpected increase in diastolic Ca^{2+} level which means there should not be a Ca^{2+} overload related leak. Danielson *et al.* (Danielson, 2018) reported SR Ca^{2+} content is responsible for the leak of Ca^{2+} to generate DADs but found no increase SR Ca^{2+} content in the RyR2 mutant heart during both rapid pacing and adrenergic stimulation opposite to WT myocyte. This approves the results we obtained from our model. Williams et al. (2011) also reported SR Ca^{2+} level depends upon RyR2 open probability (Po), higher Po lowers the SR Ca^{2+} quantity. Our simulation also could not find an increased SR Ca^{2+} level in mutant myocyte than wildtype one. Bigger Ca^{2+} sparks are generated in mutant myocytes than wildtype myocytes in each beat. When mutant myocyte paced rapidly during adrenergic stimulation, we recorded an alternate availability of SR Ca^{2+} in successive beats resulted in both amplitude and APD alternans. And, no alternans were recorded during the slow pacing. There are well recognized clinical observations that electrical instability in short cycle length (higher beating rate) is more likely to deteriorate into ventricular fibrillation (VF) (Koller, 2005) and almost all VFs are preceded by ventricular tachycardia (VT) (Nikolic, 1982) (Pratt, 1983). The results from our model show alternans in rapid pacing bring CPVT and it may end into VF or SCD.

Chudin et al. (1999) described that in rapid pacing, increased intracellular Ca^{2+} accelerates inactivation of L-type channels. In the simulation, the LCCs were inactivated when higher load SR Ca^{2+} released alternately and more Ca^{2+} in the cytosol played the role to inactivate them. When there is enough SR Ca^{2+} available for the CICR mechanism, a strong beat will be produced and less SR Ca^{2+} will be available for an

incoming beat and the beat is weaker beat. Hence weaker and stronger beats arise alternatively creating alternans.

The LOF mutation in RyR2 significantly diminishes its sensitivity towards the luminal Ca^{2+} and that causes the SR Ca^{2+} overload resulting in idiopathic behavior. But not enough explorations have been done in this field and more questions needed to be answered. It is known many instabilities carried out in the myocytes are by aberrant SR Ca^{2+} release and certainly, there is larger consequence having the bulkier SR. Beside RYR2-A4860, Roston et al. (2017), described another LOF mutation, RyR2-I4855M responsible for left ventricular non-compaction CPVT. A variation exists in types of RyR2 mutations and there are more CPVT variants too, more work in this field will shed light on them.

Conclusion

In assessing four different hypotheses to explain the mechanisms of RyR2 mutation and CPVT1, we have seen the modulation of RyR2 open probability is greatly influenced by the RyR2 mutation affecting its response towards the cytosolic Ca^{2+} sensitivity and luminal Ca^{2+} dependency. There should be primarily two categories of RYR2 mutations to answer all the questions on RyR2 mutations and CPVT1: GOF and LOF. The destabilization of binding protein mutation is a part of GOF mutation and the diastolic leakage due to this mutation is responsible for the low level of SR Ca^{2+} but not cardiac instabilities. The literature illustrates that much more work has been done in GOF mutation and still many researchers deem the LOF mutation does not exist. We have

tested the LOF mechanism in our model and retrieved those experimental findings are plausible, more experiments would shed light on it. There are still many unanswered questions in arrhythmia sudden cardiac death, the model displayed that the GOF mutation was responsible for the CPVT1 in the mutant myocyte by developing alternans. The LOF mutation also triggers arrhythmia by developing EADs. The interdomain unzipping or binding protein destabilization due to mutation in channel binding proteins is part of the GOF but deals with the RyR2 channels during the diastolic phase. We did find the increase Ca^{2+} leak due to destabilization of the closing of channels during diastole but could not have enough leak to depolarize the membrane to trigger DADs and arrhythmia. We did not find to believe in the SOICR mechanism, we agree most of the scientific community that CICR is the sole mechanism of EC-coupling in the cardiac myocytes and an increase in luminal dependency in SOICR is already a part of the CICR and explaining the same thing with different hypothesis makes no sense. With the quantitative Ca^{2+} spark analysis in the subspace, investigating quantitative variations caused by mutation and β-adrenergic stimulation in action potentials (APs), Ca^{2+} related currents, transients, and intracellular Ca^{2+} storages, the following outcomes were concluded in summary from our research:

- Alternans and EADs are the underlying mechanisms to generate arrhythmia when RyR2 mutant myocyte undergoes adrenergic stimulation either by exercise or stress or catecholamine perfusion during the condition of CPVT1.
- Fluctuation in intracellular Ca^{2+} dynamics duet to alternation in SR Ca^{2+} transients, diastolic interval, and diastolic Ca^{2+} load generate APD alternans in the cardiac

mutant myocytes. Similarly, the non-recovery of Na^+ channels from the previous inactivation produces alternate Na^+ current (I_{Na}), the alternate I_{Na} is responsible for producing AP amplitude alternans.

- Increased heart rate required to generate arrhythmia, but rapid pacing itself is not enough to generate arrhythmia.
- I_{ncx} increases APD duration in the alternans by its electrogenic property, and the frequency of EADs can be minimized by blocking this channel. It plays a positive feedback mechanism with I_{LCC}.
- SR leak is highly dependent on the diastolic SR Ca^{2+} volume. But increase release via RyR2 is not going to help it and so leaked Ca^{2+} is not enough to generate DADs.
- The SR Ca^{2+} available for the current beat is equally important as the overall SR load to bring Ca^{2+} instability in the cardiac myocytes.

References

Avila, G. K., O'Connell, K. M. S. & Dirksen, R. T. (2003). The pore region of the skeletal muscle ryanodine receptor is a primary locus for excitation-contraction uncoupling in central core disease. *Journal of General Physiology, 121*(4), 277-286.

Bagattin, A. C., Veronese, C., Bauce, B., Wuyts, W., Settimo, L., Nava, A. et al. (2004). Denaturing HPLC-based approach for detecting RyR2 mutations involved in malignant arrhythmias. *Clinical Chemistry, 50*(7), 1148 - 1157.

Bassani, J. W., Yuan, W. & Bers, D. M. (1995). Fractional SR Ca^{2+} release is regulated by trigger Ca^{2+} and SR Ca^{2+} content in cardiac myocytes. *American Journal of physiology, 268*, C1313-C1319.

Behere, S. P., & Weindling, S. N. (2016). Catecholaminergic polymorphic ventricular tachycardia. *Annals of pediatric cardiology, 9*(2), 137 - 150.

Bers, D. (2002). Cardiac excitation-contraction coupling. *Nature, 415*, 198-205.

Bers, D. M. (2000). Calcium fluxes involved in control of cardiac myocyte concentration. *Circulation Research, 87*, 275-281.

Bers, D. M. (2001). *Excitation-contraction coupling and cardiac contractile force.* Dordrecht, the Netherlands: Kluwer Academic Publishers.

Bhuiyan, Z. A. Berg, M. P., Tintelen, J. P., Bink-Boelkens, M. T., Wisefield, A. C., Alders, M. et al. (2007). Expanding spectrum of human RYR2-related disease: new electrocardiographic, structural, and genetic features. *Circulation, 116*, 1569-1576.

Blayney, L. M., & Lai, F. A. (2009). Ryanodine receptor-mediated arrhythmias and sudden cardiac death. *Pharmacology & Therapeutics, 123*, 151 - 177.

Chudin, E. J., Goldhaber, J., Garfinkel, A. C., Weiss, J., & Kogan, B. (1999). Intracellular Ca2+ dynamics and the stability of ventricular tachycardia. *Biophysical Journal, 77*, 2930-2941.

Crescenzo, V. D. Fogarty, K. E., Lefkowitz, J. J., Bellve, K. D., Zvaritch, E., MacLennan, D. H. et al. (2012). Type 1 ryanodine receptor knock-in mutation causing central core disease of skeletal muscle also displays a neuronal phenotype. *PNAS, 109*(2), 610-615.

Danielson, T. K., Manotheepan, R., Sadredini, M., Laren, I. S., Edwards, A. G., Vincent, K. P. et al. (2018). Arrhythmia initiation in catecholaminergic polymorphic ventricular tachycardia type 1 depends on both heart rate and sympathetic stimulation. *PLOS ONE, 13*(11), 1-21.

Diaz, M. S. O'Neil, S. C. & Eisner, D. A. (2004). Sarcoplasmic reticulum calcium content fluctuation is the key to cardiac alternans. *Circulation Research, 94*, 650-656.

Dobrev, D., Carlsson, L. & Nattel, S. (2012). Novel Molecular targets for atrial fibrillation therapy. *Nature, 11*(4), 275 - 291.

Eisner, D. A., Choi, H. S., Diaz, M. E., O'Neil, S. C. & Trafford, A. W. (2000). Integrative analysis of calcium cycling in cardiac muscle. *Circulation Research, 8*(22), 1087-1094.

Ganesan, A. C., Maack, C., Johns, D. C., Sidor, A., & O'Rourke, B. (2006). β-adrenergic stimulation of L-type Ca^{2+} channels in cardiac myocytes requires the distal carboxyl terminus of α1C but not serine 1928. *Circulation Research, 98*(2), e11-e18.

George, C. H., Higgs, G. V. & Lai, F. A. (2003). Ryanodine receptor mutations associated with stress-induced ventricular tachycardia mediate increased calcium release in stimulated cardiomyocytes. *Circulation Research, 93*, 531-540.

Ginsburg, K. S. & Bers, D. M. (2004). Modulation of excitation-contraction coupling by isoproterenol in cardiomyocytes with controlled SR Ca2+ load and Ca2+ trigger. *Journal of Physiology, 556*, 463-480.

Gomez, A. M. & Richard, S. (2004). Mutant cardiac ryanodine receptors and ventricular arrhythmias: is 'gain-of-function' obligatory? *Cardiovascular Research, 64*(1), 3-5.

Gonano, L. A. & Jones, P. P. (2017). FK506-binding proteins and 12.6 (FKBPs) as regulators of cardiac ryanodine receptors: Insights from new functional and structural knowledge. *Channels (Austin), 11*(5), 415-425.

Gyorke, I. N., Hester, N., Jones, L. R. & Gyorke, S. (2004). The role of calsequestrin, triadin and junctin in conferring cardiac ryanodine receptor responsiveness to luminal Calcium. *Biophysical Journal, 86*, 2121 - 2128.

Hernandez, J. J., Herron, T., Jalife, J., Maginot, K., Zhang, J., Kamp, T. et al. (2018). A CPVT mutation confers gain of function mutation to the cardiac receptor channel. Characterization using cardiomyocytes derived from patient-specific iPS cells. *Circulation, 128*, A17750.

Iyer, V. R., Hajjar, R. & Armoundas, A. A. (2007). Mechanism of abnormal calcium homeostasis in mutations responsible for catecholaminergic polymorphic ventricular tachycardia. *Circulation Research, 100*, e22-e31.

Jafri, M. S. Rice, J. J. & Winslow, R. L. (1998). Cardiac Ca^{2+} Dynamics: The roles of ryanodine receptor adaptation and sarcoplasmic reticulum load. *Biophysical Journal*, 1149 - 1168.

Jiang, D., W. Chen, R. Wang, L. Zhang, & S. W. Chen. (2007). Loss of luminal Ca2+ activation in the cardiac ryanodine receptor is associated with ventricular fibrillation and sudden death. *Proceedings of the National Academy of Sciences of the United States of America, 104*(46), 18309 - 18314.

Jiang, D. B., Xiao, B., Yang, D., Wang, R., Choi, P., Zhang, L. et al. (2004). RyR2 mutations linked to ventricular tachycardia and sudden death reduce the threshold for store-overload-induced Ca^{2+} release (SOICR). *Proceedings of the National Academy of Sciences of the United States of America, 101*(35), 13062 - 13067.

Kanaporis, G. & Blatter, L. A. (2014). The mechanisms of calcium cycling and action potential dynamics in cardiac alternans. *Circulation Research, 116*, 846-856.

Kashimura, T., Briston, S. J., Trafford, A. W., Napolitano, C., Priori, S. G., Eisner, D. A. et al. (2010). In the RyR2R4496C mouse model of CPVT, beta-adrenergic stimulation induces Ca waves by increasing SR Ca content and not by decreasing the threshold Ca waves. *Circulation Research, 107*, 1483-1489.

Kawata, H., Ohno, S., Aiba, T., Sakaguchi, H., Miyazaki, A., Sumitomo, N. et al. (2016). Catecholaminergic polymorphic ventricular tachycardia (CPVT) associated with ryanodine receptor (RyR2) gene mutations - long-term prognosis after initiation of medical treatment. *Circulation Journal, 80*, 1907-1915.

Keizer, J. & Levine, L. (1996). Ryanodine receptor adaptation and Ca^{2+}-induced Ca^{2+} release-dependant Ca2+ oscillations. *Biophysical Journal, 71*(6), 3477-3487.

Kimlicka, L., Lau, K., Tung, C. C. & Petegem, F. V. (2013). Disease mutations in the ryanodine receptor N-terminal region couple to a mobile intersubunit interface. N*ature Communication, 4*, 1506.

Koller, M. L., Maier, S. K., Gelzer, A. R., Bauer, W. R., Meesmann, M. & Gilmour Jr., R. F. (2005). Altered dynamics of action potential restitution and alternans in humans with structural heart diseases. *Circulation, 112*, 1542-1548.

Kontula, K., Laitinen, P. J., Lehtonen, A., Toivonen, L., Viitasalo, M. & Swan, H. (2005). Catecholaminergic polymorphic ventricular tachycardia: Recent mechanistic insights. *Cardiovascular Research, 67*, 379 - 387.

Kushnir, A. & Marks, A. R. (2010). The ryanodine receptor in cardiac physiology and disease. *Advanced Pharmacology, 59*, 1-30.

Laitinen, J., Brown, K. M., Piippo, K., Swan, H. J. C., Devaney, J. M., Brahmbhatt, B. et al. (2001). Mutations of the cardiac ryanodine receptor (RyR2) gene in familial polymorphic ventricular tachycardia. *Circulation, 103*(4), 485-490.

Lanner, J. T., Georgiou, D. K., Joshi, A. D. & Hamilton, S. L. (2010). Ryanodine Receptors: structure, expression, molecular details, & function in Calcium release. *Cold Spring Harbor Perspective in Biology, 2*(11), 1 - 27.

Leenhardt, A., Denjoy, I. & Guicheney, P. (2012). Catecholaminergic polymorphic ventricular tachycardia. *Circulation: Arrhythmia and Electrophysiology, 5*(5), 1044-1052.

Leong, I. S., Sucich, J., Prosser, D. O., Skinner, J. R., Crawford, J. R., Higgins, C. et al. (2015). Array comparative genomic hybridization identifies a heterozygous deletion of exon 3 of the RyR2 gene. *Upsala Journal of Medical Sciences, 120*(3), 190-197.

Liu, G., Papa, A., Katchman, A., Zakharov, S., Roybal, D., Hennessey, J. A. et al. (2020). Mechanism of adrenergic Cav1.2 stimulation revealed by proximity proteomics. *Nature, 577*, 695-700.

Liu, N., Rizzi, N., Boveri, L., & Priori, S. G. (2009). Ryanodine receptor and calsequestrin in arrhythmogenesis: What we have learnt from genetic diseases and transgenic mice. *Journal of Molecular and Cellular Cardiology, 146*, 149 - 159.

Lobo, P. A., Kimlicka, L., Tung, C.-H. & Petegem, F. V. (2011). The deletion of exon 3 in the cardiac ryanodine receptor is rescued by beta-strand switching. *Structure, 19*(6), 790-798.

Luo, C. H. & Rudy, Y. (1994b). A dynamic model of the cardiac ventricular action potential. II. Afterdepolarizations, triggered activity, and potentiation. *Circulation Research, 74*(6), 1097-1113.

Marks, A. R. (2001). Ryanodine receptors/calcium release channels in heart failure and sudden cardiac death. *Journal of Molecular Cell and Cardiology, 33*(6), 615-624.

Martin, F., Noble, P. J. & Noble, D. (2011). Ca^{2+}-induced delayed afterdepolarizations are triggered by dyadic subspace $Ca^{2+,}$ affirming that increasing SERCA reduces aftercontractions. *American Physiological Society, 301*(3), H921-H935.

Marx, S. O., Reiken, S., Hisamatsu, Y., Jayaraman, T., Burkhoff, D., Rosembit, N. et al. (2000). PKA phosphorylation dissociates FKBP12.6 from the calcium release channel (ryanodine receptor): Defective regulation in failing hearts. *Cell, 101*(4), 365-376.

McCall, E., Ginburg, K. S., Bassani, R. A., Shannon, T. R., Qi, M., Samarel, A. M. et al. (1998). Ca^{2+} flux, contractility, and excitation-contraction coupling in hypotrophic rat ventricular myocytes. *American Journal of Physiology, 274*, H1348-H1360.

Meli, A. C., Refaat, M. M., Dura, M., Reiken, S., Wronska, A., Wojciak, J. et al. (2011). A novel ryanodine receptor mutation linked to sudden death increases sensitivity to cytosolic calcium. *Circulation Research, 109*(3), 281-290.

Metzger, J. M. & Westfall, M. V. (2004). Covalent and noncovalent modification of thin filament action. *Circulation Research, 94*, 146-158.

Miriyala, J., Nguyen, T., Yue, D. T. & Colecraft, H.M. (2008). Role of Cavβ Subunits, and lack of functional reserve, in protein kinase modulation of cardiac Cav1.2 channels. *Circulation Research, 102*, e54-e64.

Mohler, P. J. & Wehrens, X. H. T. (2007). Mechanisms of human arrhythmia syndromes: Abnormal cardiac macromolecular interactions. *Physiology, 22*(5), 342-350.

Morales, D., Hermosilla, T. & Varela, D. (2019). Calcium-dependent inactivation controls cardiac L-type Ca2+ currents under beta-adrenergic stimulation. *Journal of General Physiology, 151*(6), 786-797.

Napolitano, C., Bloise, R., Memmi, M. & Priori, S. G. (2014). Clinical utility gene card for: Catecholaminergic Polymorphic Ventricular Tachycardia (CPVT). *European Journal of Human Genetics, 22*(1), 55.

Nikolic, G., R. L. Bishop, & J. B. Singh. (1982). Sudden death recorded during Holter monitoring. *Circulation, 66*, 218-225.

Oda, T., Yang, Y., Niu, F., Svensson, B., Lu, X., Fruen, B. et al. (2013). Binding of RyR2 "Unzipping" peptide in cardiomyocytes activates RyR2 and reciprocally inhibits calmodulin binding. *Circulation Research, 112*(3), 487-497.

Petegem, V. F. (2012). Ryanodine receptors: structure and function. *Journal of Biological Chemistry, 287*(38), 31624-31632.

Picht, E., DeSantiago, J., Blatter, L. A., & Bers, D. M. (2006). Cardiac alternans do not rely on diastolic sarcoplasmic reticulum calcium content fluctuation. *Circulation Research, 99*, 740-748.

Potenza D. M., Janicek, R., Fernandez-Tenorio, M., Camors, E., Ramos-Mondragon, R., Valdivia, H. H. et al. (2019). Phosphorylation of the ryanodine receptor 2 at serine 2030 is required for a complete β-adrenergic response. *Journal of General Physiology, 151*(2), 131-145.

Pratt, C. M., Francis, M. J., Luck, J. C., Wyndham, C. R., Miller, R. R. & Quinones, M. A. (1983). Analysis of ambulatory electrocardiograms in 15 patients during spontaneous ventricular fibrillation with special reference to preceding arrhythmic events. *Journal of American College of Cardiology, 2*, 789-797.

Priori, S. & & Chen, S. R. (2011). Inherited dysfunction of sarcoplasmic reticulum Ca^{2+} handling and arrhythmogenesis. *Circulation Research, 108*, 871-883.

Priori, S. G., Napolitano, C., Tiso, N., Memmi, M., Viganti, G., Bloise, R., et al. (2001). Mutations in the cardiac ryanodine receptor gene(hRyR2) underlie catecholaminergic polymorphic ventricular tachycardia. *Circulation, 103*(2), 196-200.

Priori, S. G. & Napolitano, C. (2005). Cardiac and skeletal muscle disorders caused by mutations in the intracellular Ca2+ release channels. *The Journal of Clinical Investigation, 115*(8), 2033-2038.

Prosser, B. L., Ward, C. W. & Lederer, W. J. (2010). Subcellular Ca^{2+} signaling in the heart: The role of ryanodine receptor sensitivity. *The Journal of General Physiology, 136*(2), 135-142.

Qin, J., Valle, G., Nani, A., Chen, H., Ramos-Franco, J., Nori, A. et al. (2009). Ryanodine receptor luminal Ca2+ regulation: swapping calsequestrin and channel isoforms. *Biophysical Journal, 97*(7), 1961-1970.

Qu, Z. M., Liu, M. B. & Nivala, M. (2016). A unified theory of calcium alternans in ventricular myocytes. *Scientific Reports (Nature), 6*(35625), 1-16.

Robinson, R., Carpenter, D., Shaw, M. A., Halsall, J. & Hopkins, P. (2006). Mutations in RyR1 in malignant hyperthermia and central core disease. *Human Mutation, 27*, 977-989.

Roston, T. M., Guo, W., Krahan, A. D., Wang, R., Petegem, F. V., Sanatani, S. et al. (2017). A novel RYR2 loss-of-function mutation (I4855M) is associated with left ventricular non-compaction and atypical catecholaminergic polymorphic ventricular tachycardia. *Journal of Electrocardiology, 50*(2), 227-233.

Saitoh, H., Bailey, J. C., & Surawics, B. (1989). Action potential duration alternans in dog Purkinje and ventricular muscle fibers. Further evidence in support of two different mechanisms. *Circulation, 80,* 1421-1431.

Suetomi, T. M., Yano, M., Uchinoumi, H., Fukuda, M., Hino, A., Ono, M. et al. (2011). Mutation-linked defective inter-domain interactions within ryanodine receptor cause aberrant Ca2+ release leading to catecholaminergic ventricular tachycardia. *Circulation, 124*(6), 682 - 694.

Sun, L., Fan, J.-S., Clark, J. W. & Palade, P. T. (2000). A model of the L-type Ca2+ channel in rat ventricular myocytes: ion selectivity and inactivation mechanisms. *The Journal of Physiology, 15529,* 139-158.

Takeshima, H., Komazaki, S., Hirose, K., Nishi, M., Noda, T. & Lino, M. (1998). Embryonic lethality and abnormal cardiac myocytes in mice lacking ryanodine receptor type 2. *The EMBO Journal, 17,* 3309-3316.

Thomas, N. L., George, C. H. & Lai, F. A. (2004). Functional heterogeneity receptor mutations associated with sudden cardiac death. *Cardiovascular Research, 64*(1), 52-60.

Tse, G. S., Wong, S. T., Tse, V., Lee, Y. T., Lin, H. Y. & Yeo, J. M. (2016). Cardiac dynamics: Alternans and arrhythmogenesis. *Journal of Arrhythmia, 32*(5), 411-417.

Wallukat, G. (2002). The β-adrenergic receptors. *Hertz, 25*(7), 683-690.

Wehrens, X. H., Lenhart, S. E., Huang, F., Vest, J. A., Reiken, S. R., Mohler, P. J. et al. (2003). FKBP12.6 deficiency and defective calcium release channel (ryanodine receptor) function linked to exercise-induced sudden cardiac death. *Cell, 103,* 511 - 518.

Wei, H., Zhang, X.-H., Clift, C. & Yamaguchi, N. (2016). CRISPR/Cas9 gene editing of RyR2 in human stem cell-derived cardiomyocytes provides a novel approach in investigating dysfunctional Ca2+ signaling. *Cell Calcium, 73,* 104 - 111.

Weiss, J., Garfinkel, A., Karagueuzian, H. S., Cheng, P.-S. & Qu, Z. (2010). Early afterdepolarization and cardiac arrhythmias. *Heart Rhythm, 7*(12), 1891-1899.

Williams, G. S.B., Chikando, A. C., Tuan, H.-T. M., Sobie, E. A., Lederer, W. J. & Jafri, M. S. (2011). Dynamics of Calcium sparks and calcium leak in the heart. *Biophysical Journal, 101,* 1287-1296.

Yamamoto, T. & Ikemoto, N. (2002). Peptide probe study of the critical regulatory domain of the cardiac receptor. *Biochemical Biophysics Research Communication, 291*, 1102 - 1108.

Zalk, R., Lehnart, S. E. & Marks, A. R. (2007). Modulations of the ryanodine receptor and intracellular calcium. *Annual Review of Biochemistry, 76*, 367-385.

Zhabyeyev, P., Heiss, F., Wang, R., Liu, Y., Chen, S. R. & Oudit, G. Y. (2013). S4153R is a gain-of-function mutation in the cardiac Ca^{2+} release channel ryanodine receptor associated with catecholaminergic polymorphic ventricular tachycardia and paroxysmal atrial fibrillation. *Canadian Journal of Cardiology, 29*, 993-996.

Zhang, X.-H. & Morad, M. (2016). Calcium signaling in human stem cell-derived cardiomyocytes: Evidence from normal subjects and CPVT afflicted patients. *Cell Calcium, 59*, 98-107.

Zhao, Y. G., Valdivia, C. R., Gurrola, G. B., Powers, P. P., Willis, B. C., Moss, R. L. et al. (2015). Arrhythmogenesis in a catecholaminergic polymorphic ventricular tachycardia mutation that depresses ryanodine receptor function. *Proceedings of the National Academy of Sciences, 112*(113), 1669-1677.

Zhilin, Q., Xie, L.-H., Olcese, R., Karagueuzian, H., Chen, P.-S., Garfinkel, A. & Weiss, J. N. (2013). Early afterdepolarizations in cardiac myocytes: beyond reduced repolarization reserve. *Cardiovascular Research, 99*(1), 6-15.

CHAPTER FIVE: CONCLUSION AND FUTURE DIRECTIONS

Conclusions

The heart always requires two sources of Ca^{2+} to generate a heartbeat. The channels for extracellular Ca^{2+}, LCC, and intracellular Ca^{2+} form a cluster, RyR2 via physical coupling in diadic subspace, and release both sources of Ca^{2+} in that region; collectively both channels are called Ca^{2+} release units (CRU). We worked with 20,000 CRUs in a stochastic model of Guinea pig's ventricular myocyte. In this work, we used a 6-state model for LCC and a novel 3-state RyR2 model. Besides open and closed states, the RyR2 model also includes an adaptation state which represents the adaptive behavior of the RyR2 towards the increased subspace Ca^{2+}.

Ca^{2+} releases are elementary but numerous events in a cardiomyocyte

Each cell of a heart 19,928,800±207,600 Ca^{2+} release events in every second but only 81168±2126 out of them form Ca^{2+} sparks. Out of those sparks, 52481±1523 are systolic sparks and rest are diastolic sparks or leaks. Even within a beat there are 3,915,719±255,583 Ca^{2+} release episodes are non-spark Ca^{2+} events. Each spark amplitude can elevate up to 225 μM. The data shows that massive Ca^{2+} release events occur in cardiomyocytes in each second (The above analysis was based upon 1 Hz pacing frequency in WT). The diastolic Ca^{2+} sparks were higher for 2 Hz and 3 Hz pacing but got lowered thereafter. The shorter diastolic interval in higher frequency enacts the role to lower Ca^{2+} sparks leak.

Adaptation in RyR2 channels play a major role in FFR

FFR is a survival trait in many organisms, especially in mammals. It allows the heart to adjust itself with the extension of the contractile property and regulate the cardiac output during the rapid or frequent pacing of the heart. The rapidly pacing heart brings excess Ca^{2+} per unit time. The continuous refill and replenish of SR by SERCA pump and enhancement SR Ca^{2+} release is highly critical for increased force-frequency response. Everyone talks about the SR Ca^{2+} but not many researchers write about the critical role played by RyR2 adaptation. We have found with the 20% reduction in RyR2 adaptation increased RyR2 PO by 7% while a 20% reduction in luminal dependence brought only 6% down to it. The model tells if not more but the adaptation characteristic should have similar attention like SR Ca^{2+} regulation to the RyR2 P_O in the experimental settings or modal development.

Myocyte with RyR2 mutant is a leaky machine with shorter Ca^{2+} spark amplitudes and longer spark durations

The mutation in RyR2 makes those channels super leaky during the diastolic phase. In 1 Hz pacing, there is more Ca^{2+} spark in leaks than in a beat. We found in one second, there was 143,547±6073 leak while a beat in 1 Hz had total sparks of 105,177±5249. Either systole or diastole, both phases had dominant sparks. On the other hand, in the WT myocyte the leak is 28,687±1632 in that period. Lehnart, Mongillo, Bellinger Lindegger, Chen, Hsueh, et al., (2008) observed the dramatic increase in the frequency and area of the sparks in RyR2-R2474S mutant mice.

Mutant RyR2 myocytes had small Ca^{2+} sparks with an average amplitude of 47.26±0.58. The average amplitude of Ca^{2+} sparks wild-type had 62.60±0.85. The RyR2 mutant myocyte also appeared as a leader in Ca^{2+} spark duration with an average of 175.33±1.56 ms; it proved that the RyR2 were highly leaky and continuously releasing Ca^{2+} regardless of systolic or diastolic phases. The spark duration for CASQ2 mutant and WT were 31.45±0.37 and 22.26±0.09 ms, respectively.

EADs in CASQ2 and RyR2 LOF mutations displayed different initial mechanisms

In the β-AR stimulation, both RyR2 LOF and CASQ2 deletion mutations displayed EADs as the precursors of CPVT1 and CPVT2, respectively. In the second slow phase of slow-rapid-slow simulation and with low RyR2 P_O exhibited EADs. But the onset of EADs had different mechanisms in them. The spontaneous SR Ca^{2+} release triggered EADs in mutant CASQ2 and late reactivation of I_{LCC} initialized EADs in the RyR2 mutations. But, late reactivation of the L-type current, increased SR Ca^{2+} release and elongated I_{ncx} were the parts of each EAD. In general, the EADs occur when there is a reduction in outward current and increase in inward current which reduces the net outward current required for repolarization of the heart (Weiss, Garfinkel, Karagueuzian, & Chen, 2010). When the inward Ca^{2+} via L-type current and majority outward Ca^{2+} via I_{ncx} balance out each other, there is no EAD. In simulations in RyR2 LOF, we were able to lower the frequency of EADs with a 25% reduction in Incx and they were almost disappeared with the 50% reduction in I_{ncx}. In performing slow-rapid-slow pacing of the myocyte, the rapid phase came with decreased L-type current and increased in I_{ncx} but when myocyte started beating slowly, then the L-type current increased (inward high

positive charge) which went to activate more RyR2s. The RyR2 were already operating in high SR load so they also started spontaneous Ca^{2+} release. The upsurge of cytosolic Ca^{2+} increased I_{ncx} (inward high positive charge) and the results were EADs. Since the synergy between the L-type current and the I_{ncx} is critically important to generate an EAD and the break down into this synergy without disturbing normal Ca^{2+} cycling could be a therapeutic target in an arrhythmia (Weiss, et al., 2010).

SOICR hypothesis is not the alternative to CICR

In CPVT1 mutation, GOF mutation is a highly supported mechanism. But scientists have different hypotheses besides this; we used Ca^{2+} spark analysis to find out how many of them can explain the arrhythmic mechanism in CPVT1 and SOICR hypothesis is one of them. In the CICR mechanism, the extra-cellular Ca^{2+} via L-type channels activates RyR2 channels of SR and the release of intracellular Ca^{2+} takes place. This process creates contraction of the heart to pump the blood throughout the body. The plateau phase is maintained by the continuous release of SR Ca^{2+} by RyR2 and luminal Ca^{2+} plays the role of guiding their opening and closing. Increased or decreased P_O due to RyR2's cytosolic Ca^{2+} sensitivity is regulated by SR Ca^{2+} and it is the part of the CICR (Prosser, 2010). Now, the SOICR hypothesis which essentially deals with increased RyR2 P_O in the presence of higher SR Ca^{2+} is a well-known phenomenon in CICR, why does someone need an alternative hypothesis to explain already established phenomena? To find out any existence of this hypothesis without CICR, we simulated the mutant myocyte with loaded SR with 100% more Ca^{2+} and 50% increased luminal dependency. The activation of CICR was checked with the initial value of $[Ca^{2+}]_{myo}$. The simulation could

not trigger any SR Ca^{2+} release lowering the threshold level with the SR Ca^{2+} overload. In our model setting, we were unable to verify the existence of the SOICR hypothesis and there is no experimental evidence as well as supporting this hypothesis (Prosser, Ward, & Lederer, 2010).

Na^{+} channels trigger amplitude alternans and SR load produces APD alternans

The model produced alternans with the β-AR stimulation in the myocyte with CASQ2 and RyR2 mutations. Two types of alternans were developed whereas the consecutive APs varied with amplitude and APD. Non-recovery of Na^{+} channels from the previous inactivation was the cause of amplitude alternans. Alternate activation of Na^{+} channels determined the amplitude of AP and at the same time, the alternate variation in the availability of SR load to the consecutive beats lead into APD alternans. While dealing with leaky (RyR2 mutant) and non-leaky (CASQ2 mutant) myocytes, we came to witness that a modest SR load can also generate alternans (Edwards, & Blatter, 2014). In both myocytes, the alternans depend upon the refilling of the SR in the previous beat, if the incoming beat was from higher SR load then the result was larger AP otherwise a shorter AP. Alternate APs had alternate diastolic intervals too, larger AP came after a long interval and smaller AP appeared with a short interval (Wilson, & Rosenbaum, 2007). These diastolic intervals decided the size of the SR load for the incoming beat. Therefore, not the overall SR load but the beat to beat availability of SR load was responsible for APD alternans and this causes a continuous long-short APD.

There is no single underlying mechanism to the pathophysiology of heart failure (Saucerman, & McCulloch, 2006) and it should be an integrated approach such as live-

cell imaging, animal studies, genomics, proteomics, and computational models to understand the complex process of heart failure. In recent years the computational advances in the intracellular Ca^{2+} dynamics have brought many clarities in the experimental findings and can predict many outcomes. Our approach to us multi-scale modeling to predict arrhythmia in mutant myocyte will help to understand the complex part of the heart failure towards the genetic disorder caused by a mutation in Ca^{2+} handling intracellular proteins.

Future Direction

Ventricular arrhythmia caused by CPVT may end up Sudden cardiac death (SCD) Computational models provide deep insight on calcium dynamics and disruption in the Ca^{2+} flow by mutations. Many mutations in the Ca^{2+} channels and Ca^{2+} buffers beget a great deal of damage to human cardiac health. With the developments of new algorithms, advancement in modeling tools and an increase in the simulation speed and more restrictions and regulations in using animal or human specimens, computational models are the first choices in developing new drugs or therapies. Although it's currently a Guinea pig model, the eventual goal is to develop a complete whole-cell human cardiomyocyte model. We aim to develop various cardiac models as discussed below.

Study of more arrhythmogenic mutations

Sudden cardiac death (SCD) is the leading cause of cardiac death in western countries but many of those deaths go unexplained and it is important to note sudden deaths are cardiac origin (Magi, Lariccia, Maiolino, Amoroso, & Grateri, 2017). Mutations affecting genes encoding ionic channel proteins cause channelopathies

(Behere, & Weindling, 2015). Besides studying CPVT, we can modify the current model to comprehend the other channelopathies in long-QT syndrome, short-QT syndrome, and Brugada syndrome.

Development of a computational model of atrial fibrillation

Atrial fibrillation is another multifactorial heart disease that affects 2% of the world's population and the risk jumps to 5% and 10% in the population of 65 to 75-year-olds. There is a limited understanding of AF and it is hard to design physiological therapies specific to the AF than VF (Vagos, van Herck, Sundnes, Arevalo, Edwards, & Koivuma, 2018). In such a regard, an AF specific model would provide deeper insights into understanding the basic physiology of the disease and the role of Ca^{2+} dynamics playing in some of those disease conditions. In our model, blocking L-type channels and removing subspace where RyR2 able to sense cytosolic Ca^{2+} directly will be the first critical step towards developing an atrial model in the Guinea pig.

A discordant alternans with multiple tissues

In a single myocyte, it is not possible to study the discordant (out of phase) alternans, and it requires the use of multiple cells/tissues. To develop a tissue model was out of sight a few years back because it requires massive computing power. With the advent of the powerful computing environment of multi-GPU configuration, a faster and high scale performance can be used to develop tissue models and simulate discordant alternans. Our group in the lab has already developed a spatiotemporal 2D and 3D cardiac model to understand the minimum number of myocytes required to trigger cardiac arrhythmia in a rat (Ullah, Hoang-Trong, Williams, Lederer, & Jafri, 2014). A

tissue model for discordant alternans can be developed on top of the spatiotemporal model but in the Guinea pig.

A computational model for the mechanism of central core disease

Central core disease (CCD) is a genetic disorder of neuromuscular condition caused by the mutation in the chromosome 19 (19q13.1) of RyR1 (Quinlivan, Muller, Davis, Laing, Evans, Dwyer, et al., 2003) gene in the skeletal muscle, an isoform of RyR2. In infants, this condition causes reduced muscle tone, muscle weakness, and malignant hyperthermia (MH). Since RyR1 is an intracellular channel for $Ca^{2+,}$ the effect of Ca^{2+} flux and variation in Ca^{2+} dynamics in the intracellular region plays a major role in CCD. A transformation of our current myocyte model into a skeletal muscle model is required as the first step toward this approach.

References

Behere, S. P. & Weindling, S. N. (2015). Inherited arrhythmias: The cardiac channelopathies. *Annual Pediatric Cardiology, 8*(3), 210-220.

Edwards, J. N. & Blatter, L. A. (2014). Cardiac alternans and intracellular calcium cycling. *Clinical Experiment, Pharmacology, and physiology, 41*(7), 524-532.

Lehnart, S. Mongillo, M., Bellinger A., Lindegger, N., Chen, B.-X., Hsueh, W. *et al*. (2008). Leaky Ca^{2+} release channel/ryanodine receptor 2 causes seizure and sudden cardiac death in mice. *The Journal of Clinical Investigation, 118*(6), 2230-2245.

Magi, S. Lariccia, V., Maiolino, M., Amoroso, S. & Grateri, S. (2017). Sudden cardiac death: focus on the genetics of channelopathies and cardiomyocytes. *Journal of Biomedical Science, 24*(56), 1-18.

Prosser, B. L. Ward, C. W. & Lederer, W. J. (2010). Subcellular Ca2+ signaling in the heart: The role of ryanodine receptor sensitivity. *The Journal of General Physiology, 136*(2), 135-142.

Quinlivan, R. M. Muller, C. R., Davis, M., Laing, N. G., Evans, G. A., Dwyer, J. et al. (2003). Central core disease: clinical, pathological, and genetic features. *Archives of Disease in Childhood, 88*, 1051-1055.

Saucerman, J. J. & McCulloch, A. D. (2006). Cardiac beta-adrenergic signaling from subcellular microdomain to heart failure. *Annals of the New York Academy of Sciences, 1080*(1), 348-361.

Ullah, A. Hoang-Trong, T. M., Williams, G. S. B., Lederer, J. W. & Jafri, M. S. (2014). A small number of cells is sufficient to trigger cardiac arrhythmia: stochastic computational studies. *Biophysical Journal, 106*(2), 112a.

Vagos, M. van Herck, I. G., Sundnes, J., Arevalo, H. J., Edwards, A. G. & Koivuma, J. T. (2018). Computational modeling of electrophysiology and pharmacotherapy of atrial fibrillation: Recent advances and future challenges. *Frontiers in Physiology, 9*(1221), 1-29.

Weiss, J. N., Garfinkel, A., Karagueuzian, H. S. & Chen, P.-S. (2010). Early afterdepolarization and cardiac arrhythmias. *Heart Rhythm*, 1891-1899.

Wilson, L. D. & Rosenbaum, D. S. (2007). Mechanisms of arrhythmogenic cardiac alternans. *European Society of Cardiology, 9*, 1-6.

BIOGRAPHY

Roshan Paudel born and grew up in Parbat, a mountainous district in Gandaki Province, Nepal. He received his B. Sc. degree in biology (1998) and a Master's degree in Zoology (2003) from Tribhuvan University Kathmandu Nepal. After a pause of a few years, in May 2012, he graduated Master in Science (Bioinformatics) from Morgan State University, Baltimore, Maryland. He is a Ph.D. candidate in the bioinformatics and computational biology department, college of science, George Mason University, VA. Roshan also works as a computer science lecturer at Morgan State University.